



**UNIVERSITY OF
BIRMINGHAM**

THE USE OF GEOPHYSICAL METHODS IN THE STUDY OF TREE ROOTS IN AN URBAN ENVIRONMENT

By

ANDREI EMILIAN MIHAI

**A thesis submitted to
The University of Birmingham
For the degree of
DOCTOR OF PHILOSOPHY**

**School of Engineering
College of Engineering and Physical Sciences
University of Birmingham
January 2020**

UNIVERSITY OF
BIRMINGHAM

University of Birmingham Research Archive

e-theses repository

This unpublished thesis/dissertation is copyright of the author and/or third parties. The intellectual property rights of the author or third parties in respect of this work are as defined by The Copyright Designs and Patents Act 1988 or as modified by any successor legislation.

Any use made of information contained in this thesis/dissertation must be in accordance with that legislation and must be properly acknowledged. Further distribution or reproduction in any format is prohibited without the permission of the copyright holder.

ABSTRACT

Near-surface geophysics has been increasingly applied to more and more environments, thanks to the development of both equipment and available software. As a result, non-destructive geophysical surveys in urban areas are increasingly used to solve a great deal of varied problems.

Trees provide valuable and important environmental services and play an important role in the livelihoods of humans and animals alike. However, although trees have been researched extensively, roots remain an area that is notoriously difficult to understand. Hence, robust geophysical surveys might provide an array of useful information regarding the location, size, and overall structure of tree roots, with very few practical downsides. This thesis works at the junction of several disciplines, bringing them together in a cohesive and practical manner.

The investigation focuses on two geophysical methods (GPR and geoelectrical surveying), presenting relevant surveys as well as forward models that aid survey design and data interpretation. The models also revealed why sometimes surveys are unsuccessful (or partly unsuccessful) and what can be done to maximize the odds of success.

The results show that while this task is challenging and site-specific, it is possible to study tree roots in an urban context with geophysical methods.

Dedication

To my family and close friends who have supported me throughout the endeavour in more ways than they know. To my cats who were a source of peace (and annoyance) in times of trouble. To everyone who has helped and inspired me over the years and to everyone who is working to make the world a better place. To the amazing people of the NHS, without whom I might not be here today.

ACKNOWLEDGEMENTS

I would like to thank Philip Atkins for his supervision and help, as well as his work in obtaining funding for my project.

A very special thanks goes to Alexandra Gerea, who aside from personal support, has offered academic and fieldwork help which has proven invaluable.

Many thanks to Dr. Giulio Curioni who offered his assistance when everyone else was sceptical.

I would also like to thank the COST framework and COST Action TU1208 on Ground Penetrating Radar, especially Dr. Antonis Giannopoulos, Dr. Craig Warren, and everyone else involved in developing gprMax.

In the end, one cannot help but be thankful for the entire European Union framework, without which myself and many other young researchers would have not gotten the chance to live, study, and work on their own terms.

Structure

Abstract

Dedication

Acknowledgements

Content Listings

Abbreviations

Notations

Text

Appendices

Bibliography

Table of Contents

1. INTRODUCTION	1
1.1 Background	2
1.2 Research questions	4
1.3 Aims and objectives	6
1.4 Scope	7
1.5 Summary	9
2. LITERATURE REVIEW AND GENERAL CONSIDERATIONS	10
2.1 Trees	10
2.2 Benefits of trees	12
2.2.1 Valuation of trees in the UK	17
2.3 Conflicts with infrastructure	18
2.4 Urban soils	27
2.5 Challenges to urban trees	28
2.6 Man-made surfaces	31
2.7 Geophysical techniques	32
2.7.1 Environmental Geophysics	34
2.7.2 Resistivity	36
2.7.2.1 Theoretical background	36
2.7.2.2 Range of obtainable data	48
2.7.2.3 Modern methodology	50
2.7.2.4 Advancing frontiers	51
2.7.2.5 Limiting factors	53
2.7.2.6 Impact of weather and external factors	54
2.7.2.7 Literature review: Resistivity imaging of tree roots	55
2.7.2.8 Tree as an electrode	58
2.7.3 GPR	59
2.7.3.1 History of GPR	59
2.7.3.2 Theoretical Background	61
2.7.3.3 Modern Methodology	69
2.7.3.4 Advancing Frontiers	73
2.7.3.5 Limiting factors	77
2.7.3.6 Impact of weather on GPR	78

2.7.3.7 Literature Review: GPR Imaging of Tree Roots.....	79
2.8 Survey Design Considerations	81
2.9 Data Processing & interpretation	84
3. METHODOLOGY, LAB RESULTS, AND FORWARD MODELS	86
3.1 Introduction.....	86
3.2 Lab measurements	86
3.2.1 Measuring root permittivity	87
3.2.1.1 Motivation.....	87
3.2.1.2 Choice of equipment	88
3.2.1.3 Measuring methodology	90
3.2.2 Permittivity lab measurements of tree roots.....	92
3.2.3 Forward models of tree roots	95
3.2.4 Equipment development	114
3.2.5 Software / algorithm development	118
3.3 GPR surveys.....	120
3.3.1 GPR software and processing flow	121
3.4 Resistivity surveys	123
3.4.1 Resistivity equipment.....	124
3.5 Total station	124
4. RESISTIVITY IMAGING OF TREE ROOTS.....	126
4.1 Approach.....	126
4.2 Survey 1	127
4.3 Survey 2	130
4.4 Survey 3	133
4.5 Box surveys.....	136
4.6 AC prototype.....	139
4.7 Tree as electrode	140
5. GPR IMAGING OF TREE ROOTS	143
5.1 Approach.....	143
5.2 Survey 1	143
5.3 Survey 2	150
5.4 Survey 3	152
5.5 Survey 4	154
5.6 Survey 5	157
5.7 Survey 6	158
5.8 A series of Harborne soil surveys	165

5.9 A series of Harborne asphalt surveys.....	192
5.10 An integrated GPR/ERT example.....	205
6. CONCLUSIONS AND RECOMMENDATIONS	213
6.1 Research questions.....	215
6.2 Other conclusions and secondary research questions	210
6.3 Recommendations for future work.....	222
7. APPENDICES	226
8. REFERENCES	287

List of figures

Figure 1. Commercial resistivity equipment (measuring setup).....	3
Figure 2. Commercial resistivity equipment (profile with electrodes) with 0.5 m spacing between electrodes.	3
Figure 3. Root damage caused by tree roots in the UoB campus.....	5
Figure 4. Typical GPR setup, prepared for measurement around UoB campus.	6
Figure 5. The Geometrics Ohmmapper, probably the most common capacitively-coupled resistivity meter in use at the moment, does not offer sufficient resolution to study tree roots effectively	32
Figure 6. Peak near-surface geophysics? The number of publisher papers, books, and citations featuring the terms 'Ground Penetrating Radar' and 'Environmental Geophysics'	34
Figure 7. Example of a pseudosection design, for the Wenner array, with the RES2DINV software from Loke (2010).....	40
Figure 8. Depiction of the three most common types of resistivity arrays.....	42
Figure 9. The sensitivity patterns of the three most common arrays: Wenner (a), Schlumberger (b), and Dipole-Dipole (c). From Loke (2000).	43
Figure 10. Distribution of points for a regulate Dipole-Dipole and optimized array. Both are symmetrical. From (Wilkinson et al., 2006).	47
Figure 11. The roll-along approach produces a trapezoid section with resistivity. Deepest data is disregarded (which is acceptable in this case) and there is some slight overlap in the two profiles...51	
Figure 12. Depiction of the experimental setup from Cermák et al. (2006).....	58
Figure 13. The cone of transmission, from Mihai (2014).	62
Figure 14. Visualization of Snell's equation	63
Figure 15. Depiction of the so-called 'hyperbola' effect, caused by antenna movement over an objective.....	64
Figure 16. Simplistic depiction of GPR scattering and focusing, from Mihai (2014).	65
Figure 17. Typical curve of permittivity plotted against frequency. Blue line is median value obtained after 40 measurements, brackets show minimum and maximum values (no processing or eliminating of anomalous values)	67

Figure 18. Depiction of GPR grid with the overall grid area (yellow), and two profile directions (in blue and orange), to study sidewalk damage potentially caused by a tree root, UoB campus, around Gisbert Kapp building. Direction and distance between profiles are approximate and not to scale...	70
Figure 19. Forward model of three metallic pipes of different diameters in a clay-sand soil model of. Clay-sand composition is 50%-50%.....	74
Figure 20. The GPR response for the above model.....	74
Figure 21. Depiction of the Keysight instrument used for permittivity measurements (a); root samples after drying (b); an area from which root segments were harvested (c).The GPR response for the above model.	89
Figure 22. The average (red) and median (blue) relative permittivity values for one of the samples in the entire 0.05 – 3 GHz frequency range. Values exhibit a typical variation curve, dropping down from higher values at smaller frequencies.....	95
Figure 23. Three models of a root with a relative permittivity of 3, in clay with three different levels of humidity: almost completely dry (top; permittivity 5), somewhat wet (middle; permittivity 8) and more wet (bottom; permittivity 11). Here, contrary to conventional wisdom, wetter soils make the root more easily detectable because although they lower the data quality, they accentuate the contrast between the root and the surrounding soil.....	96
Figure 24. GPR responses for clay proportion 95% (above) and sand proportion 95% (below).....	98
Figure 25. GPR responses for clay proportion 95% (above) and sand proportion 95% (below), as seen in ReflexW (with basic processing).	99
Figure 26. Longitudinal section of a thinning tree root.	100
Figure 27. GPR response of a transversal PEC root-like structure.	101
Figure 28. Example of a GPR response of a root. Several different parameters for the soil and the root were presented. Here, a dielectric contrast of 6 is depicted	101
Figure 29. Depiction of the modelled environment. A root is penetrating a water pipe.	102
Figure 30. GPR response of the modelled environment.....	103
Figure 31. Depiction of the modelled environment. A root is penetrating a water pipe, causing leakage in a randomly distributed arrangement which has not homogenized.	103
Figure 32. GPR response of the modelled environment.....	104
Figure 33. GPR response to the above-mentioned scenario	106
Figure 34. GPR response to a root neatly penetrating asphalt (top) versus a similar-sized hole (bottom).....	106
Figure 35. GPR response of a root of permittivity 12 (top) versus 8 (bottom) in an asphalt of permittivity 6.....	107

Figure 36. Depiction of described scenario with the two layers of asphalt and a root (brown) producing a bump in the second layer.	108
Figure 37. GPR response of the above-described scenario.	109
Figure 38. GPR response of a bump deformation with root (above) versus no root (below)	100
Figure 39. Simulated timeslice of bump with no root (above) and bump with root (bottom).....	110
Figure 40. Depiction of the above-described scenario	111
Figure 41. Comparison of empty cracks (top) versus water-filled cracks (bottom).....	112
Figure 42. The test environment setup was rather messy, but efficient.	115
Figure 43. Results of one of the tests, featuring 42 measurements of 16 electrodes in a Wenner array (35 positions). Minimum and maximum results compared with resistor values.....	115
Figure 44. Average values, variance and standard deviation results (top right) and standard deviation plotted as a function of resistance.....	116
Figure 45. Simplified schematic of resistivity meter.	117
Figure 46. Photo taken of the equipment on the field	118
Figure 47. Screenshots from the software: profile initialization (top), geometry selection (middle) and current electrode position (bottom).....	119
Figure 48. Typical soil survey using the 1.5 GHz Utsi antenna. Ropes and rulers were used to mark the survey area and ensure profile data acquisition on the right trajectory	121
Figure 49. Example of data inversion with Red2DInv, the lowest slice representing the final iteration with the lowest errors. High resistivity anomalies can be interpreted as tree roots, with lateral continuity serving as an important tool for identification. Here, the three black arrows indicate roots which were visible on the surface.....	127
Figure 50. Most surveys were carried out on the UoB campus, an urban area with some green spaces and plenty of tree root-infrastructure interactions.	128
Figure 51. Depiction of the survey. Stainless steel pegs were used as electrodes and the root was partially visible on the surface.	129
Figure 52. Results from two profiles 15 cm away. Results in Res2DINV.....	129
Figure 53. Data visualization showing the triangular discretization cells. Three root areas were identified and confirmed by shallow soil scratching. The overall shape of the data output by BERT is different than “conventional” inversion software, being rectangular rather than triangular. However, since there is no additional data, the extra parts (on the lower lateral sides) is gathered completely from extrapolation and was therefore discarded. This is not a major aspect in this study, since the object of interest is in the most shallow parts of the survey, but is important to keep in mind.....	131

Figure 54. The same data, viewed from a slightly different angle, and without the discretization cells.	132
Figure 55. The same data, with added visual transparency. The transparency allows an excellent visualization of the trajectory of the roots and any other elements in the subsurface.	132
Figure 56. Comparison between a Dipole-dipole profile (top), a Wenner profile (bottom), and the actual position and size of the roots (middle).	134
Figure 57. Comparison between a Dipole-dipole profile (top), a Wenner profile (bottom), and the estimated position and size of the roots (middle). The profile is parallel and 30 cm away from the previous one.	135
Figure 58. Applying a scalar clip to an ERT profile to highlight the position of the roots.	136
Figure 59. The experimental electrode setup	137
Figure 60. Survey with the Dipole-Dipole array. Top: empty soil box. Middle: buried root. Bottom: buried electrode. No difference is apparent.	138
Figure 61. A “full” ERT profile with all possible electrode configurations.	139
Figure 62. A Wenner pseudosection over the same line.	140
Figure 63. Depiction of the method setup.	141
Figure 64. Depiction of potential application scenario. If there is an active root from soil 1 to soil 2, current will be measured in the soil 2 unit.	142
Figure 65. Image from the site with potential root damage visible on the surface.	144
Figure 66. Profile from the survey with A1 and A2 depicting hyperbola from tree roots causing damage to the paved surface, and A3 depicting damage that appears unrelated to tree roots.	145
Figure 67. Yellow areas indicate root damage visible from the surface, orange area was not visible on the surface.	146
Figure 68. Profile from the survey. Unmigrated data.	147
Figure 69. Plot of tree roots. Red dots are peaked apex of root-associated hyperbolae.	147
Figure 70. Time slice at an estimated depth of 2 cm	148
Figure 71. The GPR slice map at a depth of 4.3 cm.....	148
Figure 72. A similar map, at an estimated depth of 5.4 cm, using a different colour scale.....	149
Figure 73. Comparison between the same section with the 250 MHz antenna (bottom) and the 750 MHz antenna (top). The lower frequency antenna also has lower resolution, this being the reason why it is “blind” to a root present in the first meter of the GPR section. Timeslice from an estimated depth of 6 cm.....	151

Figure 74. Two GPR profiles carried out on a sidewalk in the UoB campus near the Gisbert Kapp building. Highlighted in red are some potential tree roots or tree root damage. Red arrow indicates a pipe/cable. Static corections and background removal had not been applied yet at this point.	152
Figure 75. Simultaneous visualization of a GPR profile and timeslice can facilitate feature detection.	153
Figure 76. The same feature plotted on a 3D cube.....	153
Figure 77. Tree root damage visible on total station data (topography not considered).....	154
Figure 78. Tree root damage visible on total station data (including topography).	155
Figure 79. GPR slices at estimated depths of 3, 6, and 10 cm deep. The position of tree root damage (bump) is indicated with black dots. This position is only somewhat visible on the top section. This was the clearest example of unclear GPR results.	156
Figure 80. Representative profile with 250 MHz antenna.	157
Figure 81. Representative profile for the 750 MHz antenna.	157
Figure 82. Two roots are visible in this GPR slice at 10 cm deep. Antenna frequency: 750 MHz.....	158
Figure 83. Representative profile for the 750 MHz antenna.	159
Figure 84. A slice at an estimated depth of 10 cm with the 750 MHz antenna (left) and the 250 MHz antenna (right)	159
Figure 85. Timeslice at an estimated depth of 4 cm. Some roots are highlighted with red arrows. Living tree is highlighted in green, cut down tree highlighted in purple.	160
Figure 86. Timeslice at an estimated depth of 4 cm. The same arrows as in the image above are overlaid over the timeslice. Living tree is highlighted in green, cut down tree highlighted in purple.	162
Figure 87. Timeslice at an estimated depth of 3 cm. Thin roots not visible on the 750 MHz antenna highlighted with arrows.	164
Figure 88. Depiction of the X and Y profile lines. The approximate position of the tree is visible from the gaps in the profiles (the gaps are slightly different because the antenna wheel).	166
Figure 89. Depiction of the survey area. Image not to scale.	167
Figure 90. Time slices on the X and Y directions at an estimated depth of 1 cm.....	168
Figure 91. Time slices on the X and Y directions at an estimated depth of 3 cm.....	169
Figure 92. Time slices on the X and Y directions at an estimated depth of 4.5 cm.....	170
Figure 93. Examples of X-direction radargrams depicting the highlighted feature on profiles 25-28.	171

Figure 94. Tree root area at depths of 5-7.5 cm, highlighted in green (Y direction).	173
Figure 95. Two profiles highlighting parts of the presumed area (picks are in red).	174
Figure 96. Time slices at depths of 5-7.5 cm (X direction).	175
Figure 97. Timeslice at a depth of 1.2 cm with profiles at 20 cm (odd profiles – top, even profiles – middle) and 10 cm (bottom).	176
Figure 98. Timeslice at a depth of 1.2 cm with profiles at 20 cm (odd profiles – top, even profiles – middle) and 10 cm (bottom) on the X direction	177
Figure 99. Timeslice at an estimated depth of 2 cm with profiles at 20 cm (odd profiles – top, even profiles – middle) and 10 cm (bottom) on the Y direction.....	178
Figure 100. Timeslice at a depth of 1.2 cm with profiles on both directions overlaid at 20 cm (odd profiles – top, even profiles – middle) and 10 cm (bottom).	179
Figure 101. An image of the pre-survey setup.....	181
Figure 102. Example profiles from the X (above) and Y (below) directions). Images are not to scale.	182
Figure 103. Time slice at an estimated depth of 2 cm on the X profiles.....	183
Figure 104. Time slice at an estimated depth of 2 cm on the Y profiles.....	183
Figure 105. Time slice at an estimated depth of 5 cm on the X profiles.....	184
Figure 106. Time slice at an estimated depth of 5 cm on the Y profiles.....	185
Figure 107. Time slice at an estimated depth of 10 cm on the X profiles.....	185
Figure 108. Time slice at an estimated depth of 10 cm on the X profiles.....	186
Figure 109. Time slice at an estimated depth of 2 cm. The position of the trees is represented by brown-blue circles.....	188
Figure 110. Time slice at an estimated depth of 6 cm (left) and 8 cm(right). The position of presumed root areas is highlighted in yellow rectangles.....	189
Figure 111. An example of a profile in the surveyed area. Data are processed and migrated, Hilbert transform not applied.....	190
Figure 112. Depiction of profile geometry. The even profiles were arranged to depict the real position of the antenna. Image not to scale.	193
Figure 113. Time slice of the first half of the survey at an estimated depth of 3 cm.....	193
Figure 114. Profile 3 (at x = 0.2 m). The teal ellipses indicate probable deformation areas highlighted in the time slices. The pink ellipses indicate apparent deformations which do not exhibit lateral continuity	194

Figure 115. Profile 9 (at x = 0.8 m). The orange ellipse indicates damage visible on the surface (not the visible large discontinuity in the asphalt surface), and the teal ellipse indicates presumed deformations associated with tree roots. This was not visible on all profiles.	195
Figure 116. Time slice of the second half of the survey at an estimated depth of 3 cm	196
Figure 117. Example of deformations in the 'c' area.	196
Figure 118. Example of deformations in the 'a' and 'b' areas.	197
Figure 119. Example of deformations in the 'd' and 'e' areas.	197
Figure 120. 3D visualization with the most likely root-associated areas (highlighted in teal). Orange ellipses indicate a buried cable and a root that was visible at the surface (and therefore not revealed by geophysical surveys). Image is not to scale.....	199
Figure 121. Section of all 6 profiles depicting what was interpreted as a root penetrating the asphalt (in teal circle).....	201
Figure 122. A radargram from profile 4. The areas most likely to represent tree root damage are highlighted	202
Figure 123. Timeslices at estimated depths of 3 cm (top) and 4 cm (bottom).	202
Figure 124. The same areas highlighted on profile 4.....	203
Figure 125. Time slice at an estimated depth of 4 cm. Position of the tree is marked.....	203
Figure 126. The same areas highlighted on profile 2	203
Figure 127. The two areas are the only remarkable features on the survey.....	204
Figure 128. General depiction of the survey area. The survey areas are not to scale.....	206
Figure 129. Time slice from an estimated depth of 4 cm.....	207
Figure 130. Time slice from an estimated depth of 4 cm. Same areas as above are highlighted.....	207
Figure 131. Profile example from GPR 2	208
Figure 132. ResiPy representation of the RMS error of the 8 different profiles is very similar. Points represent iterations for every profile.	208
Figure 133. Profiles 1, 2, and 3 of the ERT.	210
Figure 134. The estimated position of roots from ERT data visualized in Paraview	211
Figure 135. GPR profile 2 and ERT profile 2 overlaid.	212
Figure 136. GPR and profile 2 overlaid, with GPR and ERT contrasts highlighted	213
Figure 137. The root trajectories inferred from geophysical surveys.....	214

List of tables

Table 1 Generally, all trees produce benefits, but larger trees produce larger benefits (Mullaney et al; 2015).

Table 2. Different valuations of trees.

Table 3. Advantages and disadvantages for common array geometries.

Table 4. Nominal resistivity of common rocks and soils, selected from Reynolds (2011).

Table 5. Typical dielectric constant of common materials measured at 100 MHz, according to Davis & Annan (1989) and Daniels (1996).

Table 6. Expected resolutions for common GPR antenna frequencies (approximate).

Table 7. Permittivity and propagation speed of electromagnetic waves for commonly encountered materials. Adapted from Conyers (2004).

Table 8. Table 1 from Mihai et al (2019). General characteristics of the measured root segments, including the diameter (Φ), wet weight (gw), dry weight (g) and water content (%)

Abbreviations

GPR	Ground Penetrating Radar
ERT	Electrical Resistivity Tomography
UXO	Unexploded Object
A-M-N-B	The four electrodes of a 'classic' geo-electrical survey, with A and B being current injection electrodes and M and N being potential electrodes (also C1-P1-P2-C2)
DC – AC	Direct Current – Alternative Current
UoB	University of Birmingham
FDTD	Finite Difference Time Domain
DGPS	Differential GPS
RTK	Real-Time Kinematic
Hz	Hertz (also MHz for Mega-Hertz and GHz for Giga-Hertz)
IDS	Ingegneria dei Sistemi
OPM	Optimized Measurement (in the context of ERT geometry)
BERT	Boundless Electrical Resistivity Tomography

Notations

α	attenuation coefficient
ε	dielectric permittivity
λ	wavelength
μ	magnetic permeability
ρ	resistivity;
σ	electrical conductivity
\emptyset	diameter
D	distance
f	frequency
R	electrical resistance
I	current
U	Voltage
T	temperature
Z	impedance

1. INTRODUCTION

Although the term itself is relatively new, mankind has been interested in geophysics for centuries, if not millennia. The reasons for this are twofold.

Above all, there is the human curiosity and ambition to know more about the surrounding environment. In 240 BC, the ancient Greek Eratosthenes of Cyrene is said to have measured the circumference of the Earth using only trigonometry and measuring the angle of the sun at different latitudes, which could be regarded as one of the first thorough geophysical studies. Even before Isaac Newton published his landmark *Philosophiæ Naturalis Principia Mathematica* in 1687, William Gilbert's *De Magnete* in 1600 noted that a compass points North because the Earth itself has a magnetic field. Newton brought forth our first understanding of gravity, and 200 years later, Maxwell's equations helped build the foundation of electromagnetism, thus offering a theoretical framework in which geophysics could operate.

The second reason for our interest in geophysics is that it enables mankind to discover and access valuable subsurface resources.

The first documented use of the term "geophysics" comes from Julius Fröbel in 1834 (in the German language). The first Geophysical Institute was founded in 1887 at the University of Göttingen and the first geophysical journal *Terrestrial Magnetism* (which would go on to become the *Journal of Geophysical Research*) was founded in 1896.

In the 20th century, the demand for petroleum and mineral resources grew enormously, and was a great motivator for the development of geophysical techniques. The interior of the Earth has been increasingly studied using seismic waves from earthquakes, and plate tectonics was supported in the 1970s by several pieces of

geophysical evidence, including palaeomagnetism, volcano mapping, and seismic studies. By then, geophysics was already an established field of science, and it continuously developed and branched out, addressing increasingly diverse issues.

Another important stage in the history of geophysics was marked by the advent of modern computers. The acquisition, processing, modelling, and interpretation of geophysical data all benefitted greatly from increased computation.

Several areas of research, including the one presented here, were empowered by increased computational power. Although many things have changed, the fundamental physical principles are still in place.

1.1 Background

The successful detection of any subsurface features through geophysical methods relies on a detectable physical contrast between the objective and the subsurface surrounding environment. Consequently, small-scale subsurface objectives, as well as objectives which share physical similarities with their surrounding environment, yield small contrasts and are difficult to detect using geophysical methods. Tree roots, which are in a constant exchange of water and chemical elements with the soil and are generally in the centimetre or sub-centimetre range, fall into both these categories, which make them one of the most challenging geophysical objectives. However, since tree roots are difficult to study directly *in situ*, geophysics offers a unique opportunity to study them remotely, particularly in urban areas where they are often covered by man-made surfaces, and excavation would be time and resource-consuming.

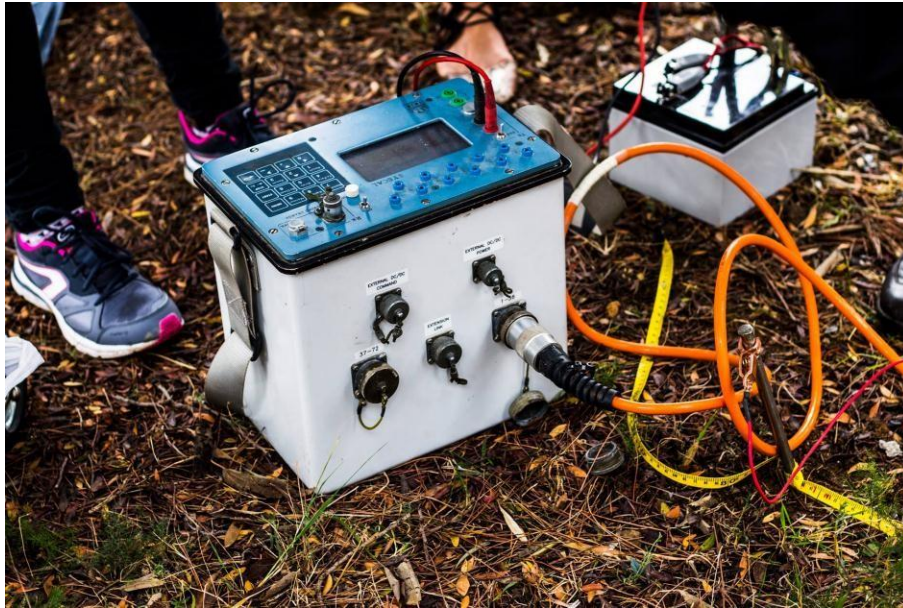


Figure 1. Commercial resistivity equipment (measuring setup).



Figure 2. Commercial resistivity equipment (profile with electrodes) with 0.5 m spacing between electrodes.

The reasons to study tree roots through geophysical methods are multifold. At a fundamental level, there are substantial knowledge gaps regarding the applicability of geophysical methods in this context and the range of information that can be obtained. Tree roots are also relatively understudied *in situ*, due to obvious practical difficulties.

There are also very practical applications to this type of study. Tree roots are often unwanted “noise” in geophysical studies (showing up on archaeological or environmental studies), but they can be an objective themselves, whether it is to provide information related to tree health, root extent, CO₂ absorption, or to study their interactions with man-made infrastructure.

Lastly, this represents an intriguing interdisciplinary field of study, occurring at the intersection of numerous different scientific fields such as geophysics, biology, soil science, and civil engineering.

1.2 Research questions

In the preliminary stages of the project, several research questions were defined, to help define the general framework for the study and the main topics of interest. These questions have been adapted and tweaked as the work progressed and serve as general objectives to be addressed here.

Main research questions:

- a) Is there a reason to study the interaction between tree roots and infrastructure with geophysics?

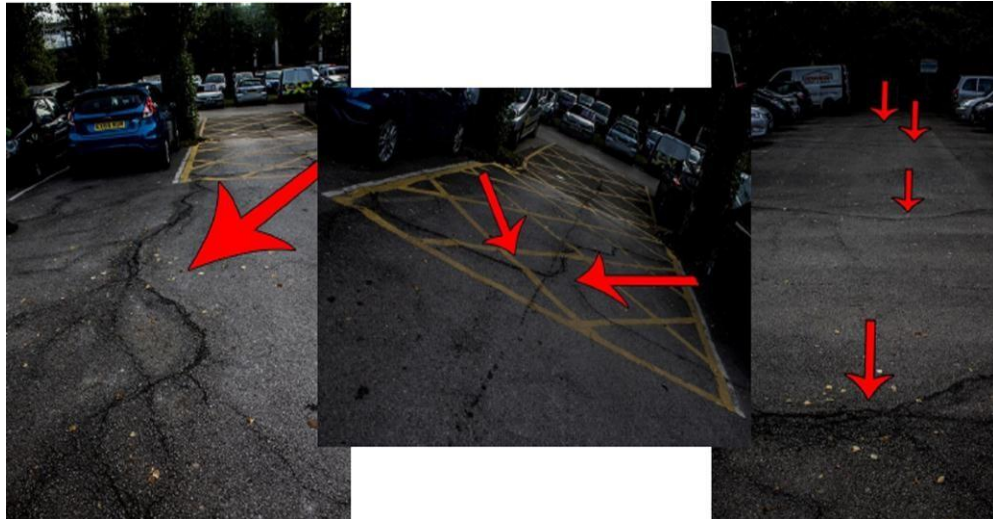


Figure 3. Root damage caused by tree roots in the UoB campus.

- b) What are the relevant and useful physical parameters of tree roots that can be used for detection, and what methods can detect them?
- c) What is the span of information we can derive by using these methods?
- d) Is there a way to predict and/or characterize the structural damage that tree roots will do using geophysical techniques?

Secondary research questions:

- a) What GPR frequency works best, and what kind of acquisition and processing flow is most suitable?
- b) What kind of resistivity measurements could be best applied, and under what circumstances?
- c) How can forward models help in the planning of surveys and in the understanding of the data?
- d) How can different types of data be best integrated?

1.3 Aims and objectives

The general objective of the study was to assess the feasibility and usability of geophysical methods in the study of tree roots. The first aim is answering the research questions as well as possible. As this is a multidisciplinary and applied study, consideration was given not only to theoretical aspects, but also to practical ones.

In addition to filling the knowledge gap at a fundamental science level, establishing and finessing a methodology for geophysical data acquisition was also given importance. Practical aspects were specifically considered given that there is real potential for applying this type of measurements in a real-life setting, offering potentially valuable information for city planners, policy makers, and urban surveyors. Insights could potentially be useful in other situations such as forestry and orchard management as well.



Figure 4. Typical GPR setup, prepared for measurement around UoB campus.

The goal was to develop a proof of concept approach, in real situations, as to how geophysical methods might be used to study tree roots and tree root damage, with the primary goal of predicting or assessing potential infrastructure damage, and the secondary goal of identifying and characterizing subsurface roots. The problem was addressed mostly qualitatively and, when possible, quantitatively, to better understand the potential and the limitations of geophysical methods in this context. The possibility of using this approach in a cost-effective manner was also considered, though it was not the primary focus of the study.

1.4 Scope

Trees are an important part of almost all environments on Earth, and urban areas are no exception. Trees also offer a great number of environmental and economic benefits, and have, therefore, been studied extensively.

Roots are a key structural component of trees, offering anchorage as well as water and nutrient absorption and distribution. Roots are also actively exchanging chemical substances with the surrounding soil (through absorption and respiration), which means that when they are taken from their natural environment, their biophysical parameters start to change, which makes any *in situ* observation even more challenging.

Geophysical methods offer a unique opportunity to study tree roots in their subsurface, natural environment. In urban environments, this is particularly important since tree roots can have a number of unwanted, destructive interactions with man-made infrastructure (roads, sidewalks, building foundations, pipes, etc.). It is not uncommon

for urban geophysical investigations (especially GPR surveys) to come across tree roots, but they are rarely regarded with any interest. Geophysical studies focusing on tree roots, particularly in urban areas, are still relatively uncommon.

A range of shallow geophysical techniques have been considered, drawing from existing evidence, particularly from the study of buried utilities or archaeological objectives. However, in the case of tree roots, there are several factors which make detection different and more challenging: the geophysical contrast tends to be less pronounced, the size of the objective is often small, and the method needs to be suitable for an urban setting. Considering all this, the methods that seem most viable are GPR and resistivity surveys (especially ERT, though other types electrical surveys are also considered).

The potential of these two methods was assessed in a variety of settings, on a variety of surfaces (both natural and man-made) and around a variety of trees from different species and of different sizes. The study does not attempt to explain the biophysical causes and parameters that are responsible for the geophysical contrast. Instead, it focuses on the detection and study of tree roots and the circumstances which make this detection possible. The causes that allow this detection are too complex to be satisfactorily covered here and warrant a separate study.

Lastly, the work also addresses how equipment can be tweaked, improved, or simply applied differently for better results. Several directions for future studies are also presented.

1.5 Summary

The work is a multidisciplinary approach on how tree roots can be detected using geophysical methods in practical, urban scenarios. The main focus is on geophysics, but the approach is multidisciplinary, considering aspects of soil science, biology, civil engineering, as well as practical considerations for the integration of the results into city planning policies.

The project aims to improve understanding of geophysical detection of tree roots as well as to provide directions in which this knowledge can be used, as well as guidance for future studies in related areas. As geophysics continues to improve and branch out, it will undoubtedly tackle problems that are more challenging (as is also the case here). Pushing these methods to their absolute maximum offers new theoretical insights, and it can also offer suggestion as to how they can be used in practical scenarios to aid in the sustainable development of our society – this has been the guiding creed of this work.

The thesis starts with a brief introduction on the interaction between trees and urban areas. The subsequent parts address the geophysical methods that can be used to study these interactions, zooming in on geo-electrical surveys and ground penetrating radar. These methods are described in detail, along with a literature review regarding their application in this context. Results of lab measurements are also included. Several representative surveys on multiple surfaces are then presented, with discussion and conclusions following afterwards, along with recommendations for future work in the topic.

2. LITERATURE REVIEW AND GENERAL CONSIDERATIONS

Since it is hoped that this work can be of use to both geophysicists and non-geophysicists, it will provide basic description of geophysical systems and principles, as well as a review of relevant aspects revolving around urban trees, including their importance and differences from non-urban trees.

2.1 Trees

Trees are perennial, non-marine plants that play a crucial role for many of Earth's ecosystems. They differ from other terrestrial plants in that they typically have a permanently woody stem or trunk and they usually grow to a considerable height. This study does not intend to provide a comprehensive definition or classification of trees and for the purpose of this work, all plants satisfying those two conditions were considered trees (although technically, some shrubs would also satisfy these conditions).

Trees were already well-developed in the Carboniferous period, 300 million years ago. It is well known (Gastaldo, 1987) that the Carboniferous was marked by vast swamp forests which produced rich coal deposits. However, recent research has shown that the oldest trees come from even earlier, emerging during the Middle Devonian, some 390 million years ago (Soria & Decombeix, 2010), where they were brought forth significant global changes (Retallack, 1997), affecting not only the geology of the planet, but also the biosphere and atmosphere.

Roots emerged during the early phases of land plant diversification, some 409-363 million years ago (DiMichele & Falcon-Lang, 2011), allowing plants to grow larger and gain more stability, improving their anchorage, as well as their nutrient and water uptake. However, plants roots, and tree roots in particular (due to their larger size) set in motion a large number of geochemical changes. Mechanically, roots fractured the rock, ploughing

and tilling the soil, allowing water to infiltrate deeper into the soil. Roots also help bind loose particles and water, preventing surface erosion. They helped to create what we today consider 'soil'.

Chemically, roots also brought massive changes. They set in motion a mineralization cycle, breaking down rocks and minerals and cycling minerals from the soil into the biosphere at an unprecedented scale (Kenrick & Crane, 1997).

Tree roots also disrupted the global carbon cycle. The uptake of atmospheric CO₂, the weathering of silicate and carbonate rocks, as well as the deposition of carbonate minerals and organic matter contributed to an important shift in the global carbon cycle (Berner, 1998).

Trees have continued to develop since the Palaeozoic, but the fundamental structure of trees (and roots) has remained largely similar. Today, trees continue to play a crucial role in the carbon cycle. Especially in the wake of global climate change, the role of trees, tree roots, and forest soils has been investigated for carbon sequestration and storage (Raich et al., 1992; Lal, 2005).

In order to address the practical feasibility and advantages of surveying tree roots in urban areas, financial considerations are also important. Ideally, tree root surveys should have a positive impact not just environmentally, but also economically. The following will present a review of why geophysical detection of tree roots is not just feasible, but also pragmatic. This is important as municipalities often remove trees due to the damage their roots cause to infrastructure; by mapping and directing interventions, geophysical surveys can help keep trees (and the benefits they produce) in place for longer.

2.2 Benefits of trees

The fact that trees provide valuable environmental and economic services (and are a pleasant sight) has been known, to some extent, for centuries. In addition to their role in the carbon cycle and soil stabilization, trees also provide a number of environmental and economic services. Trees remove air pollution (Svensson & Eliasson, 1997), help regulate the climate, offset carbon emissions, and improve the overall standard of life. In urban areas in particular, trees provide a wide range of varied benefits, and the full range of these services is still an area of active research. This is not an exhaustive discussion but will offer relevant example to give a general idea about why urban trees are important.

Urban trees make important contributions to urban air quality. They remove air pollutants such as sulphur dioxide, nitrogen oxides, ozone, carbon monoxide and particulates (Jim & Chen, 2009). It is well-established that vegetation helps to reduce air pollution but to what extent, remains site-specific and dependent on several variables. For instance, coniferous trees have a much larger filtering capacity than deciduous trees, due to two aspects (Stolt, 1982): filtering capacity increases with leaf area, which is higher for coniferous trees (this is also the reason why trees are better at filtering than most other types of vegetation), and needles are not shed during winter, when the air quality is typically worse. However, coniferous trees are sensitive to air pollution, and deciduous trees are better at absorbing gases (Stolt, 1982), which suggests that a mix of different types of trees can work best in most scenarios.

From the standpoint of filtering out PM_{2.5} alone (known to have adverse effects on human health), the impact of trees is substantial. Their exact impact is a function of many parameters (geography, local pollution, climate, etc.), but while the quantification of the effects is variable, the overall net positive impact is clear. Nowak, Hirabayashi, Bodine, & Hoehn (2013) modelled PM_{2.5} removal by trees in ten US cities and the associated health

effects. They found that reductions were typically around 1 person yr⁻¹ per city, but were as high as 7.6 people yr⁻¹ in New York City. In other words, one tree adds between 1 and 7.6 person-years every year. This translates into economic benefits ranging from \$1.1 million in Syracuse to \$60.1 million in New York City.

It is not just PM_{2.5}. PM₁₀ is also reduced substantially by trees. The potential of trees to mitigate urban PM₁₀ was analysed in the West Midlands and in Glasgow (McDonald et al., 2007). The resulting model predicted increasing total tree cover in the West Midlands from 3.7% to 16.5% would reduce average primary PM₁₀ concentrations by 10%. Tree planting schemes have been consistently shown (Tiwary et al., 2009) to be able to improve air quality, reducing the amount of air particulates and offering positive contributions to human health. It should be noted that some trees are better than others in this regard (Yang, Chang, & Yan, 2015).

California surveys assessed the environmental and economic value of the trees on the state's territory (E. G. McPherson, Doorn, & Goede, 2016). Compiling data from over 900,000 trees, the authors note that "state's street trees remove 567,748 t CO₂ (92,253 t) annually, equivalent to taking 120,000 cars off the road," providing environmental services estimated at \$1.0 billion. Trees were also found to be an excellent investment, with every \$1 spent managing the trees yielding a benefit of \$5.82 in environmental services. A similar study carried out in Lisbon, Portugal (Soares et al., 2011), found comparable results, both in terms of environmental and economic benefits.

Another study carried out in Strasbourg, France (Selmi et al., 2016) found a more modest improvement in terms of overall quality, but even so, the effect was significant. The study also suggests that the design of the city can strongly affect the importance of public trees.

Stormwater runoff, which can pose a number of problems to urban infrastructure, can also be alleviated by trees and so-called “green infrastructure” (Berland et al., 2017). Trees can help regulate the urban hydrological cycle, intercepting incoming precipitation, absorbing water from soil and improve the quality of urban soils. Studies have suggested that in the UK, tree planting policies are financially justified even when judging storm management issues alone (Stovin, Jorgensen, & Clayden, 2012). All vegetative cover (including trees) helps to intercept water, delaying surface runoff and maintaining a more stable environment, though this remains site specific. In the UK, trees have been found to reduce runoff from asphalt by as much as 62% (Armson, Stringer, & Ennos, 2013). Given the relatively uniform climate across the UK, it seems plausible that the figure is representative for many British urban areas.

Overall, a number of factors relating to the morphology, climate, soil, and overall geographical setting of the city can affect these results. A quantitative review of urban tree benefits and costs (Roy, Byrne, & Pickering, 2012) identified a wide range of demonstrated benefits (economic, visual, health, visual, aesthetic, carbon sequestration, air quality improvement, storm water attenuation, energy conservation). However, they also highlight that existing literature on urban trees is limited in terms of geographical distribution.

A different study (Gillner, Vogt, Tharang, Dettmann, & Roloff, 2015) found that trees (and, to a lesser extent, other vegetation) are also important for mitigating thermal load in urban areas. The urban heat island effect is well known for decades (Price, 1979). According to Price (1979), in many large cities, satellite sensed temperature can record temperatures 10-15 degrees Celsius higher than the surrounding rural areas. Gillner et al. (2015) notes that although different tree species differ significantly in their ability to limit both ground and air temperatures, all tree species can reduce the thermal load in the urban

microclimate, fighting the urban heat island effect and increasing the urban quality of life.

The impact of shade should also not be underestimated. Having access to shade on hot days grants not only comfort for humans, wildlife, and other vegetation, but can also save a lot of money by reducing electricity consumption for air conditioning – especially in warm climates (conversely, they can also increase heating costs in colder climates). In Sacramento, California, tree covers on the west and south side of houses reduced electricity consumption by 5.2%, whereas trees on the north and east side increased electricity by 1.5%, producing a net positive effect. The same results showed that a single London plane tree (*Platanus × acerifolia*) planted on the west side can reduce carbon emissions coming from summertime electricity usage by 31%, over 100 years (Donovan & Butry, 2009). Trees also reduce wind speeds, potentially improving comfort and reducing heating costs. Akbari (2002) finds that in the case of Los Angeles “urban tree planting can account for a 25% reduction in net cooling and heating energy usage in urban landscapes”, corresponding to an annual reduction in carbon emissions ranging from 9,000 t to 16,000 t per trees. In this sense, urban trees are much more valuable than rural trees.

While the non-urban areas tend to be larger and more effective carbon sinks, urban trees are also important, especially for the local microclimate (Nowak & Crane, 2002), helping reduce atmospheric carbon dioxide levels. They also aid local biodiversity by providing a home for numerous species, which in turn provide other environmental services themselves.

Trees also have a different type of economic value: they are valued by homeowners, and add a significant percentage to the value of a house (Pandit, Polyakov, Tapsuwan, & Moran, 2013), even when on the street and not on the property. Trees have been shown to improve the overall aspect and value of a property (Luttik, 2000).

It is not just homeowners that value trees – most people seem to do so too. Trees and urban forests play an important role in recreation, (Pandit et al., 2013; Brander & Koetse, 2011). Although urban valuation tools do not seem to incorporate the aspect of recreation into their calculations, urban woodland areas provide numerous opportunities for recreational experiences. Urban trees were also found to reduce stress, air pollution, and ultraviolet wavelengths, while also providing an area to exercise and take pleasant walks on (Cornelis, Robert, & Barfoed, 2019).

Lastly, while this relationship is still under some debate in the literature, trees also seem to have a positive effect on urban crime (Troy, Grove, & Neil-dunne, 2012), with an inverse connection between tree canopy cover and overall crime.

Overall, despite significant variation over different geographical areas, trees seem to provide quantifiable benefits urban areas. In addition to the pragmatic benefits of urban trees discussed above, life without trees is simply unimaginable. Despite these benefits though, trees also incur costs on municipalities.

It costs a significant amount of money to plant and maintain a tree in an urban area. This amount can vary greatly depending on worker salaries, available equipment, necessary pre-emptive work, etc. The cost of tree maintenance is relatively low, but applying fertilizers, pesticides, and sometimes water is sometimes necessary. Infrastructure damage can also be considered a cost.

Overall, though, previous research shows that the benefits of trees strongly outweigh the costs (at least in the vast majority of scenarios). The valuation of trees is still site-specific and it is still challenging to account for all the relevant aspects, but overall, planting trees in urban areas seems to more than pay for itself. In the case of Los Angeles, the benefit for planted trees was estimated at over \$60/tree/year, whereas in

Adelaide Australia, the benefit for a single tree was estimated at \$211/tree/year (Killicoat & Puzio, 2002), when considering shade, temperature regulation, air filtration, carbon emissions, scenic beauty, increased property values, and wildlife habitats.

While the quantitative valuation of trees remains an area of active research, urban trees have been shown to play a vital role in urban cities, and can be a key component in sustainable strategies. Collectively, their role cannot be overstated, improving environmental quality, quality of life, and urban development.

Study	Method	Yearly Benefit (US\$/tree)		
		Small	Medium	Large
McPherson et al. (1999)	Review of other studies	\$10.97	–	\$20.00
McPherson et al. (2002)	iTree	\$5.22	\$23.30	\$46.82
Bonifaci (2010)	iTree	\$38.79	–	\$166.14

Table 1. Generally, all trees produce benefits, but larger trees produce larger benefits (Mullaney et al.; 2015).

2.2.1 Valuation of trees in the UK

Since this work was carried out in the UK, and includes practical information, it makes sense to look at how the environmental services of trees are valued in the UK. Weighing these benefits against the costs of a geophysical surveys (and any potential intervention) could be of use to city planners.

In the UK, section 198 of the Town and Country Planning Act (1990) covers the local amenity value of values and encourages local authorities to protect trees. However, it does not provide a concrete tool for valuing trees. Instead, there are three valuation systems commonly used for this purpose (Sarajevs, 2011): CAVAT, i-Tree, and Helliwell. All of them offer different advantages and have different drawbacks, as there

are many complex and site-specific considerations.

However, none of these systems take into account geophysical data which can provide valuable information regarding potential conflicts with infrastructure, which in turn could be significant in the final valuation, which highlights the importance of the practical component of this work.

In addition to material benefits, reviews have also found that trees offer social, cultural, and spiritual contributions to human wellbeing, which suggests that the valuation could be significantly understated (Dwyer, Schroeder, & Gobster, 2013). Ultimately, it seems unlikely that this issue will be settled quantitatively, and may have a philosophical side to it as well. While the financial valuation is important (to policy-makers and city planners in particular), the overall value of a tree is difficult (potentially impossible) to transfer into currency. However, the key lesson is that while exceptions may exist, trees in general offer important, quantifiable services to local communities.

Anecdotally, the fact that local communities value trees was also highlighted regularly during surveys, with people from the local community regularly stopping to express concern about the health of the trees and whether the municipality was cutting them down. Some would make a passionate defence of the trees in their neighbourhood.

2.3 Conflicts with infrastructure

But looking at environmental services only tells a part of the story. Trees can also generate disservices in cities (conflicts with the existing infrastructure, cause or exacerbate health problems such as asthma through the dispersion of pollen, light attenuation, shade in cold areas) and can in some conditions, even be hazards (for instance in the case of old, heavy branches falling onto cars and people). Here, we will review some of the potential conflicts with infrastructure, caused by tree root growth, which can

be studied through geophysical methods.

McPherson and Peper (1996) estimated that municipalities in the United States spend more than \$135 million every year for tree root-related repairs – a figure which has presumably only increased in recent years, as infrastructure has become more complex and expensive itself. The main problem is the fact that trees are increasingly surrounded by impermeable surfaces (concrete, roads, foundations, etc.). This can put significant stress on the tree roots, which in their search for water, often proliferate in sites that provide more favourable conditions for growth, but where they cause infrastructure damage and pavement uplift (Mullaney, Lucke, & Trueman, 2015). This damage, which can be costly and difficult to alleviate, is almost invariably present in most urban areas – I have yet to walk in a city for a day and not see at least one instance of significant infrastructure damage caused by tree roots.

The extent of the damage can also vary substantially. Day (1991) identifies two main types of damage caused by tree roots: the first implies the growth of tree roots beneath roads, sidewalks, patios, walls, etc., causing uplift and differential movement. The second type involves roots growing beneath or in the close vicinity of foundations, particularly in clay-rich soils (but other expansive soils as well). The roots tend to absorb moisture, causing the soils to shrink, resulting in potential damage to the structure. However, it should also be noted that the opposite phenomenon can also happen in some cases: when trees are uprooted or their roots are left *in situ*, it can cause a swelling of the soil, also with potential damage to the nearby structure.

Another area of major interest is the interactions between tree roots and building foundations (Biddle, 2001). Tree roots can damage buildings directly (by penetrating or attempting to penetrate structural elements), through subsidence, or by drying and compacting soils.

Probably the most common unwanted interaction is between tree roots and road elements – sidewalks, roads, and curbs. Although this has become almost a routine problem in some areas, there is surprisingly little literature on the topic. Among existing studies, a thorough review (Randrup et al., 2001b) concludes that the potential for damage is high “when one or more of these factors are present: tree species that are large at maturity, fast growing trees, trees planted in restricted soil volumes, shallow top soil (hard-pan underneath top-soil), shallow foundations underneath the sidewalk (limited or no base materials), shallow irrigation, distances between the tree and sidewalk of less than 2-3 m, and trees greater than 15 to 20 years old” – all these are conditions commonly met in urban areas in the UK and Europe. The review also found that many cities are spending substantial sums to deal with the problem, and there is an important knowledge gap regarding these interactions.

However, in addition to the damage identified by Day (1991), another specific area of interest is the interaction with tree roots and sewer systems (pipes, joints, etc.). Interference between old systems and tree roots is not uncommon, with roots being reported to cause more than half of all sewer blockages (Randrup et al., 2001a). Especially in smaller pipes, root removal is quite common, and the replacement or repairing of the pipes is costly, time-consuming and intrusive, often disrupting nearby traffic or circulation. Randrup et al. (2001a) suggest that it’s important to carry out preventative maintenance of some parts of the sewer system. However, tree roots and water pipes are often a chicken-and-egg type of problem: tree roots are naturally drawn to any leaks, and leaks are often caused by tree roots. If damage happens, root cutting or tree removal can be desirable. However, if this is done prematurely, it can incur needless costs and prevent the trees from offering the benefits mentioned in the previous chapter. Randrup et al. (2001a) also call for more research on the distribution of the tree roots near sewers, and

geophysical methods can do much to narrow this knowledge gap.

This chicken-and-egg problem is also prevalent in many cases of pavement damage (Amato, Sydnor, Knee, & Hunt, 2002). Despite popular belief, trees are not always the main cause of damage to sidewalks. A city-wide study from Cincinnati (Sydnor et al., 2010) found no significant difference between the failure of sidewalk panels that were next to trees and panels that were not next to trees. The same study found that the correlation between sidewalk failure and trees is very low for the first 15-20 years of the trees. However, the damage caused by tree roots is evident in all environments. But the question is – does the tree root cause the crack, or does the crack “draw” the tree root, as a line of minimum resistance? There appears to be a strong relationship between the presence of a crack and whether or not a root is growing under the paved surface (Amato et al., 2002). This suggests that sidewalk that is partially damaged is particularly vulnerable to tree roots, but the literature does not seem to conclusively answer under what circumstances tree roots can cause the cracks themselves. There is also a matter of how the question is posed: if a sidewalk is used beyond its intended lifetime, but in that time, it is damaged by the tree root, is the tree root causing damage, or is the failure an expected consequence? Tree roots are also sometimes used as an excuse for improper workmanship, which might cause an increased perception of tree root damage.

Overall, while the causation may not always be easy to pinpoint, the correlation between the presence of cracks in sidewalks and tree roots is strong in most instances (Amato et al., 2002) and warrants closer monitoring – representing another research opportunity for geophysical study.

Generally speaking, the larger the tree, the bigger the environmental services provided. At the same time the bigger the tree, the bigger its roots, and the larger the chance of infrastructure damage caused by root growth. While the net impact of trees is almost always clearly positive, there is still a cost associated with tree root damage, which should be accounted for in tree valuation. The magnitude of this problem is, again, highly variable. An estimate for US cities (McPherson & Peper, 2012) finds that repair costs attributed to tree damage averaged \$4.28 per street tree and ranged from \$0.18 to \$13.65 per tree.

To make matters even more complex, it has also been shown that through shading, trees can also extend pavement life (B. E. G. McPherson & Muchnick, 2005). Again, the relationship between tree roots and paved surfaces is intricate and site-specific. The economic value assigned to street tree benefit from Mullaney et al. (2015) shows just how much different evaluations can vary in terms of costs and benefits.

Study	Evaluation method	Tree population size	Annual cost value (US\$/tree)	Total benefit for overall population (US\$)	Volume filter benefit
Stormwater					
McPherson et al. (1999)	Direct estimation	91,379	\$6.76	\$616,139	3.2 m ³ /tree
Killicoat et al. (2002)	Based on other studies	128,002	\$6.85	\$832,013	
Xiao and McPherson (2002)	Rainfall interception model	29,299	\$3.80	\$110,890	6.6 m ³ /tree
McPherson et al. (2005)	STRATUM	17,821	\$27.836	\$496,227	11.3 m ³ /tree

Bonifaci (2010)	iTree	91	\$6.47	\$588.75	
Soares et al. (2011)	iTree	41,288	\$47.80	\$1,973,613	4.5 m ³ /tree
McPherson et al. (2011)	iTree	444,889	\$2.78	\$1,236,791	5.6 m ³ /tree
		828,924	\$4.37	\$3,622,397	
Air pollution					
McPherson et al. (1999)	Direct estimation	91,379	\$15.82	\$1,442,036	7.2 t/yr
Killicoat et al. (2002)	Based on other studies	128,002	\$34.50	\$4,416,069	
McPherson et al. (2005)	STRATUM	13,184	\$0.28	\$3,715	
Bonifaci (2010)	iTree	91	\$6.07	\$552.37	
McPherson et al. (2011)	iTree	444,889	\$1.52	\$676,231	
		828,924	\$2.38	\$1,972,839	
Soares et al. (2011)	iTree	41,288	\$5.40	\$222,738	25.6 t/yr
CO2					
McPherson et al. (1999)	Direct estimation	91,379	\$4.93	\$449,445	
Killicoat et al. (2002)	Based on other studies	128,002	\$1.71	\$21,888,342	
McPherson et al. (2005)	STRATUM	17,821	\$1.53	\$27,268	
Soares et al. (2011)	iTree	41,288	\$0.33	\$13,701	
Energy					
McPherson et al. (1999)	Direct estimation	91,379	\$10.97	\$1,000,560	

Killicoat et al. (2002)	Based on other studies	128,002	\$64.00	\$8,192,128	
McPherson et al. (2005)	STRATUM	17,821	\$31.03	\$553,061	95 kWh/tree
Moore (2009)		100,000			30 kWh/tree
McPherson et al. (2011)	iTree	444,889	\$2.16	\$960,960	
		828,924	\$3.35	\$2,776,895	
Soares et al. (2011)	iTree	41,288	\$6.16	\$254,185	

Table 2. Different valuations of trees.

It would seem therefore that municipalities have an incentive of keeping older trees, rather than felling them and planting new ones if roots do start to do damage. In this case, tailored root interventions could be more pragmatic and end up reducing costs in the long run.

It is somewhat surprising to note that although root-infrastructure interactions are essentially ubiquitous, they appear surprisingly under-studied. Most studies focus on local conditions (at a city area) or are not carried out in a scientific environment, but rather for city planning affairs or by urban constructors or forestry / arboriculture organizations.

The emergence of pervious or permeable paved surfaces have been speculated to help tree roots, but there is not much evidence to support this idea – pervious concrete has not been found to significantly aid trees (Volder, Watson, & Viswanathan, 2009). However, with the rapid development of material technology (and the relatively slow rate of new studies regarding this issue), that may change not long into the future.

The existence of this damage is not restricted to a particular climate, tree type, or

city type. There is virtually no clear approach to reduce this type of damage. Many types of trees, even in their infancy, require at least 100 m² around them (Blunt, 2012), so that the rooting zone can absorb sufficient water. This corresponds to a radius of about 5.6 meters around them, which is not always the case. For mature trees, that area is double, or even beyond that. The necessary required rooting area can be reduced through irrigation, or if abundant precipitation is available. Another option is to plant trees that remain small in size. However, given that environmental services generally grow with size, that idea seems counterproductive. Another approach, which is currently carried out in some areas (Francis, Parresol, & Patino, 1996) is even more counterproductive: the planting of trees with a planned removal in 10-15 years, before the roots do any damage. Not only does this approach have the same shortfall as the previous one, but it also costs additional money to uproot and re-plant the trees, and does not guarantee that roots have not grown inside the infrastructure. If this is the case, then they will almost certainly be left in place, which makes it even more likely that the roots of future plantings will proliferate the damage. The environmental benefits of trees are also reduced considerably with this approach.

In fact, damage to infrastructure has often been cited as the most common cause of tree removal (Costello and Jones, 2003; Kirkpatrick, Davison, & Daniels, 2012). In these cases, the roots are often left in place, which, again, increases the risk of damage. A recent and notable case is in the city of Bucharest, on the Kiseleff Boulevard, where numerous trees of different ages and sizes have been cut down (according to Bucharest City Hall, this was done to reduce the risk of old branches falling down). The roots, which created visible cracks and uplifting, are still visible on the sidewalk. New trees were planted without consideration of the old ones. As the roots expand on any line of minimal resistance, it is probable that the roots of the new trees will exacerbate existing cracks, and

the damage. If this is the case, it will require a substantial and costly intervention in the not-too-distant future. Geophysical surveying could have identified the position of these roots, aiding planning.

The most comprehensive review (McPherson & Peper, 1996), spanning 15 American cities, found an average infrastructure cost of \$3.01/tree/year. Costs include pavement repair or replacement, pipe damage, tree removal and replacement, as well as legal expenses and payments due to injury claims related to tree-caused infrastructure damage (this is not considering the initial planting and management cost).

Overall, the costs associated with tree root damage remain relatively understudied compared to their advantages (Ping, Yok, Edwards, & Richards, 2018) and provide only a snapshot of costs for a single year, producing misleading lifetime results. The studies are also heavily biased towards North America, with researchers affiliated with the USDA Forest Service developing the study methodology and carrying out most local studies. More studies are required to thoroughly quantify the costs associated with different climates and environmental conditions, and there are major gaps in our quantification of street tree costs, as well as benefits. In addition, decisions regarding tree planting / uprooting are often times made based on resident attitudes rather than a cost-benefit analysis (Kirkpatrick et al., 2012).

Reducing or preventing tree root damage could increase the overall net value of trees, saving municipalities substantial costs and reducing downtime for repairs. Tree root damage happens gradually, and by the time repairs or other interventions are carried out, the bulk of the damage has already been done. Preventive geophysical measurements to survey or monitor infrastructure could enable early interventions, mapping the root distribution and evaluating existing/potential damage. For instance, a 10-year study,

comparing two different methods for reducing tree root damage (root barriers and structural soils) by *Platanus × acerifolia* roots, showed that damage is often greatest when a high surface area of roots grows in contact with the pavement surface (Smiley, 2008), something which can be highlighted through geophysical methods.

2.4 Urban soils

Urban soils have a number of significant differences compared to natural soils. These differences can change the physical parameters of soils and can affect how plant roots grow. Both these aspects can significantly influence the detectable geophysical contrast and affect geophysical surveys.

Urban soils almost always comprise of geological material that has been disturbed by human activities. As a result, parameters such as compaction and porosity are often directly affected. However, the literature shows (Edmondson, Davies, McCormack, Gaston, & Leake, 2011) that these effects are not uniform even in the same city, let alone on wider geographical scales. This adds an element of uncertainty to geophysical surveys, and any surveyor should be aware of the great variation of soil parameters in urban areas.

Since cities act as urban heat islands, higher atmospheric temperatures affect the soils as well, directly reducing humidity. The humidity of urban soils is also reduced by the fact that some of the urban rainwater falls on concrete or other infrastructure, which prevents it from accumulating in the soils as it does in natural environments. Surface runoff is typically absorbed by the sewage system.

Urban soils can also have a different chemical make-up than their rural counterparts. Increase carbon dioxide from car and construction emissions, salt or sand from the winter roads, and potential spills can all change the chemical parameters of the soil, which in turn can change the physical parameters. Urban soils also tend to

concentrate more heavy metals, particularly in topsoils (Kelly, Thornton, & Simpson, 1996). Conducting a broad survey over many areas in Britain, Kelly, Thornton & Simpson (1996) found that concentrations of heavy metals in soils in and around London is generally higher than in any other area in the UK.

Lastly, soils are very much an active ecosystem, their physical parameters being significantly influenced by the biological component they host, both at the macro- and microscopic level. Therefore, all the above-mentioned influences not only affect the soils directly, but can also affect the soil ecosystem, which in turn also affects the soil in a feedback loop. For instance, although heavy metal levels are unlikely to reach phytotoxic levels, they can still be toxic to other creatures which are more sensitive (E. Jansen et al., 1994).

Therefore, urban soils can carry a number of significant differences compared to rural soils, differences that are not always straightforward. Consequently, geophysical surveys need to be mindful of these differences and peculiarities when considering geophysical contrasts between roots and soils in urban areas.

2.5 Challenges to urban trees

In addition to different soils and higher temperatures, trees also face a multitude of other environmental stressors in urban areas, stressors that affect the wellbeing of urban trees and differentiate them from trees in forests or other wild areas. The main stressor for urban trees is that they are often surrounded by impassable, impervious surfaces. Since trees rely on roots for oxygenation, support, and water and nutrient absorption, limiting the natural growth distorts their natural development, pushing roots in unnatural directions or stunting them. Roots tend to grow on the line of minimum resistance, avoiding growing into the infrastructure whenever an alternative is possible. This often

leads to convolute root systems which cover a lower area than normal, reducing the intake of necessary fluids.

This problem is further exacerbated by another major difference for urban trees: the water absorption of soils. Paved surfaces are usually impermeable, which means that a substantial part of water from atmospheric precipitations does not enter the soil, where it can be absorbed by trees. This leaves trees starved for water, an effect that is also accentuated by increased transpiration due to the urban heat effect. Together, these two effects are also the main cause for tree root damage to infrastructure: the tree is trying to expand its roots so that it can absorb more water. This also helps to explain why the vast majority of roots are in the first 10-20 cm of the soil as that is where most of the rainwater accumulates.

Water stored by trees has also been shown to be a potential source of stress (Clark & Kjelgren, 1989). Plant use is a dynamic process, varying from species to species, depending on soil, time of year, different days, temperature, etc. These differences can be critical for ensuring urban tree survival through careful planning and irrigation. There are two main drivers of this stress: increased temperatures lead to increased transpiration, and paved surfaces prevent water absorption from urban soils. The response of trees can vary widely, but does not occur in a random manner – there is a general trend of increased stress in trees with stunted roots Clark & Kjelgren (1989) found. In particular, trees isolated in small openings in concrete tend to suffer the most.

Some challenges to urban trees are indirect and more subtle. For instance, the sum of these urban effects favours some species at the expense of others. Some tree pests have been found to be more common in urban areas than in rural areas; in particular, the scale insect *Parthenolecanium quercifex* was found to be much more common in urban

areas, largely as an effect of increased temperatures (Meineke, Dunn, Sexton, & Frank, 2013). In addition, not all trees respond similarly to stress. Urban trees seem to grow at somewhat slower rates than their rural counterparts, presumably in large part due to physical limitations on their roots, but they reach comparable ultimate sizes (Quigley, 2004). Quigley (2004) also notes that “the idea that all street trees are therefore “stressed” into reduced life spans is not supported. Rather, early to mid-successional tree species, while having smaller trunk diameters than rural conspecifics of the same age, appear to maintain a similar rate of diameter increase after a longer period of establishment.

The reaction of urban trees to climate change not been investigated, although tree ring analysis (Pretzsch et al., 2017) has found that rising temperatures accelerate tree growth and potentially shorten lifespan. However, whatever the effects may be, considering the urban heat effect, it is likely that urban trees will be affected disproportionately.

Another aspect that’s often overlooked is salt. In temperate and cold urban areas, salt is often routinely spread on streets and walkways. In addition to environmental stresses and challenges, there is another class of threats brought on by humans themselves. Aside from potential vandalism, wounds from accidents can also cause isolated problems for trees. However, a much more common and concrete threat to trees’ wellbeing is additional constructions. Foster & Blaine (1977) write that “statistically, the city engineer is the most frequent cause of tree decline”, and identify an average lifespan of approximately 10 years for sidewalk trees. Moll (1989) reports an average lifespan of 7 years for downtown trees and 32 years for suburban trees. A more recent meta-analysis (Roman & Scatena, 2011) found a mean life expectancy for street trees between 19-28 years. Even in the “best sites”, urban trees were found to have a lifespan of 60 years, compared to 150 years for rural trees

(Skiera and Moll, 1992).

Overall, there are substantial reasons to operate on the assumption that trees (and subsequently, tree root systems) in urban areas differ significantly from those in rural areas. This is a significant consideration in geophysical surveys.

2.6 Man-made surfaces

The main consideration for geophysical surveys in urban areas, however, is the presence of man-made infrastructure, and the surfaces themselves. The presence of steel, electricity wires, and other metallic structures render certain geophysical methods (such as magnetic surveys) much more difficult or even impossible. Surveys employing other geophysical methods are also made more difficult by urban constraints.

This poses an important limitation on the geophysical methods which can be used practically, especially in regards to an objective as small as a tree root. In addition to magnetic and electromagnetic field measurements, near-surface seismic measurements are also extremely difficult, and micro-gravity has also proven to be quite difficult. Given their inherent limitations (particularly in terms of obtainable resolution), these two methods are largely unsuited for an objective such as tree roots.

Resistivity measurements are also hindered by paved surfaces. Conventional electrode surveys are possible only by damaging the paved surface, which in the case of studying tree roots, is severely counter-productive. However, resistivity measurements can be carried out on soil close to paved surfaces, which offers valuable indirect information and can be used to extrapolate the direction of roots under the paved surfaces as well (in some cases). In addition, emerging alternatives for resistivity surveys are also being developed, most notably the capacitive-coupled system, which can also measure paved surfaces (Kuras et al., 2006), although unfortunately, these types of surveys have not

become commonplace in geophysical measurements yet.



Figure 5. The Geometrics Ohmmapper, probably the most common capacitively-coupled resistivity meter in use at the moment, does not offer sufficient resolution to study tree roots effectively

From a geophysical standpoint, urban surfaces might also offer some advantages, in some scenarios. For example, GPR benefits from a better coupling, which is enabled by relatively smooth surfaces like asphalt. The relative homogeneity and predictability of urban surfaces could also be an advantage in certain situations.

In some surveys, paved surfaces also substitute soils as the medium in which tree roots develop. This creates a completely different geophysical setting, where the root-soil geophysical contrast is substituted by the root-paved surface contrast. This can serve as an unlikely advantage, as roots tend to blend in with their surrounding soil, which is not possible in regards to paved surfaces. In other words, detecting tree roots in paved surfaces can, in some cases, be easier than detecting them in their natural environment.

2.7 Geophysical techniques

By this point, it has become apparent that carrying geophysical surveys in urban areas is significantly different, and often more challenging, than surveys in natural areas.

Practical concerns also exist: surveys may require stopping traffic or may be a nuisance to pedestrians or workers. These aspects were also considered in the choice of methods.

Ultimately, the choice of relevant and applicable geophysical methods was limited by the small size of the objective (tree roots) and the small expected geophysical contrast. Several methods were considered, but were not deemed satisfying, either because they could not reveal the desired geophysical information, or they could not be reliably applied in an urban setting.

The two methods which were decided upon are resistivity and GPR. Each of these methods can provide important information individually, and in conjunction, can complement each other. The following considerations make these two geophysical methods suited for the task:

- They can, under the right conditions, provide sufficient resolution to identify tree roots;
- They measure physical parameters which can reveal a contrast between the roots and the subsurface environment;
- They can operate in urban environments, which is where most of the tree-infrastructure interaction takes place, unlike magnetic methods for example;
- They are mobile and robust enough to be adapted to various environments;
- They are fast enough for research and practical purposes;
- They are both well documented methods, though for other applications.

2.7.1 Environmental Geophysics

The work presented here falls under the guise of environmental geophysics. In the broadest sense, geophysics is the application of physical studies to the Earth or other Earth-like bodies such as the Moon or Mars. From here, the field can be very broadly split into global geophysics and applied geophysics.

Historically, applied geophysical surveys have focused on deep targets, most notably resource bodies such as fossil fuels or mineral resources. More recently, applied geophysics has increasingly focused on the near-surface areas.

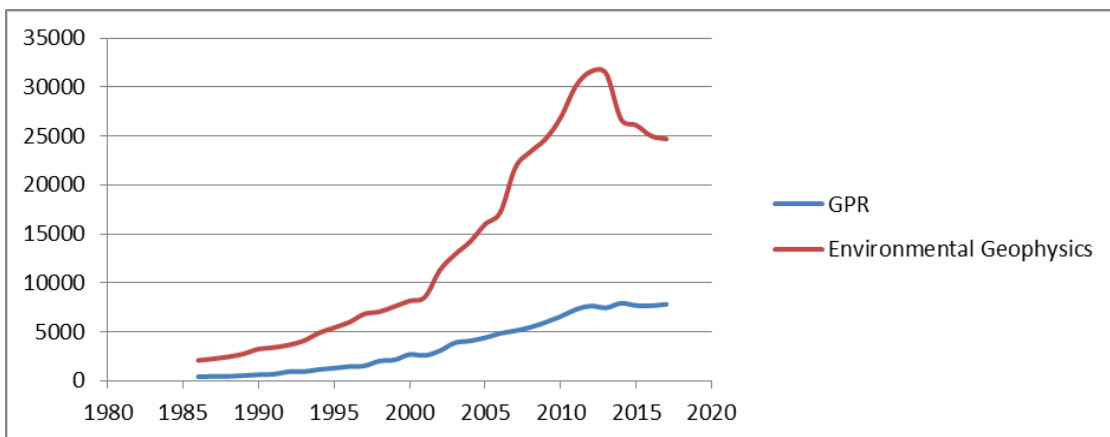


Figure 6. Peak near-surface geophysics? The number of publisher papers, books, and citations featuring the terms ‘Ground Penetrating Radar’ and ‘Environmental Geophysics’

The number of publications in the field has increased steadily in the past couple of decades, seemingly stabilizing in recent years and even decreasing, in the case of ‘Environmental Geophysics’. However, this is unlikely to be owed to a decrease in interest, but rather to an increased difficulty in publishing simple case studies and a stronger emphasis on innovations and transformative studies. This data is publicly available from Google Scholar.

Fields such as archaeology, engineering, agriculture, forensics, hydrology,

geotechnics, and many more, are increasingly turning to near-surface geophysics.

Multidisciplinary research is also becoming increasingly common, in part due to the over-specialization of researchers, in part thanks to improvements in communication technology, and also because the complexity of the addressed problems has increased (Wu, Wang, & Evans, 2018). Usually, applied near-surface geophysics is a tool which aims to help solve problems from other fields.

The most commonly used methods, according to Everett's landmark *Near Surface Geophysics* (2013) are, perhaps not coincidentally, resistivity and GPR – the same methods which have been selected for this study. This is presumably owed in part to the unsuitability of the other methods. However, it is possible that things have shifted somewhat in very recent years.

Some surveys are perhaps more under the guise of engineering, rather than environmental geophysics. Reynolds (2011) defines the two as follows:

- *Engineering geophysics is “the application of geophysical methods to the investigation of sub-surface materials and structures that are likely to have (significant) engineering implications.”*
- *Environmental geophysics is “the application of geophysical methods to the investigation of near-surface bio-physico-chemical phenomena that are likely to have (significant) implications for the management of the local environment.”*

Another important distinction is that engineering geophysics typically focuses on the material parameters and any potential damage to them, whereas environmental geophysics is also concerned with the processes involved and the natural environment. While some of the surveys presented here are carried out in a setting that fits engineering geophysics,

other surveys are carried out on urban soils, evading the engineering context. The two share numerous similarities, including the geophysical methods commonly employed in surveys.

2.7.2 Resistivity

Electrical resistivity methods have been developed since the dawn of the 20th century, but have seen important developments since the 1970s. The geophysical process was well understood in the earlier stages of the method application, but it was the computation power that allowed resistivity to truly flourish. In the past few decades, resistivity has enjoyed yet another boon thanks to, but also innovations in terms of data acquisition and processing. Today, an array of both commercial and open-source modules exist for processing and interpretation the data, further accelerating the development of the method.

2.7.2.1 Theoretical background

Electrical resistivity is a fundamental physical property of materials. Discussing resistivity in a geophysical context, however, warrants some clarifications.

Physically, resistivity (ρ) is a measure of the resisting power of a specific material to the flow of an electric current. Considering a homogeneous, electrically-uniform cube of a determined side length (L), if a current (I) is passed through it, the material of the cube resists the conduction of electricity through it. This will result in a potential drop (V) between opposite faces, and a resistance (R) will emerge, proportional to the length (L) and inversely proportional to a cross sectional area (A):

$$R = \frac{\rho * L}{A}$$

According to Ohm's Law, the resistance (R) is also defined as directly proportional to the potential drop (V) and inversely proportional to the current (I):

$$R = V / I$$

By combining the two, we can write the resistivity as:

$$\rho = \frac{V * A}{I * L}$$

The unit of measure for resistivity is then the ohm-meter (Ωm).

In most geophysical cases, the application of Ohm's Law suffices, but in cases where high current densities (J) occur, the linearity of the law can break down. If this is the case, resistivity can be written alternatively in terms of the electric field strength (E) and current density:

$$\rho = \frac{E}{J}$$

If the cube we considered has two different materials, each with their own resistivity (ρ_1 and ρ_2), both proportions and the geometrical distribution of the two materials become important considerations. Consequently, the cube (which was isotropic before), is now anisotropic. This introduces a new level of complexity, which is specific of the complexity that sometimes occurs in resistivity surveys.

In applied geophysics, there is no perfect cube or guaranteed isotropy. The resistivity method is based on the electrical response of the earth to the flow of electrical current. In general practice, current is injected through a pair of electrodes and the potential difference is measured between another pair of electrodes (several variations exist, this is just the most common practice).

Most geoelectrical methods are based on the flow of current. Considering a single electrode implanted into the earth (a homogeneous material of resistivity ρ), current flows radially, with the potential decreasing in the direction of current flow. Therefore, the current density (J) and the current (I) are divided over the area over which the current is distributed, which is generally considered to be a hemisphere. The voltage drop between any two points can be described by the potential gradient:

$$\frac{-\delta V}{\delta x}$$

In almost all surveys, electrodes can be approximated as point sources. With this approximation, it is possible to calculate the voltage at a distance (r), by considering a hemisphere with the same radius (r). The potential difference (δV) is:

$$\frac{\delta V}{\delta r} = -\rho * J = -\rho \frac{I}{2\pi r^2}$$

Thus, at the distance r , the voltage v_r becomes

$$V_r = \int \delta V = - \int \rho * \frac{I \delta r}{2\pi r^2} = \frac{\rho * I}{2\pi r}$$

However, if a new current sink is added, then a new current distribution occurs, and therefore a different expression is required to describe the voltage.

In geophysical practice, most surveys conduct measurements using four electrodes: two current electrodes C1, C2 (sometimes referred to as A and B), and two potential electrodes P1, P2 (sometimes referred to as M and N). Considering a homogeneous environment, the current is flowing between C1 and C2, taking semi-spherical shapes.

The position (geometry) of the electrodes is essential for any geoelectrical measurement. The object of the measurement is therefore a potential difference (ΔV)

between P1 and P2. In the direct current method, this potential difference is given by:

$$\Delta V = V_M - V_N = \frac{\rho * I}{2\pi} \left(\frac{1}{C1P1} - \frac{1}{C2P1} - \frac{1}{C1P2} + \frac{1}{C2P2} \right),$$

Where C1P1, C2P1, C1P2, C2P2 are the distances between electrodes. From, this the resistivity becomes:

$$\rho = \frac{\Delta V}{I} * \frac{2\pi}{\frac{1}{C1P1} - \frac{1}{C2P1} - \frac{1}{C1P2} + \frac{1}{C2P2}}$$

This equation splits resistivity into a resistance factor and a geometrical factor (K) -- again, it is important to note that in real scenarios, the subsurface does not comply to a perfectly homogeneous environment. In this case, we are not dealing with resistivity proper, which is a fundamental material property, but rather a measure called ‘apparent resistivity’. Apparent resistivity is not a true resistivity, but rather an average of the resistivity across a half-space.

Historically, the first resistivity surveys were simple in design and yielded 1D results. While this offers limited information, it was very useful in determining the depths and thickness of different geological strata.

The next step, 2D results, can either be presented in the XZ (vertical) or XY (horizontal) plane. A representation of apparent resistivity plotted in either plane is called a pseudosection (Loke, 2000). The most common representation of data is the profile. This requires first moving the electrodes along the same line, and then increasing the distance between these electrodes, to obtain data points at different depths. The resulting pseudosection is generally plotted in the shape of an inverted trapeze.

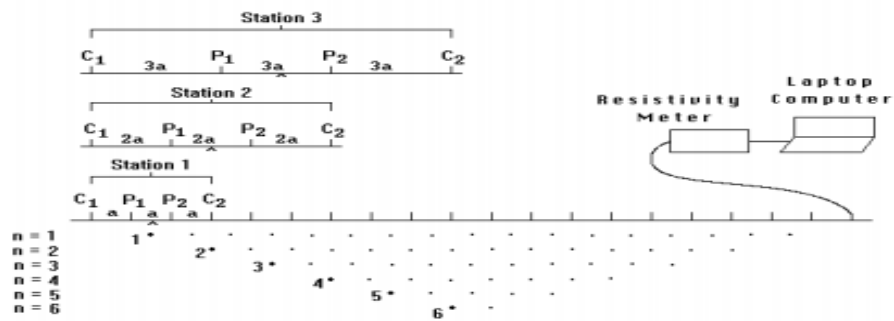


Figure 1. Sequence of measurements to build up a pseudosection using a computer controlled multi-electrode survey setup.

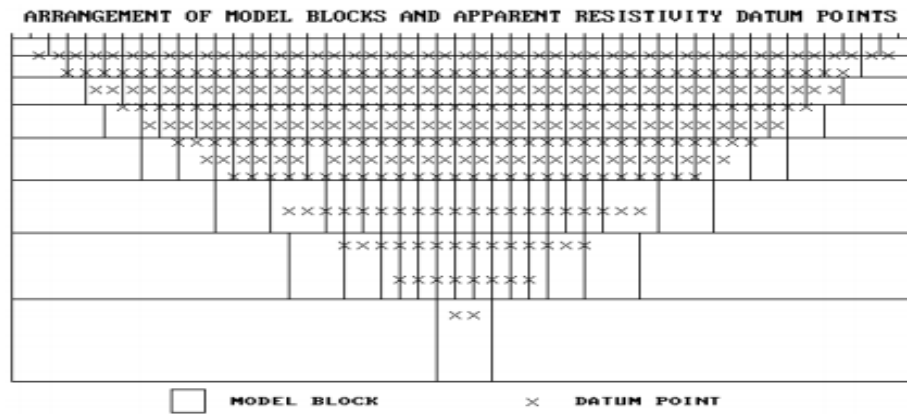


Figure 7. Example of a pseudosection design, for the Wenner array, with the RES2DINV software from Loke (2010).

The other type of 2D representation is essentially a map at a fixed depth. If the above example lies in the XZ plane, this can be seen as a visualization of the XY plane. This is essentially useful when the approximate depth of the objective is known. A simplified variant of this type of survey has become very common in archaeology, in the form of the twin probe array.

In both cases, the apparent resistivity data is inverted to obtain true resistivity data. Inversion is a computationally intensive process and was greatly facilitated and accelerated by modern computers.

Computation has also facilitated the processing and interpretation of 3D data, which allows a more comprehensive understanding of the subsurface and the target objective. Sometimes, the time-dependent monitoring of resistivity data is referred to as 4D

resistivity (Karaoulis, Kim, & Tsourlos, 2011).

Common types of arrays

Since the geometry of the electrodes is so important, several geometrical arrays have emerged for surface measurements, each with their own particularities, advantages, and disadvantages. There are 92 arrays commonly used in geoelectrical surveys (Szalai and Szarka, 2008), though a few of them are used far more than others. The three arrays which are probably the most common are Wenner, Schlumberger, and Dipole-Dipole, depicted below.

Different array may be better suited for different objectives, but on many occasions, this yields marginal benefits. The choice is often made based on the operator experience and practical constraints.

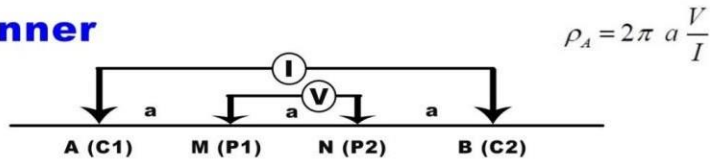
The Wenner array, named by its creator Frank Wenner, is the simplest one, but often the most effective. Electrodes are arranged in a straight line, while the distance between all electrodes is kept equal (a). The outer current electrodes C1 and C2 are on the outside and the potential electrodes P1 and P2 are on the inside. There are several variants of the Wenner array (alpha, beta, gamma), though the classic one is the most common.

The Schlumberger array, also named by its creator Conrad Schlumberger, features a somewhat similar geometry, with the defining exception that the potential electrodes P1 and P2 are much closer to the centre of the array. The C1-P1 and C2-P2 distance are always equal.

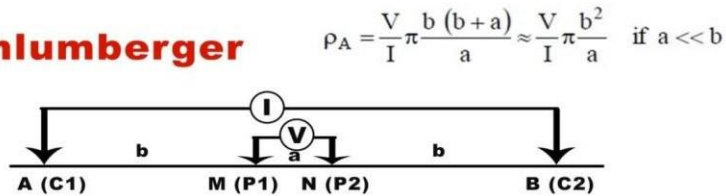
The Dipole-Dipole array employs a different geometry, with the distance between current and potential electrodes being kept equal. However, the distance between the two pairs of electrodes needs to be much larger than the distance between the electrodes in

each pair.

Wenner



Schlumberger



Dipole-Dipole

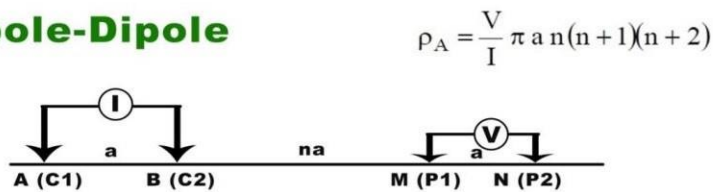


Figure 8. Depiction of the three most common types of resistivity arrays.

Due to different geometries, the arrays differ in their lateral and vertical sensitivity. All resistivity measurements are sensitive to the averages of near-surface electrical contrasts. Different array geometries lead to different geometrical sensitivities, which in turns makes them more suitable for different types of applications.

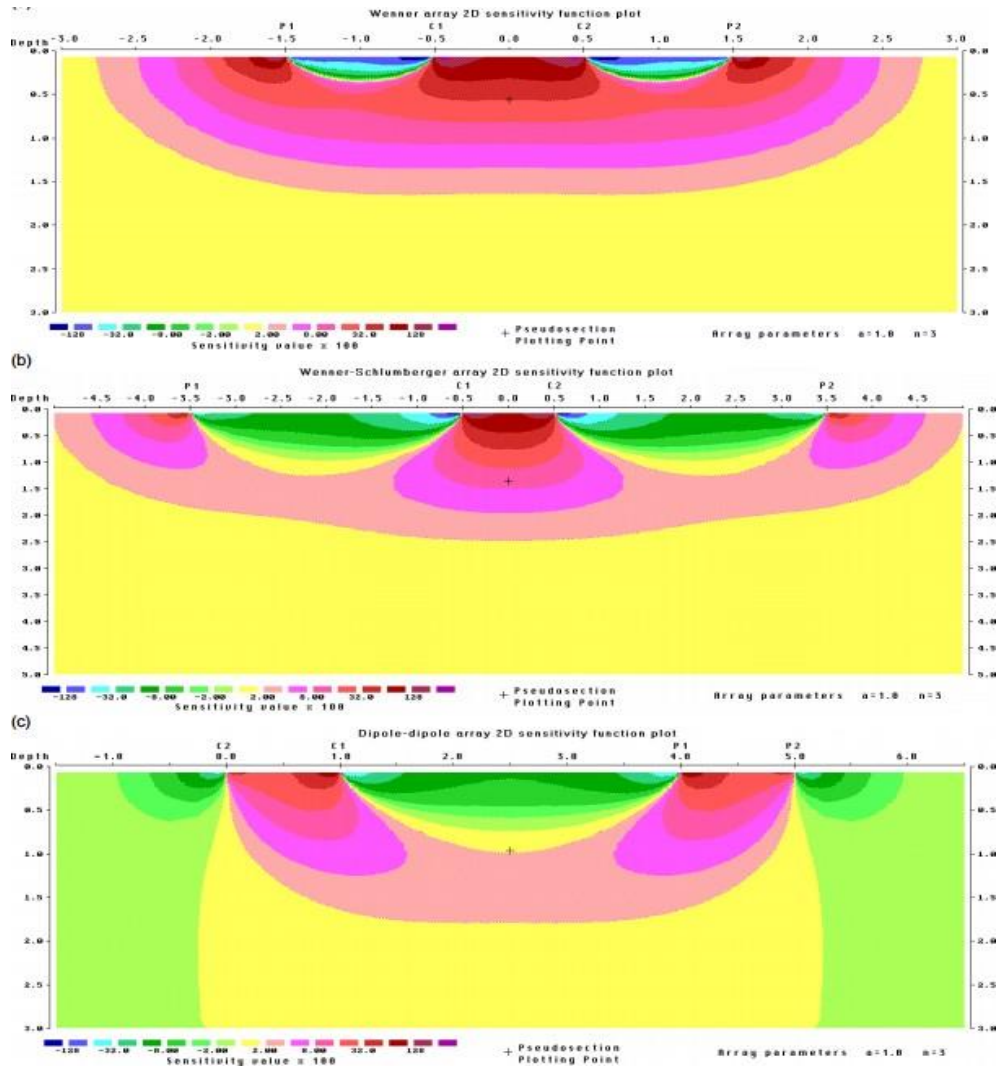


Figure 9. The sensitivity patterns of the three most common arrays: Wenner (a), Schlumberger (b), and Dipole-Dipole (c). From Loke (2000).

Reynolds (2011) distinguishes between different types of advantages and disadvantages of these three arrays. A few relevant criteria are presented below:

Criteria	Wenner	Schlumberger	Dipole-Dipole
Vertical resolution	√ √ √	√ √	√
Depth penetration	√	√ √	√ √ √
Sensitivity to orientation	Yes	Yes	Moderately
Sensitivity to lateral inhomogeneities	√ √ √	√ √ √	√ √

Table 3. Advantages and disadvantages for common array geometries.

In the case of studying tree roots, the depth of penetration is not of particular interest since most roots are in the very shallow parts of the subsurface. The sensitivity to lateral and vertical inhomogeneities, however, is of utmost importance.

Although using resistivity to study tree roots and resolve them individually has not been thoroughly addressed in the literature, there are some conclusions which can be drawn regarding the potential efficiency of different arrays for this particular objective. For instance, the Dipole-Dipole array has conventionally been used to study dikes and cavities (Loke, 2000), which resemble the structure and expected contrast of tree roots. In addition, a Wenner-Schlumberger combination can also be laid out, incorporating the data points from both arrays. It is not straightforward to understand which of these arrays (if any) is best suited of the study of tree roots, so all of them were considered as possibilities.

Other types of arrays

Other types of arrays can be routinely used (such as pole-pole, pole-dipole). A special mention goes to the twin-probe array, which has become very common in archaeological studies. The twin-probe array sacrifices some accuracy for much greater practicality, leaving one pair of electrodes (C1 and P1) at an “infinite distance” (at least 15-20 times the distance between the electrodes in the pair), and having a mobile pair of electrodes.

Another possibility worth discussing is that of doing every possible measurement. For an array with N_{el} electrodes, the total number of data points (M_{points}), considering one current source, one current sink, and two measurement electrodes is:

$$M_{points} = N_{el} (N_{el} - 1)(N_{el} - 2)(N_{el} - 3)/8$$

For an array with 32 electrodes, the value for M_{points} is 107880. Considering a measurement time in the range of 1 second, it is impractical. For even a relatively short array of 16 electrodes (as was often the case here), the number of points is 5460, bringing the required time for a single profile to more than an hour and a half (even disregarding other logistical aspects, which would further extend data acquisition time). Even trimming datapoints with the least reliability, there is still a very large number of total datapoints. This is, while feasible in an academic context, probably not realistic in a practical context, where multiple profiles are required to generate a 3D view of the subsurface.

Optimized measurements (OPM)

There is no apparent intrinsic physical law that mandates that the arrays described above (or even regular arrays in general) provide the most useful data per data point. The possibility of developing non-standard arrays that provide optimized information was analysed by Stummer, Maurer, & Green (2004). They simulated a resistivity configuration of $N_{el} = 30$, resulting in 82,215 different positions. After removing certain combinations that offer intrinsic lower-value data (such as crossed dipole, or dipole with very large offset dipole-dipole configurations), they were left with 51,373. They then generated forward, synthetic data and compared different types of arrays, finding that the best performing ~600 arrays were all non-standard versions of the dipole-dipole array. Although datasets consisting of 1000-6000 data points offered more information than

those with only a few hundred, small and optimized datasets of 265–282 datapoints offer much more useful information than standard arrays of a similar size. Notably, in the array they recommend, the first 147 electrode configurations are the initial dipole-dipole data set. The rest represent irregular dipole-style configurations.

This is not the only approach to develop optimized arrays. Wilkinson et al. (2006) developed two strategies for obtaining the maximum spatial resolution in ERT, both of which use a linearized estimate of the model resolution matrix to assess the effects of including a given electrode configuration in the measurement set. Overall, one approach was more comprehensive but took a longer time, whereas the other one was faster. However, it should be noted that all distributions operated on the assumption of a homogeneous half-space subsurface, and their performance might vary significantly from site to site.

Results were confirmed by Loke, Wilkinson, & Chambers, (2010) for different types of geological situations and objectives which, while not directly relevant to tree root measurements, is encouraging. For all forward datasets, optimized arrays performed better than Schlumberger and Wenner in terms of data misfit. Overall, regardless of the type of array, the data misfit generally increases with the median of the geometric k factor (Martorana, Capizzi, Alessandro, & Luzio, 2017), though there are still major difference depending on the depth and geometrical characteristics of the objective. Symmetrical arrays are also recommended, to reduce potential directional biases (Wilkinson et al., 2006).

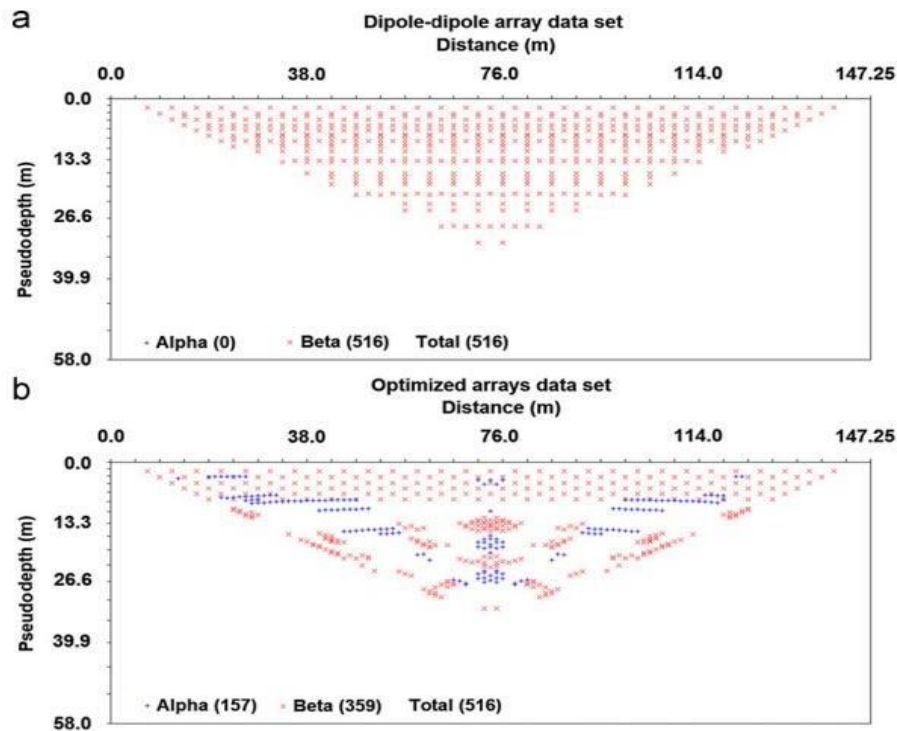


Figure 10. Distribution of points for a regulate Dipole-Dipole and optimized array. Both are symmetrical. From (Wilkinson et al., 2006).

However, OPM arrays impose extra constraints on the survey design strategy, potentially increasing polarization effects and data noise, as well as making it difficult to draw information from parallel profiles (Wilkinson et al., 2012). This can be addressed by weighing different datapoints differently, though this process does not seem to be thoroughly finessed. In conclusion, while optimized arrays show great promise, their usage in practical scenarios remains less straightforward.

Additionally, while OPM arrays can offer better results for the entire survey depth, the main focus on root detection surveys is the shallower part. The sheer number of datapoints in the shallowest parts of the surveys is significantly lower in this case than in other arrays (most notably Dipole-Dipole), potentially placing this approach at a disadvantage for the purpose at hand.

2.7.2.2 Range of obtainable data

Since geophysics relies on a detectable contrast, let us first consider the common values for the relevant parameters: resistivity and relative permittivity (commonly, dielectric constant). The values of common geological formations and soils, as well as those of man-made constructions have been much better documented than the values of tree roots.

In both soils and man-made materials, both resistivity and the dielectric constant are influenced by water content. There can be a great variation between different types of rock and soils, or even between similar materials with different water content or different porosities or stages of weathering.

The resistivity values of different soils and rocks have been studied and discussed at great length in relevant literature, and it is important to note the huge range of variability for some materials.

Material	Nominal resistivity (Ωm)
Quartz	300-10 ⁶
Granite	300-1.3 x 10 ⁶
Granite (weathered)	30-500
Slates	600-4x10 ⁷
Marble	100-2.5x10 ⁸
Conglomerates	2x10 ³ -10 ⁴
Sandstones	1-7.4x10 ⁸
Limestones	50-10 ⁷
Clays	1-100
London clay	4-20
Lias clay	10-15
Boulder clay	15-35
Very dry clays	50-150
Alluvium and sand	10-800
Soil (40% clay)	8
Soil (20% clay)	33
Topsoil	250-1700
Gravel (saturated)	100
Gravel (dry)	1400
Quaternary (recent) sands	50-100

Lateritic soil	120-750
Dry sandy soil	80-1050
Sand clay / Clayey sand	30-125
Dry sandy soil	80-1050
Sand and gravel	30-225

Table 4. Nominal resistivity of common rocks and soils, selected from Reynolds (2011).

Among others, Davis & Annan (1989), Annan (2009), and Daniels (1996) have discussed the dielectric constant values for common natural materials. Most if not all values discussed in the literature fall within this general range. It should be also kept in mind that the dielectric constant varies with frequency, which can cause significant variations.

Material	Dielectric constant	
	<i>Davis & Annan</i>	Daniels
Air	1	1
Distilled water	80	
Fresh water	80	81
Sea water	80	
Dry sand	3-5	4-6
Saturated sand	20-30	10-30
Limestone	4-8	
Soil, sandy dry		4-6
Soil, sandy wet		15-30
Soil, loamy dry		4-6
Soil, loamy wet		10-20
Soil, clayey dry		4-6
Soil, clayey wet		10-15
Shales	5-15	
Silts	5-30	
Clays	5-40	
Granite	4-6	
Dry salt	5-6	4-6
Ice	3-4	

Table 5. Typical dielectric constant of common materials measured at 100 MHz, according to Davis & Annan (1989) and Daniels (1996).

Regarding man-made structures, there is a wide variety of different materials to be considered. It is noteworthy that structures such as cubic pavement or rebar mesh can

be severely detrimental to a GPR survey, potentially rendering it impossible to acquire any relevant data. Different elements of stone masonry, bricks, tarmac, concrete, can have very different dielectric properties. However, root detection in such surfaces is aided by the fact that roots are unlikely to be tucked neatly within the man-made material -- they will likely generate cracks and potentially be surrounded by air or water, which facilitates detections, as the forward models in a following chapter suggest.

2.7.2.3 Modern methodology

Most resistivity surveys involve some form of ERT with 16 or more electrodes. Most commercial units feature predetermined geometries of arrays and combinations of arrays. Whether they come with a dedicated software or not, acquired data is typically inverted, resulting in pseudosections. Anomalous datapoints can be statistically eliminated based on how well they fit the inverse model, though this procedure should be done with care so as not to eliminate any accurate yet anomalous values (which is a particular concern in the near-surface measurements of minute objects with high, localized contrasts). Few commercial measurement kits can accommodate custom arrays.

Electrodes are usually planted in a line (though exceptionally, other geometries are also used). The distance between electrodes governs both the resolution and the depth of penetration, so the survey must be carefully designed with this in mind. Since the number of data points invariably decreases with depth, better data quality can be expected in the first part of the pseudosection (the portion nearest to the surface). Advancing a profile is typically done through the “roll-along” method, covering a continuous section down to a desirable depth. 3D data has become common in modern surveys, obtained through parallel profiles. The distance between profiles should also be carefully designed with this in mind.

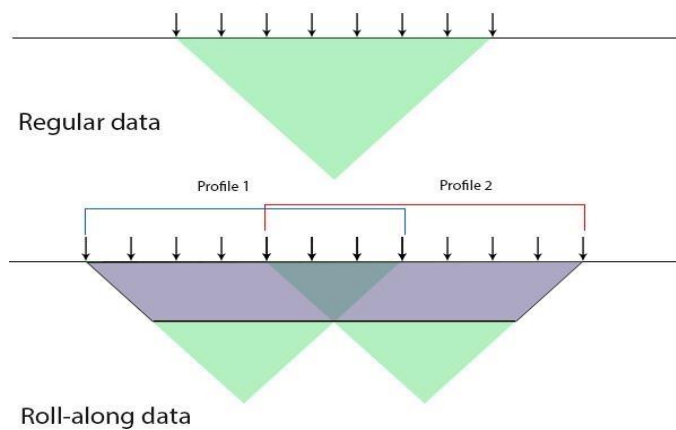


Figure 11. The roll-along approach produces a trapezoid section with resistivity. Deepest data is disregarded (which is acceptable in this case) and there is some slight overlap in the two profiles.

2.7.2.4 Advancing frontiers

Several ideas were considered to improve existing capabilities. A custom electrode switchbox allows for full flexibility, enabling a comparison between different regular geometries as well as the implementation of unorthodox arrays (Wilkinson et al., 2012), something which is not possible with most commercial devices. This is a simple but significant advancement to commercial devices.

The most important advancements in the field of resistivity surveys have been at the data processing and software level, although advancements exist at all levels. For instance, the usual practice is to apply a direct current, but there is also equipment that uses commutated direct current (i.e. a square wave) or even alternating current. Direct current allows greater depth of penetration and eliminates the complex issues presented by ground inductance and capacitance, but can produce polarization and telluric effects. Alternative current is sometimes used to eliminate these polarization effects, but the period is generally low (20 Hz), to ensure that the resistivity is essentially the same as the direct current resistivity. In modern equipment, multiple channels with several different frequencies can be used to minimize this effect, or if a DC equipment is used, the

polarization is switched multiple times for a single measurement. Modern resistivity meters are also equipped with digital signal processing to eliminate potential noise.

An area of particular interest, especially in urban surveys, is the capacitive method (Wilkinson et al., 2012). This method has the very important advantage of being usable on surfaces where electrodes cannot be implanted – in urban paved surfaces, this has proven to be an ‘Achilles Heel’ for resistivity measurements.

In theory, capacitive methods would be perfectly suited for the detection of tree roots. However, as of this writing, the technology is not robust enough for this type of small-scale objective. The quality of the data can be improved through careful survey design and planning.

If the objective is something relatively small (as is a tree root), the distance between electrodes must also be planned accordingly. Furthermore, electrodes are often regarded as a “point source”, and for the vast majority of surveys, that is a satisfactory approximation. However, when the distance between electrodes becomes comparable in size to the electrodes themselves, it is not entirely clear whether the electrodes can be considered point sources.

Modern inversion software also gives the possibility to improve overall survey quality compared to previous decades. The softwares used here are RES2DINV (with stand-alone plotter), Resipy, and BERT, which was operated with the open-source plotter Paraview.

RES2DINV (along with its 3D ‘sister’, RES3DINV) is one of the most popular geophysical inversion software, working with apparent resistivity and using smoothness-constrained Gauss-Newton least-squares inversion technique (Sasaki, 1992) to produce a 2D model of the subsurface, supporting all common arrays, as well as non-conventional arrays.

BERT is an ERT inversion software package described by Gunther et al. (2006) and Rucker et al. (2006). The current version is based on GIMLi (Generalized Inversion and Modelling Library), a C++/Python library used mostly for geophysical methods. It is based on the finite element modelling techniques discussed by Rucker and Gunther (2011), generating an inversion mesh. The software operates as a bash script in Windows or Linux. It works with all array geometries.

The ResiPy GUI, which integrates the meshing and inversion packages R2, cR2, R3t and cR3t (Boyd et al., 2019) was also used. These packages offer 2D and 3D forward/inverse solutions for current flow in an unstructured (tetrahedral) or structured (triangular prism) mesh, as well as in a rectangular mesh for 2D profiles. The inverse solution uses a regularised objective function combined with weighted least squares (an ‘Occams’ type solution) as defined in Binley and Kemna (2005). This is an open-software package.

These inversion packages are customizable in terms of array geometry, inversion parameters, and data output, which is an important advantage in the context of detecting tree roots.

2.7.2.5 Limiting factors

Regardless of advances in data acquisition and processing, and even with there are still inherent limitations to the method.

The distance between electrodes has a major influence on the resolution, but there comes a point after which placing electrodes closer than 5-10 cm is unrealistic and impractical. At those distances, positioning errors (both horizontal and vertical) become very significant and difficult to account for. Given the scale of the objective and the distance between electrodes, several problems which are rarely considered in surveys

become significant: the size of the electrodes and factors which affect current injection (the depth of the electrode insertion and the geometry of the electrode themselves). In surveys, electrodes are considered point sources, which is a convenient and satisfactory approximation even in near-surface applications such as archaeology or engineering geophysics, but might not be sufficient here. Extra precautions (such as taping a part of the electrode) had to be taken to ensure that these factors are not affecting the measurements in any significant way.

The detection of tree roots can also be made more difficult by environmental conditions, and topsoil conditions in particular. It is expected that not all roots are resolvable through electrical methods, especially due to resolution challenges.

2.7.2.6 Impact of weather and external factors

In many geophysical surveys, the impact of weather and climate is not significant. However, in the near-surface surveys, seasonal effects can have important effects (Fry, 2014). In the study of tree roots, which lie at the very shallow part of the soil, that impact can be reasonably expected to be significant at times.

The impact of precipitations on all resistivity surveys is well-known, but in this particular scenario, it is not clear exactly how a higher water intake affects the measurements. Although the roots themselves have a higher resistivity than the surrounding soil, studies looking at the root area as a whole (Amato et al., 2008) find a lower resistivity areas associated with the root areas. As roots grow, they create channels which facilitate water flow and storage. In this case, it's not clear how increased or reduced precipitation affects the detection of tree roots.

Since the survey focuses on the very part of the topsoil, lack of precipitations, leading to very dry soil, can cause cracks which cause improper continuity within the

topsoil.

2.7.2.7 Literature review: Resistivity imaging of tree roots

Tree roots have appeared in geophysical surveys for years, but most often, they have been regarded as noise, most notably in archaeology (Matos, Kipnis, & Lu, 2010). The studies that do exist tend to focus on the overall tree area and not individual roots.

For instance, al Hagrey (2007) presented a case study in an olive orchard in southern Italy (a particularly dry area). Remarkably, al Hagrey found that directly below the stem, there are “central negative ρ anomalies, increasing with depth and concentrating below the tree.” This is explained by al Hagrey thusly: “Certainly, the root-zone and its water content and redistribution are responsible for these concentric low resistivities”. In a previous paper, al Hagrey (2004) reports similar findings, and addressed the possibility of distinguishing woody roots from absorptive roots, though this remains highly challenging.

The effect of plant roots on soil resistivity is not always straightforward. Even as woody plant material has large values of resistivity, only in some cases do they occupy a large enough soil volume that their effect may be viewed as a quantitative contribution of resistive material to the soil (Rossi et al., 2011). In addition to this direct contribution and other practices that may affect resistivity patterns (ie soil management practices), processes such as root water uptake and evapo-transpiration can also play a role in resistivity patterns, by influencing the soil moisture content around the roots (Cassiani et al., 2015). While these factors have been shown to change during the day, they seem to be often associated with high-resistance geophysical anomalies. In the case study of Cassiani et al (2015) the high-resistivity area around an orange tree test site has been interpreted as “a dry region where root water uptake manages to keep soil moisture

content to minimal values”. In this particular case of an orange tree, it was noted that roots keep the soil around them so dry that even irrigation only increases electrical conductivity by no more than 20%. Amato et al (2008) present another case study, using resistivity to analyse tree root distribution and measure root biomass. While the work did not focus on individual tree roots, it found a “resistive response from coarse roots”. The same work notes that resistive responses to roots are caused by “large structures (>2 mm diameter) only”. In general, though, large root densities are associated with a stronger resistive response.

However, this effect may not always be straightforward. Zenone et al (2008) note that “the density of roots may be related to the accumulation of capillary water and to the presence of low-resistivity haloes around the tree”. This effect has also been highlighted by Rodríguez-Robles et al (2017) which, in a natural setting, showed a “relationship between the position of roots, low soil resistivity (greater water availability), and greater bedrock fracturing”. While this geological setting is less likely to be encountered in urban areas, it seems important to be aware of the potentially counterintuitive effects roots can have on subsurface resistivity. Additionally, in single measurements, Zenone et al (2008) were able to discriminate between poplar areas in a loamy soil, but were not able to discriminate pine roots in resistive sandy soil, showcasing the challenges associated with this method. In the same work, it was observed that the position of the roots (which were excavated following the survey) does not coincide neatly with geophysically anomalous areas. Leucci (2010) also asserts that thick roots have a higher resistivity than the surrounding soil, but soft, fine roots can have a lower resistivity than the surrounding soil. The same work notes that the root network of the trees seems to be characterized by “a high resistivity zone within an area of low resistivity”, and documents changes in the resistivity distribution following an irrigation, hinting at similar effects based on

precipitation patterns.

Ultimately, while it is expected that coarse roots will produce resistive results, the mechanisms and relationships between tree roots and the surrounding soil are complex and insufficiently understood, with numerous factors potentially playing a role (including but not limited to type of soil, tree species, precipitation regime, and root diameter). The resistivity surveying of roots appears site-specific and greatly variable.

The distance between electrodes is certainly a critical aspect of these studies. Both al Hagrey and Amato et al. employ a distance of 0.25 m, which while adequate for a general overview, is likely still insufficient to resolve all but the coarsest roots; other studies used an even greater electrode separation.

A study which did look at single roots (Zanetti et al., 2011) employed a variation on the conventional geoelectrical surveys, using the spectral induced polarisation (SIP) method. They report that conductivity varies with diameter and species, which is not surprising. However, their study was carried out in a controlled lab environment, which may not be relevant to a real-life case study. There is also a possibility of roots changing physical parameters after collection. Roots are in a constant and active exchange of fluids and nutrients with the surrounding environment, and after they are removed from this setting, their parameters start to change. This is why lab studies on tree roots are so difficult, and *in situ* measurements so important (and challenging).

Another study that looked at individual roots (Zenone et al., 2008) noted the potential of using both the GPR and ERT methods in conjunction, but upon excavation, it was found that the geophysical anomalies were not an ideal predictor of root position. The same work calls for a standard field procedure in performing such geophysical work.

2.7.2.8 Tree as an electrode

Another unorthodox possibility which has emerged is the use of the tree itself as a current electrode. The physical feasibility and safety of the method has been established by (Cermák et al., 2006). However, the range of useful information which can be derived through this method is still a matter of debate.

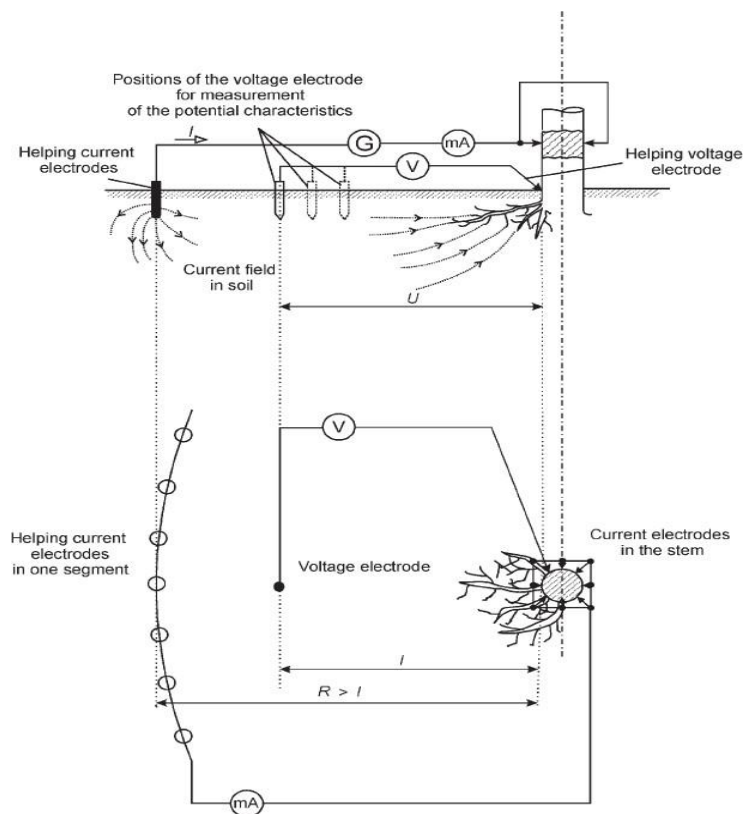


Figure 12. Depiction of the experimental setup from Cermák et al. (2006)

Cermák et al. (2006) used it to determine the root absorbing surface, not to resolve individual tree roots. The main difficulty of the approach is the fact that it's not possible to fully control the influx of and geometry of current flowing into the soil. This can be partially alleviated by inserting a potential electrode at the very bottom of the tree and eliminating the influence of the trunk. However, all conductive roots can pass current into the soil, while their position and physical parameters are not known.

Notably, some subsequent work (Urban et al., 2011) was unable to experimentally

replicate the results from Cermák et al. (2006), casting doubt on how exactly this method could be applied.

Still, using the tree as an electrode can be a noteworthy approach assessing the total tree root absorbing surface, which might potentially serve as a useful proxy to assess whether the absorptive area of the roots extends into paved surfaces, though this assumption remains unverified and still a work in progress. A much simpler usage of this method is can be used in assessing whether the tree roots have completely penetrated a paved area (see chapter 4.7). For instance, given a green area split in two by a thick paved area, current can be inserted through the tree and if it is measured on the other side, it can be inferred that the roots have broken through the surface. There are a few very important drawbacks to this approach; it can only work in situations where the soil unit is completely separated in two by the paved surface – often times, this surface only covers the soil, and there is still a soil continuity beneath it. Secondly, it only works if the roots have completely broken through the surface – if there is only partial damage, the current will still not reach other side. Lastly, there is also a chance of non-root damage penetrating from one side to another, creating a conductive corridor. However, given all these important shortcomings, this method might still be useful as a quick verification in some niche scenarios and was deemed to warrant further investigation.

2.7.3 GPR

Ground penetrating radar is a relatively new option in the geophysicist's toolkit. However, it has proven invaluable, particularly useful in settings where other geophysical methods find it difficult to operate: urban environments.

2.7.3.1 History of GPR

GPR is a tool that seems well equipped for tree root location although presumably, most people would find the idea of using radar to look for roots rather bizarre. However,

using radio waves to sound the subsurface was considered for decades, even before the first results were obtained (El Said, 1956). A pivotal point for radar in geophysics was in 1961 when Waite and Schmidt showed that aircraft radar altimetry was returning substantial errors on icy surfaces. This kickstarted the use of radar waves to probe the subsurface, setting in motion gradual improvements and mushrooming applications.

Especially since the 1990s, GPR has become increasingly popular, thanks to theoretical advancements as well as progress in equipment and computers. In a rough classification, GPR applications can be split into two main categories: geological (for which the depth of penetration is crucial) and environmental/engineering, for which higher frequencies are used (400 MHz and above), which offer much higher resolution at the expense of penetration depth.

The range of applications for GPR is impressive and continues to grow every year (the detection of tree roots, or at a broader scale, the application of GPR to plant studies, is also an emerging application).

There are, of course, limitations to GPR. Perhaps the most pervasive and infamous limitation is the limited performance GPR exhibits in strongly dispersive environments. In practice, conductive soils with high water content (and especially clays) are often too dispersive to ensure reliable GPR data. This also makes it an excellent complement to resistivity, which thrives in these conditions.

Overall, although it has its own shortcomings, as any other method, GPR has established itself as a valuable tool and should always be at least considered for near surface studies.

2.7.3.2 Theoretical Background

The foundations of GPR usage are grounded in Maxwell's equations, which mathematically describe the physical behaviour of electromagnetic fields:

$$\begin{aligned}\nabla \times \vec{E} &= -\frac{\partial \vec{B}}{\partial t} \\ \nabla \times \vec{H} &= \vec{J} + \frac{\partial \vec{D}}{\partial t} \\ \nabla \cdot \vec{D} &= q \\ \nabla \cdot \vec{B} &= 0\end{aligned}$$

where E is the electric field strength vector (V/m); q is the electric charge density (C/m^3); B is the magnetic flux density vector (T); J is the electric current density vector (A/m^2); D is the electric displacement vector (C/m^2); t is time (s); and H is the magnetic field intensity (A/m).

The other side which governs the propagation of radar waves in the subsurface is represented by the constitutive relationships which approximate how different atoms and molecules in a certain material respond as a whole to the application of an electromagnetic field.

$$\begin{aligned}\vec{J} &= \sigma \vec{E} \\ \vec{D} &= \epsilon \vec{E} \\ \vec{B} &= \mu \vec{H}\end{aligned}$$

where conductivity σ characterizes free charge movement in the presence of a current and dielectric permittivity ϵ characterizes the displacement of charge constrained in a material in the presence of the same electric field. Magnetic permeability μ describes how the magnetic moment of the molecules in the material reacts to the electric field.

For both theoretical and practical considerations, it is important to understand how

these EM waves propagate through the soil: in a cone, commonly called the ‘cone of transmission’ (Conyers, 2004). The dimensions of this cone are a function of the transmission frequency and subsurface conditions. Higher frequencies generally tend to have narrower cones, whereas lower frequencies and unfavourable soil conditions lead to broader cones. This is not of upmost importance for something like tree root detection as the objective lies very close to the surface, but it is still an important factor which need to be considered and accounted for.

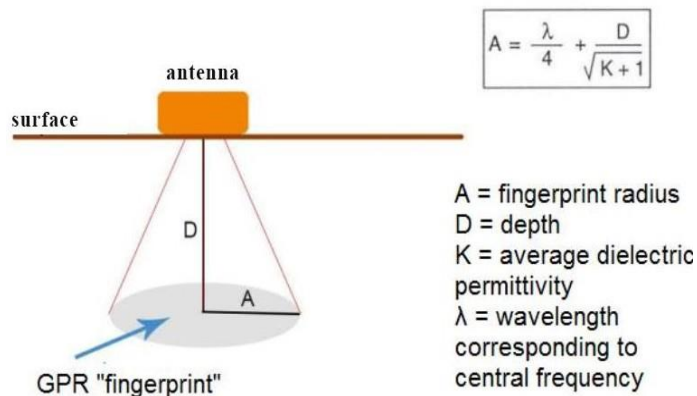


Figure 13. The cone of transmission, from Mihai (2014).

GPR waves are subjected to the phenomena of reflection and refraction, like any other EM wave. Any time it encounters a discontinuity, a part of the wave is reflected back towards the surface. This discontinuity could be any object or structure (a stratigraphic boundary, a buried object, a void, etc.), and the strength of the reflection is a function of the physical differences between the two objects or structures which make up the discontinuity. This essentially defines the geophysical contrast – the stronger the contrast, the stronger the reflection, and the easier the geophysical detection of the discontinuity. A subsurface object which does not manifest a geophysical contrast to its surrounding environment may not be readily detected. This is particularly relevant

because, according to Mihai et al. (2019), the permittivity of roots can sometimes coincide with the permittivity of the surrounding soil, making detection more difficult or even impossible.

The signal is also weakened as the wave moves beneath the surface (again, this is dependent on the frequency and soil conditions – higher frequency yields better resolution but lower depth of penetration).

The GPR wave follows the well-known laws of reflection and refraction (Snell's law). Considering a smooth planar surface, the angle of incidence will be equal to the angle of reflection:

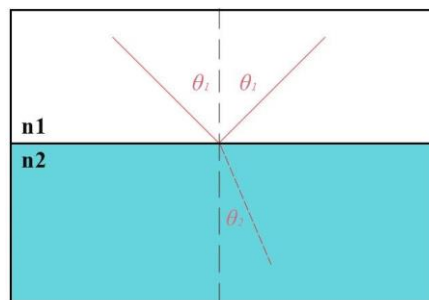


Figure 14. Visualization of Snell's equation.

The part of the wave that is not reflected back is refracted, changing its speed and bending in a manner described by Snell's law of refraction:

$$n_1 \sin\theta_1 = n_2 \sin\theta_2$$

where n is the refractive index of the respective medium and θ is the angle measured from the normal to the boundary.

Another fundamental physical process relevant for GPR is diffraction. Generally speaking, diffraction happens when an EM wave encounters an obstacle or a narrow slit. In GPR, this phenomenon is important because it is responsible for producing point-source hyperbolas. Considering the cone of transmission and an antenna moving over a flat surface, energy will be reflected not only from directly below the antenna, but also on

oblique trajectories, where the reflection will be recorded at greater depths. As a result, a point discontinuity will not produce a visible point on the radargram, but rather a hyperbola. It is important to note that the location of the point coincides with the apex of the hyperbola, but given a larger, spherical object, the hyperbola does not necessarily correspond to the shape and size of the object (Conyers, 2004).

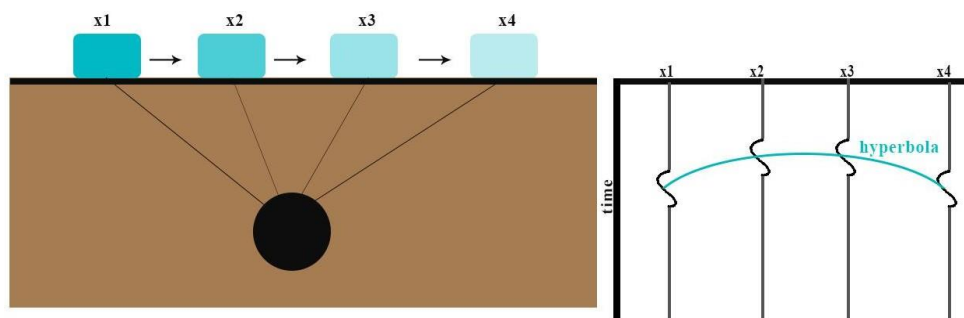


Figure 15. Depiction of the so-called 'hyperbola' effect, caused by antenna movement over an objective.

The classic hyperbola in GPR is a well-described and useful feature caused by the movement of the antenna over an objective and the electromagnetic waves encountering it at different times. In the case of a point-based objective, the apex of the hyperbola coincides with the position of the point. However, the size of the hyperbola is not indicative of the object size and should not be used as an approximation. The hyperbola can be used to infer some aspects of the reflective object but can also be a problem, especially when attempting to integrate multiple profiles into 3D data. Hyperbolae can be reduced to their apex through the process of migration.

Scattering (and its opposite phenomenon, focusing) also affects GPR waves. Sometimes, waves get reflected outside the range of the antenna and are not collected. This becomes particularly important when dealing with convex or near-vertical discontinuities, as well as some topographic surfaces. Meanwhile, focusing occurs when

waves are reflected from surfaces sloping towards the antenna, resulting in high-amplitude and multiple waves being received by the antenna when this would not be the case. Both phenomena can mask or distort subsurface features.

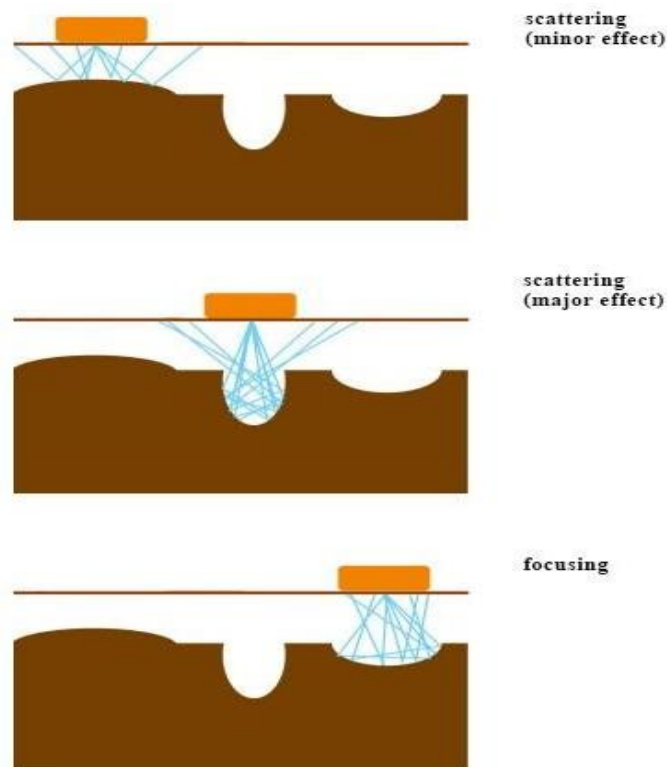


Figure 16. Simplistic depiction of GPR scattering and focusing, from Mihai (2014).

Of course, other EM phenomena (i.e. dispersion, dissipation, ringing) also affect the GPR waves, although they are generally of secondary importance to the ones presented above.

A GPR system typically consists of what is called an “antenna” (comprising of one or more transmitting and receiving antennas) and a console which is used to interact with the user. The console can be either stand-alone, or in some equipment, could employ a typical laptop, tablet, or even smartphone.

The resolution of the objective should be considering when selecting the antenna. The higher the central frequency, the higher the resolution. In theory (considering a homogeneous, isotropic subsurface), vertical resolution can be considered one-quarter of

the wavelength λ (Reynolds, 2011).

$$\lambda = \frac{V}{f},$$

where V is the radiowave velocity and f is the frequency. A few common examples adapted from Reynolds (2011) give an indication of what kind of resolutions can be expected:

Antenna Frequency	120 MHz	500 MHz	900 MHz
Soil			
Wavelength (cm)	62.5	15	8
Resolution (cm)	15.6	3.75	2
Bedrock			
Wavelength (cm)	92	22	12
Resolution (cm)	23	5.5	3

Table 6. Expected resolutions for common GPR antenna frequencies (approximate).

The propagation of GPR waves and the overall performance of the geophysical method is governed by the dielectric parameters of the soil. This dielectric behaviour is typically described in terms of complex permittivity (ϵ^*) and complex conductivity (σ^*). The former, and particularly the real part of permittivity is of principal importance. In practice, the real permittivity (ϵ_r) of a material is expressed as a function of its relative permittivity to that of air. This is routinely simply called permittivity, although it is technically a relative permittivity (in practice, it is also commonly called the dielectric constant).

Real permittivity is a function of frequency, decreasing as the frequency increases.

In most realistic scenarios, the permittivity curve follows this general shape:

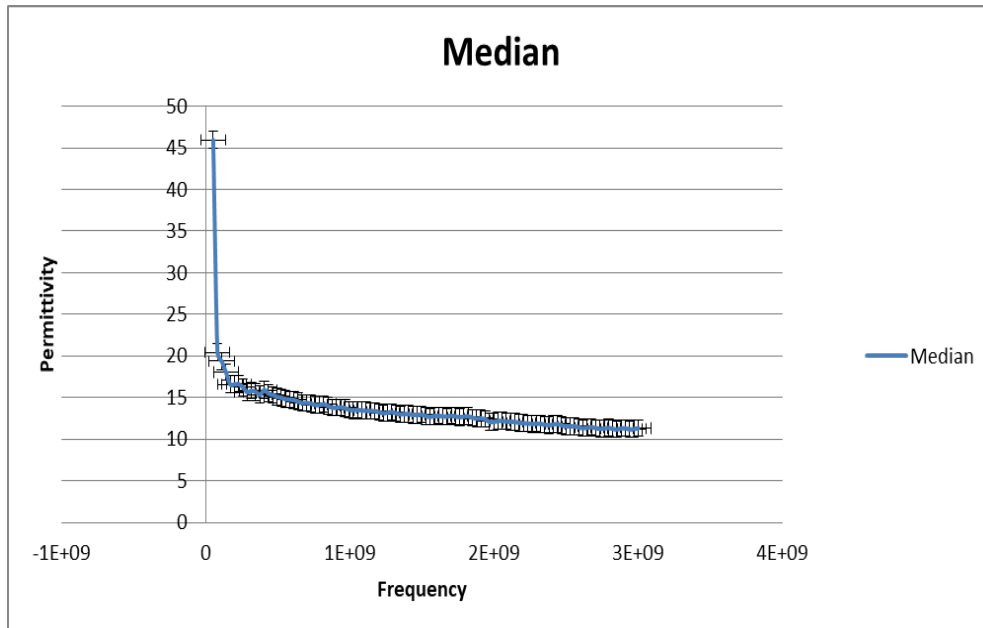


Figure 17. Typical curve of permittivity plotted against frequency. Blue line is median value obtained after 40 measurements, brackets show minimum and maximum values (no processing or eliminating of anomalous values).

Much like the different subsurface mediums have different resistivities, they also have different dielectric constants, although the range is substantially lower than in this case, ranging from 1 (air) to 80 (water). Consequently, the speed of GPR waves from air to water also ranges from 0.06 m/ns to 0.2998 m/ns. In practice, the value for almost all materials ranges between 3 and 30, which corresponds to speeds up to 0.175 m/ns.

In natural environments, the dielectric constant is often related to the porosity and water saturation.

Material	ϵ_r	V (mm/ns)
Air	1	300
Water	81	33
Pure ice	3.2	167
Permafrots	2-8	106-212
Gravel	5	134

Sand and gravel (unsaturated)	3.5-6.5	118-160
Sand and gravel (saturated)	15.5-17.5	72-76
Sand (dry)	3-6	122-173
Sand (wet)	10-32	53-95
Silt (unsaturated)	2.5-5	134-190
Clay (dry)	2-5	134-212
Clay (wet)	8-40	47-106
Marsh	12	86
Agricultural land	15	77
Pastoral land	13	83
Soil (fine-grained)	41-49	43-47
'Average' soil	16	75
Granite	5-8	106-120
Limestone (dry)	4-8	100-113
Limestone (wet)	6-15	77-122
Dolomite	6.8-8	106-115
Basalt	8	106
Shale (wet)	6-9	100-122
Sandstone (dry)	4-7	113-150
Sandstone (wet)	6	122
Concrete	4-30	55-150
Asphalt	3-5	134-173
PVC, epoxy, polyesters	3	173
Quartz	4.3	145

Table 7. Permittivity and propagation speed of electromagnetic waves for commonly encountered materials. Adapted from Conyers (2004).

It is important to note that in surveys carried out on natural surfaces, water content is an extremely important parameter directing the permittivity. Conyers (2004) identifies water content as the “single most significant variable” in this context.

2.7.3.3 Modern Methodology

Modern GPR surveys involve one or several antennas in a joint system. Antennas are defined by a central frequency, which typically varies between 10 MHz and can go up to 4 GHz or even above. The lower frequencies are used for deeper studies, whereas the highest frequencies are used for engineering purposes such as detecting cracks or fissures in man-made materials.

Although the antenna is defined by its central frequency, the transmitted energy is not restricted to that frequency alone. Generally speaking, antennas have a ‘two octave’ bandwidth – they transmit energy from half of the central energy to two times the central energy. However, the antenna is shielded so that its energy is sent downwards. Coupling the antenna properly to the surface is also important to ensure good data quality. As the antenna is pulled over the ground, any time the ground coupling is imperfect (due to a bump, sudden changes in micro-topography, or any surface irregularity), this will affect penetration depth, data quality, and antenna tilt, all of which can further affect the data quality.

The scope of GPR surveys has also expanded as the available technology improved. Pseudo-3D has generally become the norm when it comes to resolving subsurface environments. This means that surveys should be carefully planned in advance, to select an antenna frequency that optimizes relevant feature detection, but also consider other survey parameters such as transect spacing and orientation.

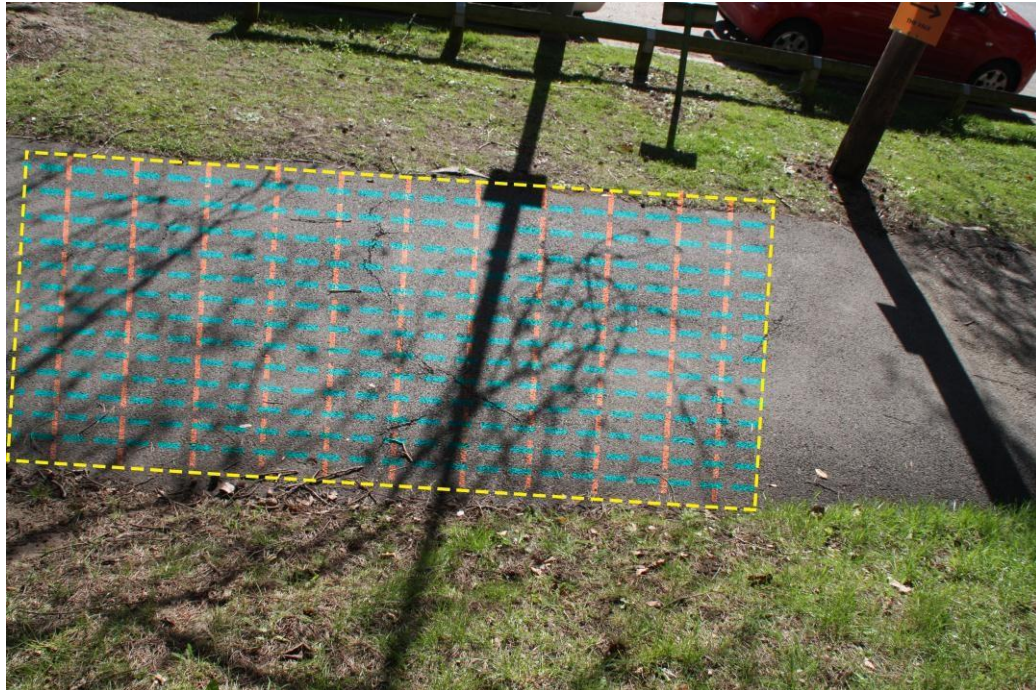


Figure 18. Depiction of GPR grid with the overall grid area (yellow), and two profile directions (in blue and orange), to study sidewalk damage potentially caused by a tree root, UoB campus, around Gisbert Kapp building. Direction and distance between profiles are approximate and not to scale.

Transect spacing are a crucial parameter for the quality of a GPR survey. For an elongated objective, it is ideal to develop profiles perpendicular to the preferential elongation direction. However, the direction or shape of the objective might not be known, in which case the transect spacing should be selected with care. The first consideration is to have the transect separation small enough so that an objective is not missed in between two profiles. For tree roots, this is nigh impossible if profiles are carried out in one direction since the diameter of tree roots is in the centimetre range. This would suggest that perpendicular profiles are generally better-suited for tree root studies. It has been suggested several times that carrying out perpendicular profiles is most often the best way to carry out surveys in general. Neubauer et al. (2002) conducted surveys in the x and y directions with transect spacing 0.5 m and 1.0 m, in the study of buried walls. They found that the walls were best resolved in perpendicular directions, but the resolution for surveysonly conducted in the x

direction with a spacing of 0.5 meters was higher than surveys carried in both the x and y direction at a spacing of 1 meter. The question of whether a fixed amount of profiles offers the best resolution in one direction or in perpendicular directions remains far from solved, however. Pomfret (2006) carried another transect experiment, finding that perpendicular profiles offer the best resolution. Studies on clandestine graves by Schultz and Martin (2011) also found that x and y surveys are the most efficient method. It seems plausible that the ideal configuration is site specific, depending on the geometry of the objective. However, given the peculiarities of tree roots, the only case in which one-direction profiles are preferable in which the direction of the tree roots is known and profiles can intersect the roots perpendicularly, or when only roots on one direction are of interest.

Most modern equipment also allows the selection of a few important parameters related to data acquisition. Tree root surveys, just like all GPR surveys, should consider these parameters carefully:

- Time window – is the length of time the antenna still collects the two-way wave travel time. The ‘rule of thumb’ suggested by manufacturers is to allow a 100 ns time window to reach 2-3 m depth. Conyers (2004) suggests that the time window should be at least equal to the time it takes to resolve the maximum depth, but for a precise estimate, the optimum depth can be calculated thusly:

$$W = 1.3 * \frac{2D}{V}$$

where W is the time window, D is the maximum depth to be resolved, and V is the minimum velocity through the material (or different materials) in m/ns. Of course, this requires some knowledge of the surveyed material. A

10-30% increase can be added as a safety buffer, as the only downside the a large time window is the data size.

- Sampling interval – the interval between two consecutive data points on the same wave. It should not be longer than the half-period of the antenna's frequency. It can be calculated with:

$$t = \frac{1000}{6f} ,$$

where t is the sampling interval in ns, and f is the central frequency of the antenna in MHz.

- Step size – the spatial sampling interval, controlling how often a trace is collected spatially and improving overall resolution.
- Samples per trace – the number of incremental pulses used to construct a reflection trace. This parameter also improves spatial resolution, but requires longer time window for collection.

The Nyquist frequency is also important to consider for surveys. The Nyquist frequency is essentially the maximum frequency that can be recorded at a given sampling rate. Any higher frequencies are aliased. In order to properly reconstruct features, 3D GPR surveys must fulfil the Nyquist criterion for sampling requirements. In the case of a 1500 MHz, for example, a distance between 1.6-2 cm is required to completely eliminate the risk of any aliasing. However, the practicality of the situation renders it virtually impossible to ensure that accuracy (even for experienced and very careful operators). In practical standards, sampling at half the antenna size (or less) is rarely justified, particularly for high-frequency antennas.

Modern surveys also use digital processing aids. There is a range of available

processing suites, both free and paid, with different capabilities. Most tools offer some similar processing tools, although there are also particular differences in how these processing steps are applied and how the results are visualized.

Survey design should be analysed carefully. An antenna suitable for the objective is required, capable of resolving the target and also of having a depth of penetration sufficient to reach the target. Prediction of whether the GPR approach will “work” is not always possible—something that is often a fact of life with applied geophysics.

2.7.3.4 Advancing Frontiers

Several innovations can be incorporated into GPR surveys, both at the acquisition and the processing stage, as well as through the use of forward models. GPR forward models are very computation-intensive and have proven difficult to carry out. However, this field has benefitted greatly from increasing processing power, the democratization of software and the open-source movement, which have led us to a point where such forward models can be created with relative ease. A solution which stands out is gprMax (Giannopoulos, 2005; Warren et al., 2018), an open source software freely available at <http://www.gprmax.com>. This software uses the Finite Difference Time Domain (FDTD) to simulate the propagation of electromagnetic waves and is well suited for GPR. Results can be simulated in 2D or 3D, and all relevant parameters can be modified: the geometry and dielectric parameters of the subsurface, the position and characteristics of the transmitting and receiving antenna, the time and space discretisation, as well as the waveform and the absorptive characteristics of the “edge” of the model.

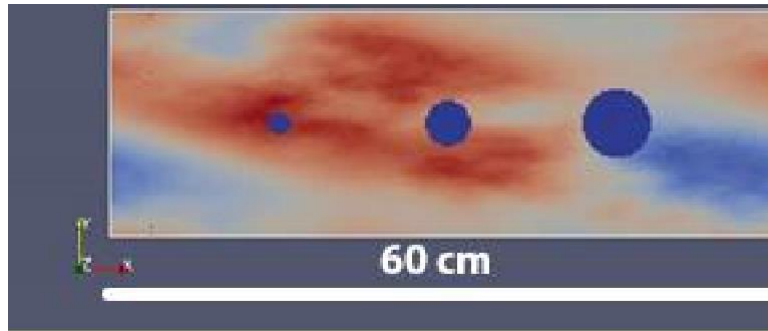


Figure 19. Forward model of three metallic pipes of different diameters in a clay-sand soil model of. Clay-sand composition is 50%-50%.

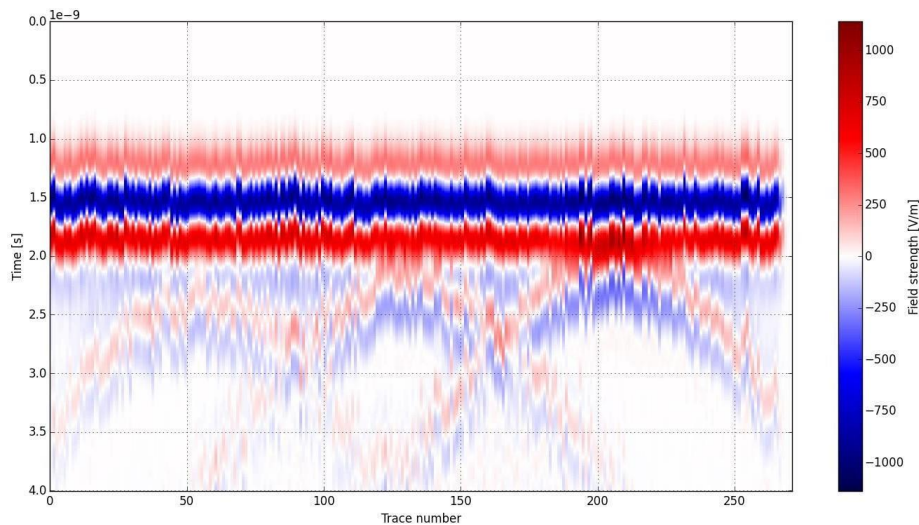


Figure 20. The GPR response for the above model.

Numerical modeling can become an important interpretation aid, and FDTD has become one of the most popular techniques in modeling, as it is robust, flexible, and accurate (Cassidy and Millington, 2009b). The optimization of FDTD GPR modeling has been an area of active research (Millington and Cassidy, 2010), and the method has become additionally appealing thanks to its ease of implementation. The main drawback of the FDTD approach is the need to discretize both the space and the time continua, which could lead to excessive computer memory requirements and the staircase representation of curved interfaces (Giannopoulos, 2005). However, the recent increase in computation power has made such approaches more appealing.

In order to simulate the GPR response from a target or set of targets, Maxwell's equations are solved subject to the geometry of the problem and its initial conditions

(Giannopoulos, 2005). The numerical solution is obtained in the time domain. The domain is divided into a grid, with individual cells called Yee cells, after Kane Yee, one of the pioneers of the FDTD (Yee, 1966). The numerical solution is obtained by applying a discretized of Maxwell's curl equations, and then the process is reiterated. Each iteration corresponds to a unit of time and is indicative of how the electromagnetic field propagates throughout the domain.

Forward models are useful for a better theoretical understanding of the subsurface environment, as well as serving as an interpretation aid for practical surveys. For instance, a forward model can offer more indication as to what the best suited antenna would be for a particular survey, or what type of contract can be expected. If the soil and the general subsurface layout are known, a basic forward model could be generated to offer some indication about what can be expected in the survey. The interpreted features can also be simulated to verify if the models coincide with the results at an acceptable rate. Particular inferences can be made about the range of obtainable information (for instance how water-filled cracks greatly facilitate the discovery of tree roots penetrating into concrete or asphalt; these cracks can be even more visible than the root itself).

However, despite progress at the interpretation side of surveys, innovation around data acquisition and processing is more common. Positioning has long been a problematic issue for high-precision near-surface geophysics, and GPR is no exception. The most common data acquisition process is still the establishment of a grid and the surveying of parallel profiles in one or two directions (Conyers, 2009). While this approach can be subjected to manual errors, a careful survey design and data processing (particularly when it comes to geometry) can ensure that the errors are minimized and the results are accurate. A more technology-heavy approach would rely on a total station to ensure a reliable position. This can not only save time, eliminating the need to carefully setup a grid, but can potentially also be carried out with a single surveyor with

the aid of “smart” total stations which can automatically track the surveyor’s movements. This is particularly useful in surveys where precise positioning is required. This approach has also demonstrated an unforeseen benefit in the study of tree roots: because the total station tracks positioning not only in the XY plane but also on the vertical Z direction, it can also be used to map slight deformations (uplift) caused by the tree root, even when this is not evident to the naked eye.

Another emerging approach for positioning is using Differential GPS (DGPS) or Real-Time Kinematic GPS (RTK), which have a much better precision than conventional GPS systems. These approaches can also be relatively low-cost and applicable in a broad range of situations. Radiolocation can also be employed for a similar purpose, as can a range of other positioning methods. These are of particular interest in Indoor Positioning Systems (IPS), where conventional GPS or total station systems struggle. In addition to better positioning, this also allows the surveying in unconventional or irregular geometries, which are sometimes preferable over regular grids. All in all, while there is no one positional technique that has imposed itself as dominant over the others, there is a range of approaches in development, and a precise method such as GPR has much to gain from these positional improvements.

Another significant improvement is the use of multiple-channel GPR. Multi-channel systems involve several antennas tied together in a system and can best be defined as full resolution GPR systems when crossline separation of the antenna approach the $1/4$ wavelength of the transmit pulses in the ground (Annan 2009). This offers several very important advantages. For starters, it greatly increases the coverage, enabling the surveyor to cover a much broader area in a similar time – which, as any surveyor can attest, is a godsend. Additionally, the antennas are often in different polarizations, which allows better detection of some subsurface features. For instance, one such piece of equipment

(the IDS Stream C) features 34 antennas with two different polarizations, covering a swath of 1 meter. However, for all their advantages, multi-channel systems remain quite expensive, this being the principal drawback.

There are multiple software packages and processing tools, both open-source and commercial. However, in terms of scope, robustness, and ease of use, commercial ones were found to be superior.

2.7.3.5 Limiting factors

Although GPR is a very detailed geophysical method, it remains primarily used for qualitative purposes. However, while many problems can successfully be addressed this way, research is increasingly addressing quantitative analysis of GPR data. This is where forward models, precise equipment, and powerful processing come into play.

The multidisciplinary approach is also important. As a result, progress was not always linear. Being a multidisciplinary approach, different sources of information were considered and used to improve surveys. For instance, the initial assumption was that root size was the main parameter in GPR root detection, given a low permittivity variation between different root segments. However, direct permittivity measurements (Mihai et al., 2019) showed great permittivity variation, which meant that even larger roots might not be readily detected in a soil setting. Additionally, forward models revealed that oftentimes, detecting the root-caused damage can be easier than detecting the root itself, which is a significant aid. The biophysical complexity was also considered, as well as the peculiarities of urban surveys, which render GPR surveys more difficult (for instance, due to scattered noise throughout the soil and different geophysical soil parameters).

However, these aspects were also considered as limiting factors. An important limiting factor for tree root detection is the size of the tree root – quite possibly the

smallest size considered in practical geophysical surveys. This size might be smaller than the equipment resolution.

The lack of geophysical contrast is another important parameter to consider and potential limitation. This was analysed in detail in the paper presented in Appendix D. The possibility of a lack of dielectric contrast between the surrounding subsurface and the root should always be considered.

2.7.3.6 Impact of weather on GPR

Since water content is one of the most important variables in a GPR survey, weather (and particularly precipitations) can also have a significant impact on GPR surveys. In most situations, it is advisable to avoid surveys immediately after rainfall or after precipitations in general. Of course, surveys on snow and ice are also not advisable.

However, in the context of a tree root study, the situation is more complex. In the case of surveys on man-made surfaces where tree root damage is suspected, carrying a survey after a rain might be more favourable, since forward models seem to suggest that water infiltrated in the cracks makes them easier to detect. Ideally, this would be done after the water on the surface has dried up, but not too long after that, so that subsurface water is still in place. Meanwhile, in the case of surveys carried out on natural soil, the interplay between roots, soil, and water is even more complex. Forward models have also shown that there is a significant likelihood that tree root has a similar permittivity to that of the surrounding soil. Tree roots are also known to absorb more water and keep it in their vicinity. It is not clear what the optimum humidity range would be for a survey, but it seems reasonable that a period when the soil is neither too wet or too dry is desirable on soil. Water tends to create worse GPR surveying conditions, creating a dispersive medium that reduces data quality and the depth of penetration. Forward models showed that in

some fringe cases, precipitation can actually favour GPR surveys, when roots are dry and the surrounding soil is very wet. It is expected that roots will absorb some of the surrounding water relatively quickly, so there is probably a window of time right after rain when survey results might be favoured by precipitations, but this is a fringe scenario.

2.7.3.7 Literature Review: GPR Imaging of Tree Roots

In the past two decades, several studies present the usage of GPR to detect and study tree roots. In a 2013 review, Guo et al. summarized the state of the art thusly:

“As a noninvasive method, GPR has been proved to be a valuable technique for detecting coarse roots in low moisture and electrically-resistive soils. However, the detection and quantification of coarse roots using GPR is still in its infancy and not all roots or soil conditions are suited for this technology. Most GPR root detection studies have been conducted under controlled experimental conditions or within plantations. [...] Overall, successful GPR-based coarse root investigation is site specific, and only under suitable experiment conditions can reliable measurements be accomplished.”

While the field has seen a growth since 2013, the summary mostly stands true. It is perhaps debatable whether the method is still in its infancy, but it has certainly not matured to its potential, and remains challenging and site-specific. What exactly constitutes a reliable measurement and how reliable such measurements are is also likely a matter of debate (recently, in 2018, Alani et al. noted that with the aid of specialized processing algorithms, surveys can become much more reliable).

In one of the first such studies, Butnor et al. (2003) used GPR to study root biomass in a forest setting. Barton et al (2004) used three GPR antennas in the 0.5-1 GHz frequency range to detect tree roots in an ideal setting. This was further confirmed by Bassuk et al. (2011) in a more realistic soil medium under pavement. However, while

over the past decade it has become clear that GPR can often detect tree roots, the exact parameters and conditions under which this detection can be achieved are not fully known. This is owed, in part, to the very site-specific nature of this issue.

Root mapping in an urban environment represents the main objective of this work. While such studies are fewer in number, they do exist (Guo et al., 2013). Still, reconstructing root architecture from GPR alone is challenging; often when radargram results were compared with root excavations, only partial similarities are found (Stokes et al., 2002). Hirano and Yamamoto (2009) also noted that distinguishing between different roots in the same area is not always possible. Differentiating between signals from roots and other objects of similar geometry (PVC tubes, old pipes, pebbles) is also extremely challenging as there are no evident differences in signal between roots and these other buried objects (Guo et al., 2013; Zenone et al., 2008).

While fewer in number, quantitative studies also exist in the literature. Xihong et al. (2011) presented a way to model tree root diameter based on GPR results, and Satriani et al. (2010) performed laboratory experiments of both ERT and GPR surveys. Tanikawa et al. (2013) showed that root orientation can significantly affect detection, while Butnor et al. (2016) showed that even under stumps, GPR surveys tend to underestimate root biomass and some roots escape detection. It should be mentioned that in the case of laboratory studies, root samples (or sometimes, even branch samples) were harvested and placed in the controlled setup. However, there is good reason to believe that this might not be an entirely accurate methodology. Mihai et al. (2019) found remarkable variation among the permittivity of roots of the same tree or in the same unit, and the separating the root from the tree likely induces substantial biophysical changes in the roots, changes which can be relevant for GPR surveys. Most notably, roots will partly dry up after separation, which makes them more easily detectable by producing a stronger geophysical

contrast to the surrounding soil. While this has not been yet investigated in great detail, it remains a significant point to consider for existing studies.

However, as Isaac and Anglaaere (2013) note, the detection of tree roots with GPR is hindered by methodological challenges and a lack of non-destructive validation of results. The same work highlights another important aspect: the distinction between fine and coarse roots. Different works draw a different line between these two categories. In general, coarse roots are defined arbitrarily (Guo et al., 2013). Overall, the feasibility of the usage of GPR for detecting tree roots has been demonstrated in the literature, though the limitations of the method are still imperfectly defined, and relatively few studies focus on urban areas (instead, opting for case studies in agricultural or forestry settings).

In addition to root mapping, the literature also seems to focus on calculating root biomass and information about GPR tree root detection in realistic urban scenarios remains very scarce. There is clearly potential to build on the existing literature and fill knowledge gaps. However, although other approaches are also feasible, the mapping of subsurface coarse roots appears the most practical and reliable application of GPR in tree root study, though in general, some roots seem to escape detection.

2.8 Survey Design Considerations

Although good practices exist, there is no universally applicable established methodology when it comes to geophysical surveys. Different authors (and companies) seem to use slightly different techniques, and the specifics of the survey should always be customized based on objectives, methods, and site-specific characteristics. Here, it was attempted to best adapt existing techniques to the situation and, where it was possible, improve the existing approach for this type of objective.

There were several considerations regarding, for instance, the type of ERT array

which is best suitable for detecting tree roots -- is it one of the existing, regular arrays, a combination of several, or something different altogether? What direction should the profiles be carried out on? If the dominant orientation of the objective is well known, then carrying perpendicular profiles will likely be satisfactory, but oftentimes the position and orientation of tree roots might not be known, and therefore profiles on perpendicular directions are best carried out. Several types of trials have been carried out comparing the results and although no definitive answer can be given (as the answer always depends on the exact scenario), some conclusions are discussed in a further chapter.

Several different survey designs and methodologies were tried for this study. Results were compared and future surveys were optimized based on the comparison. However, the general approach was to define a survey area of interest, design a simple grid of parallel profiles in one direction (as per Annan, 2009), and ensure a satisfactory distance between profiles. The area was carefully delimited with tape measure and where a total station was not used, a basic verification was made to ensure that the survey lines are indeed parallel (and where necessary, perpendicular). Notes and images were taken by the surveyed area, describing the general area and the objectives to be investigated. Results from initial surveys guided subsequent ones. Lessons were also drawn from other fields of geophysics. For instance, since archaeology is often focused on small-scale objectives located in the shallow part of the subsurface, lessons were drawn geophysics applied to archaeology (Gaffney, 2008), as well other reference works on geophysical practice (Conyers, 2004; Reynolds, 2011; Everett, 2013)

The starting hypothesis was that that since tree roots are often small in size and often only have a minor contrast compared to the surrounding environment, resolution is of utmost importance, and distance between profiles or measuring points should be as

small as reasonably possible. Therefore, the distance between profiles was carefully considered. However, since having profiles spaced at 1-2 cm is not realistic, the minimum considered distance between transects was 5 cm. Distances of 10, 15, and 20 cm were also considered and tested. Distances of over 20 cm were considered suitable for only a preliminary survey.

The weather and the weather forecast were also considered before a survey. Given the close distance between transects, surveys were time-consuming, and it was attempted to carry out all the surveys in one area in the same day, under the same weather conditions (although this was not always possible).

The surveyed areas were in general kept to a small size. As a “rule of thumb”, it was aimed to keep surveys to an area less than 100 square meters. This was done as surveys had, in general, one localized objective (ie mapping the root system around a single tree, or mapping a sidewalk area that was suspect of root damage). After an area of interest was drawn, the survey area was extended by a buffer of approximately 10%, to reduce the chance of a significant geophysical feature emerging on the very edge of the survey.

Although all available GPR antennas were trialed, surveys in the latter part of this work used higher-frequency antennas. There is no fixed rule for choosing the optimum antenna frequency for a given survey (Guo et al., 2013), but ideally, the antenna central frequency should be able to ensure that a propagated wavelength in a medium is at the very least comparable in size to the half-length of the smallest target (Daniels, 2004). However, the highest frequency antenna (4 GHz) was not deemed suitable for the task. It was expected that the roots of interest would lie in the first 20 cm of the subsurface, and the 4 GHz antenna could not reliably reach this depth. Survey particularities for ERT and

GPR are presented in sections 3.3 and 3.4 respectively.

2.9 Data Processing & interpretation

There are several different approaches when it comes to processing and interpretations. The data could be analysed directly, numerically, or using academic or commercial software – each with their own advantages and shortcomings. Here, I have used the following softwares:

- GPR processing (ReflexW, GPRSoft Lite, matGPR);
- Resistivity processing (RES2DINV, BERT, ResiPy);
- Data visualization (Paraview, Golden Surfer);
- Forward modelling (GPR-Max, RES2DINV, ResiPy);
- Algorithm development (Matlab, Python 3.0, Arduino);
- Image processing (Paint, GIMP, Adobe Photoshop);
- Mapping (Google Maps, Google Earth, QGIS).

It is important to emphasize the difficulty of interpreting tree root GPR data. In most instances, shallow digging was not possible on soil to assess the validity of the geophysical interpretation. No digging was allowed by local authorities on paved surfaces, but several cues can be used to infer the presence of a tree root under such structures. The first is lateral continuity – the geophysical contrast of the objective needs to be continuously visible. If this continuity has been established, then the source of the contrast must be determined. In urban areas, the most common sources are typically pipes and cables. However, these can generally be distinguished from tree roots by the strength and overall appearance of the contrast.

The range of contrasts between the subsurface environment and the tree root can be determined through forward models and lab measurements, but in practical surveys, there

is a large variation between both environmental and tree root parameters. The geophysical identification of tree roots remains a challenging, but in some cases, feasible affair.

3. METHODOLOGY, LAB RESULTS, AND FORWARD MODELS

3.1 Introduction

This work comprises various methods and activities, often carried out independently, and sometimes carried out in conjunction (i.e. joint GPR and resistivity survey).

The first part of activities involves lab measurements. Permittivity measurements were carried out directly on tree roots, assessing their relative permittivity on a range of relevant frequencies, as well as other parameters such as their weight and water content. Large plastic boxes were used for lab GPR and resistivity surveys. Electrical measuring equipment was also developed and tested in the lab (measurement equipment in alternative current which was only used in preliminary surveys, and switchboxes for direct current, described in the following sections). For the surveys, both commercially and lab-developed equipment was used.

The field surveys were carried out with a close consideration to the huge variability of the environmental parameters. Different types of geometries and arrays were trialled out, assessing the comparative quality of the data. All surveys were used to improve the design of further surveys and overall, there was an improvement of the quality in the later surveys.

Lastly, combined surveys were carried out, where the objective was to draw as much geophysical information as possible in a practical scenario.

3.2 Lab measurements

Lab measurements were mostly carried out in the electrical engineering department at the University of Birmingham, but some were carried out in the civil engineering lab.

3.2.1 Measuring root permittivity

3.2.1.1 Motivation

Along with the permittivity of the surrounding subsurface environment, root permittivity is the decisive factor that determines the effectiveness of GPR surveys. Given the expected variability of different types of roots, it was not the purpose of this study to create an exhaustive list of measurements for permittivity depending on parameters such as species, diameter, water content, etc. The main objectives were to assess a range of expected permittivity values for tree roots in a practical context, to see whether branches can be used as proxies for roots, and to use the obtained values in forward GPR models. A secondary objective was to see how the permittivity relates to parameters such as diameter, weight, and particularly, water content.

While the root permittivity has been estimated based on other parameters, most notably water content (Cui, Guo, Chen, Chen, & Zhu, 2013), a direct and comprehensive measurement survey on tree root permittivity has not been carried out, to my knowledge. Additionally, Mavrovic et al. (2018) report a permittivity variability of up to 300% on the trunk of some species, hinting that a large variability could also be present in the case of roots.

Such electromagnetic measurements are becoming more and more common, especially in the medical world, for diagnostics and therapeutics (La Gioia et al., 2018). It was considered that a similar approach could also hold value for measuring tree root parameters. Measurements on vegetal tissues do exist in the literature (Mavrovic et al., 2018), as do measurements on soil (Demontoux et al., 2017) and man-made materials (Villain et al., 2017), but roots have not been studied thusly.

Overall, direct permittivity measurements appear to be a reliable method to

measure the dielectric constant, a parameter that is relevant for forward models. The real part of permittivity (called the dielectric constant or simply relative permittivity) was used in the forward models. The imaginary part of the permittivity (sometimes called the loss factor), which represents the dissipative nature of the object, absorbing the energy and partially transforming it into heat, is linked more to conductivity and was not used in the models.

3.2.1.2 Choice of equipment

Multiple techniques have been used in the literature to measure the dielectric properties of biological materials, including transmission line and waveguide, coaxial probes, tetrapolar impedance, and perturbation cavity methods (La Gioia et al., 2018). However, the open-ended coaxial probe is the most commonly used because it does not suffer from many of the drawbacks that other methods suffer. At least in regards to tissue imaging, this method appears to be the most used one, according to La Gioia et al. (2018), and seems to be a good option in the case of tree roots as well.

Modern commercial coaxial probes are accurate but can only fit samples of specific size (not too big). Here, the permittivity measurements were carried out with a Keysight 85070E dielectric probe, an open-ended coaxial probe. The 85070E can measure complex permittivity over a broad range of frequencies.



Figure 21. Depiction of the Keysight instrument used for permittivity measurements (a); root samples after drying (b); an area from which root segments were harvested (c).

Measurements were first taken from 5 MHz to 3 GHz. Then, in some instances, the interval was trimmed from 100 MHz to 3 GHz, which is a sufficient frequency range for the expected GPR data. A three step calibration is done before any measurement. The three most common standards used are open circuit, short circuit, and a broadband load; this was also the case here. The probe was calibrated with hydrogen peroxide and special instruments provided by the producer. If the calibration is stable and successful,

the “real” measurement can proceed.

The method also has some drawbacks, most notably the small volume of the sample considered (~1 cm). A very good contact between the probe and the sample is also required, both in the case of biological sampling and in the case of soil sampling (Demontoux et al., 2018). Overall, though, the method seems well-suited for the task.

3.2.1.3 Measuring methodology

The measuring process involved keeping the samples firmly pressed on the probe surface for a few seconds. It is important that the plant has a smooth surface as any surface roughness could lead to the probe measurement incorporating tiny air pockets, thus altering the overall results. As Mavrovic et al. (2018) note, one of the main practical challenges in this type of measurement is to obtain a surface smooth enough to ensure contact. Therefore, roots were cut smoothly into centimeters of approximately 10 cm long. Their shape was sometimes irregular which made measuring more difficult and these samples were cut into smaller segments, but never smaller than 5 cm.

Since the ultimate objective is detecting coarse roots, only measurements on coarse roots were carried out. However, because the root samples were harvested from living trees, a careful consideration was given to the trees’ wellbeing. Therefore, only relatively smallcoarse roots were harvested, and where possible, roots were harvested towards their end segments, so as not to disturb a longer section of the root. Roots were only harvested from mature trees, only when no significant harm was done to the tree. Roots were harvested from trees in public areas in Birmingham (an representative area is depicted in Figure 21).

The root is a living part of the tree, and the moment it is cut away from the rest of the tree, its bio-physical parameters start to change. Since the measurements could not be

performed out *in situ*, it was imperative that they were carried out as quickly as possible after the samples were harvested. The general procedure involved cutting up root segments with a wood saw (so as to leave the section smooth). The samples were then immediately taken to the lab, a process which took between 30 and 60 minutes, depending on practical considerations. The roots were labelled and sealed in plastic boxes for transportation (see Figure 21).

The first measurements were carried out as a proof of concept. For subsequent measurements, roots were weighed with a high precision scale, measured, and placed into an oven for 24 hours, after which they were weighed again, to calculate the water content of the samples and compare this against permittivity.

The measurements on the first samples were taken by manually pressing the root sample on the probe. To reduce the potential for human error and accelerate the process, subsequent samples were held in place by an adjustable chemistry stand. Each measurement takes only a few seconds, after which the analyser displays a graphical representation of the data, which serves as an initial calibration – if it is a reliable measurement, the curve will be relatively smooth, as there are no air pockets to influence the measurement. If it's not, then the measurement was retaken until a smooth curve was obtained. This proved to be a reliable method, despite initial concerns. However, although the measurements themselves are mediated, 40 continuous measurements were carried out for each sample, to further ensure statistical relevance, and the process was tedious and time-consuming.

Because permittivity measurements can sometimes exhibit variability (La Gioia et al., 2018; Mavrovic et al., 2018), and because this is a novel approach for tree roots, the same measurement was repeated multiple times for consistency. The self-imposed goal

was to have at least 30 viable measurements, and an extra 10 were taken as a buffer; so in total, 40 measurements were made of every sample, with the idea that if a few of them were unsuitable for unforeseeable reasons, there would still be at least 30 measurements remaining, which was considered a satisfying number for this purpose. This was also carried out to see whether the properties of the roots would change over the course of 30-60 minutes, which is how long it took for the measurements to take place. Since it did not seem to be the case, it can be inferred that the measurements equate to *in situ* measurements.

3.2.2 Permittivity lab measurements of tree roots

This chapter, along with the results obtained with this methodology, are illustrated by the following special issue article published in *Near Surface Geophysics*: “Direct measurements of tree root relative permittivity for the aid of GPR forward models and site surveys,” by Mihai et al. (2019), <https://doi.org/10.1002/nsg.12043>. The paper is reproduced in its entirety in Appendix D, but the main findings are described and summarized here as well.

A critical challenge in developing GPR forward models is knowing what permittivity value to input for the tree roots. This was addressed by the direct permittivity measurements explained above. The first comparison analyzed the relative permittivity of two roots and a branch, to assess whether the two have similar or comparable values for this parameter. This was not found to be the case: the permittivity roots and branches from the same tree, and of very similar diameter, were found to be quite different, indicating that branches are not a useful proxy for root models and measurements.

A second, larger survey (also presented in Appendix D) describes multiple root

segments extracted from the same soil unit, from trees on a public natural pathway called the Harborne Walkway. A total of 20 segments from 10 roots were analyzed. Several root samples were harvested and immediately transported to the laboratory, where permittivity measurements were taken using a coaxial probe, as described previously.

The roots exhibited a very large permittivity variation, despite being in the same soil unit, having a similar diameter, and coming from the same species. Observed relative permittivities at 1 GHz ranged from 11 to over 30. This range is so great that it has significant potential of overlap with the permittivity soil values as described by Hubbard et al., (1997), Davis & Annan (1989), and Daniels (1996). If such an overlap does happen, it means that there is a very low dielectric contrast between the root and the soil, making GPR detection difficult or impossible. In addition, some roots (presumably diseased or inactive) exhibited very low permittivities (under 5).

The root values for diameter and permittivity were then input into forward models using gprMax. These models underscored that in permittivity values that could be expected for urban soils, there could be a very low contrast between the root and the soil. Even in the presence of a thin bark (a scenario which was also simulated in forward models), detection is not guaranteed if the permittivity value of the root and the soil are too close – regardless of root size.

This was interpreted as a potential explanation for something that was reported several times in the literature: that some roots (even coarse roots) sometimes escape GPR detection. Being aware of this spread of permittivity values is extremely important for surveyors and geophysicists looking to map subsurface root systems. This large permittivity spread is the main outcome of this now-published work presented in Appendix D and was used to direct future work.

Another notable finding is that roots can have both higher and lower permittivity than what would likely be expected for soils in urban areas. If this is the case, it would mean that in different situations, roots can exhibit both a positive and a negative permittivity contrast to the surrounding soils. This would suggest that although higher permittivity soils are generally an unfavorable environment, they could favor the detection of lower-frequency roots, especially diseased or inactive roots.

After the measurement, the root segments were weighed and then placed in a civil engineering oven to dry for 24 hours. They were then weighed again to assess the water content. While water content appears to be an important factor in the roots' permittivity, it does not appear to be the only one. Further research is required to better understand the bio-physical factors behind this permittivity variability and what factors influence or define it.

This finding is consistent not just with what has been reported in the literature, but also with the surveys presented in subsequent chapters. In surveys carried under unfavorable conditions (such as the “Harborne Leaf Fall” survey in chapter 5.8), just a small part of the root system is mapped, which was unsurprising. But even under favorable conditions, using multiple high-frequency GPR antennas, some roots escape GPR detection, and it is not always clear why. Granted, there could be other reasons (resolution, noise, cluttered objects), but an insufficient contrast between roots and the surrounding soil could help explain why even coarse, isolated roots are sometimes not detected with GPR alone.

The permittivity and diameter parameters obtained through these direct measurements, along with soil permittivity parameters existing in the literature were used in the forward models presented in the following chapter.

3.2.3 Forward models of tree roots

The median value was selected for models because it provided smoother curve than the average or value (although there were no major differences, particularly at high frequencies such as the ones used for GPR surveys here).

Sample comparison between average and median permittivity

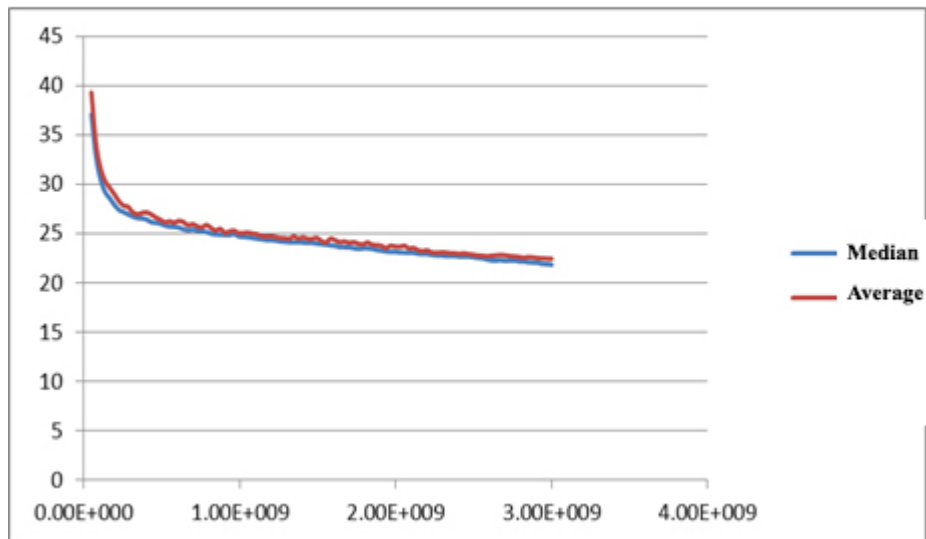


Figure 22. The average (red) and median (blue) relative permittivity values for one of the samples in the entire 0.05 – 3 GHz frequency range. Values exhibit a typical variation curve, dropping down from higher values at smaller frequencies.

The first models simulated simple reflections in various soil-root geophysical contrasts, attempting to quantify the contrasts and what contrasts are detectable. These models were considered an ideal, unrealistic scenario. Even with added noise, the real-life soil environment is much more challenging to GPR surveys than the forward models. Therefore, the models are considered as an indicator of what can be seen in the field. If something cannot be detected or differentiated in the models, it also cannot be detected in the field (where conditions are more difficult). If something is barely detectable in the models, there is a chance it might also be visible in the field, but this is not necessarily the case.

The following models (and those presented throughout the section) use a discretization grid of 0.002 m in all directions (x, y, z), unless otherwise specified – a

resolution that should be more than enough for the objective at hand.

The following scenario (where a root has lower permittivity than the surrounding soil) was selected because in direct measurements, some roots were found to have very low permittivity, and it seems plausible that they would have a negative permittivity contrast compared to the surrounding soil (a scenario rarely explored in the literature).

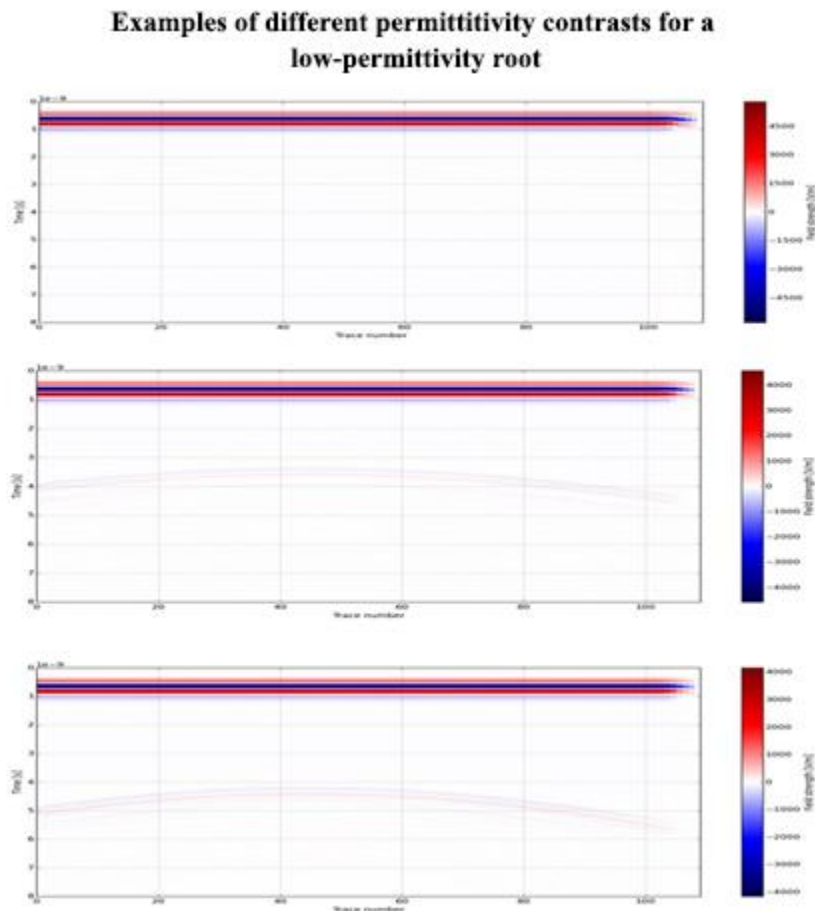


Figure 23. Three models of a root with a relative permittivity of 3, in clay with three different levels of humidity: almost completely dry (top; permittivity 5), somewhat wet (middle; permittivity 8) and more wet (bottom; permittivity 11). Here, contrary to conventional wisdom, wetter soils make the root more easily detectable because although they lower the data quality, they accentuate the contrast between the root and the surrounding soil. The rationale of this model was to highlight this aspect.

Quantifying detectable contrasts remains challenging, but in surveys with reasonable amounts of noise, it can be assumed that a permittivity contrast of 4 and above might be detected (in a medium that is not particularly lossy). The mineralogical components of the soil are also significant. Models in several environments were created to highlight this.

The basic model presented in subchapter 2.7.3.4 was tweaked to consider different clay/sand compositions and see how these compositions would affect the identification of tree roots, using permittivity values existing in the literature (Hubbard et al., 1997; Davis and Annan, 1989). Thankfully, gprMax offers a readily available algorithm to create a randomized distribution of user-input clay-sand fractions, which is excellently suited for this purpose.

The first models mimicked metallic pipes (perfect electrical conductors - PEC) instead of tree roots, as a range of permittivities for tree roots had not yet been determined, and this was meant to be a preliminary model. The following models show a GPR B-scan (profile) of 3 such pipes of 1, 2, and 3 cm diameter in a mixture containing clay-sand mixtures of 50-50%, 95-5%, and 5-95% (at the same humidity).

The GPR response for equal clay-sand components is presented as an example in 2.7.3.4. Here, a comparison between dominant clay and dominant sand distributions is presented.

The sand composition yields a substantially stronger reaction, even at the same water content. This is not surprising, due to the different dielectric properties of these soils (sandy soils being much better suited for GPR surveys).

The models were subsequently transformed into SEG-Y files, to enable ReflexW visualization and further processing.

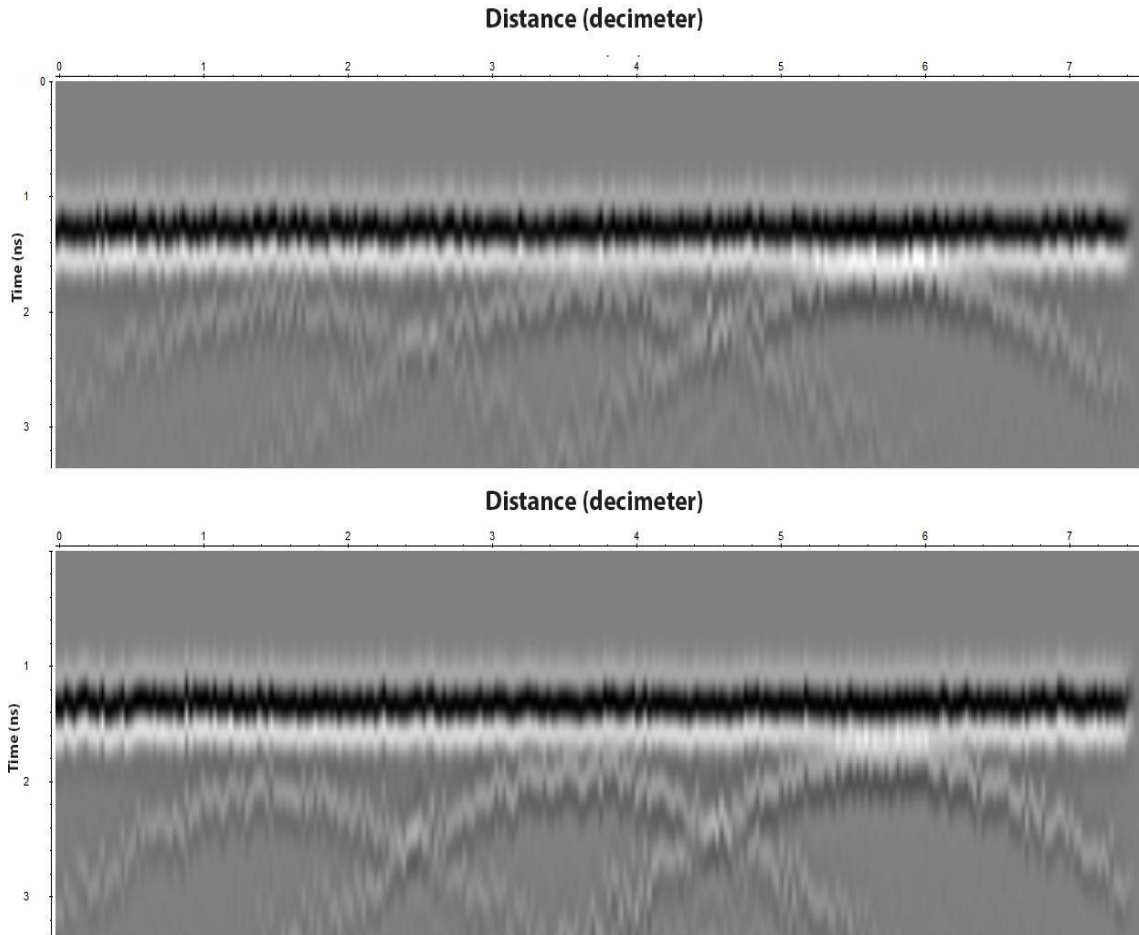


Figure 24. GPR responses for clay proportion 95% (above) and sand proportion 95% (below), as seen in ReflexW.

Unlike the gprMax interface, ReflexW also enables the user to process the data. When simple processing is applied as would be the case in a regular survey (trace stacking to reduce soil inhomogeneity effects, background removal, and static corrections), the difference between clay and sand is even more noticeable.

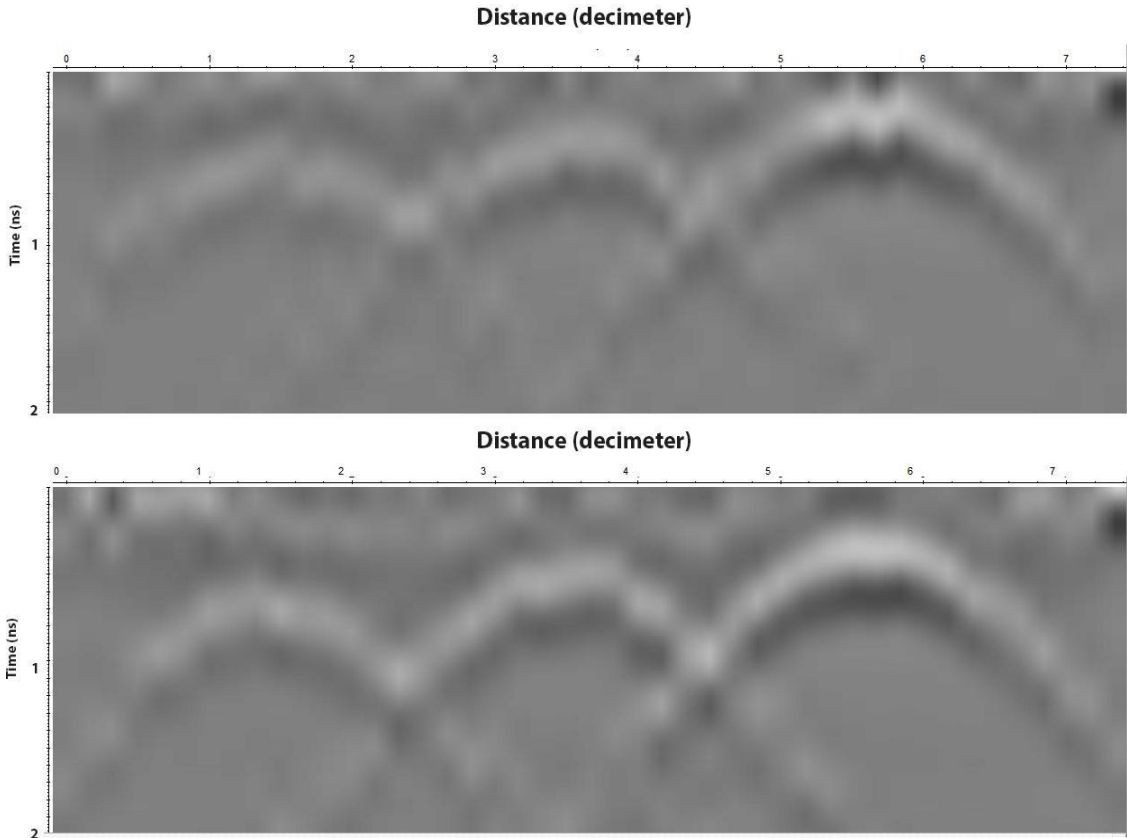


Figure 25. GPR responses for clay proportion 95% (above) and sand proportion 95% (below), as seen in ReflexW (with basic processing).

When instead of metal pipes, the model simulates roots (and instead of the PEC, a realistic permittivity value for roots is inserted), this difference can become crucial in determining whether tree roots can be identified or not. This is owed, in part, to the more lossy clay environment, but also to the different permittivity values of soil and clay at the same watercontent. It should be also considered that in the case of a dried root (such as a diseased or inactive root), the roles might be reversed, and the contrast might be stronger in clay versus sand (although the overall data will still have lower quality on the clay environment).

The contrast should not be analyzed in a vacuum, however. In lossy environments, where data quality is reduced, a similar contrast dielectric can be harder to detect. Therefore, positive and negative contrasts are not equivalent: high-

permittivity roots in low-permittivity soils are more likely to be observed than low-permittivity roots in high-permittivity soils.

Longitudinal models of roots and root-infrastructure interactions were also created, the rationale being that they could serve as an aid in visualization and interpretation of real data. While it is unlikely that a GPR profile will occur exactly in the direction of the root, these can still help in interpreting real GPR data (for instance, this type of profile could be regarded as an interpolation between parallel profiles, or serve as an indication as to what may be seen on a timeslice).

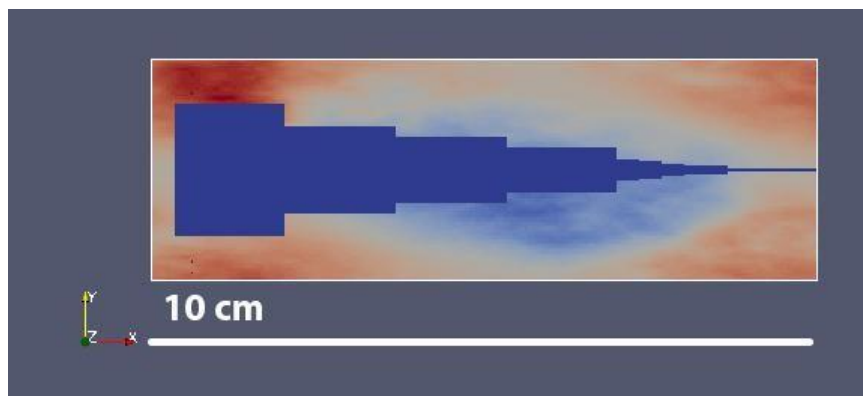


Figure 26. Longitudinal section of a thinning tree root in a clay-sand mixture.

Here, once again, the model started with a PEC structure, which was replaced with realistic root permittivity values. As expected, the PEC structure yielded a strong reflection.

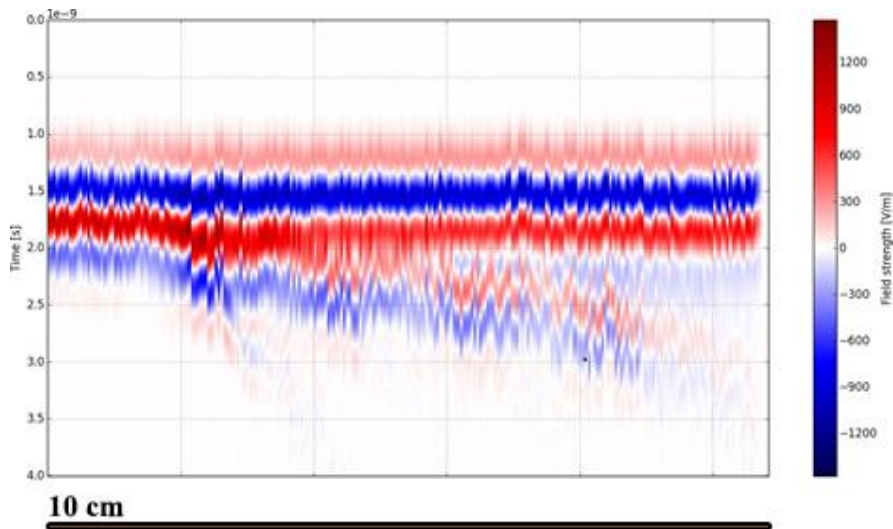


Figure 27. GPR response of a transversal PEC root-like structure.

However, when realistic permittivity values are introduced for a tree root, the contrasts become less pronounced. In the following image, there is a permittivity contrast of 6 between a homogeneous soil and the root depicted in Figure 26.

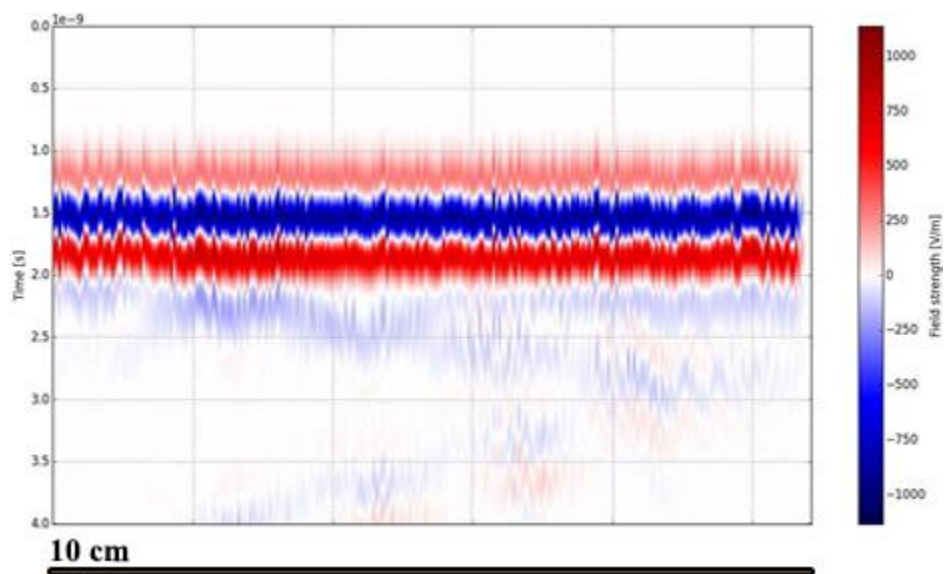


Figure 28. Example of a GPR response of a root. Several different parameters for the soil and the root were presented. Here, a dielectric contrast of 6 is depicted.

The thinning of the root is clearly exaggerated. However, this highlights the idea that individual contrasts alone are not sufficient for root determination and lateral continuity is essential for the identifying tree roots. It also showcases what type of

reflection could be encountered in the unlikely case of a real survey in the direction of the root.

Other scenarios more likely to be encountered in practice were also reproduced. Another point of interest for surveys is the detection of potential damage to pipes, along with potential leakage. The topic of GPR investigations for pipe leaks has been addressed in the literature several times (Plati and Dérobert, 2015), but it remains challenging. The interference of tree roots (which can often be the cause of damage or can exacerbate existing damage, per Day, 1991) adds another layer of complexity, which has not been addressed thoroughly yet. It is unclear if the existence of roots would potentially mask the leakage. The following two models simulate this scenario in a 60 x 20 cm environment, the rationale being that it could help surveyors know what type of contrast to expect.



Figure 29. Depiction of the modelled environment. A root is penetrating a water pipe.

Several soil variations were considered for this task. Here, the soil was considered to be a very wet clay. This parameter was chosen because one of the goals of this scenario was to detect whether the leakage could be detected in a challenging, realistic urban scenario.

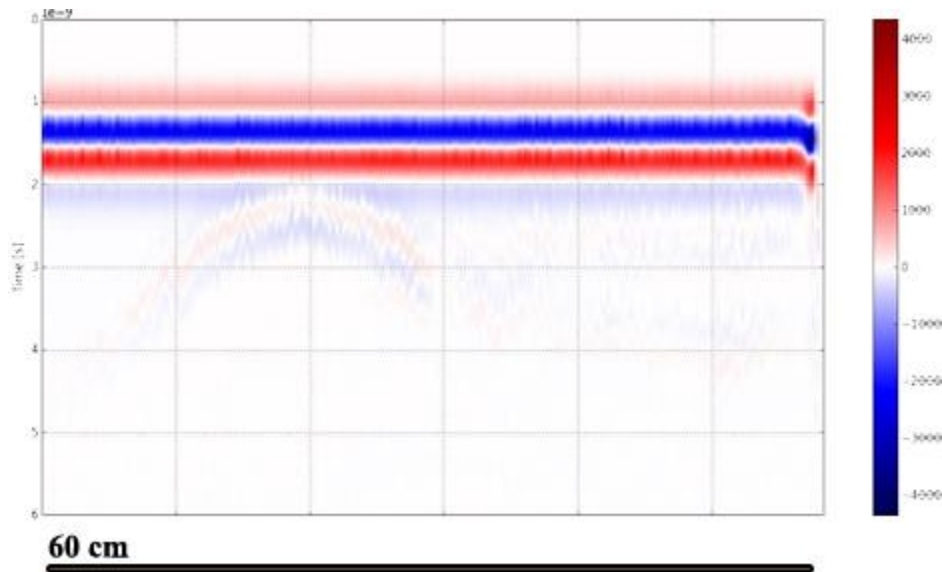


Figure 30. GPR response of the modelled environment. Again, the permittivity contrast between the soil and the root is 6, but this shows up fainter than the model above, due to the lossy medium.

However, regardless of the permittivity of the soil or the root, cracks in the pipe are not detectable. The overall impact of the PEC material is too strong and masks potential cracks (which are also expected to be small in size). It might be possible to reveal whether a root is in the close vicinity of the pipe, but assessing whether or not the root has penetrated the pipe is likely not a realistic expectation. However, pipe leakage is more likely to be detected, in the same scenario.



Figure 31. Depiction of the modelled environment. A root is penetrating a water pipe, causing leakage in a randomly distributed arrangement which has not homogenized.

This leakage does produce a response.

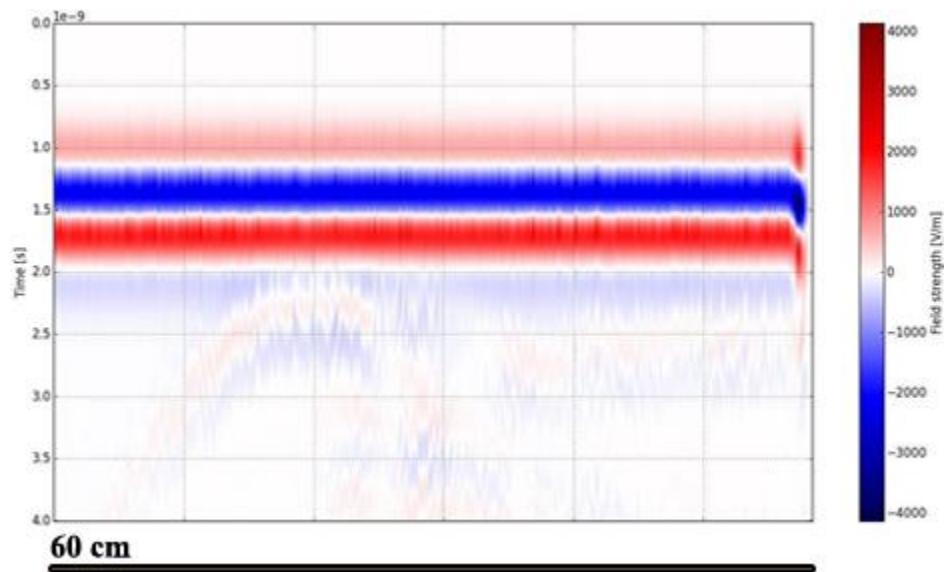


Figure 32. GPR response of the modelled environment.

Whether or not this response is detectable (particularly at low amounts of leakage) remains site-specific. The exact dynamic of the leakage is not fully known and therefore models remain an approximation. Unsurprisingly, in drier soils, the leakage is more readily detectable.

Although this does not explain whether the root itself is causing or exacerbating cracking the pipe, this can be useful for monitoring at-risk pipes. Measurements can be carried out, and if a root is detected in the vicinity of the pipe (or developing towards the pipe), this can be a reason for concern – even without any leakage. If leakage is detected and a root is nearby, it can be expected that the root will exacerbate the damage. In this case, even if it is a minor leak, it should not be ignored. The main conclusion of these models is while establishing the proximity of a root to a pipe can be done, actually identifying whether the root is protruding into the pipe is not realistic. Additionally, pipe leakage may carry a specific signature that facilitates detection.

Other models were also produced to better understand the interaction between roots and the damage they produce and to aid in particular interpretations of data. The rationale

for these models comes from an unexpected question that arose during surveys: when a GPR survey suggests that tree roots have penetrated a paved surface, is it the actual root that is detected, the damage that the root causes, or both? The following set of models explores this question.

Firstly, simple root models were simulated in a homogeneous material with permittivity values of what you would encounter in asphalt. The more homogeneous the subsurface environment, the easier it is to detect any geophysical contrast. Asphalt is a more homogeneous environment than soil, and much less prone to changes (such as those caused by rain or extended periods of drought). Although asphalt is not a perfectly homogeneous environment, it was considered as such in the models. It should be mentioned that modelling the diversity and complexity of asphalt, concrete, and other materials used as pavement warrants additional study in itself, but this was not the goal here.

A root with a diameter of 1.5 cm and permittivity 12 was used as a model. A permittivity value of 6 was considered for asphalt, and a frequency of 1.5 GHz was used for the antenna. The root is easily visible on the radargram in this scenario. Again, the modelling box measures 0.6 x 0.2 m.

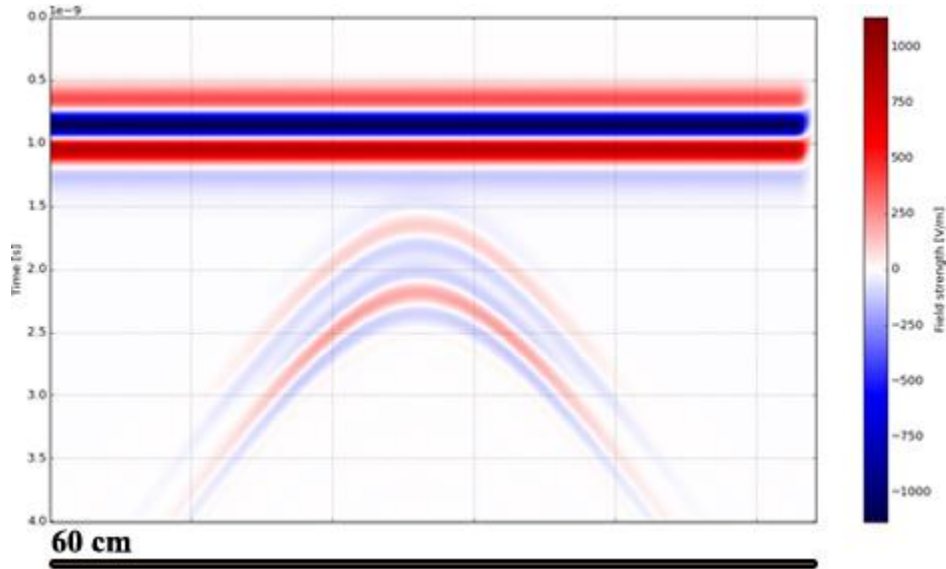


Figure 33. GPR response to the above-mentioned scenario.

The data was again migrated into ReflexW, where a random noise distribution of 10% was added to make the data more realistic. Even without any processing (such as stacking traces), the difference from the inhomogeneous soil is clear. However, when the modelled root was replaced with a similar-sized air-filled hole, the results are similar.



Figure 34. GPR response to a root neatly penetrating asphalt (top) versus a similar-sized hole (bottom).

However, this is a result of the contrast between the modelled root and asphalt. If the root permittivity value is closer to that of the asphalt, for instance at a value of 8 (as is the case here), the contrast is much fainter. The following forward model aims to provide a visual aid, depicting how the permittivity contrast can look fainter depending on the root permittivity.



Figure 35. GPR response of a root of permittivity 12 (top) versus 8 (bottom) in an asphalt of permittivity 6.

It is not even clear that such a faint contrast can be realistically detected in real surveys; it is quite possible that it will be obscured by other contrasts or noise. Essentially, if the permittivity value of the root is too close to that of the asphalt, the contrast might be too small to detect the root itself. This possibility cannot be ruled out, particularly as roots under the asphalt are expected to be drier (as the asphalt is warmer and accelerates transpiration).

However, roots are unlikely to protrude neatly into the asphalt, and are more likely to produce cracks as they go in. Centimetre-sized cracks in asphalt are expected to produce detectable results, although it should be added that cracks are not expected to be perfectly cylindrical or follow a regular form, and therefore the GPR response will be more challenging to interpret. Still, discontinuities of any shape (such as cracks or

fissures) are likely to make detection easier. This suggests that while detecting root-crack systems is likely, it is not always easy to distinguish between the root itself and the cracks, and caution should be employed when interpreting such data.

There is one indication, however, that might help distinguish positive from negative contrasts (and to an extent, this might help differentiate roots from voids): individual trace shapes. In a negative contrast (fissure), the negative side of the trace corresponding to the contrast is expected to be dominant, whereas in a positive contrast, the opposite is expected to happen. Similarly, in the scenario with the root with higher permittivity, reflections indicative of both the top and the bottom are visible. In a practical scenario, these differences can be hard to identify as the interferences are far more complex and this is not always reliable, but it can be a pointer nonetheless. Yet, in a relatively common scenario, presented below, even this information might not be useful.

Another common scenario was modelled next: a root buried under asphalt, causing a bump deformation (something which is commonly encountered in urban areas in Birmingham and presumably, in most places around the world). The goal was to assess how this type of scenario would be visible on the radargram, and how different variations would affect the GPR data. The asphalt features 2 layers (permittivity 4 and 6 respectively) in all situations, as can be often encountered in practice (Conyers, 2004). This scenario was selected because it was commonly encountered throughout surveys.

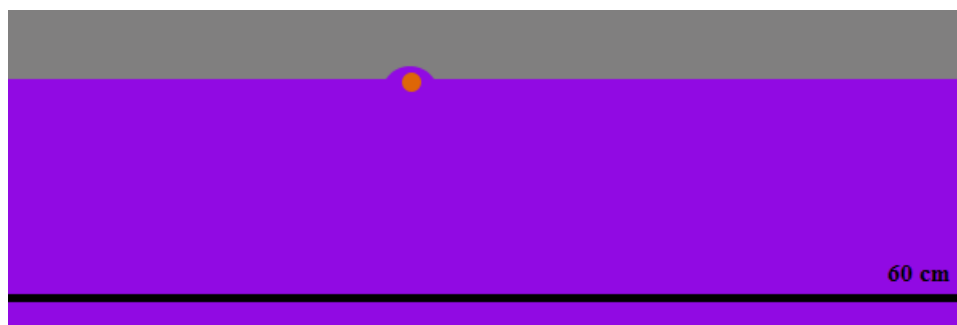


Figure 36. Depiction of described scenario with the two layers of asphalt and a root (brown) producing a

bump in the second layer.



Figure 37. GPR response of the above-described scenario.

However, although asphalt bumps are quite common, it is likely that not all of them are caused by roots. Thus, the next forward model compared a bump caused by a root, with a bump when no root is present. Background removal has been applied for simpler visualization.



Figure 38. GPR response of a bump deformation with root (above) versus no root (below).

The two radargrams appear very similar, and any existing difference is not obvious. The contrast is slightly stronger when the root is present, but it is probably not possible to assess the presence or absence of a root from this alone. Since there is a positive contrast between the second and the first layer of asphalt, the pointer mentioned in the previous example is also not useful. This is a significant conclusion: when identifying a bump, it may be challenging to assess whether that bump is caused by a

root or not.

It is worth reiterating that establishing lateral continuity is key to identifying tree roots. Many of the GPR root surveys indicate the presence of roots through hyperbolae, suggesting the existence of an actual object – but without lateral continuity, this might only be an isolated inhomogeneity or some buried object (such as a pebble or any other object).

A timeslice was also generated from multiple such models, for comparison. This was useful as an aid for interpretation, highlighting that often, roots appear on timeslices as a negative (dark) anomaly surrounded by positive (white) stripes or viceversa. Again, the contrast is stronger in the root section, but not much else can be said. The bump itself doesn't appear to produce a major difference in the simulated timeslices.

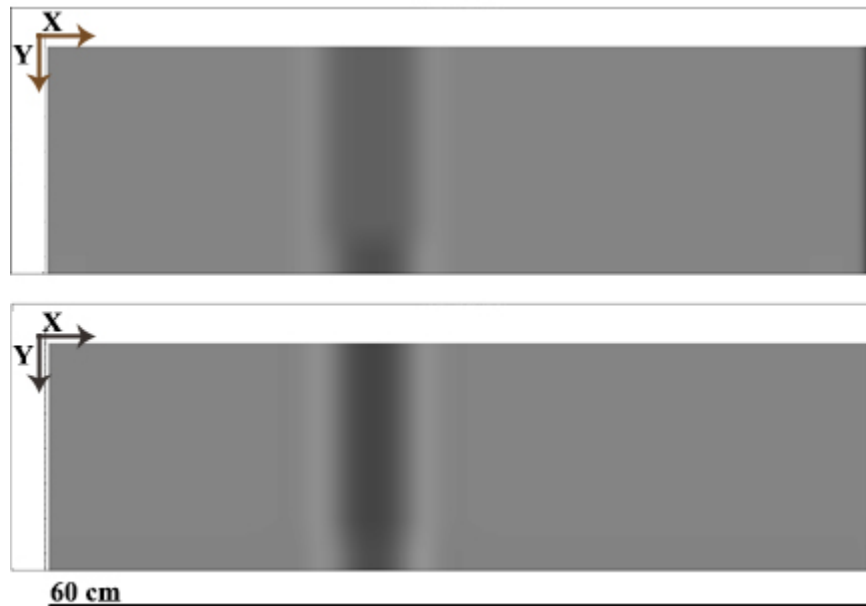


Figure 39. Simulated timeslice of bump with no root (above) and bump with root (bottom).

The above forward simulations assume that the root would penetrate the asphalt “neatly”, without producing cracks or other deformations. In this case, the only geophysical contrast would be between the root and the asphalt and the root. However,

this is not necessarily always the case. Roots penetrating asphalt cause a series of deformations, including cracks and bumps. The mechanical interplay between roots and paved surfaces is not entirely understood and again, only basic approximations of these processes.

Another likely scenario was represented in the following forward models: a root penetrating asphalt, causing a bump, as well as a system of small cracks (diameter: 1-4 mm) around it. The rationale for this is to create scenarios closer to what may be encountered in real life.



Figure 40. Depiction of the above-described scenario. Cracks are represented around the root.

When the cracks are so small, the difference they cause is negligible. But in the presence of water, the situation changes. When the same model is simulated but the cracks are filled with water, the difference is notable, with water significantly amplifying the contrast. It is notable that once again, water can facilitate detection rather than impede it (which is often the case in GPR).



Figure 41. Comparison of the same system of cracks, air-filled (top) versus water-filled cracks (bottom).

Until now, the existence of water has been neglected in these simulations. Asphalt (as most types of paved surfaces), is waterproof and should not allow the presence of water. However, deteriorated asphalt, and particularly asphalt that has been penetrated by a root, could have water-filled pores or cracks, whether due to transpiration from the root or due to leakage. If this is the case, existing water can make an important difference, as seen in Figure 41. The water-filled pores in the simulation cause reverberation-type effects that have a visible impact.

As the simulated cracks become larger (and especially as they become closer in size to the root itself) their impact will become more and more significant, regardless of whether or not they are water-filled. However, it should be noted that water, commonly an ‘enemy’ of GPR, can make this sort of contrast much more visible to the GPR.

These are a few representative scenarios replicated in forward models that summarize what was learned over this process. Numerous variations (especially varying permittivity contrasts and antenna frequency) were trialed and exemplifying them would produce redundancy. The way tree roots affect the asphalt at a localized scale is not fully understood – it is still unclear what type of fissure system they create when penetrating

into the asphalt. This limits the utility of forward models as it is unclear what situation should be replicated. Since subsurface voids are an early sign of deterioration, this is an area of interest even without studying even without tree roots (Hoegh et al., 2015). Should this gap be filled, the simulations would gain a layer of confidence. However, a few conclusions can still be drawn.

The contrast between tree roots surrounding soils remains a major challenge in detecting roots. However, on paved surfaces, it is unlikely that detection relies merely on a contrast between the root and the surrounding paved surface because the root is unlikely to protrude neatly into the surface, and is expected to create a system of fissures. If these fissures are small and air-filled, they are unlikely to aid detection. If they are large enough or water-filled, then they may be easier to detect than the root itself. In addition, it is not always straightforward to determine whether a road or sidewalk deformation is caused by a root or not.

The large variability of materials used in paved surfaces warrants further inspection. These examples aimed to serve only as a reference, but having access to an encyclopedia-type reference with simulated paved surfaces (and their interaction tree roots) would be useful. This is expected to become a growing area of interest as there is already an established interest in monitoring asphalt quality using GPR. The scenarios presented here feature roots with permittivity values relatively close to those of the asphalt. However, roots can easily have permittivity values two times larger, in which case, much stronger contrasts are to be expected.

Ultimately, these forward models help in understanding and interpreting GPR data. Overall, given the complexity of subsurface interactions and the knowledge gap regarding root-infrastructure interactions, these models serve as a general indication and establishing

a clear quantification of detectable contrasts and scenarios remains site-specific and challenging.

3.2.4 Equipment development

For this study, both commercial and lab-developed equipment was used.

The available commercial resistivity meter only had 4 channels, which was unsuitable for the desired approach. Also, most commercial resistivity meters only allow for pre-determined electrode configurations (Wenner, Schlumberger, etc.), which was also unsatisfactory. So a box to switch electrode positions (from here on called a switchbox) was developed to address this. In addition, the equipment developed here also comes at a lower cost than existing commercial alternatives.

The switchbox featured 4 input channels, for P1, P2, C1, and C2, and 32 output relays. The goal was to mimic and then improve multielectrode resistivity meters. The power input came through a conventional 12V battery, and the connection to a computer was done via USB. The box was commanded through a Matlab algorithm that directed the geometry of the ERT.

In order to assess the accuracy and precision of the system, a simple test environment was set up. The environment featured 13 resistors connected in series on a breadboard. The switchbox outputs were connected to take measurements on these resistors, mimicking a Wenner array.

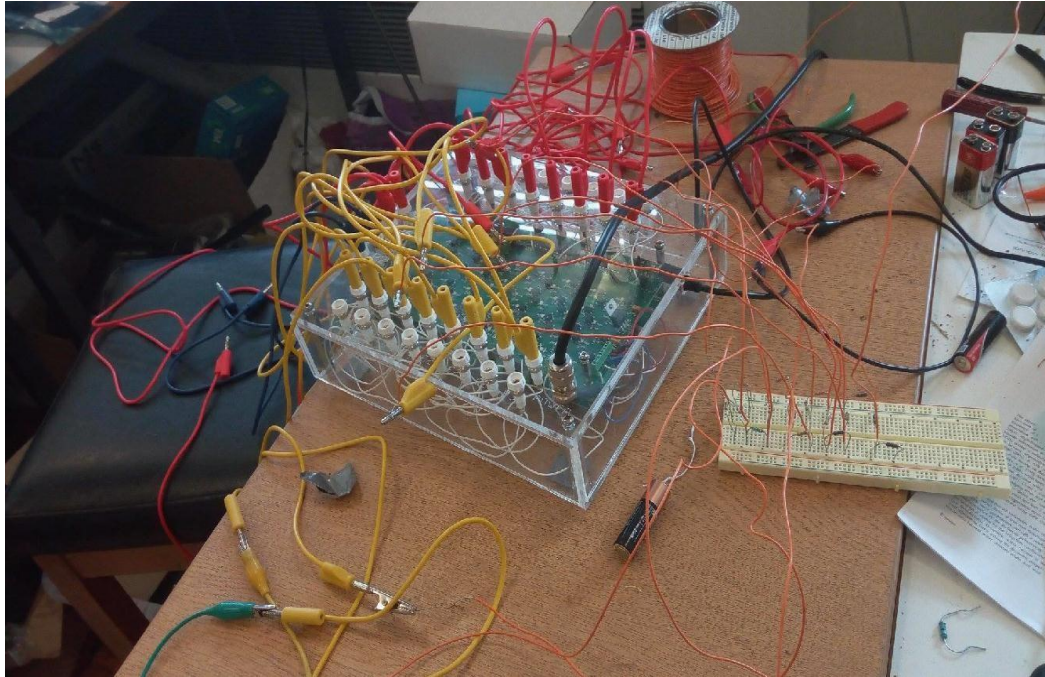


Figure 42. The test environment setup.

In total, 30 measurements were carried out to verify the precision and accuracy of the setup. The average and median values were well within the resistors' fabrication variation value, and there was no significant variation between different iterations of the same measurement. The minimum and maximum values of the 30 measurements were also well within the resistor fabrication values:

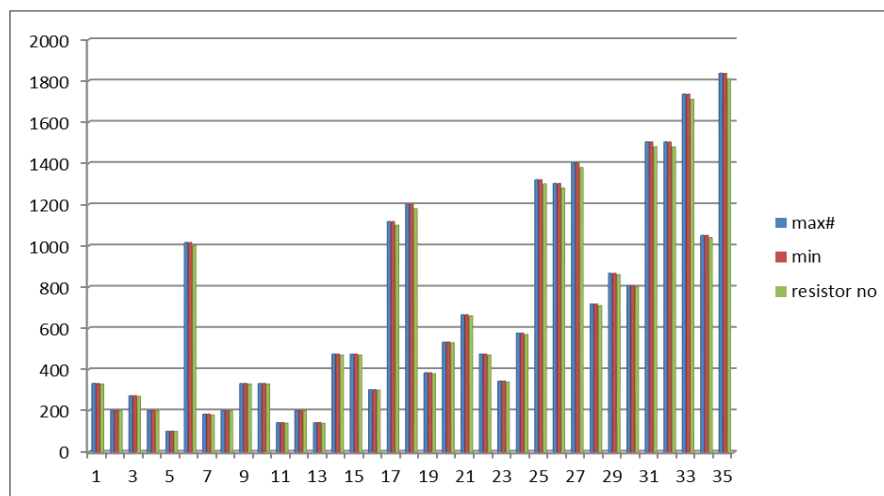


Figure 43. Results of one of the tests, featuring 42 measurements of 16 electrodes in a Wenner array (35 positions). Minimum and maximum results compared with resistor values.

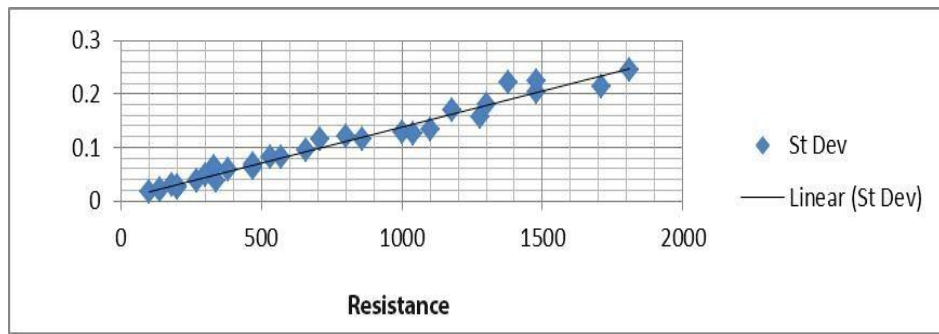


Figure 44. Average values, variance and standard deviation results (top right) and standard deviation plotted as a function of resistance.

Thus, the equipment was deemed sufficiently accurate and precise for the task at hand, with errors within $\pm 2\%$ of the resistance value.

Over the course of the study, another switchbox was also developed using a somewhat different approach. The reasons for a second such device were twofold: first, it was to have a backup on hand in case the first one was damaged. Secondly, there was a curiosity to see whether such a device could be made with a lower cost and with more readily available materials. Geophysical equipment can be expensive, and for such an approach to be routinely applied in a practical context, reducing existing costs could prove to be an important consideration. While the first one was already substantially cheaper than existing commercial opportunities, the second one was even more so.

While the first switchbox was built by soldering relays onto the board, the second one was designed using readily available relay boards and an Arduino Mega board. This setup proved to be much more affordable and equally capable, precise, and accurate.

The ease of data acquisition was also considered. Unlike most commercial equipment, which is cumbersome and heavy, this was more lightweight and can be easily used with a tablet or smartphone, as the algorithms were exported as stand-alone applications. Tweaking the geometry with the ease of a smartphone or tablet proved to

be a valuable advantage in the field. This not only enabled data acquisition in any desired geometry, but also substantially facilitated the acquisition of resistivity data, allowing monitoring and other forms of long-term data acquisition.

Another approach was also considered for the acquisition of resistivity data. A prototype developed in the lab conducted AC measurements, sending a sine wave into the ground.

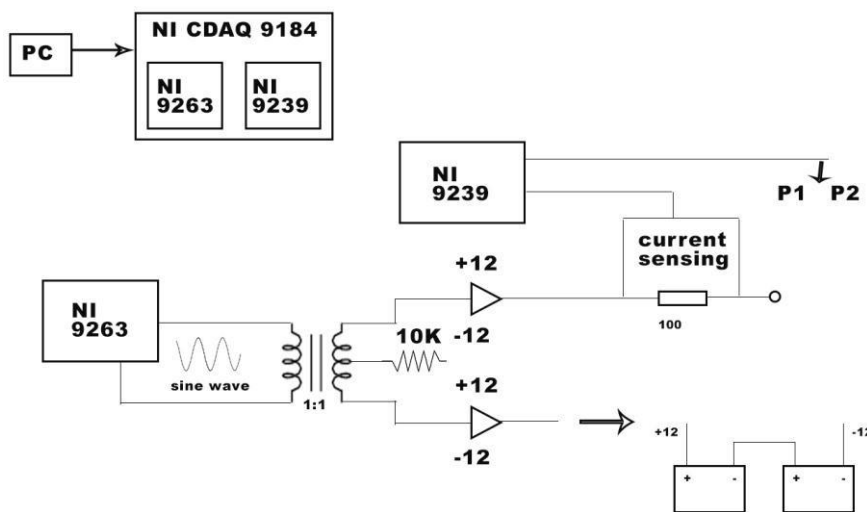


Figure 45. Simplified schematic of resistivity meter.

The prototype connected a computer with a National Instruments (NI) CDAQ 9184 4-Slot Ethernet Chassis. The chassis was designed for remote or distributed sensor and electrical measurements. A single NI CompactDAQ chassis can measure up to 128 channels of electrical, physical, mechanical, or acoustic signals. The CDAQ 9184 contains two modules, and analogue to digital and a digital to analogue. The digital to analogue is a NI 9263 module, ± 10 V, analog output, 100 kS/s. This inserts a sine wave signal, through a 1:1 non-grounded transformer. This then goes in a 10k resistor and splits on two branches, each with an amplifier; one branch is connected to the batteries (resulting in the C1 and C2 electrodes), while the other is responsible for the current sensing, through a 100

ohm resistor. This current sensing then passes through an analogue to digital module, the NI 9239, which has a 24-bit resolution. Two other channels from the NI9239 are responsible for the P1 and P2 electrodes. In order for this to work an effective ERT, everything passes through a custom switchboard, which basically has an on and off relay for each electrode, with a 40 dB on-off isolation. The frequency for the data is 775 Hz.

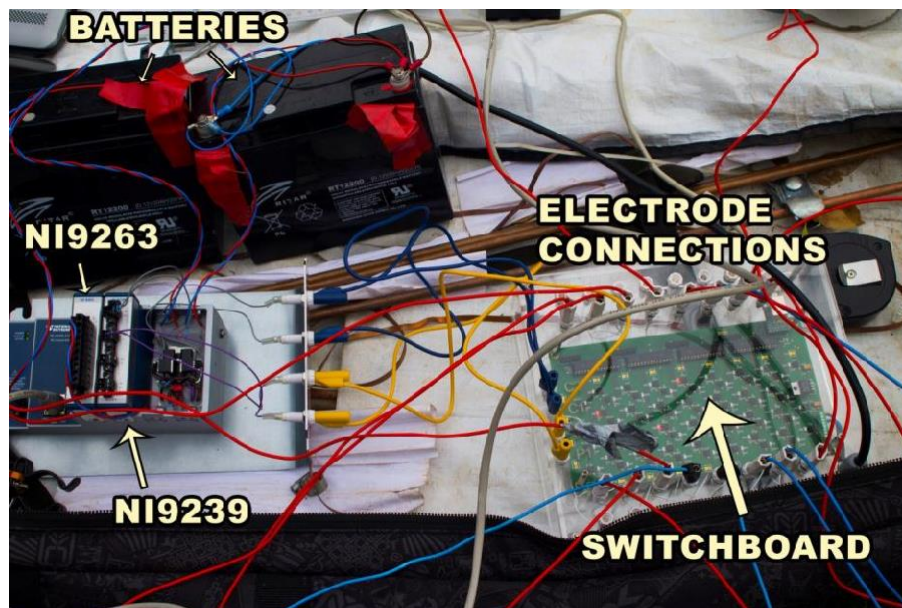


Figure 46. Photo taken of the custom equipment on the field.

However, while the approach has promise and warrants a separate investigation, it was not possible to eliminate all uncertainties from the system and therefore this equipment was only used for preliminary surveys. A result with this equipment is presented in section 4.6.

3.2.5 Software / algorithm development

In order for the switchbox to function properly, it must be controlled by an algorithm. The main advantage here is the flexibility and customization: every geometry and combination of geometries of ERT, be it regular or irregular, can be designed, at the will of the operator.

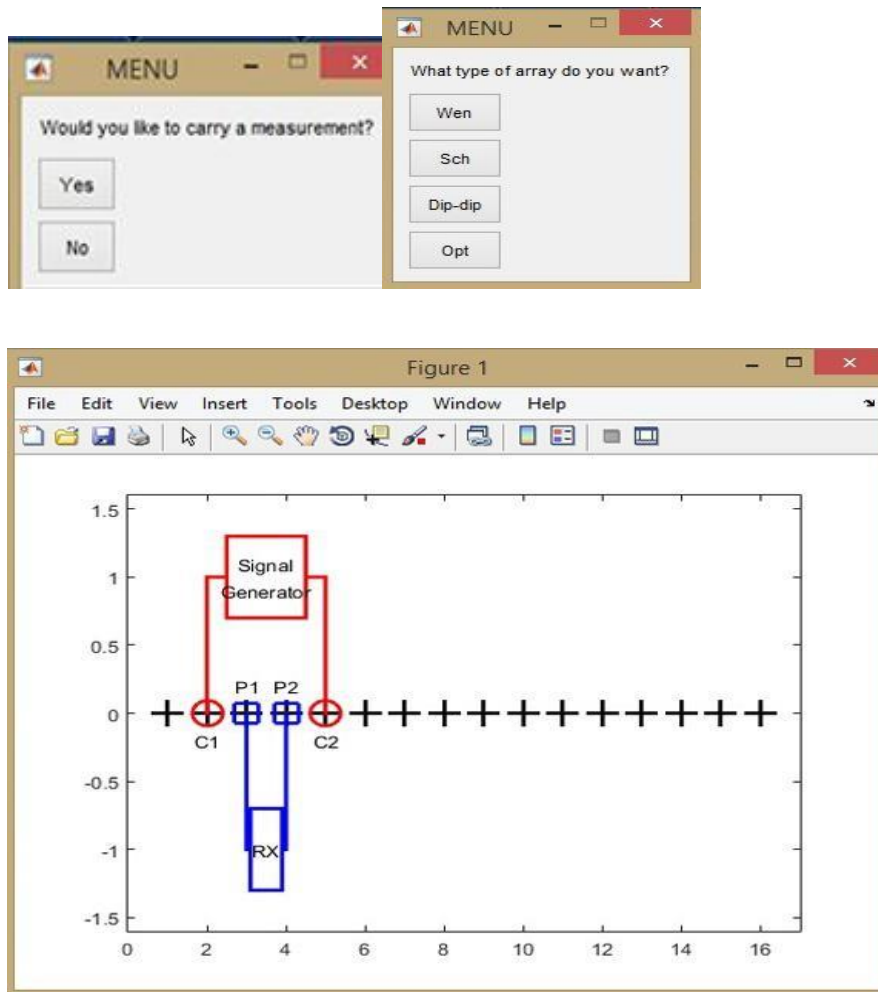


Figure 47. Screenshots from the software: profile initialization (top), geometry selection (middle) and current electrode position (bottom).

The first operating algorithm was designed in Matlab and was trialed in various situations, both in lab measurements and real-life scenarios, using different geometries. A significant advantage of this algorithm is that it enables to operator to ‘see’ the measurements in real time, which has practical advantages while doing measurements in the field.

Conversely, for the second switchboard, algorithms were designed in the open-source Arduino IDE, mirroring the Matlab ones. This second device was tested in the

same lab environment, with a similar resistor test.

3.3 GPR surveys

GPR surveys are an integral part of this study. GPR is one of the most high-resolution geophysical methods, can be carried over most surfaces (both natural soils and man-made structures), offers excellent resolution (depending on the antenna frequency), and is generally a fast method. Still, measuring something as minute and low-contrast as tree roots is pushing the method to the very limit, and in many cases, the physical limitations of the method become obvious.

There is no shortcut to developing an effective survey. All surveys require careful planning, backed up by a sound understanding of the geophysical method, the objective, and the environmental conditions. Careful consideration must be given to site-specificity and the objective of the survey. Surveys were carried out over both natural soils (with or without vegetation). The data acquisition methodology was not much different between the two, though the processing and interpretation were somewhat different.

Two different commercial GPR systems were used for this research. The first one is a dual system IDS GPR, incorporating a 250 MHz and a 750 MHz antenna. The second one is an UTSI Electronics system. Two antennas were also available here, a 1.5 GHz and a 4 GHz antenna. Both systems come without a console and require a computer or tablet running a designated software. Both systems were tested over a known setup (pipes on campus that were clearly marked by the construction crew) to verify their accuracy and precision.



Figure 48. Typical soil survey using the 1.5 GHz Utsi antenna. Ropes and rulers were used to mark the survey area and ensure profile data acquisition on the right trajectory.

The broad range of frequencies offers flexibility between depth of penetration and resolution. With the detection of tree roots, the latter is much more important than the former. As a result, the 250 MHz antenna offered little useful information, being usable for only the coarsest of the tree roots. At the other end of the spectrum, the 4 GHz antenna also proved to be limited in its applicability due to its extremely high frequency which limits its depth of penetration to only a few centimeters in practical scenarios, rendering it unusable in most situations.

3.3.1 GPR software and processing flow

In general, and perhaps moreso in urban areas than in other sites, GPR radargrams are cluttered with noise and extraneous reflections. Consequently, they must be cleaned up before interpretation (Guo et al., 2013). The general objective of GPR processing in this case was to

prepare an image that improved the signal-to-noise ratio, making it easier to interpret (per Daniels, 2004). The first advanced processing flow was described by Butnor et al. (2003), and Guo et al. (2013) mention that in the literature, GPR surveys for tree roots include radargram standardization, signal amplification, migration, and Hilbert transformation.

The guiding principles of data processing here were those discussed in Cassidy (2009a): “keep it simple; keep it real; understand what you are doing; be systematic and consistent”. The GPR processing was carried out in ReflexW, a commercially available software which offers a robust filtering capability. After the raw data was imported into ReflexW, a number of processing steps were applied. Depending on the site-specific requirements and conditions, some or all of the following were applied:

- static corrections (geometry, start and end point, time cut);
- de-wow;
- butterworth bandpass (typically starting from 0.5x to 2x the central frequency);
- gain;
- background removal;
- trace stacking (0-4 traces);
- Kirchoff migration;
- Hilbert transform.

All these filters and their parameters are described in great detail in the ReflexW manual (https://www.sandmeier-geo.de/Download/reflexw_manual_a4_booklet.pdf).

Unless otherwise specified, all GPR surveys follow this general processing flow, though not all steps are necessarily applied (ie some surveys did not include trace stacking, or migration, etc).

Multiple alternative processing flows and various alternatives were trialed, often

to comparable results. However, the above-mentioned were chosen as a standard flow (though in some cases, the radargram appeared easier to interpret pre- migration and Hilbert transform).

Ultimately, a 3D file was generated from 2D profiles in most situations, as the continuity of the root is essential in this type of identification (since roots can have varying permittivity values which do not serve as a good diagnostic tool, this lateral continuity was regarded as the best indication for identification of tree roots; the root can be distinguished by man-made linear features such as cables or pipes based on strength of reflection and, almost always, by irregularities in the linear geometry). As it has been previously discussed (Jol, 2009), 3D visualization and time slices are an important aid in interpreting data – especially in this type of scenario.

3.4 Resistivity surveys

Resistivity surveys have been used in a wide range of environments, with many and varied objectives. The application of electrical measurements (particularly resistivity) to identify a biological objective is unusual, however. The tree roots lie in the shallow parts of the soil, so the surveys fall under the umbrella of near-surface geophysics. The objective in case seems to be at the intersection of environmental and engineering geophysics. Tree root measurements carry a resemblance to agricultural geophysics, but there are differences in the scope, as well as environment. Agriculture geophysics focuses more on determining soil parameters such as water content (Huisman, Hubbard, Redman, & Annan, 2003) and conductivity (Corwin & Lesch, 2005). Even when the focus is on plant roots, the emphasis is usually on the overall root biomass rather than individual roots (Konstantinovic, Wöckel, Lammers, Sachs, & Martinov, 2007).

This distinction is not just semantic, because the methodologies in the different parts

of geophysics vary. Therefore, approaches from all areas were considered, and different parameters were tried out (for instance distance between electrodes and type of array).

3.4.1 Resistivity equipment

The main measurement unit was a 4-electrode TAR-3 Resistance Meter from RM Frobisher. The unit was designed specifically for archaeology resistance mapping (reasonably similar in scope), and generally outputs data in a grid geometry. However, this data was always discarded – only the resistance value was recorded directly, and the geometry was noted separately. The equipment was tested in the lab, using a series of resistors connected to a breadboard, confirming its precision and accuracy. For multi-electrode and ERT measurements, the device was connected to a custom switchbox, as described in subchapter 3.2.4.

The size of the electrodes was also a significant consideration. Since most commercial electrodes are on the order of size of the geophysical objective, an alternative was used: thin, stainless steel pegs. Thick electrodes seemed to have a notable effect on surveys, which is not present in the case of thinner electrodes.

3.5 Total station

Some surveys were accompanied by a total station survey. The usage of a total station to track GPR movements is, while not a novel technique (Trinks et al., 2010), still a state-of-the-art approach, helping to limit operator missteps and applying other corrections (i.e. minor topography modifications) that would escape the open eye. Here, the total station has also been used to map asphalt and concrete cracks caused by tree roots (for comparison with geophysical data), as well as the deformations associated with cracks (slight positive topography caused by the roots). The total station surveys were temporarily brought to a halt by a campus-wide ban on all laser usage.

Ultimately, the goal of these surveys was to assess the feasibility of identification of individual roots and the potential of ERT as a complement to GPR in identifying tree roots.

4. RESISTIVITY IMAGING OF TREE ROOTS

As any other geophysical method, GPR has inherent limitations and even without these limitations, the permittivity contrast between tree roots and soils is sometimes insufficient to allow detection (Mihai et al., 2019). As it is often the case, a second geophysical method adds another dimension of subsurface understanding, and resistivity is a viable (albeit more cumbersome) alternative.

Without using capacitive (or other types of non-contact) equipment, resistivity can only be applied non-destructively on soil surfaces. Since capacitive method is still insufficiently developed and matured to be applied robustly, only resistivity soil surveys were considered for this study. Even so, in addition to the study of tree roots under these soil surfaces, some deductions can be made about roots under paved surfaces. For instance, the direction of roots penetrating into the sidewalk and asphalt can be extrapolated from measurements on neighbouring soil surfaces.

4.1 Approach

Thanks to the recent increase in computation power, most modern geoelectrical studies use some form of a multielectrode setup, which enables a more robust and capable measurement system than just the 4 “traditional” electrodes. This allows more data to be gathered in a short amount of time, and offers flexibility – tree root surveys benefit from this just as any other type of survey. The data is acquired, processed if necessary, and inputted into the software, where it is inverted. To test the suitability of the method, the first surveys were carried in areas where root areas were visible on the surface (or their position could be inferred from segments visible on the surface).

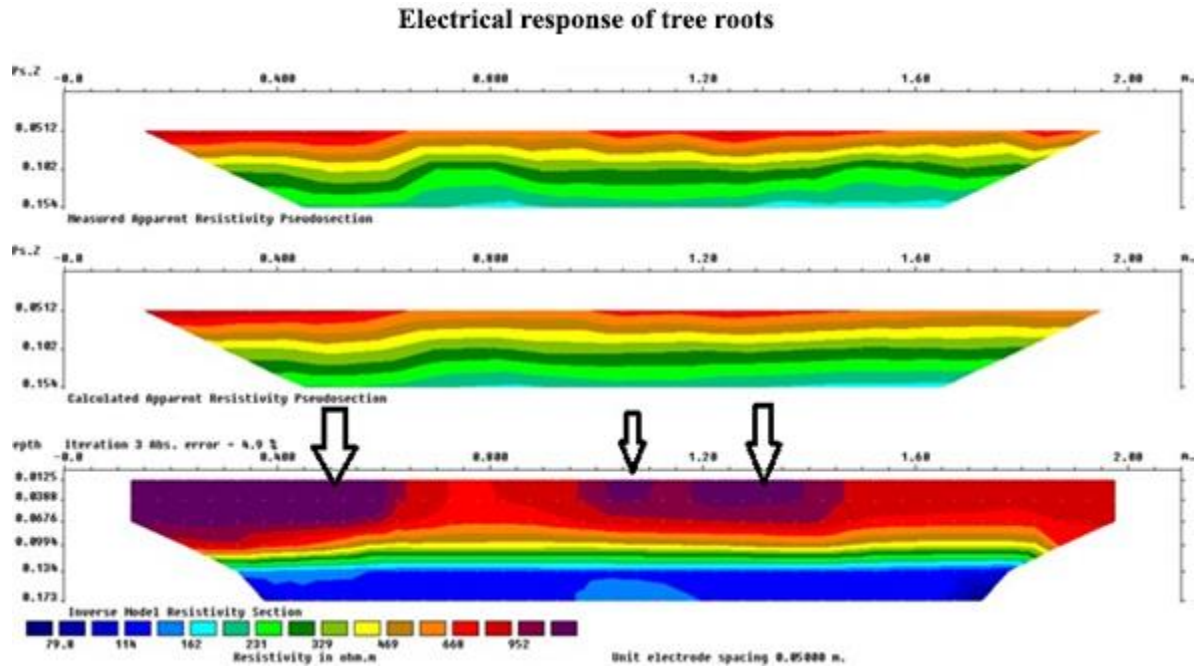


Figure 49. Example of data inversion with Red2DInv, the lowest slice representing the final iteration with the lowest errors. High resistivity anomalies can be interpreted as tree roots, with lateral continuity serving as an important tool for identification. Here, the three black arrows indicate roots which were visible on the surface.

A number of different surveys were carried out. Not all are presented here – a selection is made for the ones that hold distinctive results.

4.2 Survey 1

The first ERT surveys used an established methodology. The survey exemplified here was carried around an apple tree (*Malus* genus) in Hornton Grange, in the campus of UoB, close to the Gisbert Kapp building.

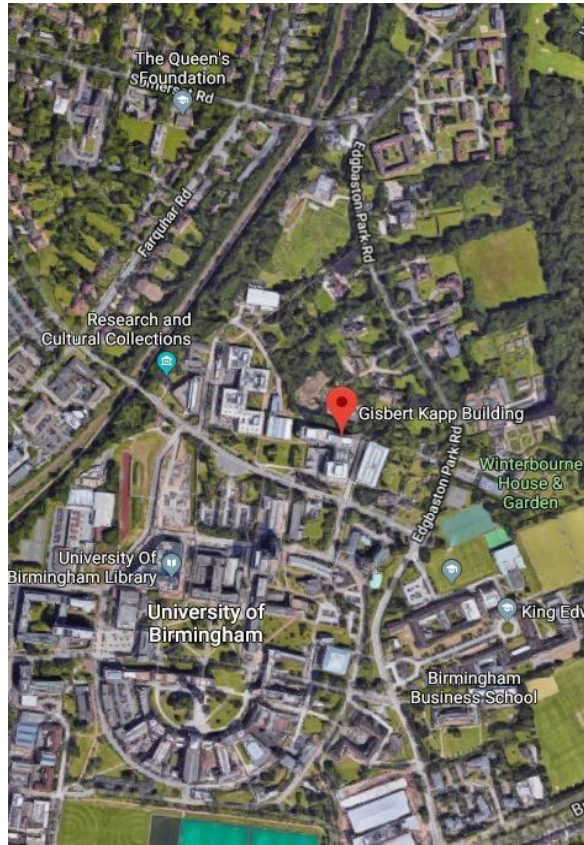


Figure 50. Most surveys were carried out on the UoB campus, an urban area with some green spaces and plenty of tree root-infrastructure interactions.

The purpose was to test the method in a practical setting in the detection of tree roots. The terrain was flat, the soil was a wet clay, and one of the roots was slightly visible on the surface. This was actually why the site was chosen as a test, because the position of at least one root could be confirmed visually without any digging.

The survey essentially consisted of 4 parallel profiles carried out perpendicular to the visible root, at a distance of 10 cm one to the other. The distance between consecutive electrodes was 10 cm. A total of 16 electrodes were employed, using a Wenner Array.



Figure 51. Depiction of the survey. Stainless steel pegs were used as electrodes and the root was partially visible on the surface.

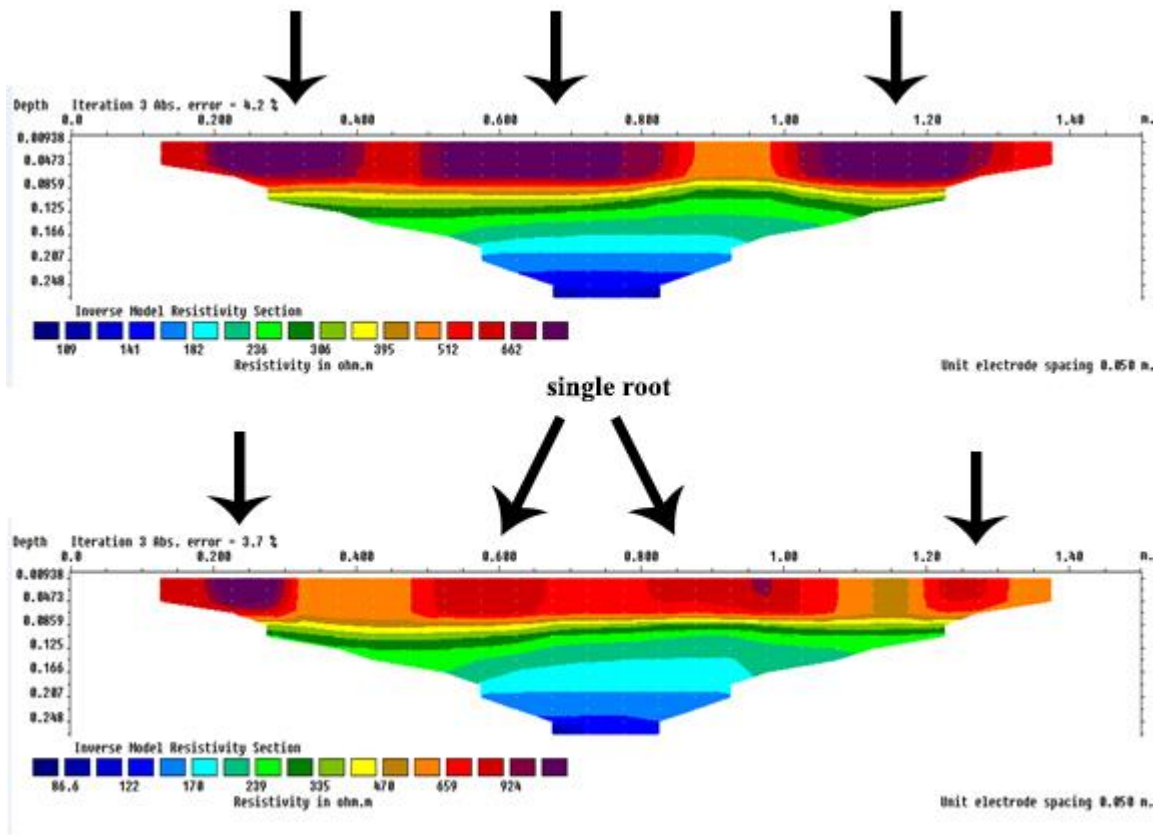


Figure 52. Results from two profiles 15 cm away. The same three roots are visible on both profiles (highlighted by arrows), but in the second profile, one root appears as two separate anomalies. Results in Res2DINV.

Aside from the root segment which was visible on the surface, two other roots were

identified (and confirmed by scratching away the topsoil). However, they were not equally visible on all profiles, and one profile seemed to depict one root as two separate contrasts.

The survey confirmed that the approach can indeed resolve at least some (thick) individual woody roots in real-life conditions. However, while the presence of roots could be inferred from the high resistivities and lateral continuity, there was significant ambiguity regarding the exact position of the roots and their width, as well as uncertainty regarding the potential to identify thinner roots. In different profiles, the position and width of the root appeared to be somewhat offset. High lateral soil variation was also experienced. However, it is plausible that these aspects are an artifact of the data inversion and have no physical significance.

It also became apparent that resistivity anomalies overestimate the size of the roots, this being potentially the reason why roots immediately below the surface appear, on resistivity profiles, to extend to the surface.

4.3 Survey 2

After confirming the feasibility of the method in several situations, the shift focused towards a mapping of the root system. The survey presented here involved a similar methodology, though with more parallel profiles, so that the representation of a 3D area would be possible. A similar equipment was used, using the same geometry, electrode spread, and type of array.

However, for the data inversion and representation, a combination of BERT and Paraview were used.

The measurements were carried out in the immediate vicinity of an apple tree (*Malus* genus). No roots were visible on the surface, but given the proximity to the tree, it was assumed that there were some roots beneath the surveyed area – an assumption which

turned out to be true.

Since the data visualization is a bit more difficult to view on paper or in a still medium, several images are presented below to depict the advantages (and disadvantages) of this type of visualization. The data was visualized in BERT and Paraview as this offers a way to add transparency into the models (see figure 55), which was deemed useful.

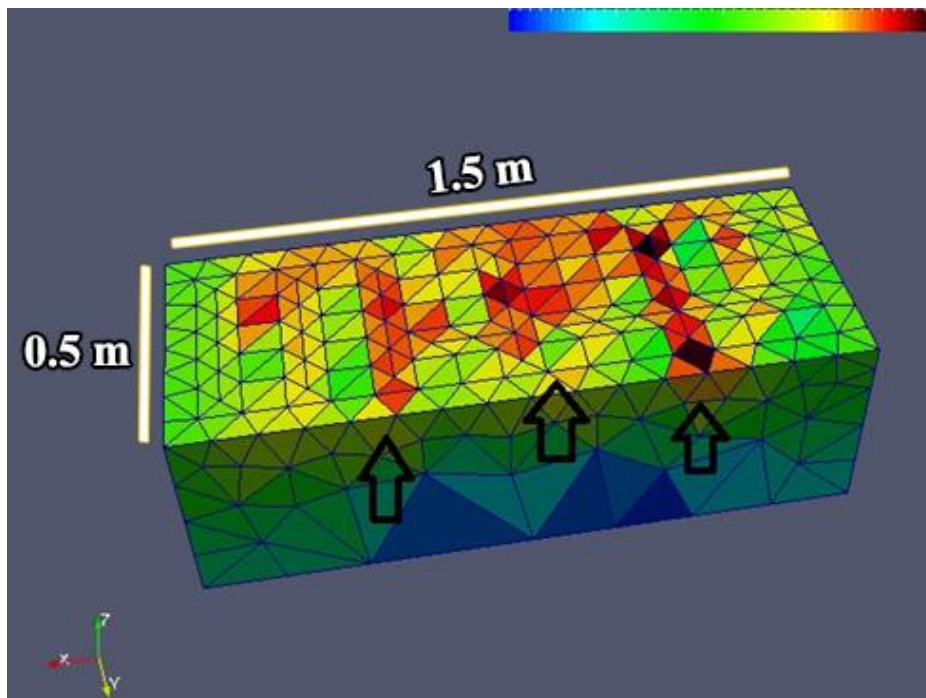


Figure 53. Data visualization showing the triangular discretization cells. Three root areas were identified and confirmed by shallow soil scratching (highlighted in arrow). The overall shape of the data output by BERT is different than “conventional” inversion software, being rectangular rather than triangular. However, since there is no additional data, the extra parts (on the lower lateral sides) is gathered completely from extrapolation and was therefore discarded. This is not a major aspect in this study, since the object of interest is in the shallow parts of the surveyed area, but is important to keep in mind.

It is noteworthy that although the roots were not visible on the surface (approximately 10 cm deep), they appeared to be on the surface when visualized on the resistivity data.

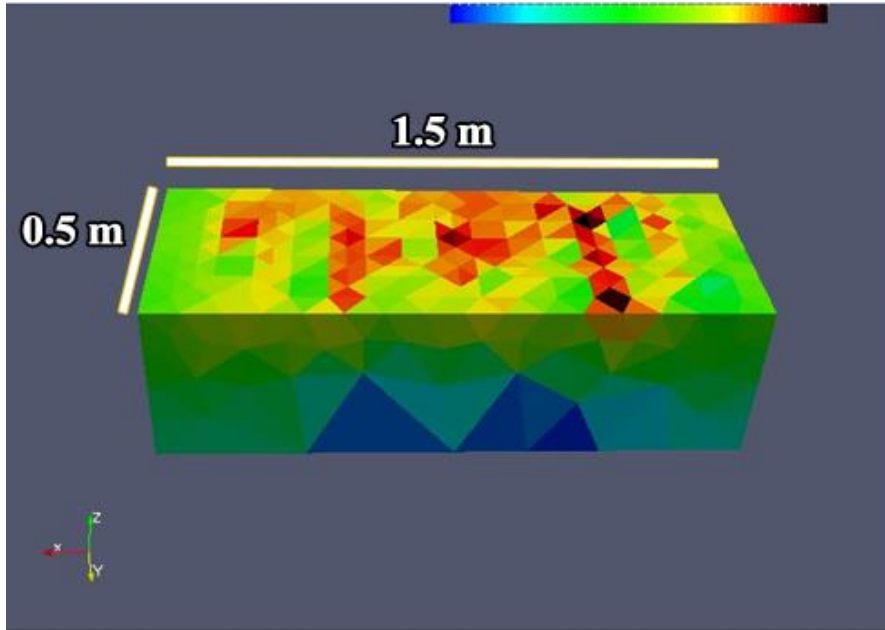


Figure 54. The same data, viewed from a slightly different angle, and without the discretization cells borders.

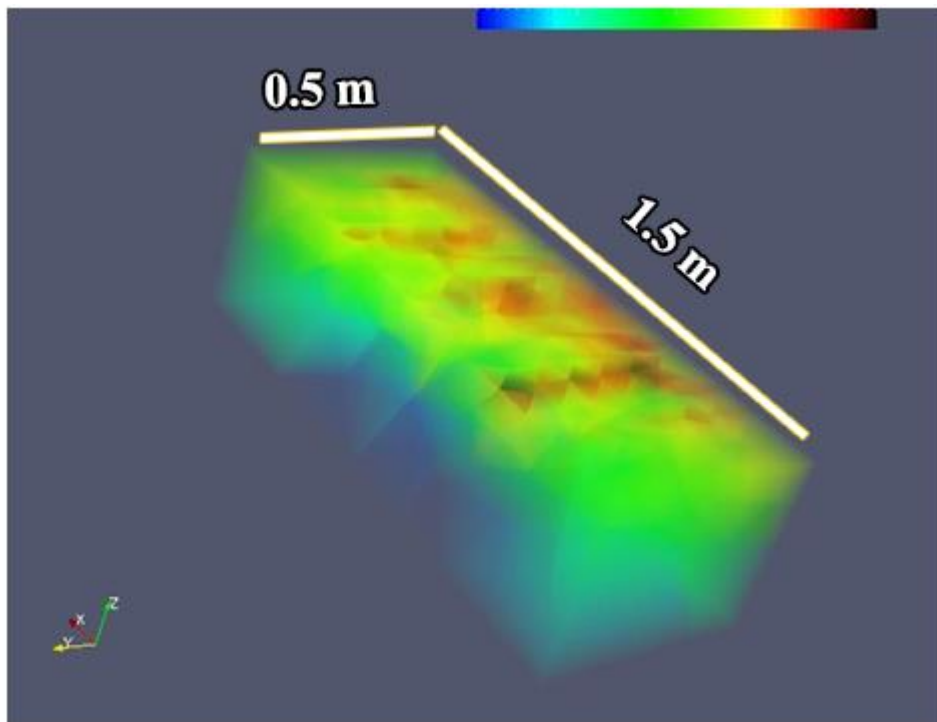


Figure 55. The same data, with added visual transparency. The transparency allows an excellent visualization of the trajectory of the roots and any other elements in the subsurface.

At this stage, still only the Wenner array was used, highlighting that even this simple array (with only 35 data points per 16 electrode profile) is capable of imaging roots successfully. Four individual coarse roots were successfully identified, as well as an area which contained numerous thin roots. These individual thin roots could not be

resolved individually, but the root area was revealed as an area of high resistivity.

Again, the position of the anomaly oversize the root itself, but nevertheless, individual roots were resolved with resistivity measurements, proving the potential applicability of this method.

4.4 Survey 3

Several comparison surveys were carried out with different arrays. In this type of surveys, not only was the distance between electrodes very small (5 or 10 cm), but the geophysical contrasts also vary sharply over small areas. This poses unique challenges to ERT arrays, pushing the approach to its very limit. Consequently, it was not overly uncommon for the inversion algorithms to produce larger RMS errors or even to not reach a convergent solution. The OPM array was the most vulnerable to this type of scenario, potentially owed to the fact that it concentrates its data points in some particular areas, while leaving other areas sparser. Although the array seems to perform well at larger electrode spacings and holds promise in multiple scenarios, it seems less well suited for this type of survey. Unexpectedly, the Schlumberger array also reported similar errors. RMS errors in an unacceptably high range of 15-20% were not uncommon for the Schlumberger array, and were not owed to one or two anomalous data points. In order to reduce the errors to an acceptable range, so many datapoints had to be eliminated that the Schlumberger array became virtually indistinguishable from the Wenner. As a result, most surveys focused on the Wenner and Dipole-Dipole arrays. While this was mostly an empirical conclusion, the Dipole-Dipole and Wenner arrays seemed to consistently yield more reliable results.

The two arrays performed surprisingly similar, despite their noted differences. The

Dipole-Dipole array tended to produce larger exaggerations of the root size but was more sensitive to lateral changes across the entire profile, whereas the Wenner array had more mixed results: sometimes, it produced more accurate representations of roots, but other times, it appeared to not detect fine roots at all, or split a single root into two different anomalous areas, suggesting the existence of two roots, where this is not the case. This is excellently represented on the survey presented here. Overall, the Wenner array produces surprisingly adequate data despite a reduced number of data points. This is encouraging and suggests that, given the short time of acquisition, the classic Wenner array is still a consideration in this type of study.

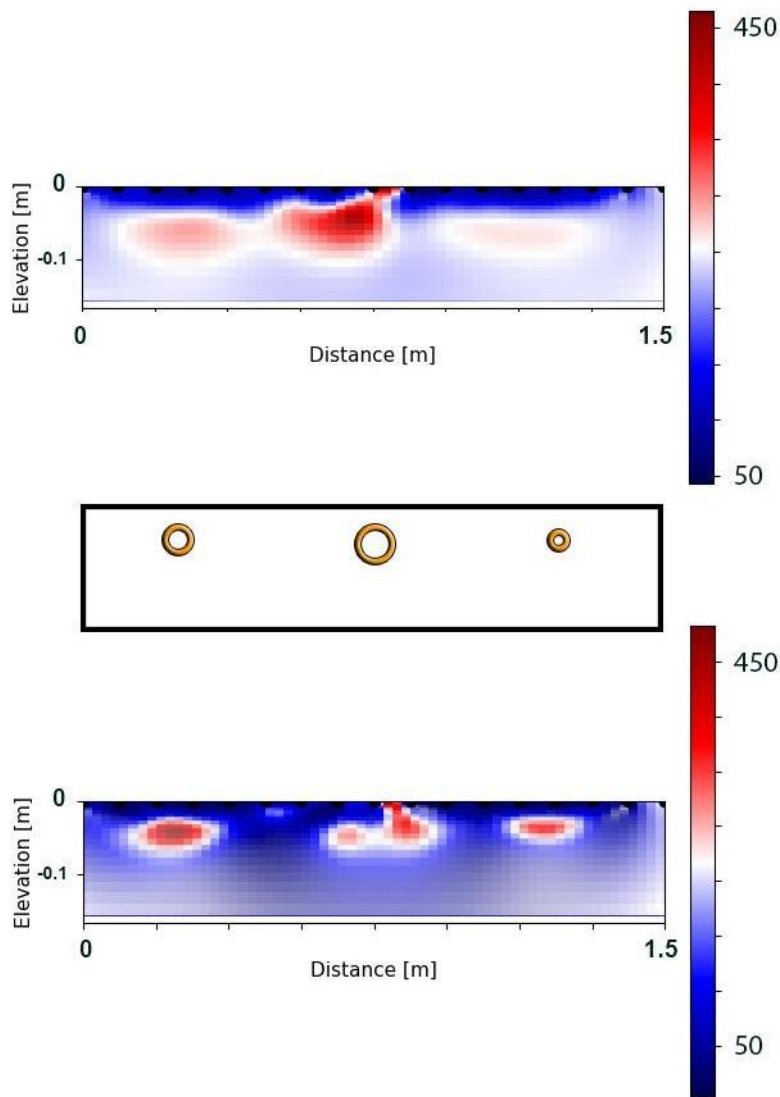


Figure 56. Comparison between a Dipole-dipole profile (top), a Wenner profile (bottom), and the actual

position and size of the roots (middle).

The middle root was indeed slightly visible on the surface in one point, as indicated by both arrays in image 56. However, this was the only position where the middle root was visible on the surface. The Dipole-dipole profile exaggerates the lateral dimension of the roots even further. Meanwhile, the Wenner profile did not continue to separate the anomaly from one root into two separate anomalies on other profiles (see following image).

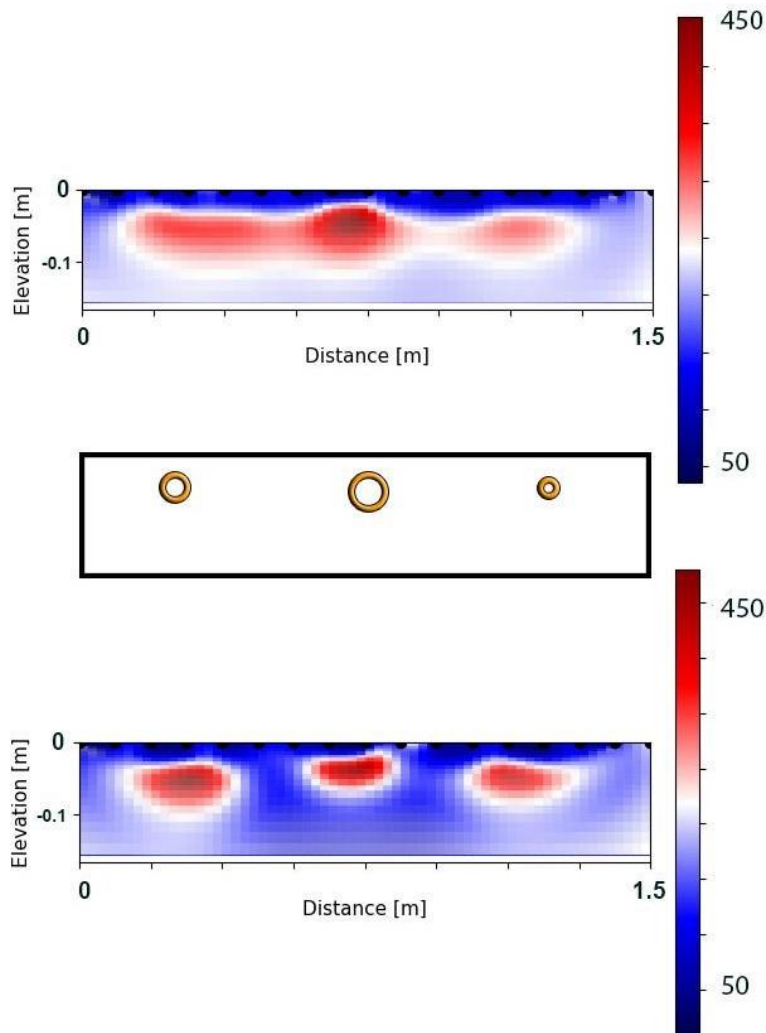


Figure 57. Comparison between a Dipole-dipole profile (top), a Wenner profile (bottom), and the estimated position and size of the roots (middle). The profile is parallel and 30 cm away from the previous one.

While the positive anomalies are indicative of the root positions, they don't

completely coincide. However, this is likely to be an inversion artifact and not relevant in a practical scenario given the scale of the surveys. Establishing the existence of roots is the main objective, and this is possible using ERT.

Unlike the GPR surveys, the absolute values of resistivity are not of interest – the geophysical contrast and detectability were the main objectives. In addition, the data were migrated into Paraview, where several visual processing steps were applied for better data visualization (this being the reason for including this separate visualization). A more complex survey of integrated GPR-ERT data is presented in subchapter 5.10 using these techniques.

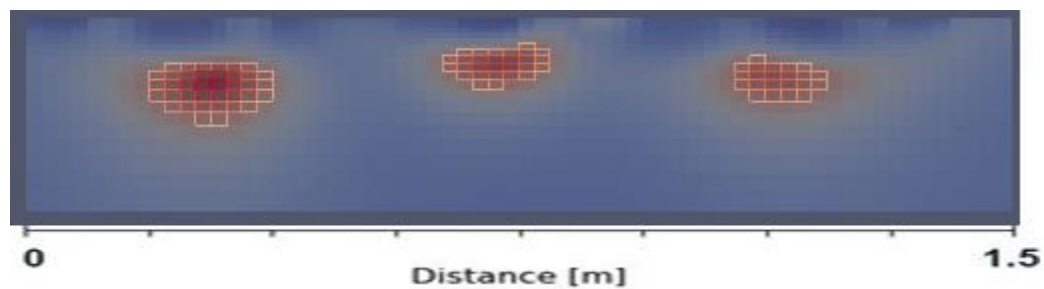


Figure 58. Applying a scalar clip to an ERT profile to highlight the position of the roots.

4.5 Box surveys

Several surveys were also carried out inside a test box filled with soil. The main objective was to test several scenarios in a controlled environment, since the resistivity parameters of roots have not been thoroughly analysed. Experimental observations from controlled and natural environments (Amato et al., 2009; Werban, Attia, & Rabbel, 2008) suggest that coarse roots produce high-resistivity anomalies, but it is less clear what type of resistive anomaly thin, conductive roots produce, particularly in relationship to the observation of Zenone et al. (2008), that “the density of roots may be related to the accumulation of capillary water and to the presence of low-resistivity haloes around the

tree”. This was explored experimentally with one, and then up to 3 single thin roots. The goal was to see what type of anomaly (if any) would be observed, and how pronounced it could be. Even if no response would be observed (which turned out to be the case), this can still be considered a positive result, as it underscores a limitation of the method.

A single type of soil was used: a clayrich in organic matter, commercially acquired. It is worth noting that this cannot be assumed to be representative of all scenarios. The sheer variability of soils, in terms of chemical and mineral make-up, water content, porosity, and micro-ecosystem should not be underestimated. The impact that all these parameters have on geophysical surveys is significant, and was not replicated here. We must not fall into the trap of believing that one experimental setting is representative for all real-life scenarios. Instead, this was only meant to serve as an indicator for detectability. The electrode positions were marked with a drilled acrylic plate according to the methodology described by Gerea et al. (2019).

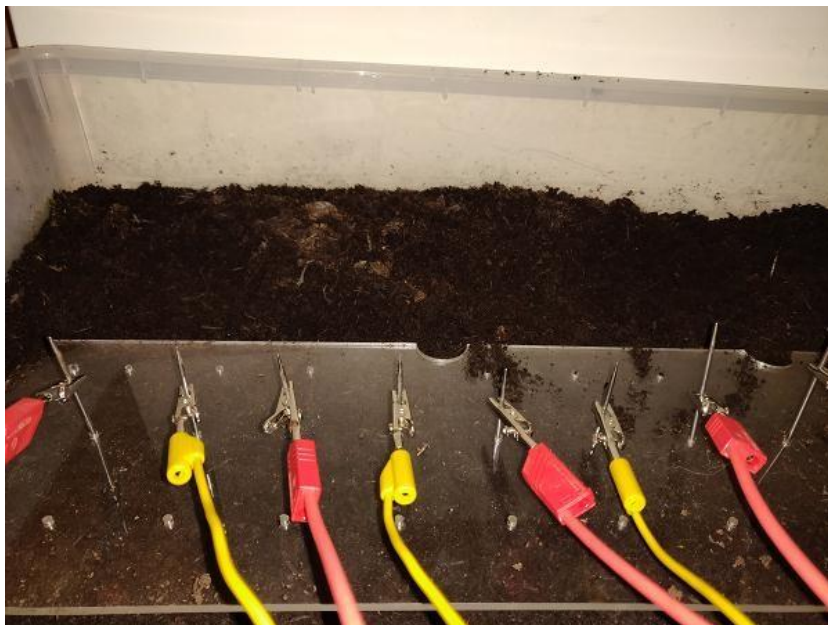


Figure 59. The experimental electrode setup.

No significant resistive effect was noticed. Thin roots (diameter < 0.6 cm) were buried but did not produce a detectable contrast, and are considered unlikely to be detected

in a real scenario, if they are not detectable even under ideal conditions with no clutter or noise. Thin conductive electrodes were also buried, and they were also not detected.

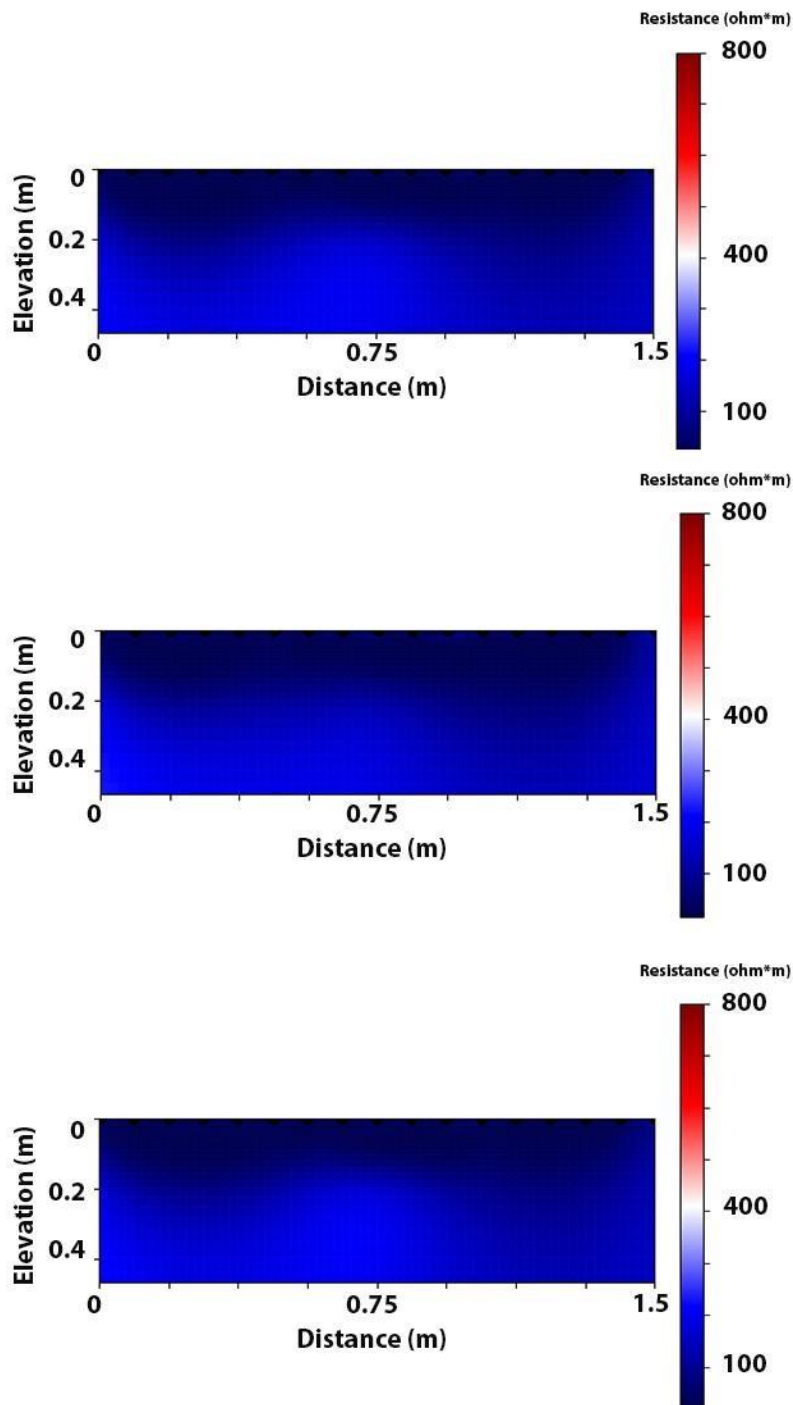


Figure 60. Survey with the Dipole-Dipole array. Top: empty soil box. Middle: buried root. Bottom: buried electrode. Nothing but the background values is detected.

The results may yet be noticeable under different environmental conditions (in some

types of soil), but this suggests that detecting very thin roots is unlikely, and the subsequent measurements were focused on coarse roots expected to produce a detectable positive resistivity anomaly.

4.6 AC prototype

A proof of concept measurement was made using the prototype described in Chapter 3.2.4. The measurements were carried out in Hornton Grange, in the UoB campus.

Although the design prototype was not used in further surveys, it is worth noting as it has a few specific strong points (discussed in the above-mentioned chapter), which warrant its mention here. In addition to differences caused by differences between DC and AC, the speed of data acquisition was much higher – a significant practical advantage. As a result, this enabled the acquisition of a full tomography – with all possible non-symmetrical electrode configurations in a reasonable amount of time. The data was inverted and plotted in BERT. A representative profile is highlighted below.

The electrode spacing was 0.5 meters and a total of 32 electrodes were used for the profile. The survey covered a large tree as well as a shrubby area.

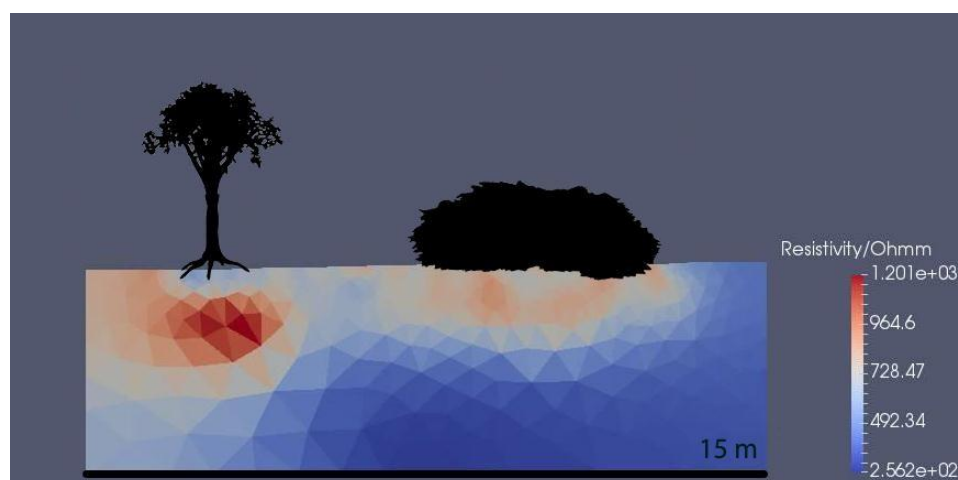


Figure 61. A “full” ERT profile with all possible electrode configurations.

Several aspects are remarkable here. Notably, there is an area of high resistivity as

well as an area of low resistivity. This could be owed to the fact that the roots themselves produce a positive contrast, but some root absorptive areas ‘hold’ water around them, producing a negative contrast.

The Wenner configuration produces results that are not too different, highlighting once again that there is not a direct relationship between the number of data points and data quality. This relationship has been addressed in the literature and is an area of active research; it was not expanded upon here, merely used as a comparison.

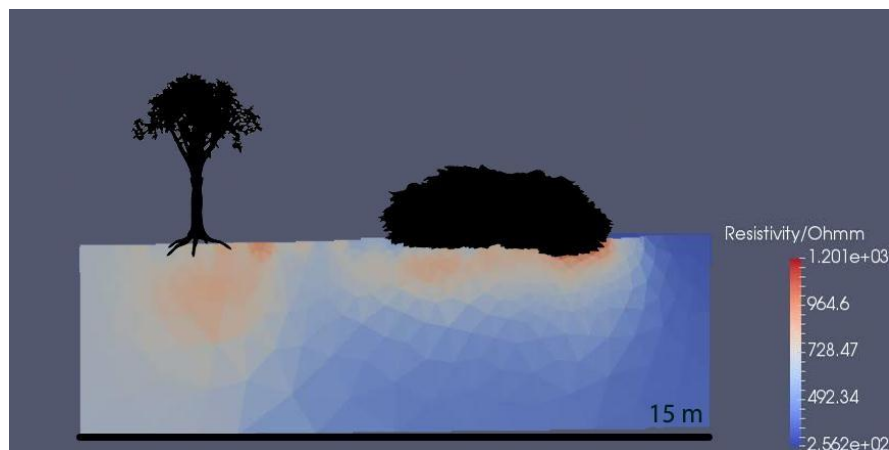


Figure 62. A Wenner pseudosection over the same line.

4.7 Tree as electrode

Another approach which was considered was using the tree itself as an electrode, so inserting current through the tree itself. This was not the first time this has been considered (Cermák, Ulrich, K, & Koller, 2006), yet this approach remains understudied and rather empiric. The quantitative replication of this approach has proven problematic and there are still many unknowns regarding the flow of current in this scenario and the potential utility of this approach. Since it is used for establishing root area and not distribution, it is not usable in its current state for the purpose at hand. However, this remains a qualitative approach usable in some niche scenarios, as was revealed by a number of preliminary surveys. In particular, a very simple method derived from this can

be used to assess if a root has penetrated from one side of the asphalt to the other.

The method is straightforward but limited, and only works in a particular setup. It relies on the conductivity of some roots, which has been verified. Given a tree in the vicinity of a paved surface, if there is a suspicion that one or several of the roots of the tree has penetrated the paved surface and reached another soil area, this can be tested thusly. Current is injected through the base of the tree as described. The current is then measured in the other soil surface. If the measurement is successful, this is an indicator that the root has indeed reached the other side.

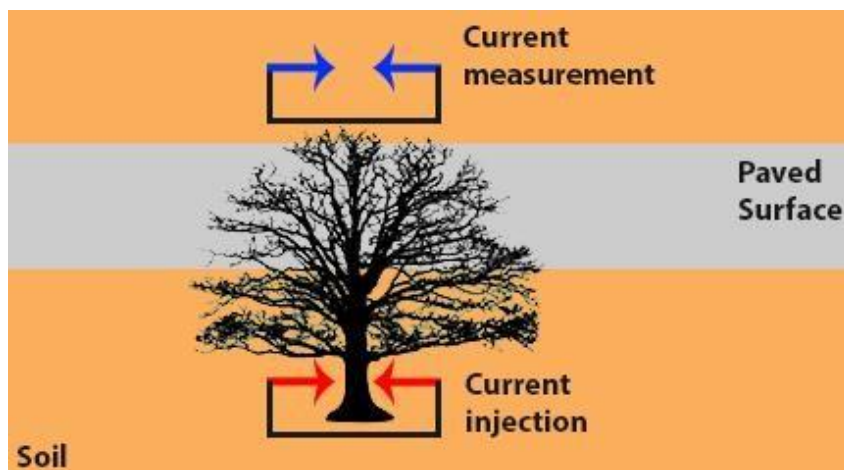


Figure 63. Depiction of the method setup.

There are clear limitations to this method. First, the root must have penetrated the paved surface completely to ensure conductivity between the two soil areas. Secondly, the root must be active and not diseased or inactive, in which case they would likely not be conductive. In addition, it must be ensured that the two soil areas are truly separated (and are not communicating in any way beneath the paved surface, as is often the case).

This is a minor but potentially significant finding whose implications have not been explored thoroughly. It has only been tested empirically, and more research is required to establish the potential and limitations of this method, as well as the full range of potential applications. Nevertheless, it is not impossible to envision the method

being applied in some scenarios as it involves a quick, low-cost setup, and can give immediate results. In particular, the method could be considered in areas where trees are planted in a small patch of soil (as is often the case in many cities).

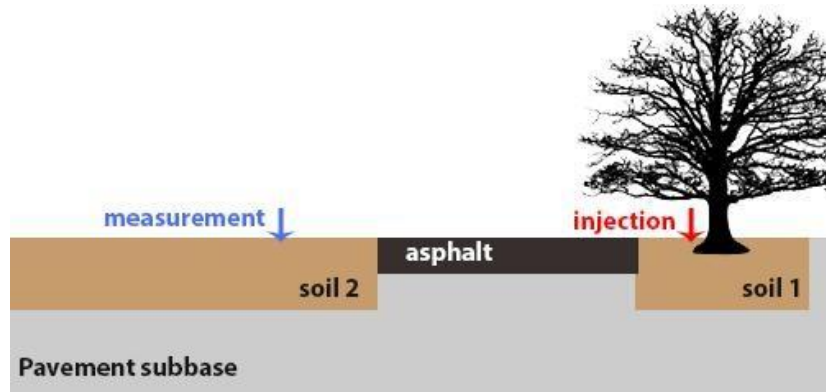


Figure 64. Depiction of potential application scenario. If there is an active root from soil 1 to soil 2, current will be measured in the soil 2 unit.

In addition, if the root area can indeed be assessed through the method described by Cermák, Ulrich, K, & Koller (2006), some assumptions can be made about how far the roots have spread. For instance, if the root area is calculated to be too large for a confined tree, there is a significant chance that the roots have spread beyond the confinement.

5. GPR IMAGING OF TREE ROOTS

The following will be a representative selection of GPR surveys, highlighting both the positive results, as well as the shortcomings and challenges of this method.

5.1 Approach

The detection of tree roots has been addressed a few times in the literature, so that was used as the starting point for GPR surveys: replicating the potential detection. The initial surveys started out in the close vicinity of trees, where the likelihood of tree roots beneath paved surfaces was high, and areas where tree root damage was visible on the surface.

After this, the mapping of tree roots was attempted on multiple types of surfaces, both paved and soil surfaces. Emphasis was placed on realistic scenarios, attempting to replicate a scenario in which a surveyor would attempt the mapping of tree roots and potential root-associated damage.

Unfortunately, digging under paved surfaces and verifying the results directly was not possible due to logistical reasons. In some cases, a shallow verification on soil surfaces was allowed but on paved surfaces, it was not possible.

A number of surveys have been carried out. Representative results are presented here.

5.2 Survey 1

Given the inherent variability between relevant environmental factors, numerous surveys were carried out in various settings, attempting to characterize root detection in multiple situations. Several of these surveys are presented in the following, highlighting different situations and scenarios.

Poplar Tree survey (Poplar 1)

The following survey was carried around a very large poplar tree (*Populus* genus) in what was the North Gate parking lot in the Birmingham University campus. That part has since been demolished but unfortunately, no access was permitted to see the actual location of the roots during the demolition.

In total, 27 profiles spanning 6 meter in length were carried out (total area: 3.9 x 6m). The data was acquired in one direction, with a distance between profiles of 15 cm. The 750 MHz antenna was used. No migration was applied. 2D profiles were merged into a 3D file.



Figure 65. Image from the site with potential root damage visible on the surface.

Damage from the poplar tree roots was visible on the surface in some instances (though it was not always clear if the damage was caused by roots). The goal was to assess whether the GPR data correlates with surface observations, and if other tree roots can be

detected. Another objective was to assess whether the tree root damage is shallow only, or if it also extends in depth, which would also be an indicator of the position of the root.

Discontinuities in pavement continuity associated with a hyperbola were considered a strong indicator for tree root detection, especially where lateral continuity could be established. Such areas were “picked” in ReflexW.

As expected, the two areas where damage was visible on the surface were also visible in GPR data.

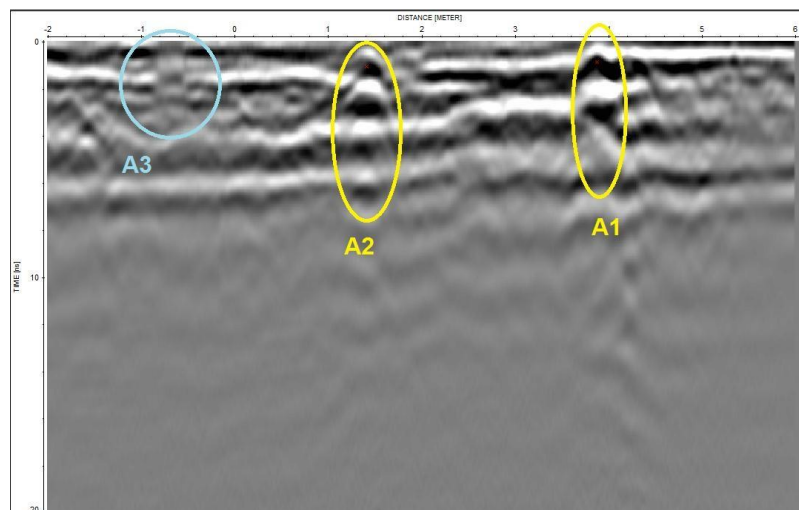


Figure 66. Profile from the survey with A1 and A2 depicting hyperbola from tree roots causing damage to the paved surface, and A3 depicting damage that appears unrelated to tree roots.

The areas highlighted in yellow (Poplar1_A2 and Poplar1_A2) can serve as models for tree root detection, with the pavement’s continuity is interrupted by the hyperbola caused by the root. Meanwhile, the area highlighted in light blue (Poplar1_A3), while also featuring a discontinuity, does not seem to be associated with a hyperbola and therefore represents an area of degraded pavement, but it is not clear if a tree root is causing the damage. This is consistent with the forward models simulated in chapter 3.2.3 – the damage to the asphalt is sometimes easier to detect than the presence of a

root.

The extent of the damaged pavement area is presented below, largely but not fully corresponding with the distribution of tree roots.

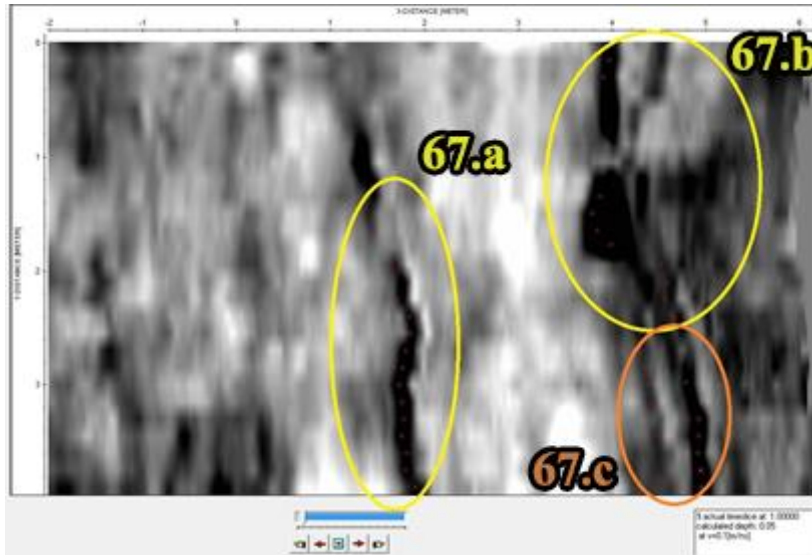


Figure 67. Yellow areas indicate root damage visible from the surface, orange area was not visible on the surface.

The two areas highlighted in yellow (67.a, 67.b) were also visible on the surface, but a third area (potentially consisting of two separate roots) also emerged, highlighted in orange (67.c). The two roots appear to branch out from a larger one – one is in direct continuation to the visible surface damage, whereas the other one branches at a slightly different direction. This signal from the second root was, while detectable, much fainter. The lateral continuity enabled its identification as a root which had not yet caused visible damage to the surface.

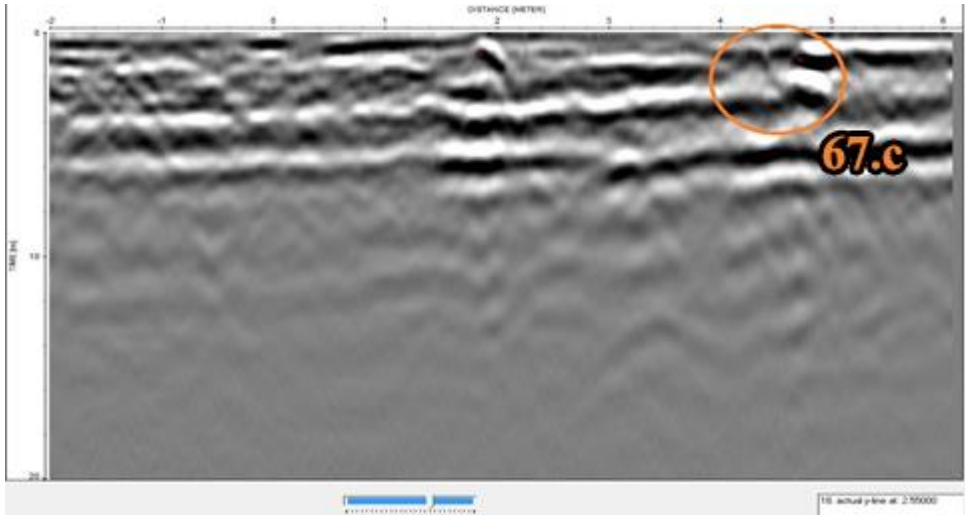


Figure 68. Profile from the survey. Unmigrated data.

Interpreting the data is challenging, and also provides lessons for future surveys. The profiles and slices must be analysed together for better interpretation. A single reflection is not sufficient to indicate a root, and lateral continuity must be established. Similarly, a faint or inconspicuous feature can be indicative of a root provided that it has lateral continuity. Picking potential roots and then visualizing their projection can help to delimitate roots.

Hyperbolae suspected of being roots were “picked” in ReflexW and the lateral continuity of 3 roots was determined (although this was not always visible on the time slices). This seems to suggest that the 67.c feature consists of two separate roots.

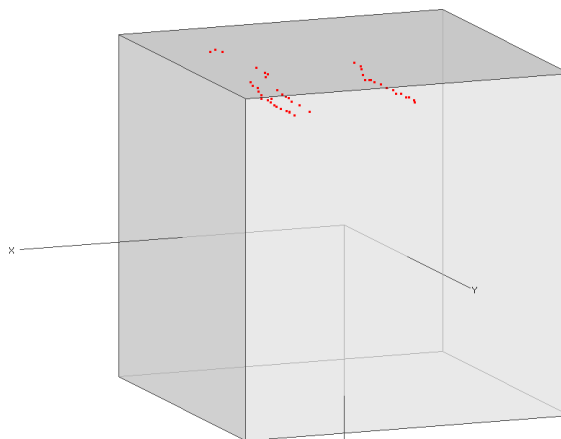


Figure 69. Plot of tree roots. Red dots are peaked apex of root-associated hyperbolae.

Different colour scales can ease visualization. Here, blue and violet indicate pavement degradation/discontinuities (not necessarily tree roots). Visualizing timeslices at different depths can also help identifying the position of roots.

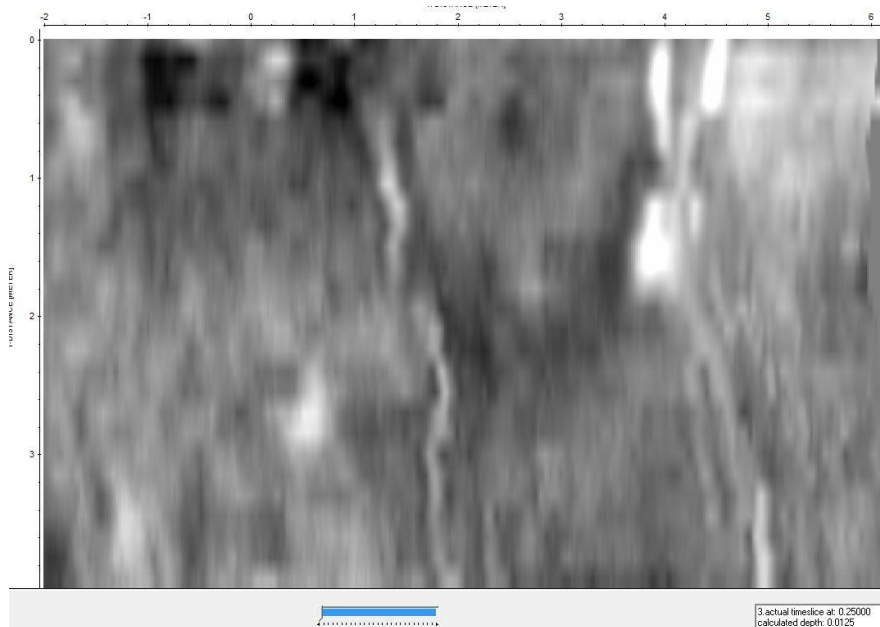


Figure 70. Time slice at an estimated depth of 2 cm.

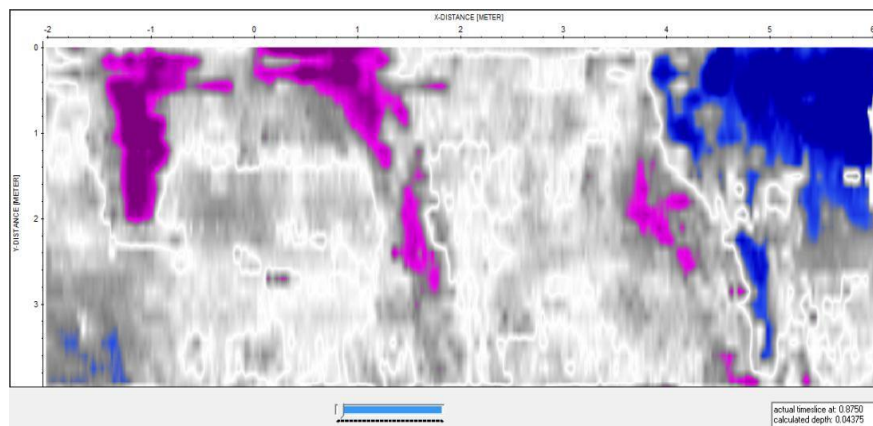


Figure 71. The GPR slice map at a depth of 4.3 cm.

It should be noted that the visualization results can vary significantly with depth, even within one centimetre.

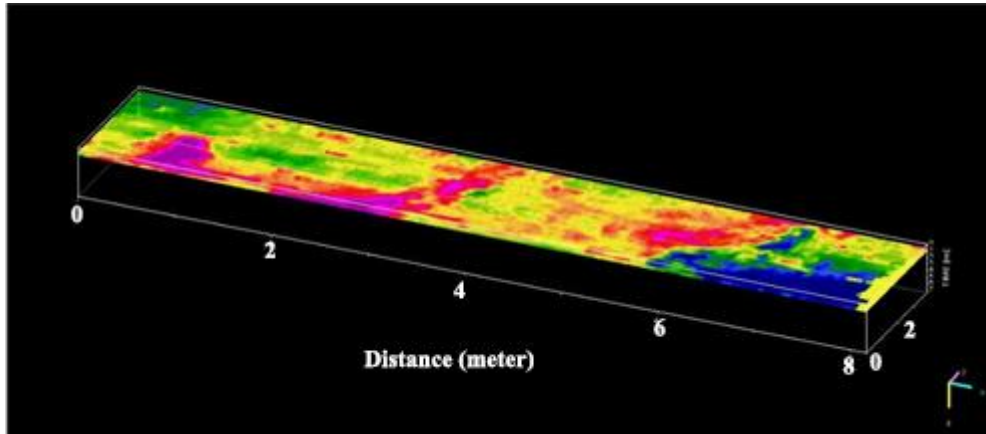


Figure 72. A similar map, at an estimated depth of 5.4 cm, using a different colour scale.

Discontinuities indicative of damage were observed until an estimated depth of 27-30 cm. This is important because it can serve as an indicator for infrastructure managers, indicating that “patching” the damage will be counterproductive, as the damage is deeper and adding more material to the surface will add even more load, leading to more long-term damage.

Overall, the GPR data confirms visual observations regarding tree root damage. The data also highlights another patch of degraded pavement, without tree root damage, as well as a tree root which has penetrated the pavement but has not yet caused visible damage.

However, while the results are relatively clear and striking in this survey, it should be noted that these were old poplar trees with massive roots (poplar trees are very tall and they have strong roots that extend far). It would be too optimistic to assume that surveys would have such large roots producing large contrasts.

5.3 Survey 2

Pine Tree 1 survey

The following survey was carried out in a largely similar setting, around the UoB campus. The survey was carried in the vicinity of pine trees, not poplar trees, and again, root-caused pavement damage was visible on the surface. Parts of the root itself were visible on the surface.

Here, both the 750 MHz and the 250 MHz antennas were used, and comparing the results between the two antennas was one of the main objectives of this survey. Although the latter was not particularly well-suited for the task, it was also used to see whether in practice it could also derive useful information. The surveyed area also included a small pipe or cable, which was marked by a distinctive asphalt patch used to cover it. Another unmarked pipe was identified after the survey.

The main objective of this survey was to locate individual roots, which were expected to be quite large given the large height of the poplar trees (which have since been removed from the UoB campus due to infrastructure re-planning). Significantly, a comparison between the two antennas was also carried out.

Unsurprisingly, the 250 MHz antenna had a substantially lower resolution. The differences between the two antennas were highlighted by timeslices. In particular, there is one clear indication of a root that entirely escapes detection on the lower frequency antenna. This confirms that the 250 MHz antenna can only be relied on to detect the coarsest roots.

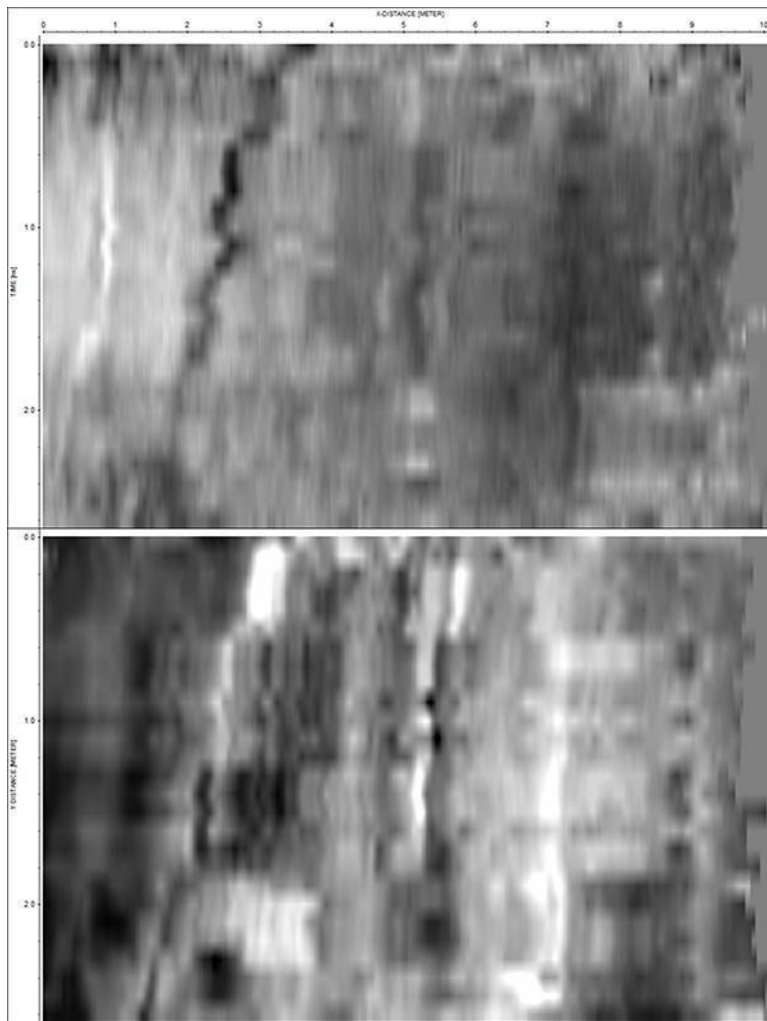


Figure 73. Comparison between the same section with the 250 MHz antenna (bottom) and the 750 MHz antenna (top). The lower frequency antenna also has lower resolution, this being the reason why it is “blind” to a root present in the first meter of the GPR section. Timeslice from an estimated depth of 6 cm.

Another notable phenomenon is that one root appears to change its polarity over its length.

5.4 Survey 3

Part A

Another relevant survey assessed the usability of the 1.5 GHz antenna. Two long profiles of approximately 40 meters were carried out. The objective was to assess the performance of the antenna in a real-life scenario and identify tree root damage not visible at the surface using single profiles – without creating slices or any form of 3D results.

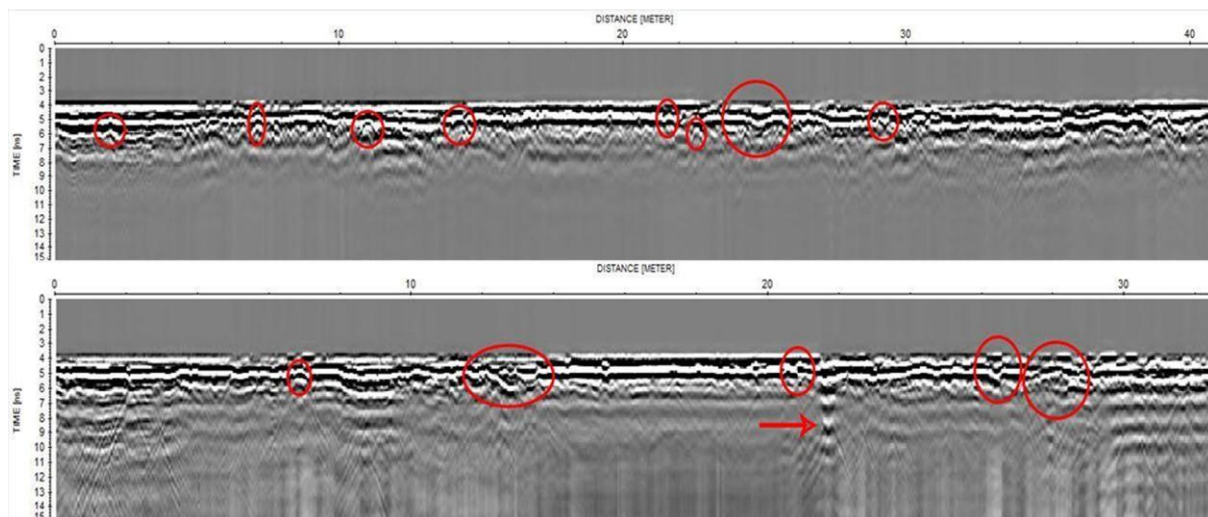


Figure 74. Two GPR profiles carried out on a sidewalk in the UoB campus near the Gisbert Kapp building. Highlighted in red are some potential tree roots or tree root damage. Red arrow indicates a pipe/cable. Static corrections and background removal had not been applied yet at this point.

While the results from this survey were encouraging and showed a clear improvement in resolution compared to the 750 MHz antenna, it became clear that without establishing lateral continuity, determining the presence of tree roots is very challenging.

Irregularities in asphalt (or other paved surfaces) can be detected, but attributing whether these are caused by roots or something else is not possible. The profiles above highlight several deformations (uplifts, downlifts, discontinuities), but while some of them show strong indications of tree roots, the determination is ambiguous.

For the purpose of antenna testing, this survey was successful in highlighting the antenna's improved resolution compared to previous surveys.

The higher resolution appears to be better suited to this purpose compared to the 750 MHz antenna, however the depth of penetration was low, and at this point, it was unclear whether this depth was sufficient in all cases.

Part B

Similar measurements were carried out in a neighboring area around the Gisbert

Kapp building, attempting to also generate timeslices and try out different visualization techniques that facilitate the root of roots and asphalt damage.

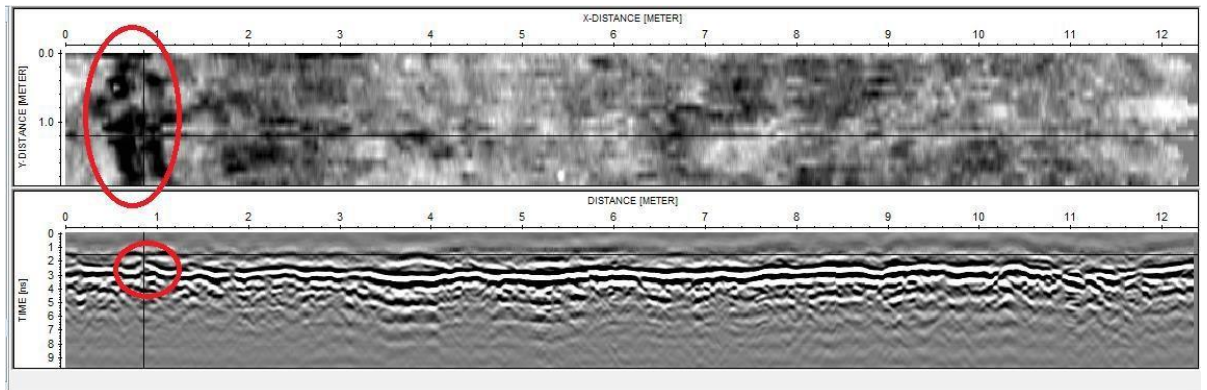


Figure 75. Simultaneous visualization of a GPR profile and timeslice can facilitate feature detection.

This confirmed the importance of establishing lateral continuity when it comes to the roots (or the damage caused by roots), a theme that would define many surveys. In particular, one area of asphalt damage was identified and highlighted.

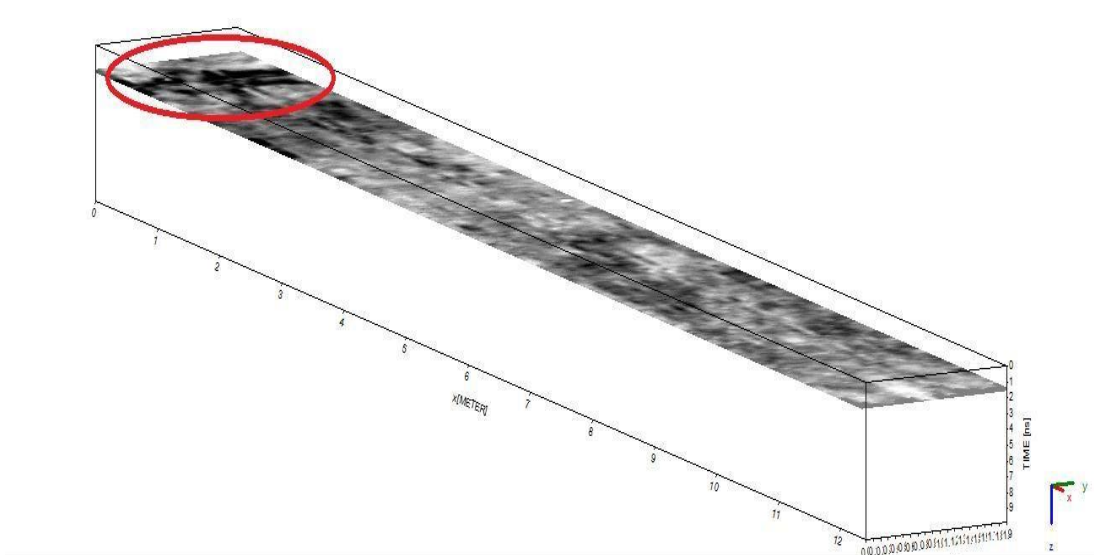


Figure 76. The same feature plotted on a 3D cube.

Lessons learned from these preliminary surveys were applied in the subsequent more detailed profiles. However, the difference between the forward models and real data becomes apparent here. The paved surface damage in Figure 75 is apparent, but it looks

different (and not as neat) as the same scenario simulated in Figure 39. This speaks to the more challenging interpretation of real data.

5.5 Survey 4

This survey involved the use of a total station for positioning. Before the GPR survey was carried out, a general 3D mapping of the surveyed area was carried out. The area was chosen with visible tree root damage (bumps and cracks) on the surface. The bumps were visible on the total station data. The distance between profiles was 10 cm. Remarkably, however, the total station data also revealed some small bumps which were not visible on the surface to the naked eye.

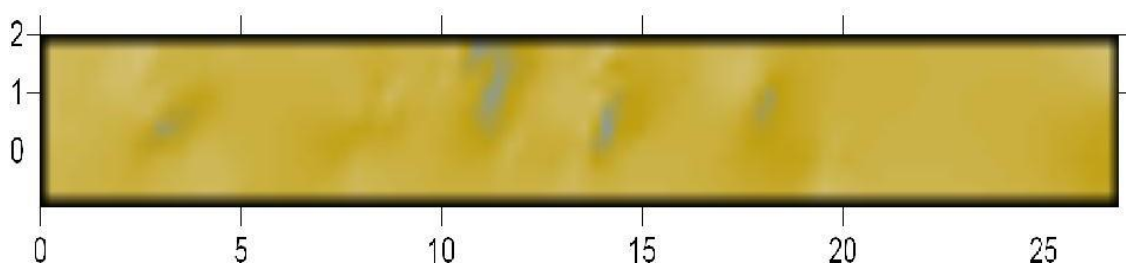


Figure 77. Tree root damage visible on total station data (topography not considered).

The data was gathered on a sloping area, which was also visible on the total station data. This was a secondary objective of the study, to use total station data to correct for the slope.

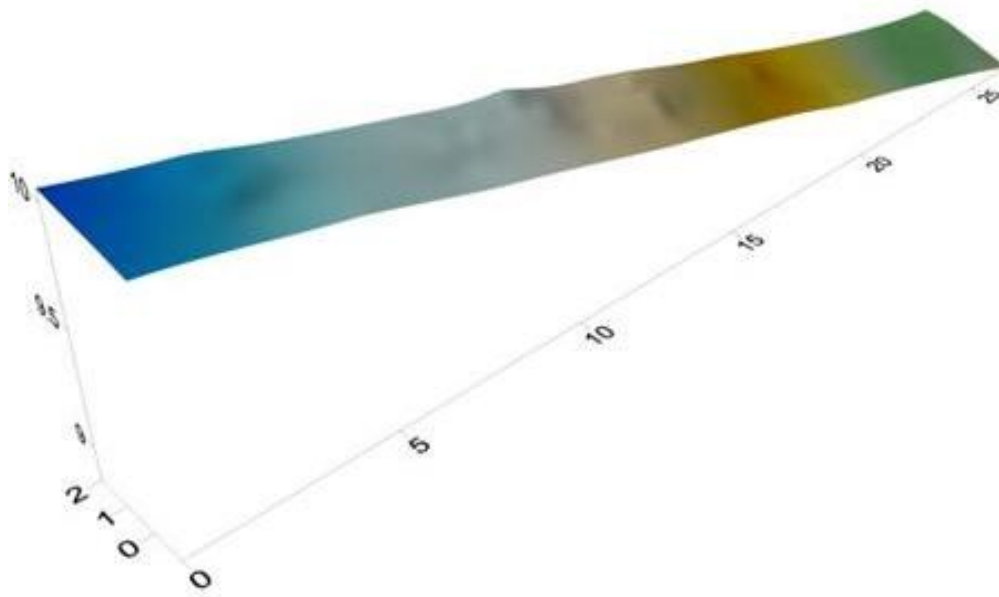


Figure 78. Tree root damage visible on total station data (including topography).

The data integration was done seamlessly, and the slope did not seem to affect the quality of the data. However, the GPR data itself was less clear.

The GPR data did not readily reveal the positioning of all these roots – with the exception of the features which were clearly visible on the surface, few features could reliably be identified. For instance, an area of approximately 2 x 4 meters is presented below. The area features points corresponding to small bumps revealed by the total station (in black dots), overlaid in Golden Surfer over GPR timeslices.

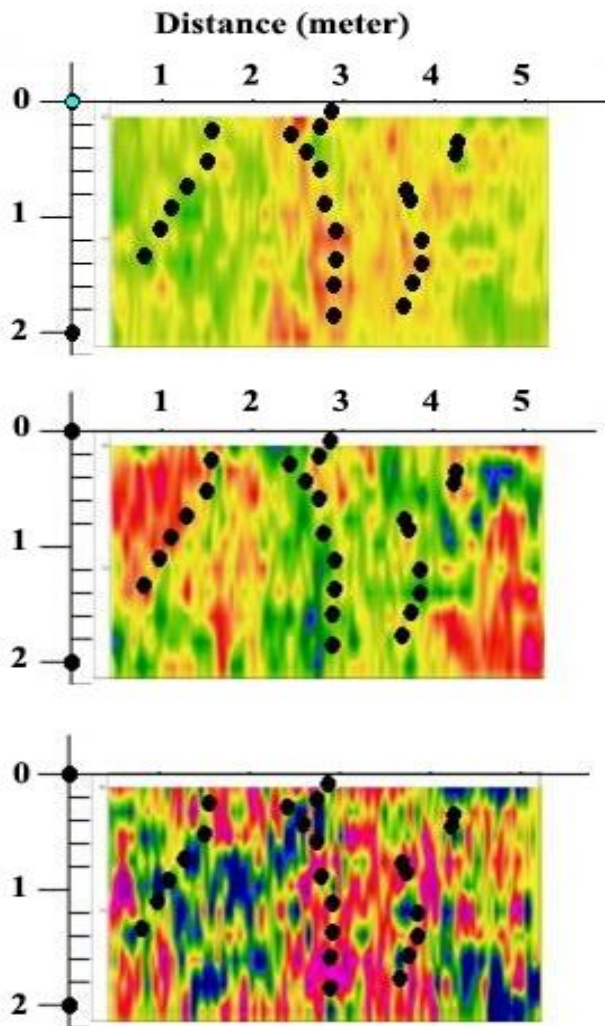


Figure 79. GPR slices at estimated depths of 3, 6, and 10 cm deep. The position of tree root damage (bump) is indicated with black dots. This position is only somewhat visible on the top section. This was the clearest example of unclear GPR results.

While the central area is suggestive of root damage, it is not clear from the radargrams if other two areas are also indicative of root damage. This survey is a good example, highlighting that it is not always possible to detect roots using GPR alone, showing the limitations of the method.

As a proof of concept for total station data integration, this survey was successful. Total station substantially eased data acquisition and added an element of geometrical certainty to the survey. Unfortunately, however, the total station surveys were brought to a

halt not long after this, due to a department-wide ban on all laser usage (which included total stations).

Looking at this data through the lens of the simulated forward models, it appears that general deformation in the paved surface (whether caused by roots or not) can mask the presence of roots.

5.6 Survey 5

The subsequent survey was a short survey carried on a soil area, as opposed to a paved surface. The area was surveyed with three available antennas (250 and 750 MHz antennas). Surveys were carried out in perpendicular directions, at a distance of 10 cm.

As expected, roots on soil surfaces are generally harder to detect than on smooth paved surfaces (with strong exceptions such as rebar concrete or paving cobbles). The 750 MHz antenna was again the better suited of the two, and several roots were detectable.

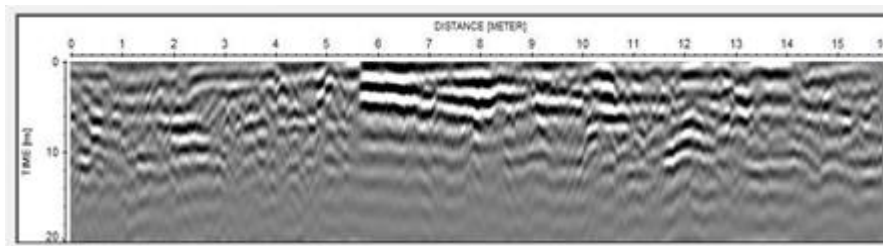


Figure 80. Representative profile with 250 MHz antenna.

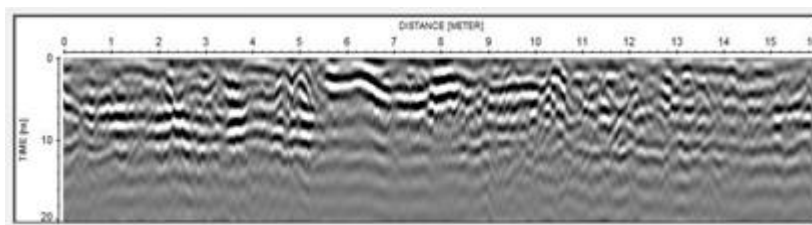


Figure 81. Representative profile for the 750 MHz antenna.

The timeslices do reveal some tree roots, but interpreting the data is challenging. Overall, while the earlier surveys revealed roots more clearly, this one highlights the

type of difficulty and ambiguity that can be encountered in this type of surveys.

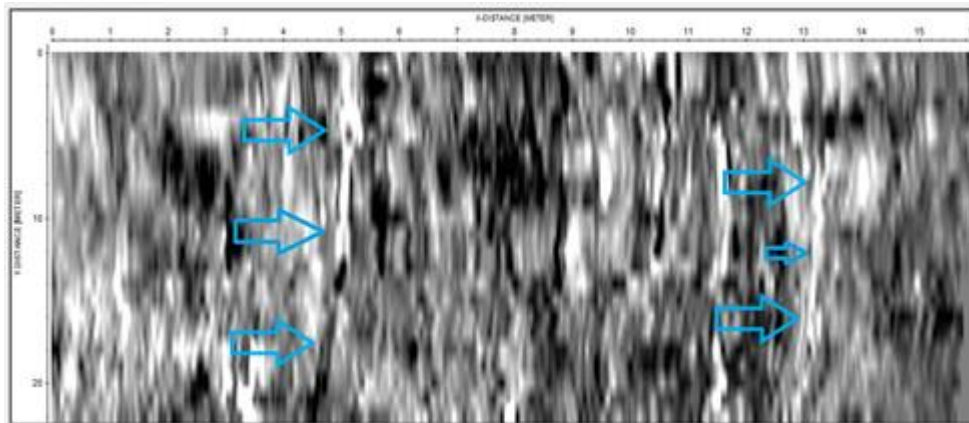


Figure 82. Two roots are visible in this GPR slice at 10 cm deep. Antenna frequency: 750 MHz.

The timeslices do reveal some tree roots, but interpreting the data is challenging. Overall, while the earlier surveys revealed roots more clearly, this one highlights the type of difficulty and ambiguity that can be encountered in this type of surveys.

5.7 Survey 6

A number of surveys were carried out in a similar context, with the results being generally consistent: the 750 MHz antenna is well-equipped to detect coarse roots. The thinner roots escape detection, but coarser roots can be resolved using this approach. In this survey, all the three antennas (250, 750, and 1500 MHz were used).

Another particularity of the survey area, significant due to its implications, was that there were two trees on the survey area – one of which had been cut down for several years. It is unclear how cutting a tree would affect root detectability, but it is likely that this does happen, and change the root-soil contrast, though it is not entirely clear how.

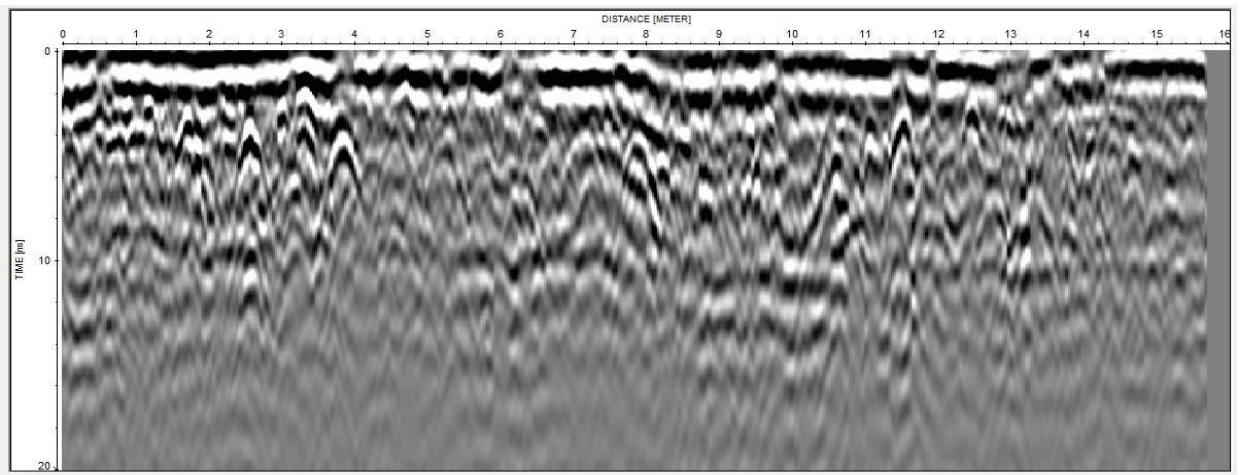


Figure 83. Representative profile for the 750 MHz antenna.

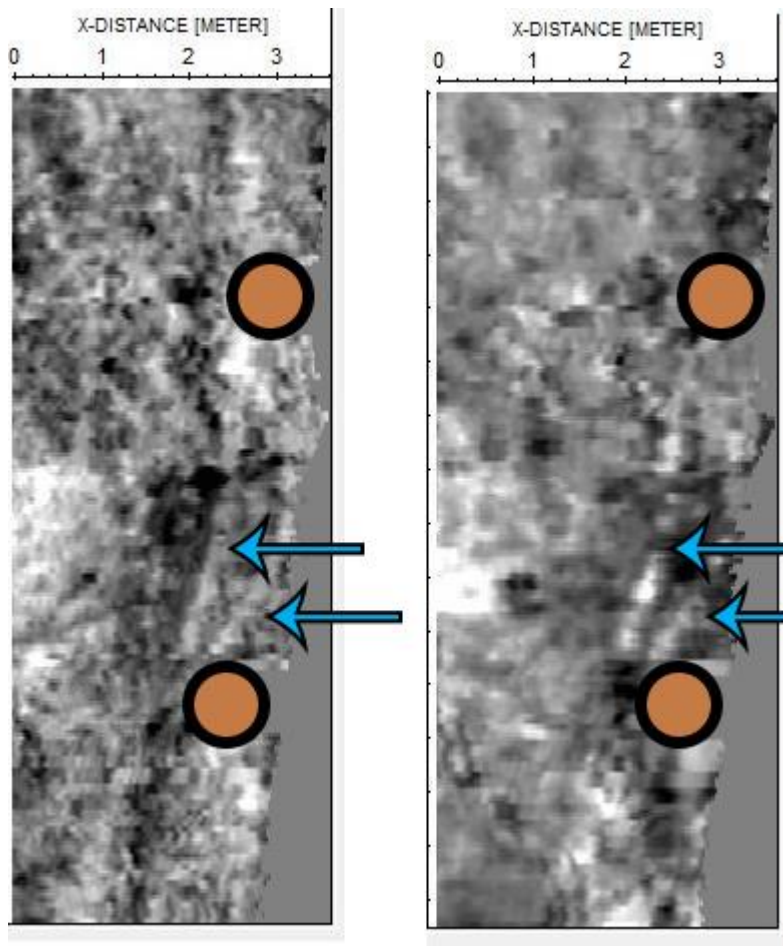


Figure 84. A slice at an estimated depth of 10 cm with the 750 MHz antenna (left) and the 250 MHz antenna (right). Trees marked with brown ellipses (the “top” tree had been cut down). Two of the roots highlighted with blue arrows.

The difference in resolution is clear. While the 250 MHz antenna does reveal a feature (presumably a cable) running through the lower-left side of the survey, but when it

comes to the roots, the 750 MHz antenna does a better job at resolving features. This is important as it suggests that in some scenarios, some thinner, deeper roots are undetectable with most antenna frequencies: neither the higher and the lower frequency antennas have sufficient resolution in the deeper parts of the survey. However, in the shallower parts of the survey, the 750 MHz antenna does highlight other parts of the root system (highlighted in red arrows).

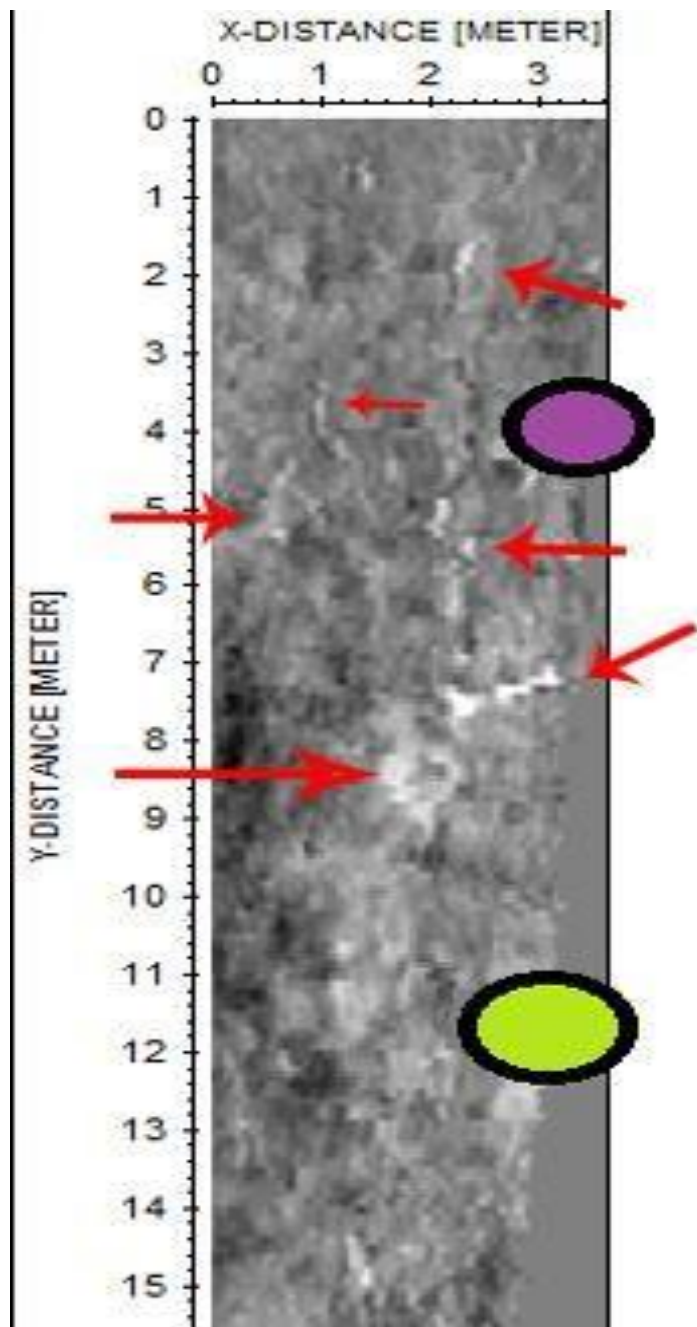


Figure 85. Timeslice at an estimated depth of 4 cm. Some roots are highlighted with red arrows. Living tree is highlighted in green, cut down tree highlighted in purple.

The roots from one tree, the living one, extend far beyond the canopy. However, not much is visible from the other tree, the one that had been cut down. The most plausible explanation for this is that its roots had started to rot and change their dielectric properties, becoming less distinguishable from those of the soil. This has significant implications for other surveys around trees that had been cut down for a long time, and would suggest that if mapping the position of a root system for a cut down tree is of interest, this is best done either before the tree is done or shortly after.

Measurements were carried out only in one direction (the short one in the image above), which also helps to explain why most of the identified roots are on a perpendicular direction to the profiles.

Measurements were also carried out with the 1500 MHz antenna. All the measurements were taken on the same day, in a time interval of a few hours, in a day without any precipitations. All the processing was done in the same way (a similar bandpass of $\frac{1}{2}$ - 2 times the central frequency was applied, and all other steps were similar). However, these revealed a surprising aspect: even at very shallow depths of a few centimetres, the 750 MHz antenna can sometimes outperform the 1500 MHz one.

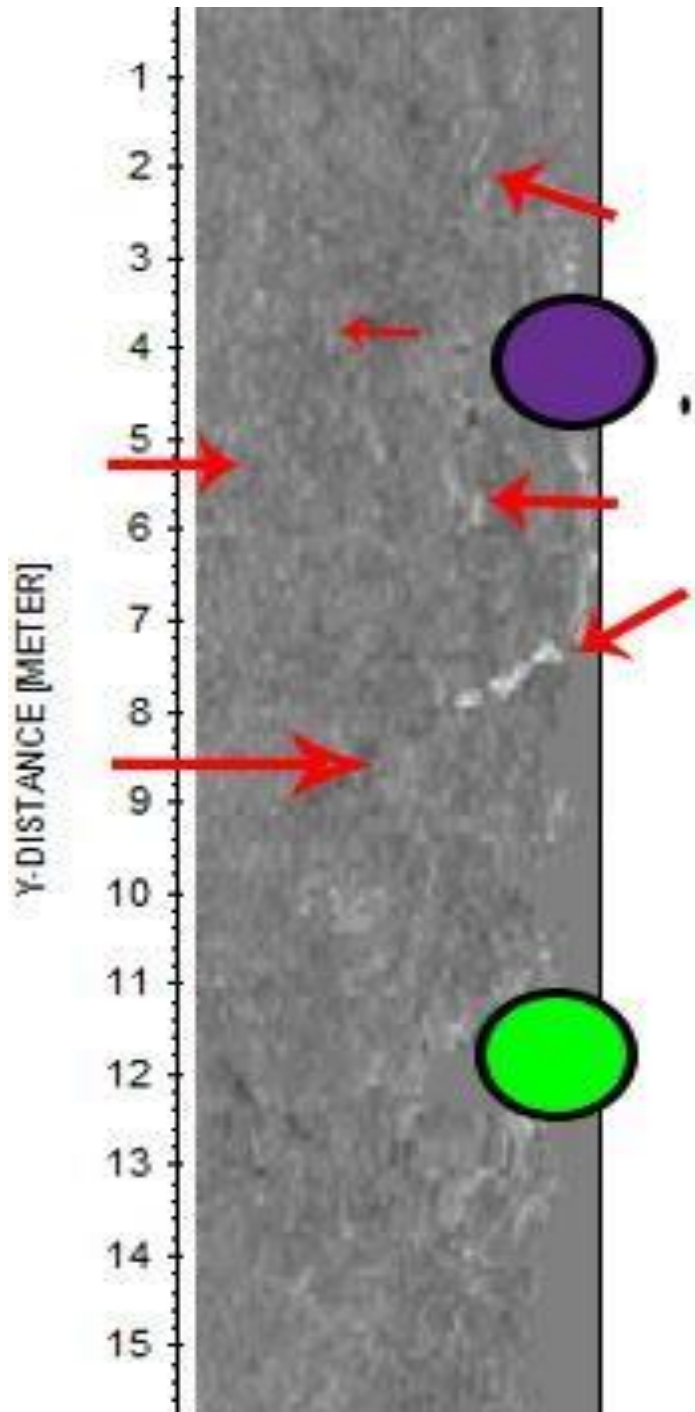


Figure 86. Timeslice at an estimated depth of 4 cm. The same arrows as in the image above (Figure 85) are overlaid over the timeslice. Living tree is highlighted in green, cut down tree highlighted in purple.

Essentially, the roots on the 750 MHz time slice at this depth are more visible on the timeslice or the 1500 MHz antenna. Barring lower equipment quality and positioning errors, this is most likely explained by the lossy environment in which the survey was carried out (a rather wet clay, very compact, and highly anthropized), which is more

unsuitable for higher frequencies.

Nevertheless, the higher frequency antenna did provide some advantages: it revealed surprisingly thin roots. Identifying these was only possible on timeslices thanks to their remarkable lateral continuity; one root, highlighted below in a blue arrow, turned out to have a diameter of approximately 1 cm, which is very close to the limit of detectability.

Another Y-shaped root, indicated by a pink arrow, is also expected to be similarly fine. The 1500 MHz antenna was also found to be much more sensitive to vertical changes. Viewing these changes as a continuous animation can also aid root identification, helping the interpreter determine that this it is not a false positive (though this is not possible to reproduce on paper).

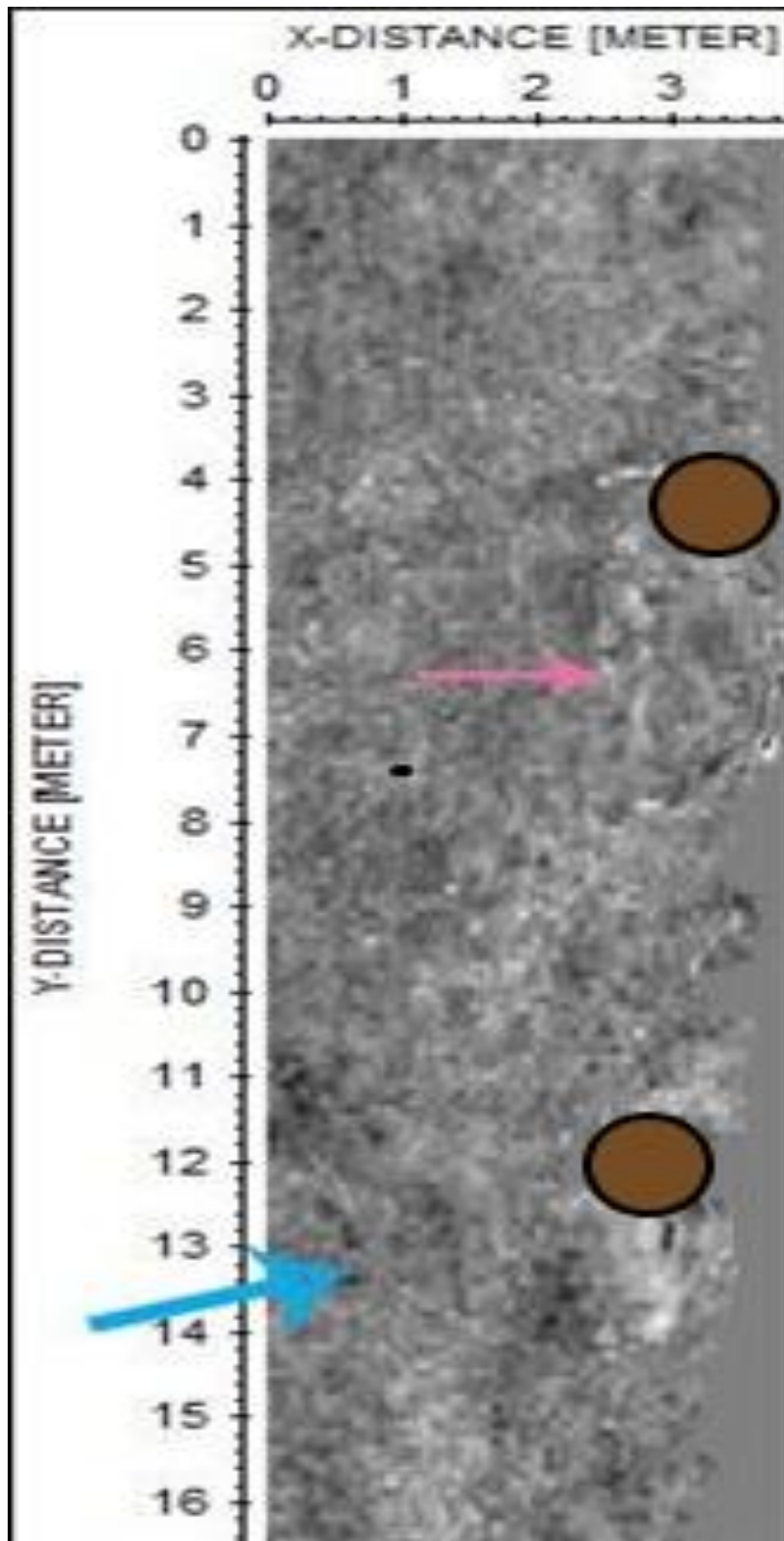


Figure 87. Timeslice at an estimated depth of 3 cm. Thin roots not visible on the 750 MHz antenna highlighted with arrows. Trees marked with brown ellipse.

This type of survey suggests that choosing antenna frequency is not a trivial step and should not be done on the “higher is better” assumption. No doubt, all things being

equal, a 1500 MHz antenna has better resolution in the top 10 cm than a 750 MHz antenna, but in an unfriendly environment, the opposite might stand true. This is particularly significant on soil surfaces, and wet clays in particular. This type of practical finding was not expected based on the forward models alone, showcasing the importance of avoiding over-reliance on models when interpreting data.

The limits of the 1500 MHz antenna were further put to the test in the following series of surveys.

5.8 A series of soil surveys in Harborne

The following is a series of surveys carried in the Harborne area in Birmingham. Because of the numerous and often unpredictable construction works taking place on campus, the area was preferred for these trials. Unlike the above-mentioned surveys, which were carried out in the summer, these were carried out in the late autumn.

In principle, the Harborne area is just as well-suited for tree root surveys. There are multiple green areas and parks, a large number of trees of varying ages and species, and visible evidence of root damage to the infrastructure. Overall, this is an ideal setting for surveys mimicking a real-life challenge of identifying roots and root damage. The 1500 MHz antenna alone was used in the following surveys. There were two different types of surveys: the first part, carried on soil (or mostly on soil), whereas the second part focused only on paved surfaces (asphalt sidewalk).

Harborne 1

The survey was carried out in the Harborne area. The surveyed area was approximately 7.1 m by 4.4 m. A relatively young tree was present in the survey area, representing the main objective of the investigation. GPR profiles were carried in two perpendicular directions (X and Y), at a distance of 10 cm between profiles. The areas

covered by X and Y profiles were only slightly different.

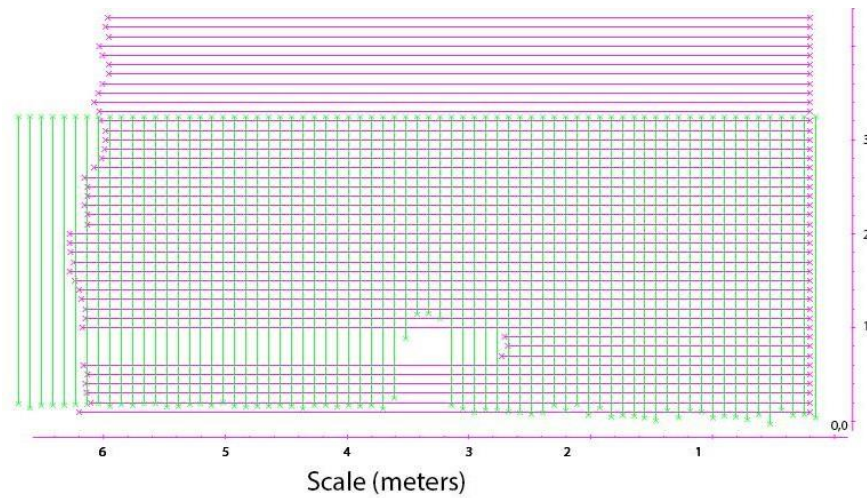


Figure 88. Depiction of the X and Y profile lines. The approximate position of the tree is visible from the gaps in the profiles (the gaps are slightly different because the antenna wheel).

The imperfect overlap is partially due to an antenna asymmetry that was not considered in the initial stages of the survey. However, a buffer distance was taken to ensure that the features of interest are covered by profiles in both directions. The following two surveys also followed a similar plan. This offset is also responsible for the positioning of the tree and certain anomalies at seemingly different locations on the X and Y profiles (because the '0' of the two don't coincide).

Studying the differences in data revealed by data on X and Y profiles was a secondary research question of this survey; a point of interest was to see if there would be any notable features between the two, or if the data would be identical. Additionally, given a practical time constraint, would it be better to spread the profiles at twice the distance, but cover perpendicular directions, or "thicker" profiles on just one direction? Other facets were also of interest in this survey.

Several prior trial surveys have revealed that the presence of structural subsurface elements (pipes, tunnels, etc) can mask the presence of closeby roots. So this survey was also carried out in the vicinity of an active duct, which was clearly visible on the

radargrams.

The survey was also carried out on two different surfaces: grass, pavement, and grass again. The survey was carried out to mimic a real-life situation in which the objective would be to study the distribution of tree roots and potential damage done to infrastructure.

Survey area representation

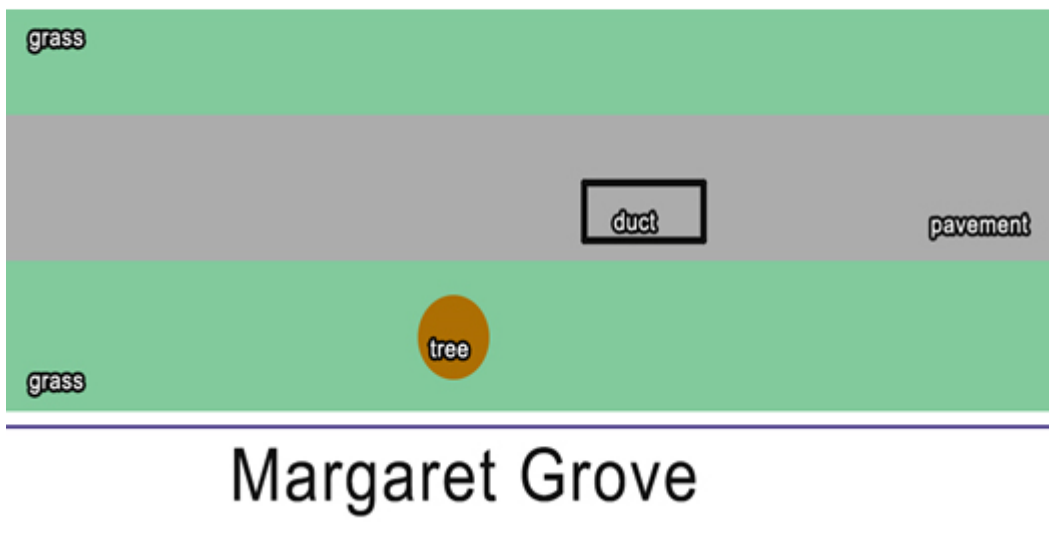


Figure 89. Depiction of the survey area. Image not to scale.

The migration was a particularly challenging processing step. As is often the case in this sort of survey, migration only offers marginal improvements, and in some cases, can actually be make the results more difficult to interpret. In addition, migration is bound to be imperfect since the survey covers two different subsurface environments (soil and asphalt), so there is no one uniform migration speed. Nevertheless, migration was chosen here as it seemed to produce a marginal improvement of the data quality (at least at the visual level, in time slices).

Data gathered from both directions revealed largely similar structures. However,

the results were not identical. From the very start, the different interpolation artifacts are clearly visible on the two different directions. Below is a comparison of timeslices at a depth of 1 cm. This falls in the GPR's so-called blind zone and is not reliable or relevant for subsurface information, and is presented only for comparison purpose.

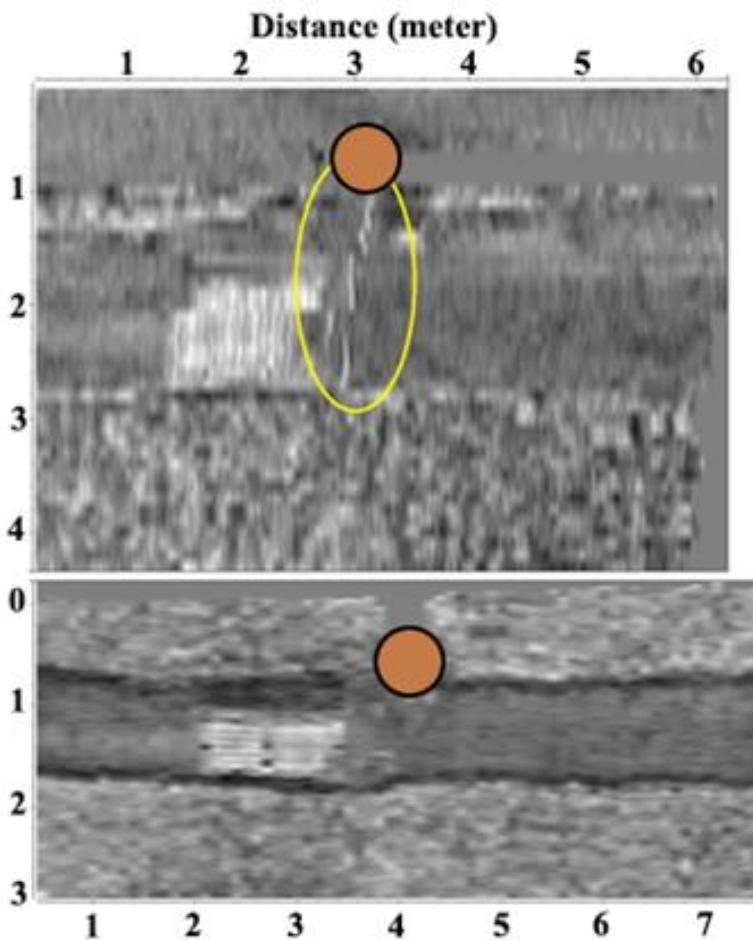


Figure 90. Time slices on the X and Y directions at an estimated depth of 1 cm. Position of tree marked with brown ellipse.

The data looks rather similar, as expected. But there are a few notable differences. For starters, the bottom slice shows some structural elements of the duct (in black, on the white rectangular shape). It also appears to offer a generally clearer view of the general structure. However, more intriguingly, the above slice appears to depict a feature (highlighted in yellow) moving from the close vicinity of the duct.

This feature appears completely absent on the other direction. This could be discarded if it was only visible in only the first centimeter, but the trend continues at

further depths.

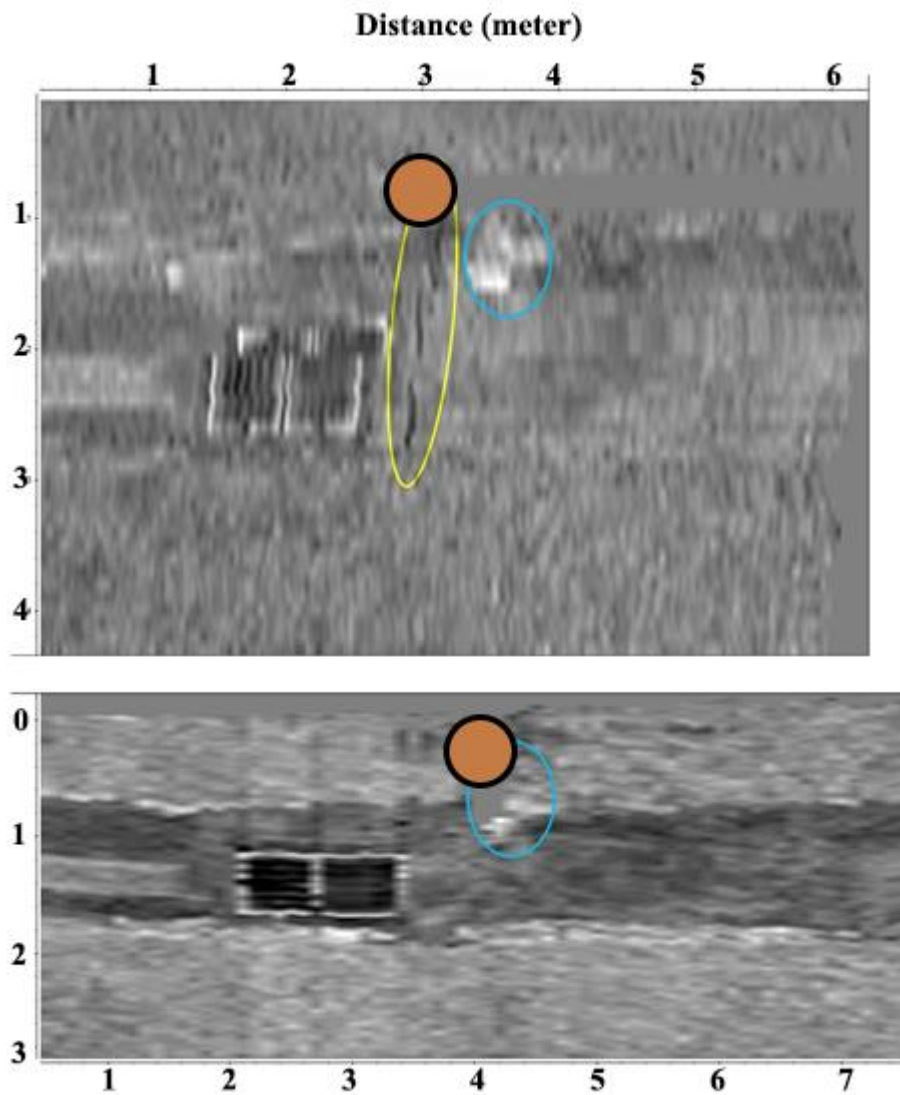


Figure 91. Time slices on the X and Y directions at an estimated depth of 3 cm. Different tree location is owed to the physical antenna impediments (ie the '0' on the X and Y locations did not coincide), see Figure 88.

Again, the bottom timeslice reveals the details of the duct in much higher detail, but the linear feature highlighted in yellow is completely invisible. Another interesting feature emerges in the vicinity of the tree: potential damage to the road which, given the location, is likely to be caused by the root system.

The feature is visible until an estimated depth of approximately 5cm.

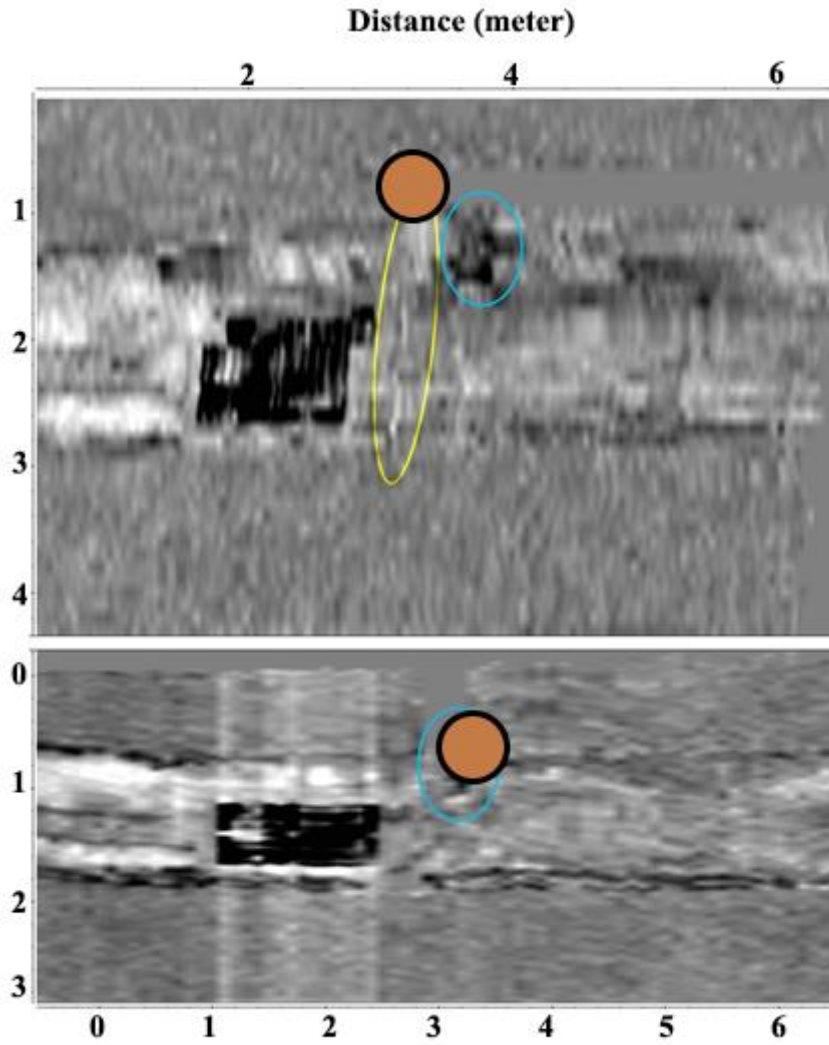


Figure 92. Time slices on the X and Y directions at an estimated depth of 4.5 cm.

Although the feature is not clearly distinct on all profiles, it is sufficiently visible on some.

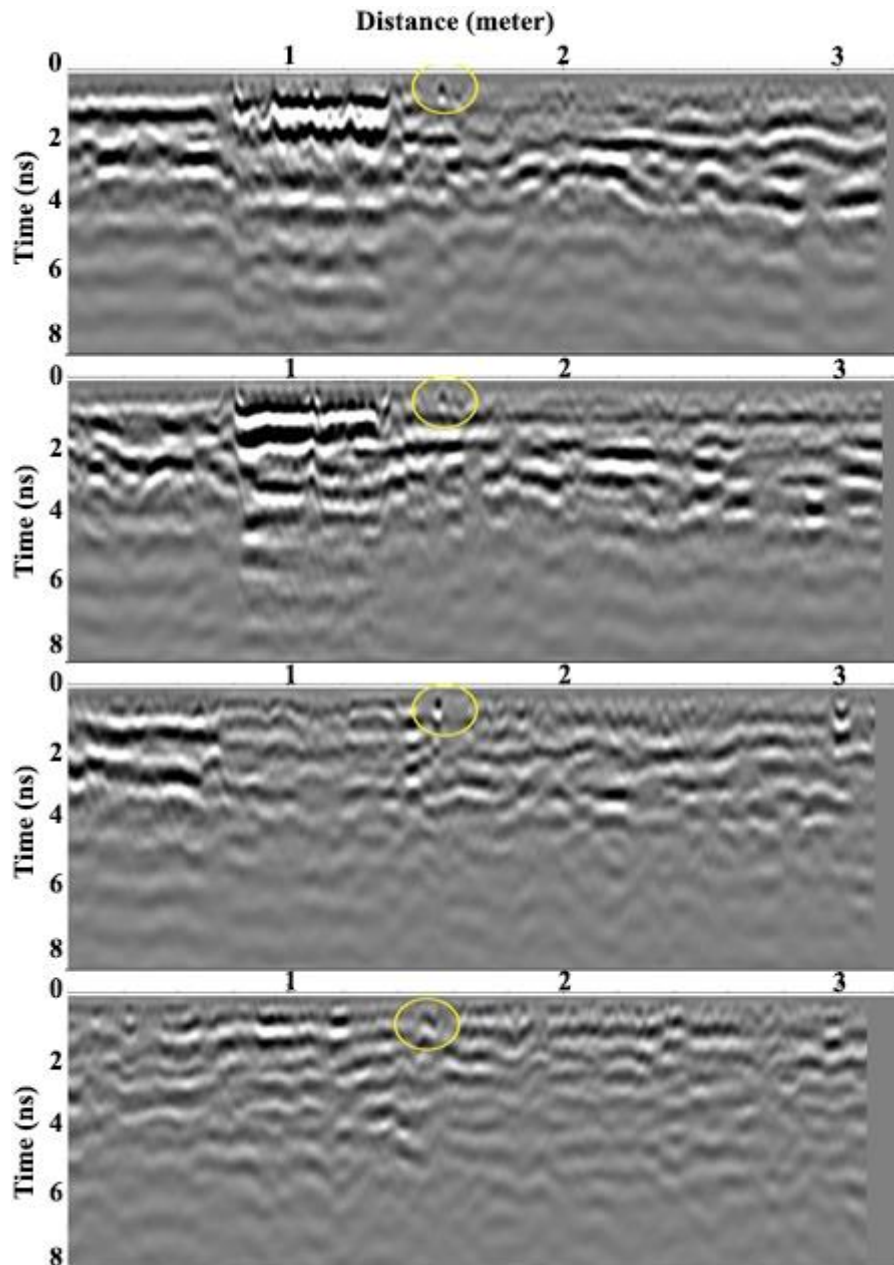


Figure 93. Examples of X-direction radargrams depicting the highlighted feature on profiles 25-28.

At first, the feature was dismissed as a structural element related to the duct. However, it does not seem to be separated from the man-made structure, and only located in its vicinity. Furthermore, it appears to continue beyond the duct. It cannot be a pipe or cable as it would not be so close to the surface. The duct itself and its main line are visible in the above mentioned profiles.

All this indicates that the feature is indicative of a shallow root passing through the asphalt and damaging it. The lack of continuous visibility of the feature would suggest that these are cracks rather than the root itself, although this could also be potentially explained by variations in the dielectric permittivity of the root. In this situation, it can be inferred that the root has penetrated the asphalt and caused damage to it. This is an important finding, and if the root trajectory can be inferred to be directed towards the asphalt from the soil part, then it would be a significant predictor of damage.

Another takeaway from this survey is that surveys on asphalt, and with man-made structures in general, obstruct the visibility of tree roots. It seems therefore advisable to carry or interpret surveys separately on soil and on asphalt, as mixed surveys (such as this one) raise additional challenges if interpreted together.

An inspection of the profiles in the perpendicular direction shows that it is, indeed, not possible to detect this feature with this setup. As expected, linear features are more visible to profiles perpendicular on their direction.

Unfortunately, not much can be said about the distribution of the tree roots. A part of the tree root system is visible in the vicinity of the tree. The features are not easily visible, but are nonetheless distinguishable on profiles in the Y direction. The flow of consecutive timeslices, however, does indicate the presence of root elements (images have been flipped vertically).

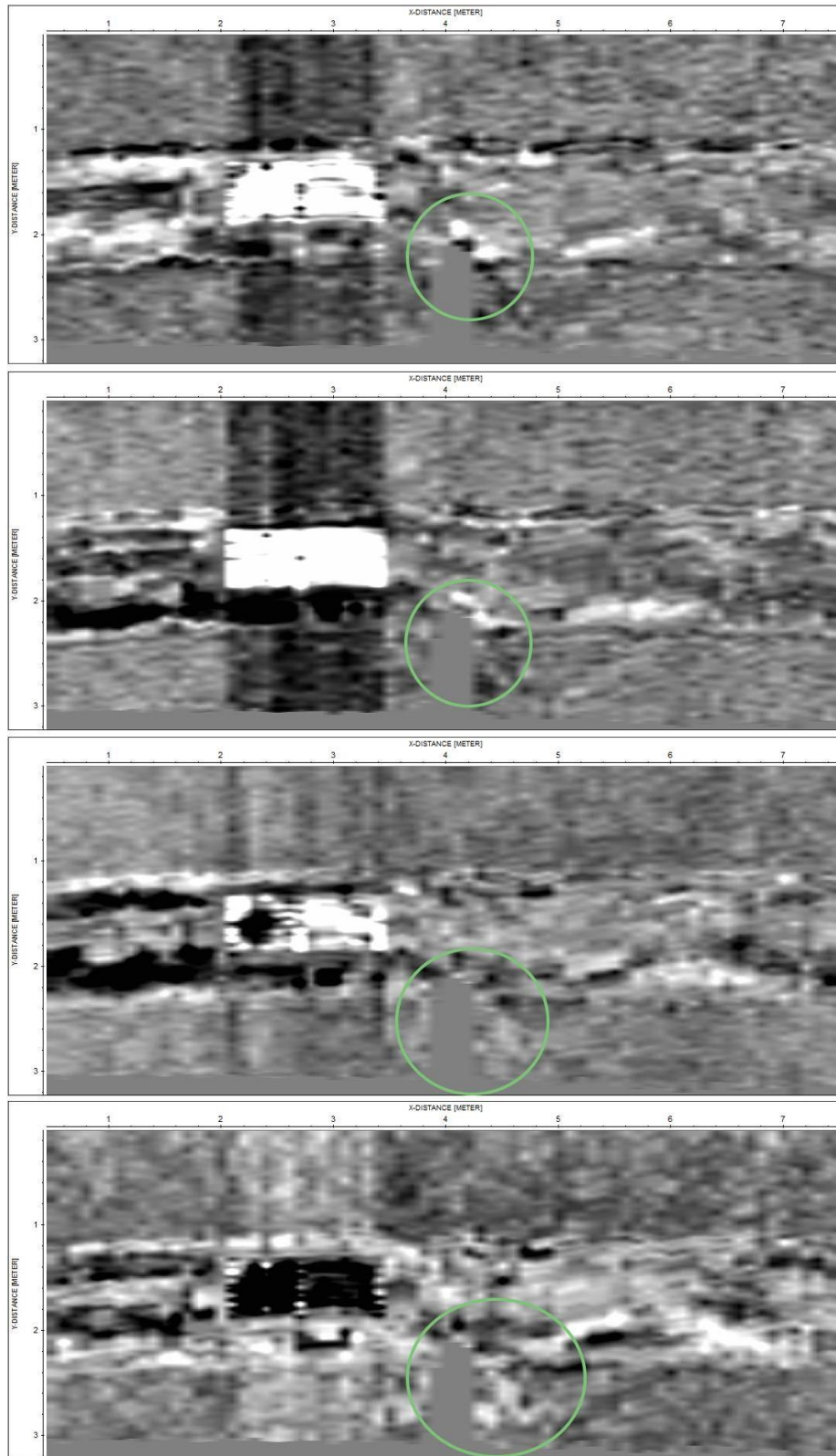


Figure 94. Tree root area at depths of 5-7.5 cm, highlighted in green (Y direction). Tree position unmarked so as not to distract or cover relevant data.

These roots are also in the close vicinity of the asphalt, where they seem to have caused detectable deformations. It is unclear to what extent these are the roots or deformations caused by the roots, but it is very likely that they can be ultimately traced back to roots. The area was “picked” in the ReflexW software to see the corresponding areas in radargrams.

The areas are visible, but their nature is not clear. Therefore, lateral continuity is crucial to their identification and analysis (as is almost always the case in the detection of tree roots).

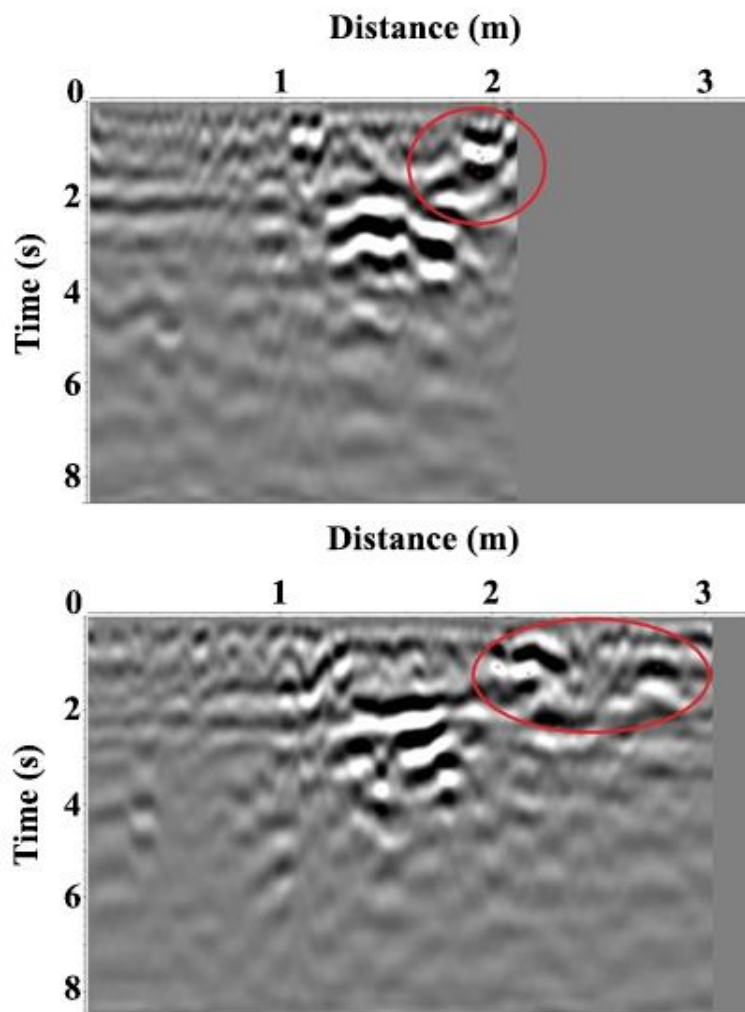


Figure 95. Two profiles highlighting parts of the presumed area (picks are in red).

Remarkably, however, the root area is not visible on the X profiles. A flow of slices at the same depth reveals very few noticeable features.

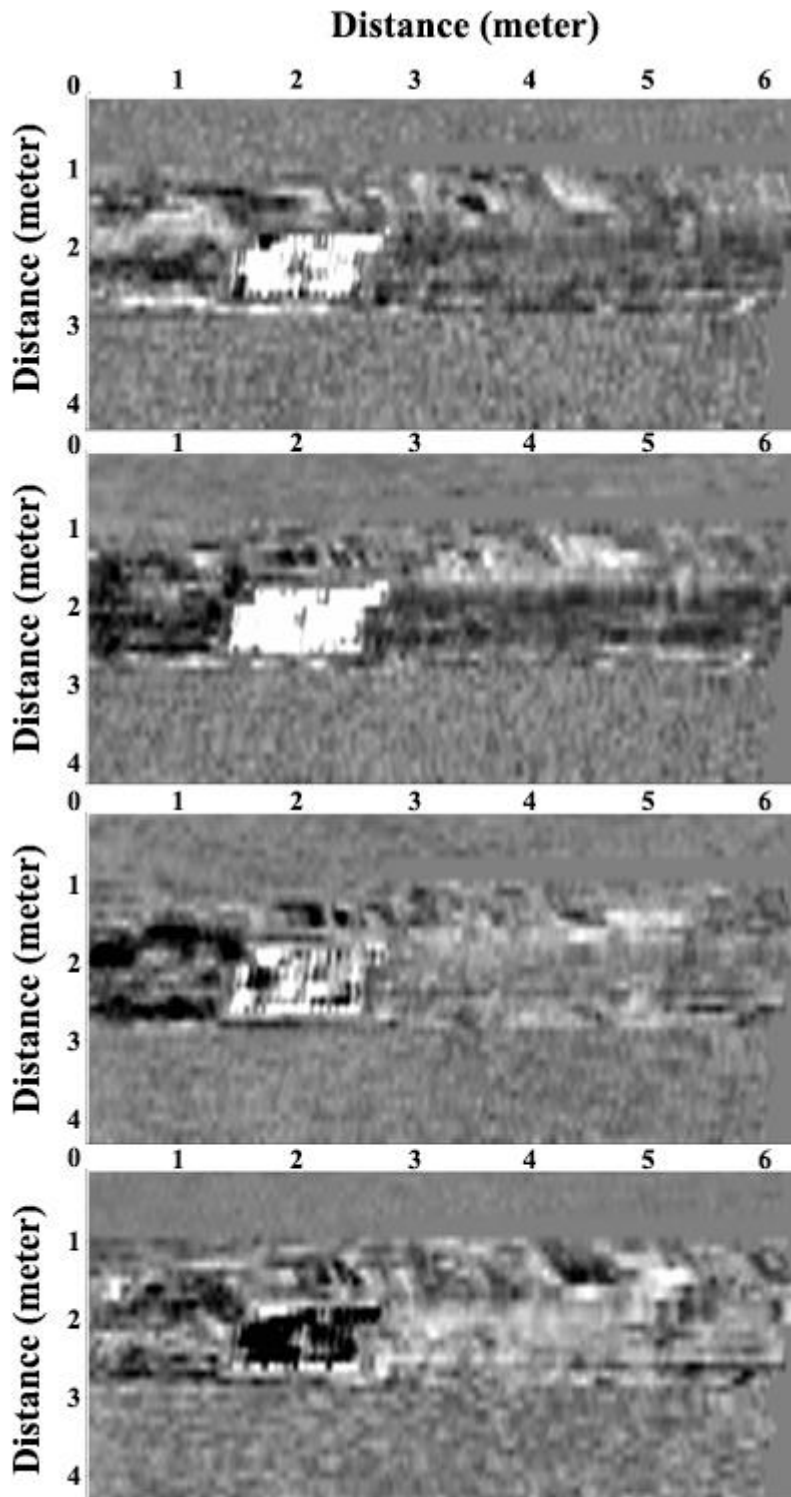


Figure 96. Time slices at depths of 5-7.5 cm (X direction).

The asphalt-soil disparity appears much stronger than in the Y direction, potentially due to anisotropic properties of the asphalt. From these slices alone, it would be impossible to identify any features related to a tree. This also seems to suggest the utility of acquiring data in two perpendicular directions.

Another secondary objective was to compare the data quality at two different distances between profiles: 10 and 20 cm respectively. The appearance of a significant feature on profiles in one direction but not on profiles in the other direction is an important indication to the necessity of carrying out profiles in perpendicular directions. For comparison, 3D radar files were also generated as if the data had been acquired at distances of 20 centimeters (using both odd and even profiles).

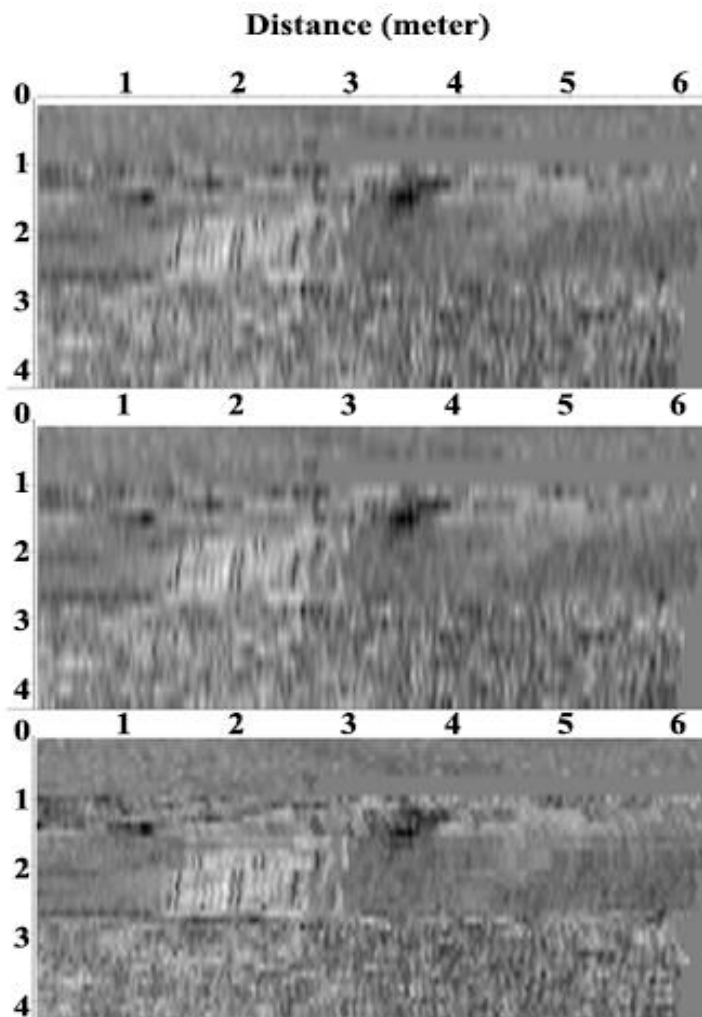


Figure 97. Timeslice at a depth of 1.2 cm with profiles at 20 cm (odd profiles – top, even profiles – middle) and 10 cm (bottom).

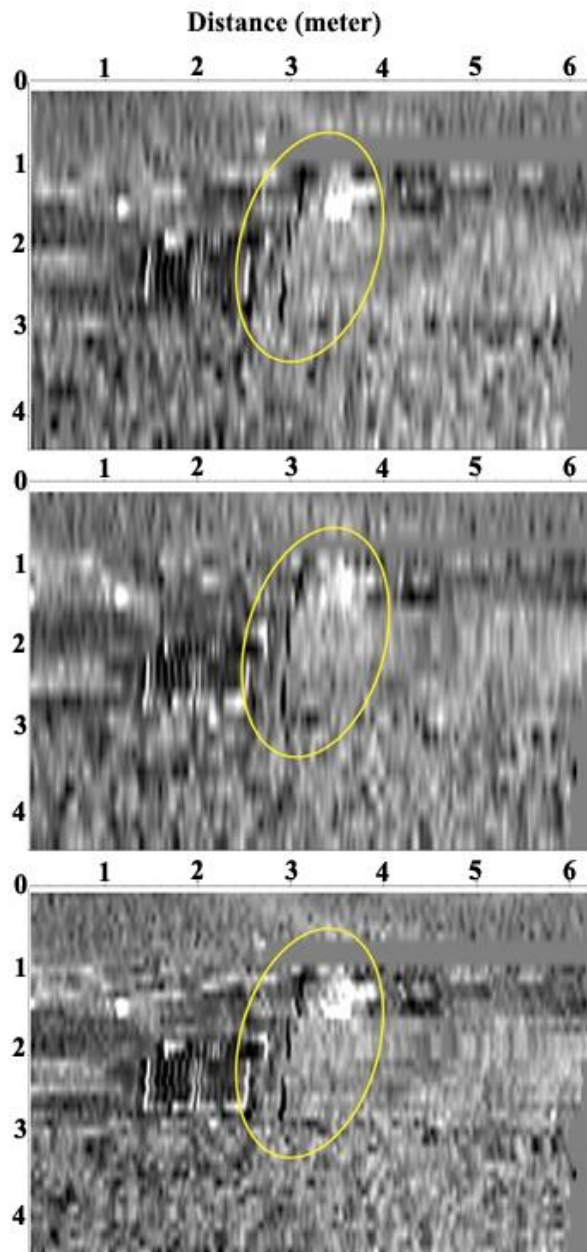


Figure 98. Timeslice at a depth of 1.2 cm with profiles at 20 cm (odd profiles – top, even profiles – middle) and 10 cm (bottom) on the X direction.

The main features are visible in all the profiles, although resolution of the profiles at 0.1 cm is significantly better. However, given the choice between more profiles in one direction or fewer in both directions, the latter certainly seems preferable here.

The same thing can be noticed on the profiles in the Y direction: the resolution is significantly better on the full data, but the general features are also visible.

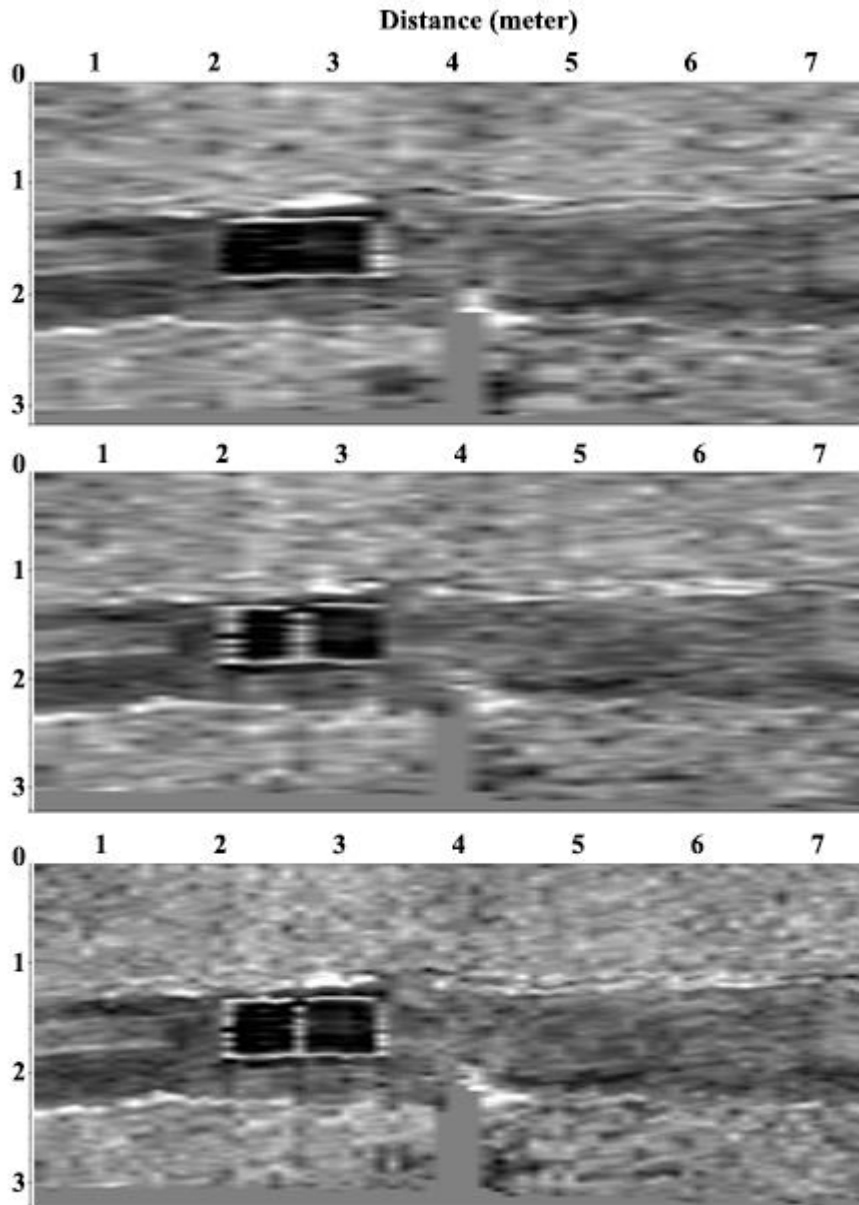


Figure 99. Timeslice at an estimated depth of 2 cm with profiles at 20 cm (odd profiles – top, even profiles – middle) and 10 cm (bottom) on the Y direction.

The improvement in resolution at a profile distance of 10 cm vs 20 cm is not insignificant. Overall, this indicates that a distance no greater than 10 cm is preferable for the purpose of tree root detection. However, given a very tight time constraint (for instance, survey on a road temporarily closed down), the sacrifice in resolution is preferable if profiles are gathered in perpendicular direction. Unless the orientation of the objective is well known (in which case profiles should be carried perpendicularly to the objective), profiles at a distance of 20 cm on both X and Y directions are preferable to profiles at a distance of 10 cm in either direction.

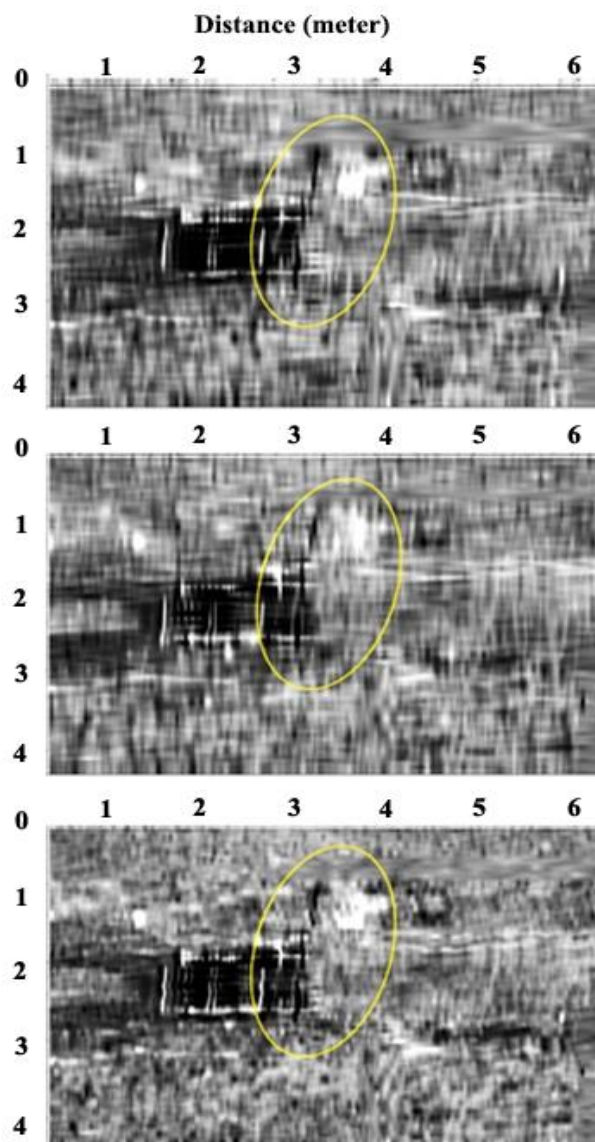


Figure 100. Timeslice at 1.2 cm, with profiles on both directions overlaid at 20 cm (odd profiles – top, even profiles – middle) and 10 cm (bottom). Tree position not superimposed as not to cover data

Overall, several features were identified on the radargram. In particular, one root appears to be extending around the duct (and potentially to it), penetrating the asphalt. However, few roots were revealed by the radargram (presumably the coarsest ones). This is potentially owed to the high soil humidity, but can also be owed to low root-soil contrast.

Harborne 2 (“Willow Tree”)

The survey was also carried out in the Harborne area, around a willow tree. The objective was to assess the detectability of the willow’s roots. The site was chosen due to the rather unusual tree species and its root characteristics, which are noteworthy in this context. The tree is generally considered to produce an extensive and aggressive root system. A University of Florida catalogue (<https://edis.ifas.ufl.edu/st576>) states that willow “surface roots can lift sidewalks or interfere with mowing” and that willows should not be placed in proximity to septic tanks as they can cause damage.

Profiles were acquired in two perpendicular directions (X and Y). The surveyed area was approximately 6.5 x 9 meters.



Figure 101. An image of the pre-survey setup.

Although the survey could be carried out, the general conditions were not well-suited to the survey. Although it had not rained for several days at the time of the survey, the soil was still relatively wet. The soil was also rich in clay, with the combination of clay and water being notoriously difficult for GPR surveys. These have taken a toll on the results. Two representative profiles are presented below, highlighting the reflections in the first 4 ns.

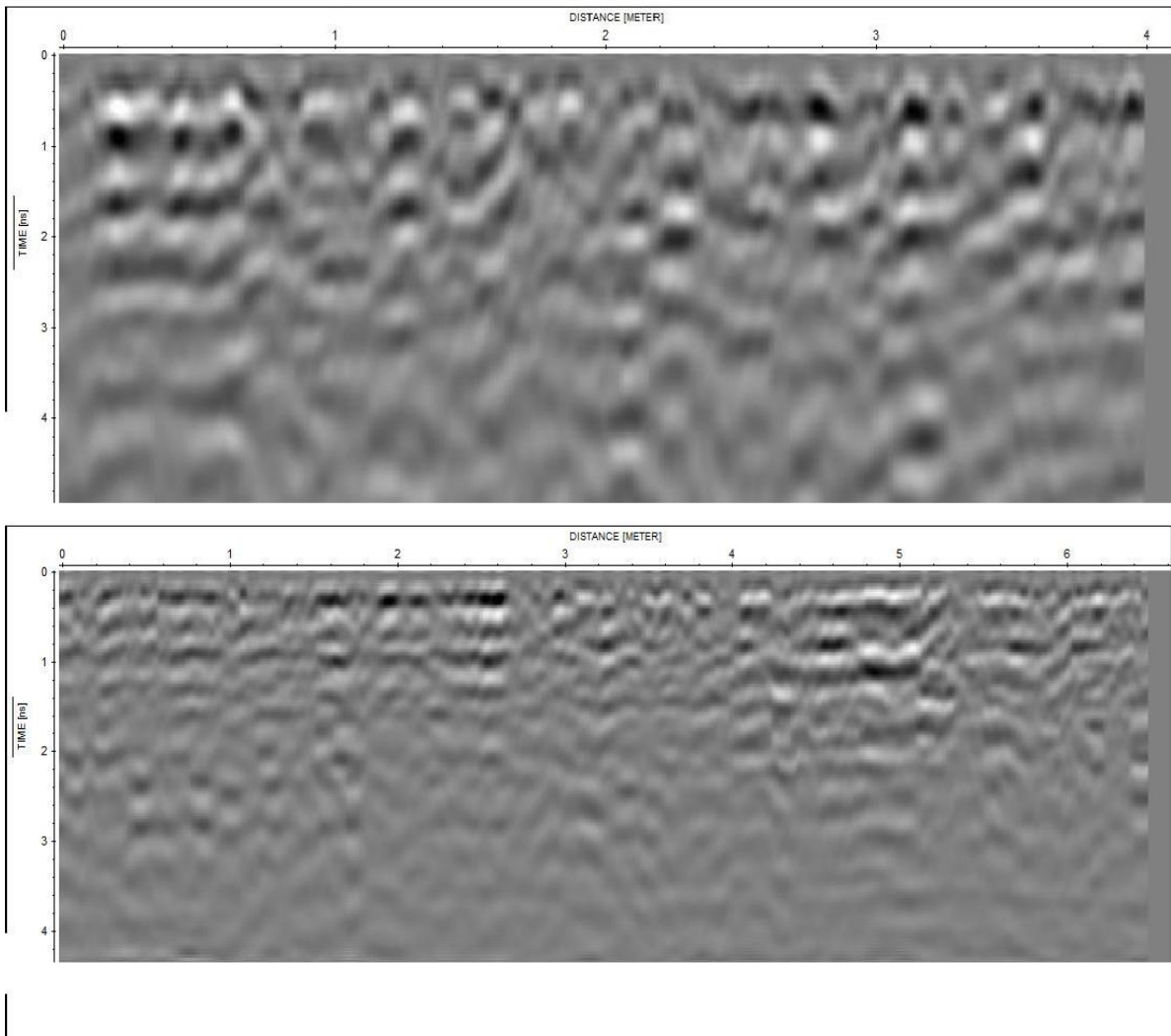


Figure 102. Example profiles from the X (above) and Y (below) directions), relatively low quality data. Images are not to scale.

The X profiles reveal a part of the root area located very close to the surface (but not exactly at the surface), as is depicted below.

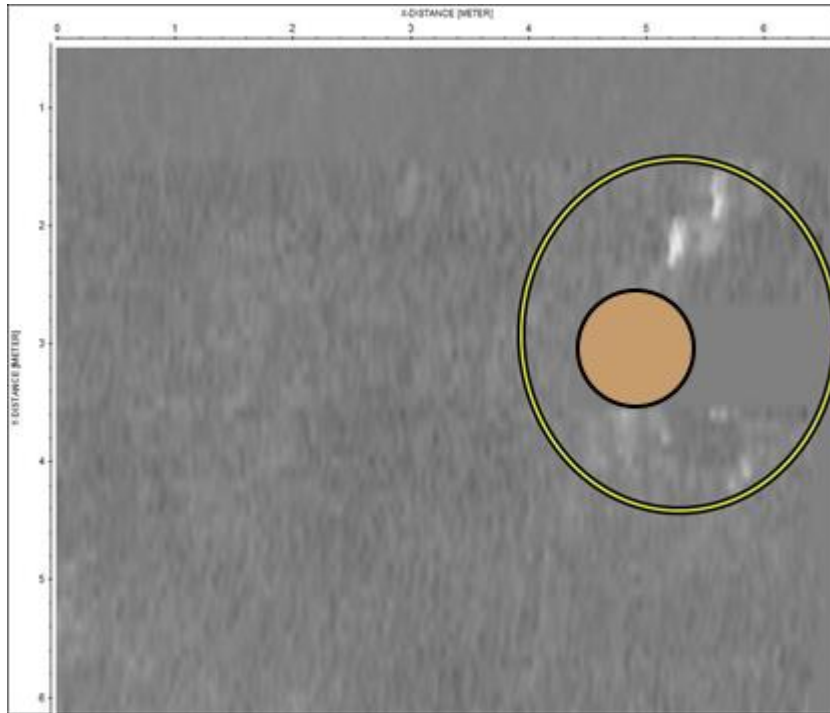


Figure 103. Time slice at an estimated depth of 2 cm on the X profiles. Tree position marked in brown ellipse. Tree size not to scale.

The same root area also appears on the Y profiles, and is better represented on that direction.

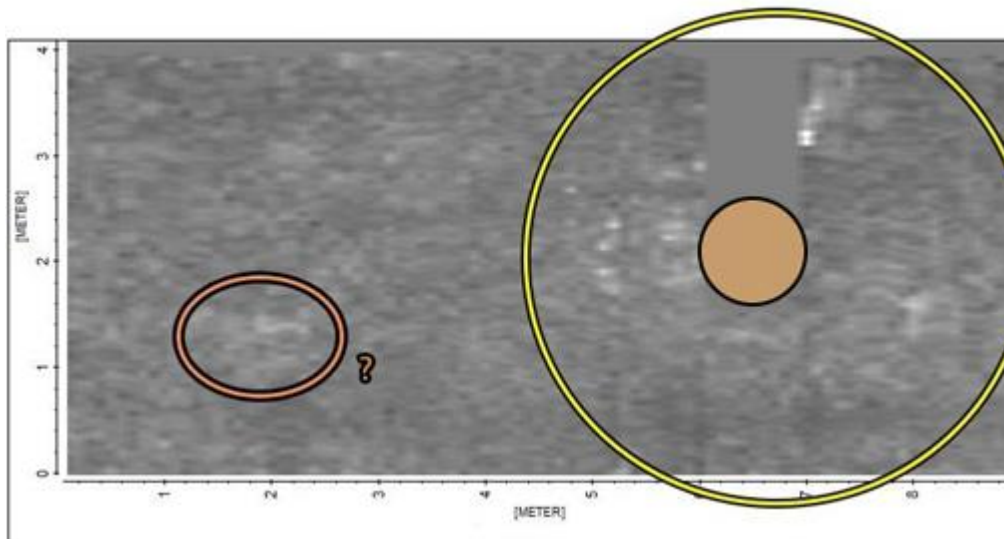


Figure 104. Time slice at an estimated depth of 2 cm on the Y profiles.

Strong reflections indicative of roots are visible in several directions, extending from all around the tree area. However, while the tree root area is well represented (highlighted

in yellow ellipse) and a few of the roots can be resolved individually (top and right of the ellipse respectively), the left side of the area shows a root area rather than individual roots.

There also appears to be another small reflective area (highlighted in orange) of unknown nature. It does seem to have some limited lateral continuity but is unlikely to be connected to the willow tree. This does not appear to be a tree root and is therefore likely not a feature of interest for this survey.

Similar observations can be made in slices a bit deeper on the X slices, suggesting that these are indeed very thick roots. Unfortunately, no additional roots could be detected.

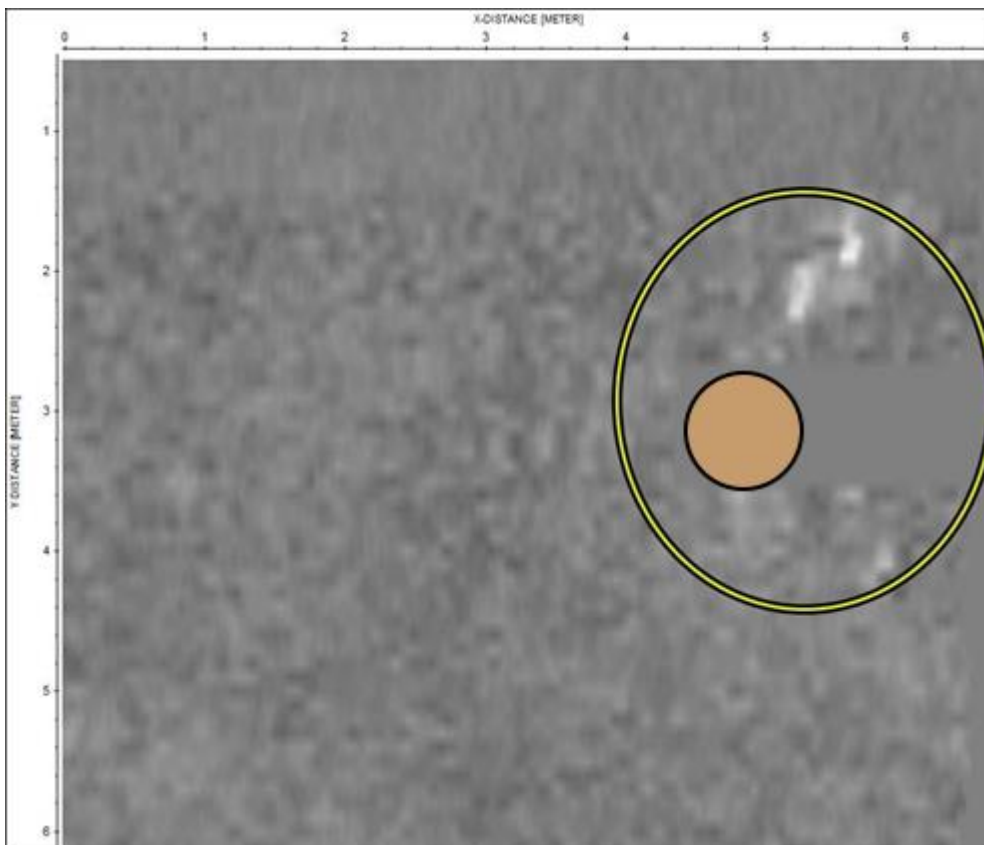


Figure 105. Time slice at an estimated depth of 5 cm on the X profiles.

Overall, the survey results were very underwhelming. Few features can be identified, and the existence of a root area around the tree can not be satisfying on its own. these are indeed very thick roots. Unfortunately, few individual roots could be detected,

and only in the vicinity of the tree.

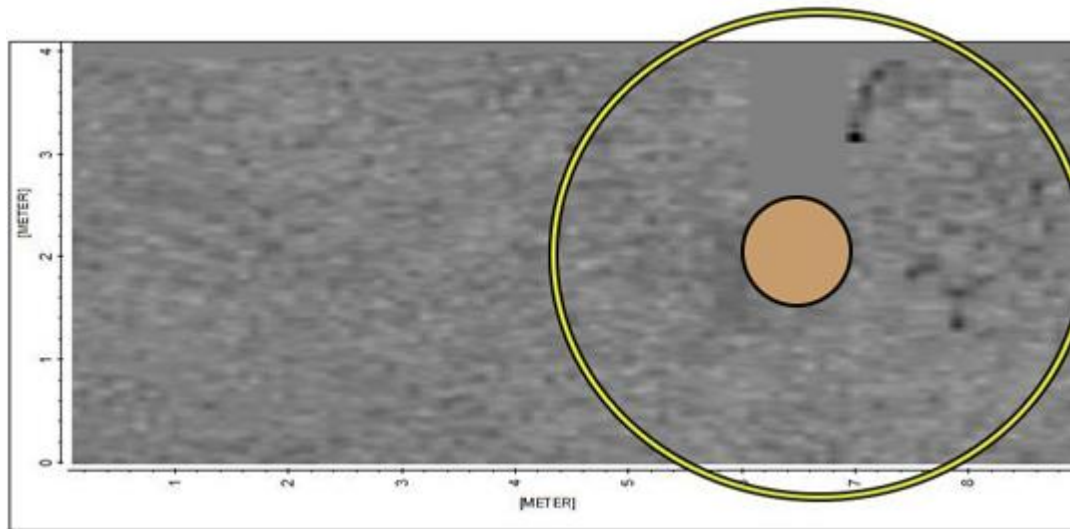


Figure 106. Time slice at an estimated depth of 5 cm on the Y profiles.

The root area in the vicinity of the tree is detectable up to a depth of 10 cm. The X profiles highlight a part of the root which was not visible at shallower depths, suggesting that the root is sloping downwards (top right of timeslice). However, the visible root area is still limited to the near proximity of the tree.

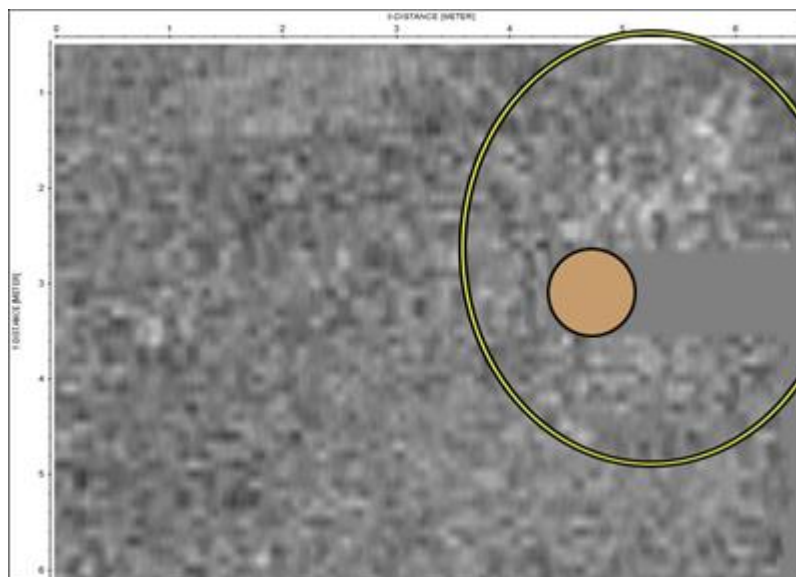


Figure 107. Time slice at an estimated depth of 10 cm on the X profiles.

A similar trend is observed on the Y lines: some parts of the root system are more visible a few more centimetres down.

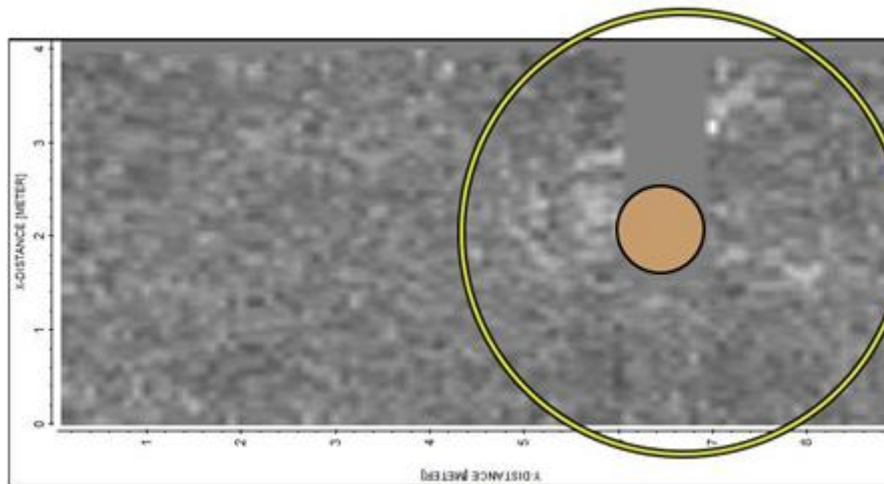


Figure 108. Time slice at an estimated depth of 10 cm on the X profiles.

However, after this depth, the quality of the data quickly degrades and no more valuable information is revealed.

It is slightly surprising that not much more can be said about the willow’s root structure – a testament to how much unsuitable conditions can affect the measurements, and even the root system a large tree expected to have thick, woody roots, cannot be reliably mapped. A root area in the immediate vicinity of the tree was identified, but no roots extending more than a couple of meters from the tree were detected. It is unlikely (though not impossible) that the tree did not have roots extending beyond this range. Instead, it is more likely only the coarsest roots could be detected, and not the thinnest ones – despite the high-frequency antenna. This would suggest either a lack of dielectric contrast, strong signal attenuation, or most likely, a combination of the two.

An important mention is to be made regarding the soil. The dielectric properties of the soil indicate that this is not similar to “natural” soil (soil from un-altered rural areas). The soil appears to be more compact, with a higher electromagnetic velocity, and riddled with noise. These factors are significant in detecting tree roots and highlight once again

the added difficulty of urban surveys. From the forward models alone, this type of unfriendly scenario would be hard to anticipate.

There is no indication that the tree is affecting nearby paved surfaces, particularly given the significant distance from the willow tree to any paved surfaces. If this was a diagnostic survey, there would be no reason to suspect impending damage in the near future.

Harborne 3 (“Leaf fall”)

The survey was also carried out in the Harborne area, but had a different secondary objective. The survey was purposely carried out in rough conditions, in the leaf fall season, in soil with a high moisture levels, and on a surface of fallen leaves. To my knowledge, no prior survey had been specifically designed to deal with these conditions. Given the fact that this season accounts for approximately 2-3 months of the UK year, it could be important to assess the feasibility of a survey over fallen leaves. It is unclear to what extent the fallen leaves interfere with the GPR signal and to what extent a survey under these conditions would be advisable (or if it would be better to remove the leaves or delay the survey to a later time), but it was expected that this would make for a very difficult GPR survey.

The survey spanned the area around two large linden trees (*Tilia* genus) in the Harborne area. Profiles were acquired in two perpendicular directions (X and Y). The surveyed area was approximately 16.1 x 6.4 meters. The distance between profiles was 10 cm in both directions. However, upon processing, it became apparent that due to a technical malfunction, the profiles on the X direction were unreliable as some of the files were corrupted. Nevertheless, this was treated as an instructive survey, using only the

files on the Y direction. The quality of the data was visibly lower than in other neighbouring areas.

Several variations were trialed in an attempt to improve the quality of the data, but yielded limited success. In a separate processing flow, a Hilbert Transform was also applied to improve visibility in some instances. This processing flow was applied to all the surveys presented here.

The Y profiles are partly successful at revealing a part of the tree root area in the immediate vicinity of the trees. As expected, there is a thick root area around the trees.

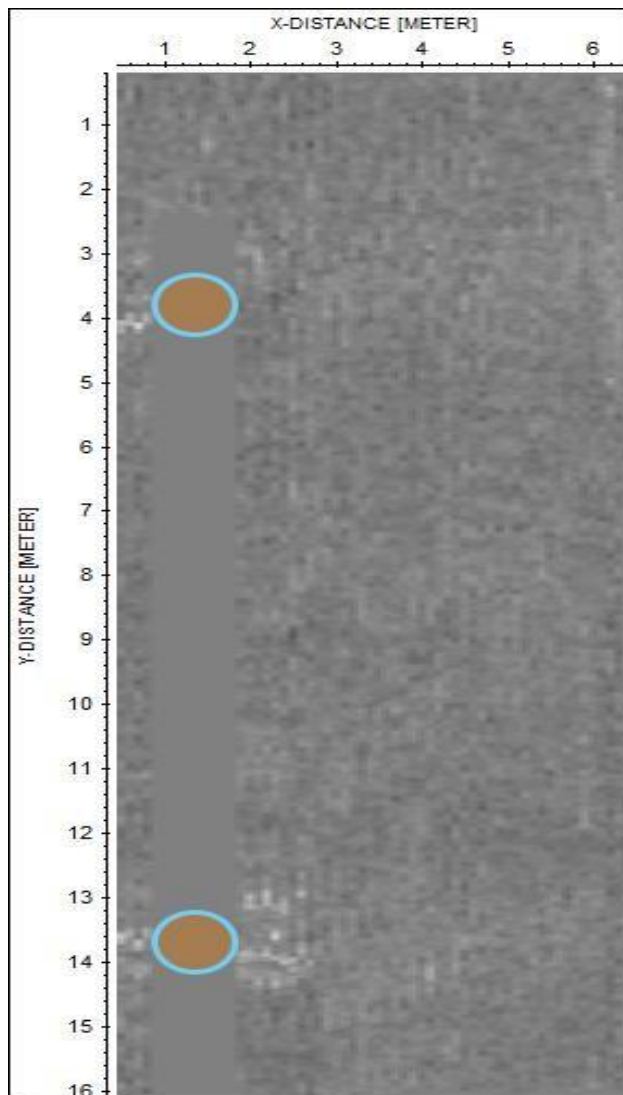


Figure 109. Time slice at an estimated depth of 2 cm. The position of the trees is represented by brown-blue circles.

However, it is very challenging to accurately assess the distribution of roots in the subsurface. While an area believed to be associated with roots is visible, this is probably only representative of the thickest, coarsest roots. Again, this is a case of low-quality data with few identifiable features.

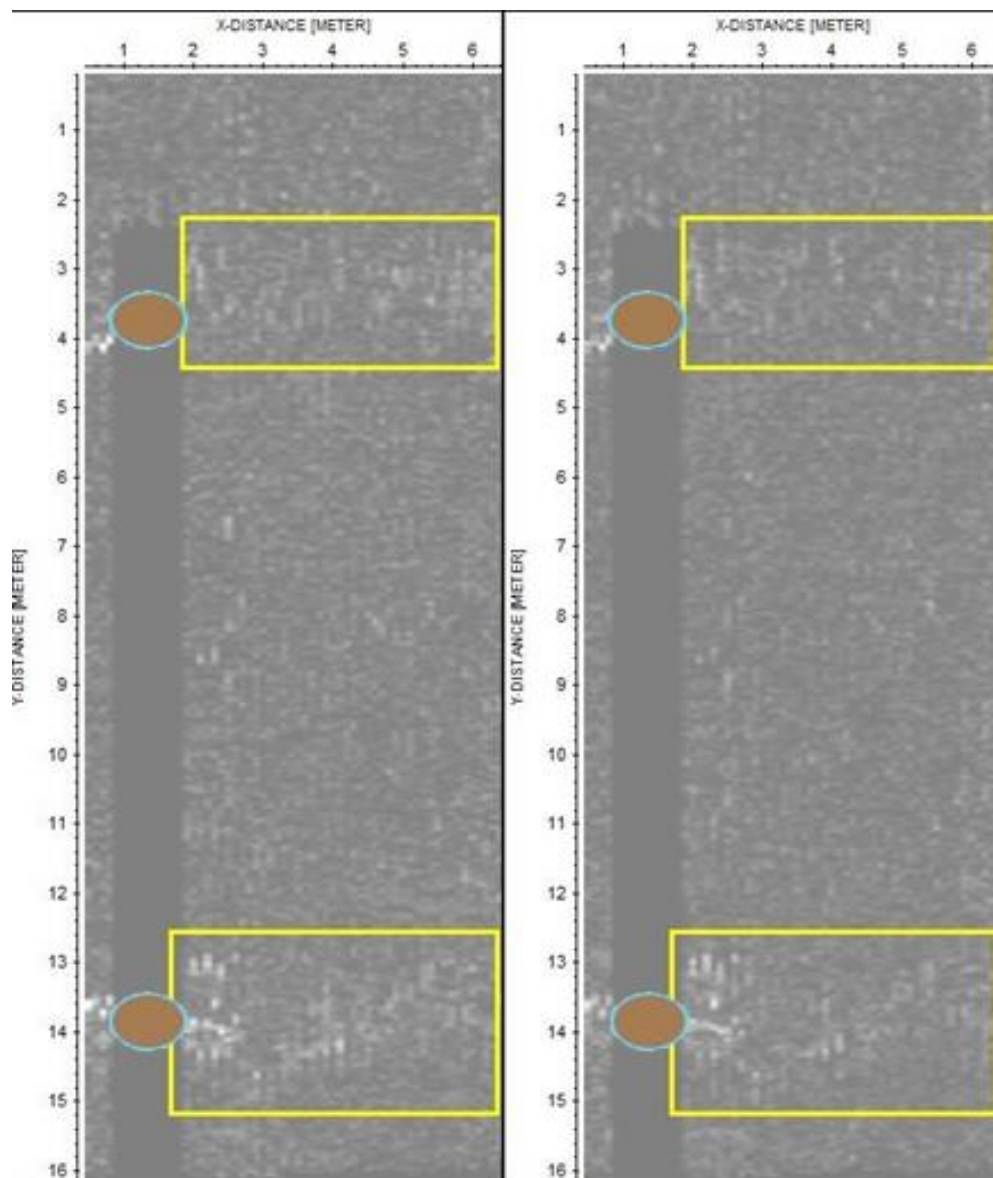


Figure 110. Time slice at an estimated depth of 6 cm (left) and 8 cm(right). The position of presumed root areas is highlighted in yellow rectangles.

Analysis of individual radargrams does not reveal much additional information. There are numerous reflections of different intensities and shapes, but the distribution

appears to be chaotic, with few discernible patterns that could lead to root identification. This is comparable with what was obtained in the previous survey.

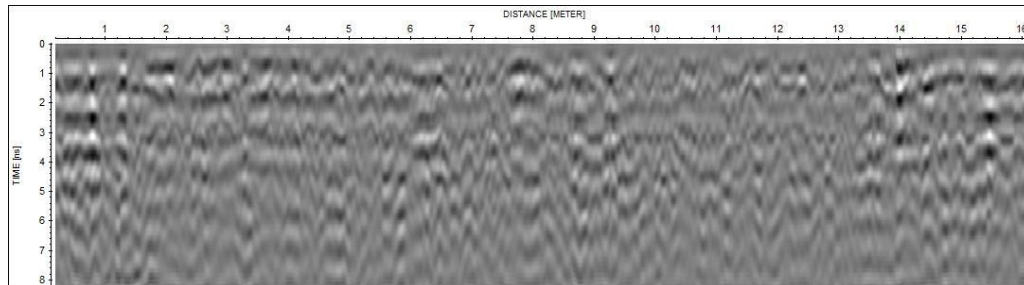


Figure 111. An example of a profile in the surveyed area. Data are processed and migrated, Hilbert transform not applied. Of note is the noise and overall low quality of this data.

Given the size of the trees, the presence of numerous roots can be safely inferred. Nevertheless, these roots are not apparent in radar data and lateral continuity cannot be established with accuracy. This could happen due to the dielectric properties of the soil (given that it is Autumn time, the soil is moister than usual), or potentially due to the fallen leaves on the ground. Since the trees were old and quite large, it is also possible (though purely speculative) that the trees' roots created a thick mesh all around the soil, making detection of individual roots more difficult.

Overall, the quality of the survey data can be considered very low. There is some useful information that can be derived, but useful data is very limited. Nothing but the coarsest roots can be reliably detected, and even for those, there is a substantial degree of uncertainty. It is not entirely clear if the issues are also related with the urban nature of the soil. Nevertheless, given these results, it seems advisable to not carry additional surveys under these conditions.

Already, several preliminary conclusions can be drawn at this point.

Carrying out GPR surveys on soils featuring fallen leaves is not advisable.

Identifying thin roots cannot be guaranteed, even with a high-frequency antenna,

especially in a non-friendly environment. Acquiring data on both directions seems desirable, but a distance between profiles of 20 cm and higher is also not advisable. Interpretation of the data is challenging, and using the position of the tree as a geometrical indicator is a useful indication. However, this opens an interesting question: if the trees had been completely removed but the roots had been left in place, would identification of the roots still be possible?

The above question, made under the assumption that roots will have the same dielectric properties, is moot. If the root system is no longer connected to the living tree, it will dry out and start to rot. This would change the roots' dielectric properties. More research at the junction of biology and soil science is required how to understand just how this process would happen, and how it would happen differently for different species. This is likely a function of tree species, soil moisture, and soil biosphere. For instance, the sap of coniferous trees is a good preservative and can help maintain roots for a longer time. A moist soil rich in fungi and decomposing microorganisms can accelerate the decay of a root, but again, the timeline and physical changes associated with this decay are not well known. For practical purposes, it can be assumed that the longer a decaying root spends in soil, the more likely it is to mimic the properties of the soil even more. However, there is a time window shortly after the tree was fallen where the roots dry out and have not yet started to decay – in this situation, detection is expected to be significantly easier as the dielectric contrast would be stronger.

Overall, however, the data in these surveys is significantly lower quality than that presented in survey 6, for instance. If this is an indication, then all these above-mentioned considerations fade in the face of a simple survey acquisition parameter: the time of year. While it is unclear whether the contrast between the roots and soil is larger in the colder or warmer time, it is clear that, especially in a climate and soil system such as England's,

summer is a significantly better time for survey acquisitions. Winter, autumn, and early spring are more likely to produce wetter soils, which worsen the detectability of all subsurface features, including tree roots. This is unsurprising, but it was worth putting to the test to see if potentially stronger contrasts outweigh this disadvantage. This is not the case.

5.9 A series of Harborne asphalt surveys

An additional set of surveys was carried out on paved surfaces (essentially, on sidewalks and walkways). These were mostly small surveys, of only a few parallel profiles (in one direction), carried out to assess potential damage to the paved surface. The survey areas were chosen where longer profiles could be carried out on a direction perpendicular to the presumed root direction.

These surveys would mimic a low-cost, quick survey designed to assess potential root damage.

Harborne asphalt 1

The survey was carried out in the Harborne area. Parallel profiles were carried out at a distance of 10 cm, going in one direction and returning from the other. Special attention was paid to the positioning of the profiles – and in particular to the antenna positioning.

For a simpler analysis, the profiles (which are over 15 meters long) were split into two halves.

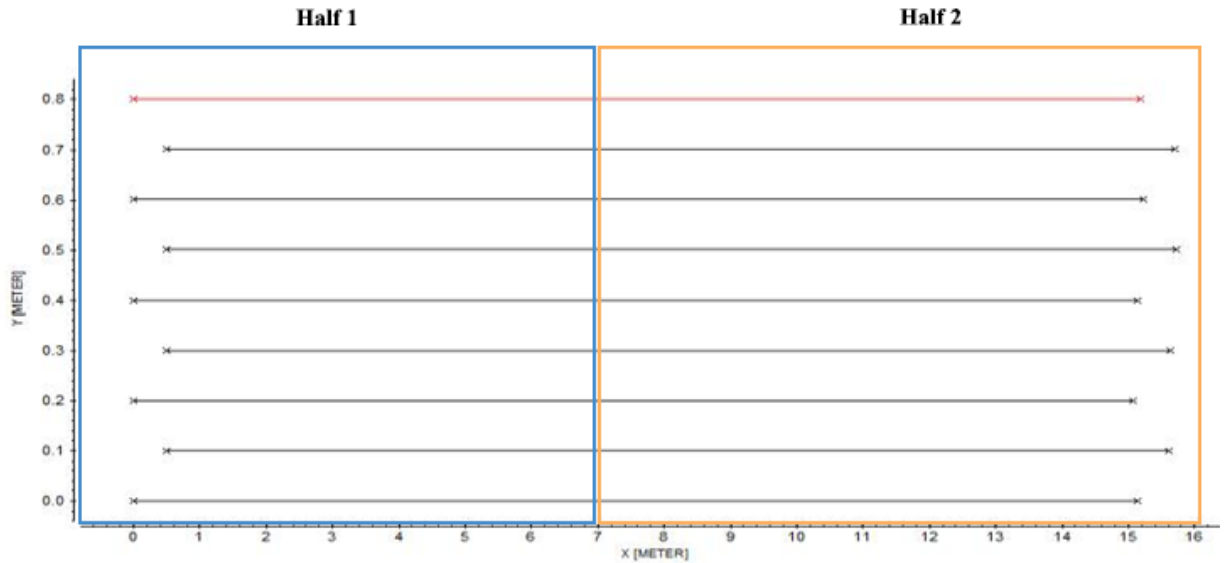


Figure 112. Depiction of profile geometry. The even profiles were arranged to depict the real position of the antenna. Image not to scale. Half 1 corresponds to Figure 113, Half 2 corresponds to Figure 116.

Some damage associated with tree roots was visible on the surface, and the position of this damage was noted. The focus was exclusively on the top 10 centimeters. All potential tree root damage appeared limited to this interval.

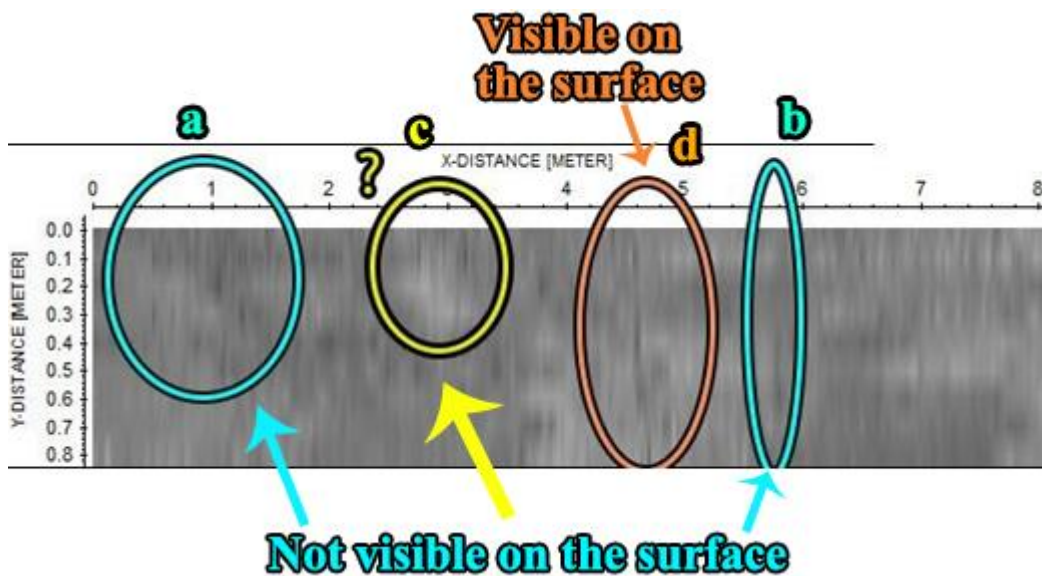


Figure 113. Time slice of the first half of the survey at an estimated depth of 3 cm.

The orange highlight (d) marks the position of tree root damage that was visible at the surface. It can be observed in all the radargrams, although the interpolation algorithm

suggests gaps or discontinuities (this is, perhaps, an indication that a 10 cm separation between profiles is too much). However, the fact that even tree root damage which is visible on the surface produces such faint contrasts is telling to how difficult the detection of these roots can be. The other suspected areas of root damage are much harder to interpret.

A few areas (most notably, the one highlighted in yellow) could suggest incipient. Several reflections can be noticed in the first half, particularly on the middle profiles, but given their lack of lateral continuity, these cannot be assumed to be roots. This was interpreted as an area that potentially has incipient damage, but it is not possible to trace this to tree roots.

However, there are two areas which could potentially be associated with roots (highlighted in teal ellipses). The first one (a), around the 1 meter mark, is reflected by what appears to be a series of irregularities with potential (but unconfirmed) lateral continuity. It is not clear what these could represent – it is unlikely that they represent actual roots, but could be associated with roots in the form of cracks or asphalt deformations.

In this case, investigating individual profiles can help reveal the nature of this contrast.

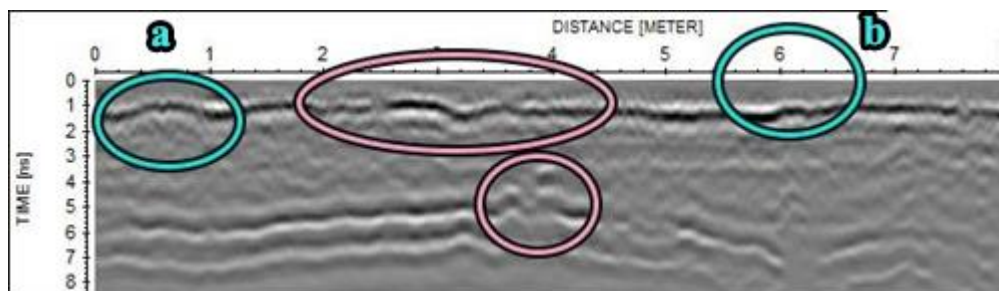


Figure 114. Profile 3 (at $x = 0.2$ m). The teal ellipses indicate probable deformation areas highlighted in the time slices. The pink ellipses indicate apparent deformations which do not exhibit lateral continuity.

The profiles highlight apparent irregularities in the asphalt, including some at the very surface level (which was not visible on the surface). However, it is not clear if this is related to tree roots, but it is an indicator of stress on the asphalt nonetheless.

The second (b), around the 6 meter mark, represents a thin line; on the profiles, it appears as a very subtle but distinguishable deformation in the surface layer of the asphalt. This is quite likely associated with tree roots, although is only barely visible in the time slices. It is an example when, even without lateral continuity, there are strong indications of existent tree root damage.

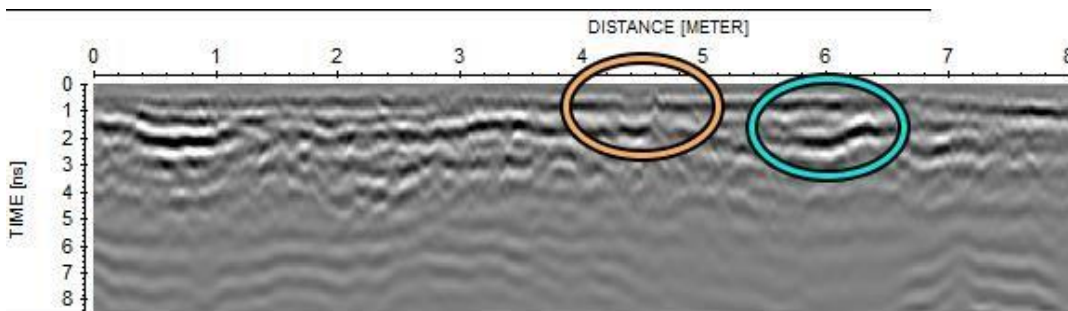


Figure 115. Profile 9 (at $x = 0.8$ m). The orange ellipse indicates damage visible on the surface (not the visible large discontinuity in the asphalt surface), and the teal ellipse indicates presumed deformations associated with tree roots. This was not visible on all profiles.

There are a few notable things about the visible crack as well. The crack was only 1-2 cm wide, but it appears much wider on the profile. Additionally, the root itself is not visible on the radargram.

In the second half of the surveyed area, there are even more areas of interest where tree root damage is suspected, though data interpretation is challenging.

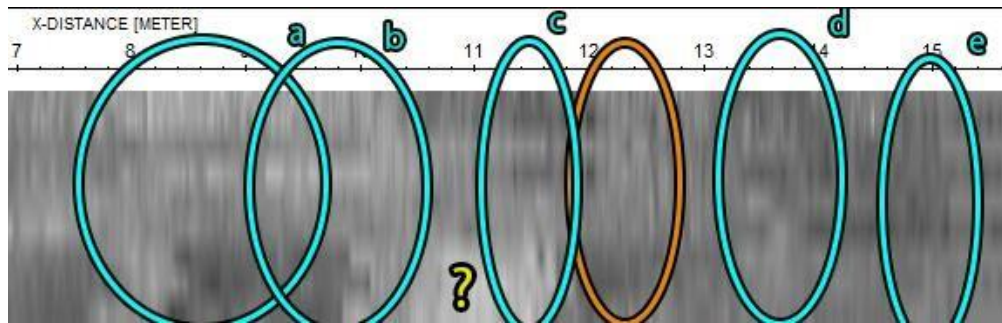


Figure 116. Time slice of the second half of the survey at an estimated depth of 3 cm.

While not evident at first glance, there are several features that are likely correspond to tree root damage. The orange ellipse indicates root damage that was visible on the surface, and this area was not analyzed here since it was already visible. However, five other areas were identified (a-e), highlighted here in teal ellipses.

The 'c' ellipse may exhibit tree root damage, as it showcases two potential lines associated with tree roots. These areas are visible as discontinuities and clear reflections on the profiles, indicating that there is indeed asphalt damage. The lateral continuity suggests and corresponding profiles exhibit a potential root connection. Individual profiles are also consistent with tree root-caused damage. This area was interpreted as likely to have root-induced damage.

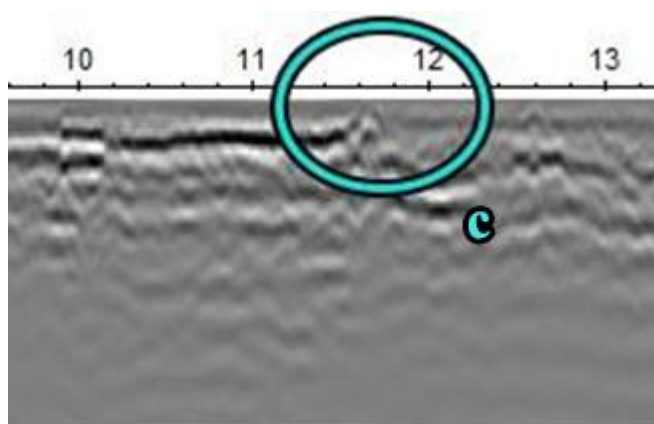


Figure 117. Example of deformations in the 'c' area.

The 'a' and 'b' areas shows radargram features similar to the ones in the first half

(vertical deformations), but unlike a “messy” radargram, they are more hyperbolic in nature, and more suggestive of an intrusion. These both seem indicative of asphalt damage, which is likely root-related.

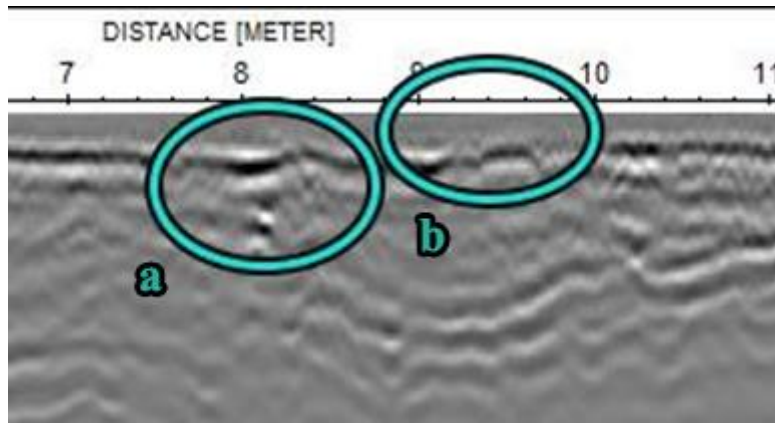


Figure 118. Example of deformations in the ‘a’ and ‘b’ areas.

These areas have some similarities to the forward models produced in Figure 41, though if this is indeed the scenario present in this area, it appears that the fissures are not water-filled.

Similarly, the ‘d’ and ‘e’ area are indicative of asphalt damage, but it is less clear whether this could be caused by tree roots. The ‘e’ area, despite being less clear on individual profiles, appears to have lateral continuity, which is consistent with root damage.

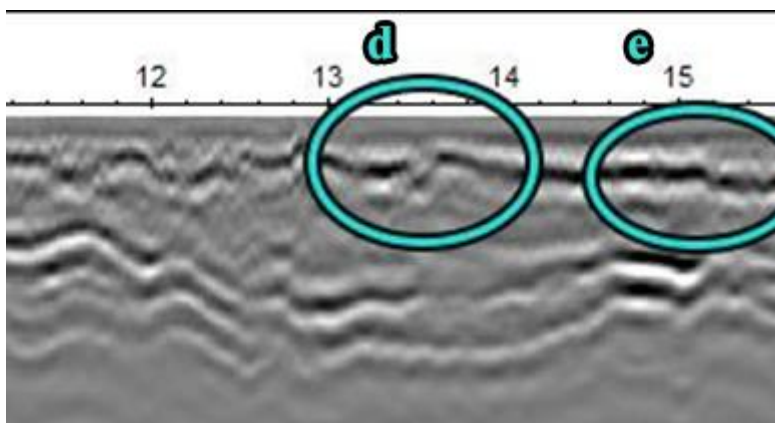


Figure 119. Example of deformations in the ‘d’ and ‘e’ areas.

Deeper timeslices were analysed and interpreted in a similar fashion. However, no additional features were identified, suggesting that asphalt damage is mostly limited to the very surface parts, as was expected.

It is also important to note that since surveys were only carried out in one direction, it is possible that root deformations parallel to the survey directions were completely missed by the GPR data. The chosen direction was perpendicular to the expected direction of the tree roots. It is also important to consider that asphalt also tends to accumulate damage and distortions, even without tree roots. Not every such feature should be associated with a root.

In the end, the areas most likely to be associated with tree-root damage were identified, and highlighted in teal ellipses below. Had this been a monitoring survey, in addition to the areas where root damage was visible on the surface (highlighted in orange ellipses), these would have been the areas of maximum interest (teal ellipses, corresponding to a and b in the first half of the survey, and c and e in the second half of the survey):

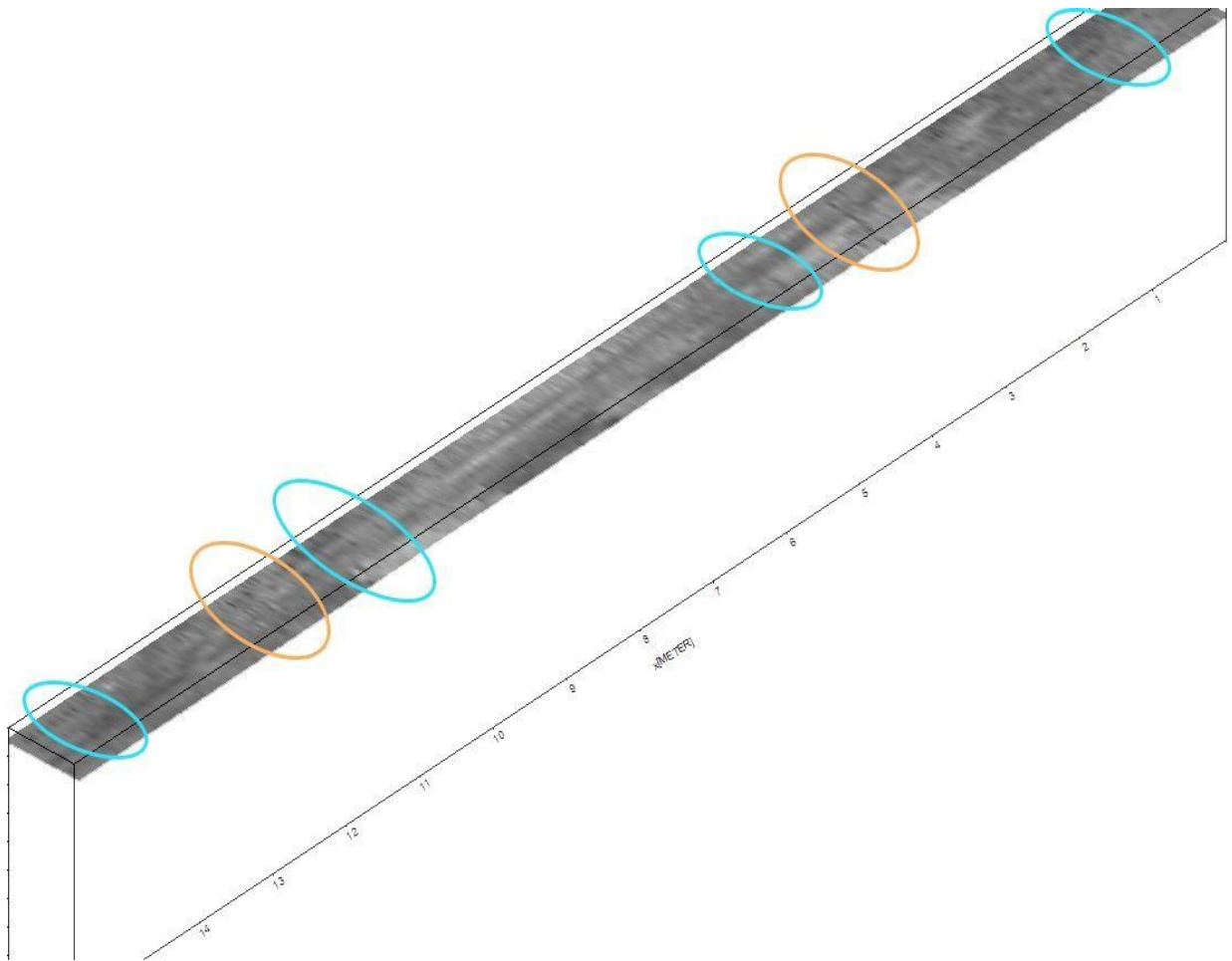
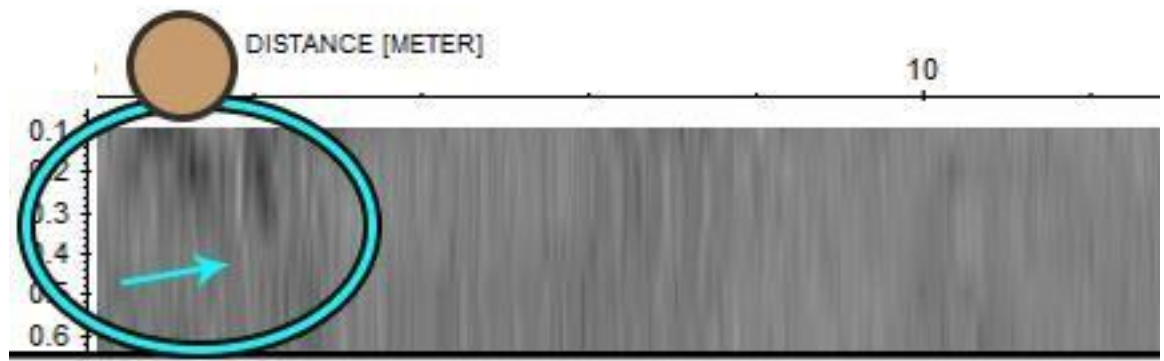


Figure 120. 3D visualization with the most likely root-associated areas (highlighted in teal). Orange ellipses indicate a buried cable and a root that was visible at the surface (and therefore not revealed by geophysical surveys). Image is not to scale.

Harborne asphalt 2

The second survey was also carried out in the Harborne area, and also consisted of 6 long parallel profiles carried out in one direction, at a distance of 10 cm between profiles. As the profiles are around 34 meters long, they were split into 3 parts. The data was not migrated, which in this case, aided interpretation of data.

The first part of the surveyed area shows more signs of degradation than the previous survey. Emphasis was placed on features which were likely to represent root-associated damage or roots themselves.



Timeslices at estimated depths of 3 cm (top) and 4 cm (bottom). Brown circle marks the position of a tree.

Teal ellipse marks area of root-associated damage.

As expected, the vicinity of a tree is more likely to lead to pavement root damage. The arrow indicates a signal very likely to be associated with a root. It has lateral continuity, a relatively strong contrast. Around it is another area which could be indicative of asphalt damage. This interpretation is confirmed by individual profiles, which show a root penetrating into the asphalt.

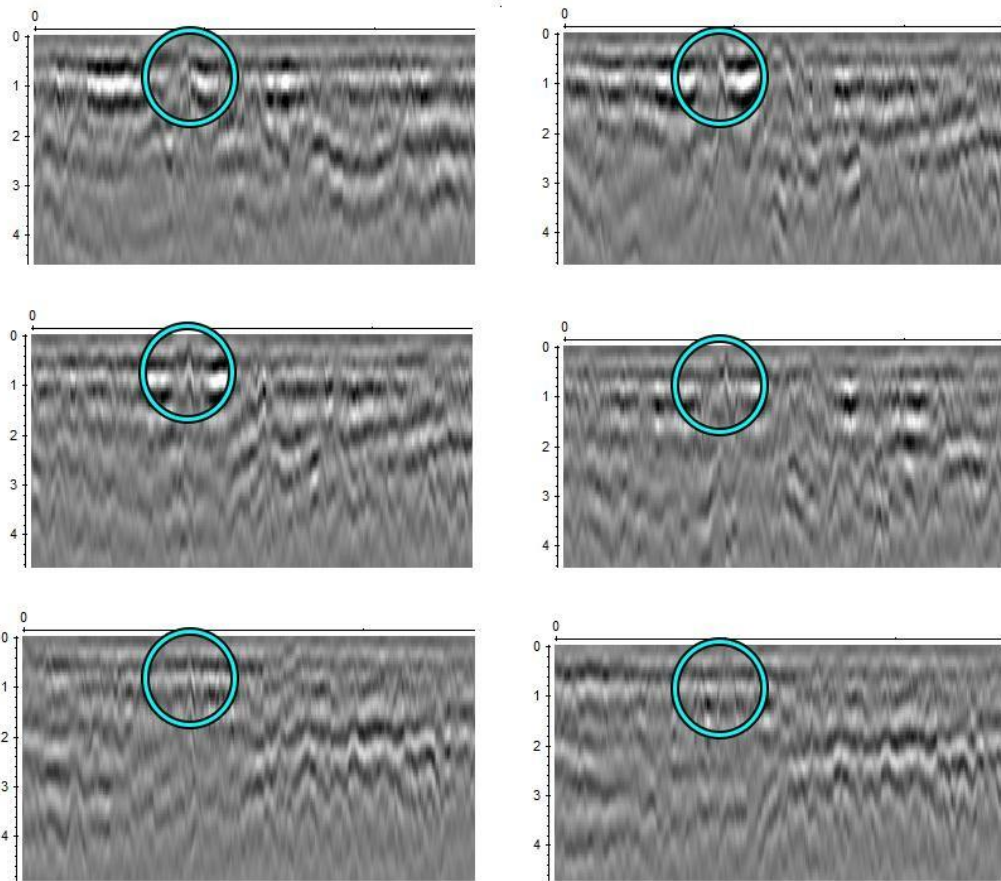


Figure 121. Section of all 6 profiles depicting what was interpreted as a root penetrating the asphalt (in teal circle).

The root appears to be visible on all 6 profiles, to an extent. It appears hyperbolic as the data is not migrated. However, it appears to be becoming less visible towards the later profiles, suggesting that the damage is less severe as we move away from the tree. In the 6th profile, it is hardly visible at all. Overall, this is interpreted as compelling evidence of active root damage, and this damage is largest in the area closest to the tree. This conclusion could only be reached by analyzing both the profiles and the timeslices in conjunction. Other deformations consistent with tree root damage can be seen in this area of the survey. Multiple hyperbolae potentially consistent with tree roots were identified.

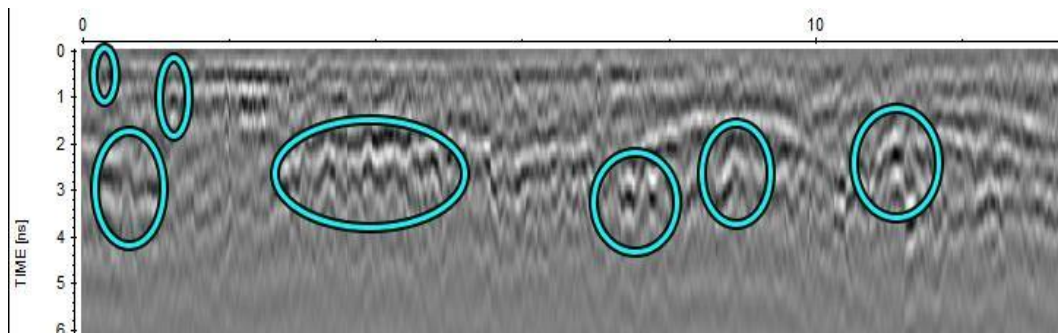


Figure 122. A radargram from profile 4. The areas that can potentially represent tree root damage are highlighted.

However, despite such a large number of suspected areas, their lateral continuity cannot be established and therefore, it can also not be established whether they are tree-root-related or not. As a whole, however, the entire area appears to be actively affected by tree roots, or at the very least, appears damaged.

Two other areas appear consistent with tree root damage. They both appear to have some lateral continuity but appear very faint.

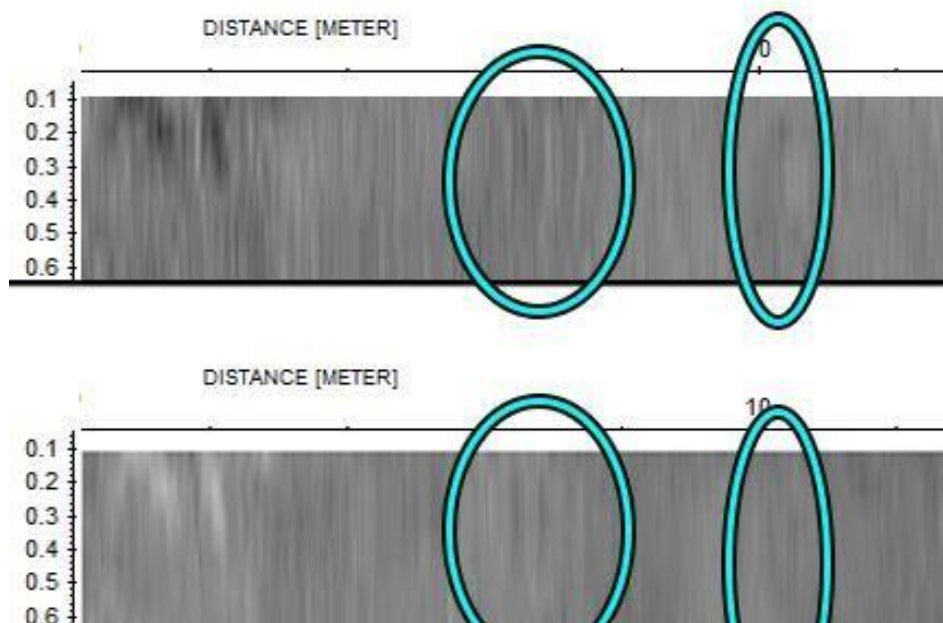


Figure 123. Timeslices at estimated depths of 3 cm (top) and 4 cm (bottom).



Figure 124. The same areas highlighted on profile 4.

The second part of the survey revealed three additional areas consistent with root damage. Two are highlighted in the larger ellipse (with white hues), and one in the smaller one (black hue).

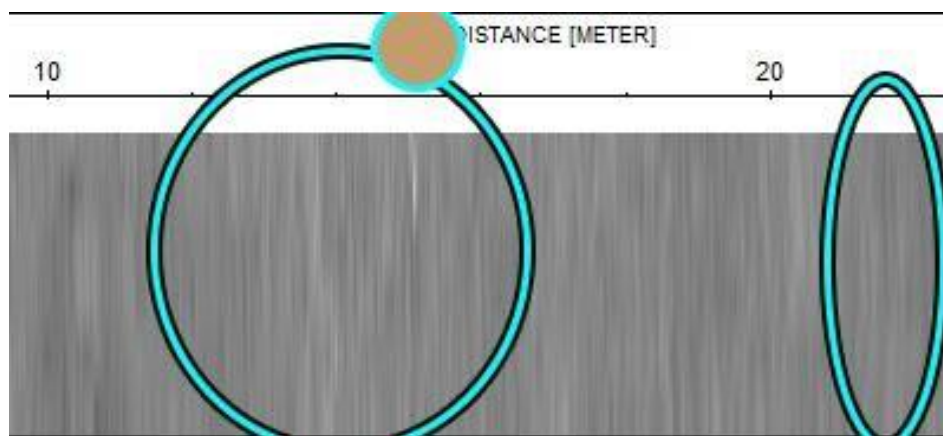


Figure 125. Time slice at an estimated depth of 4 cm. Position of the tree is marked.

These areas are also faint, but do exhibit lateral continuity, as exemplified below, which makes them like to be incipient areas of tree root damage.

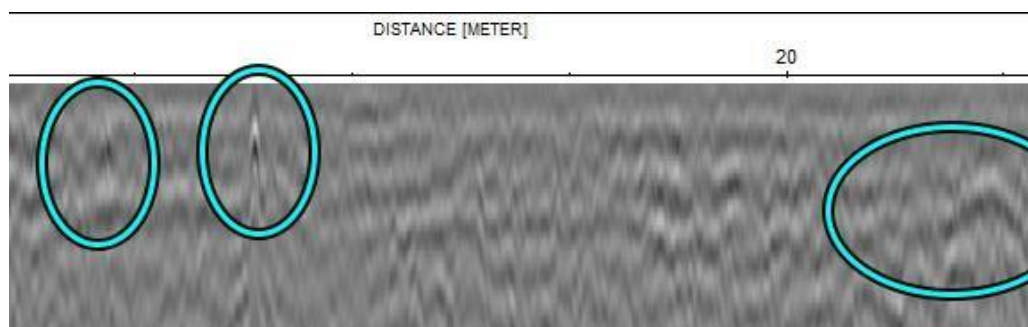


Figure 126. The same areas highlighted on profile 2.

It is important to note, when analysing tree root damage, the distance to existing trees (and in some cases, tree roots that may have belonged to felled trees). However, the distance at which urban tree roots can spread should not be underestimated. This survey was carried out in an area where trees were essentially surrounded by asphalt, and only had access to a small soil surface area. In these conditions, roots can extend far beyond into the asphalt, and the roots of mature tree can easily reach 10 meters or even more.

The third section of the survey is dominated by two duct areas. These areas were paved with a different material than the rest of the sidewalk. They were very clearly visible, but no root areas of tree root interest were identified.

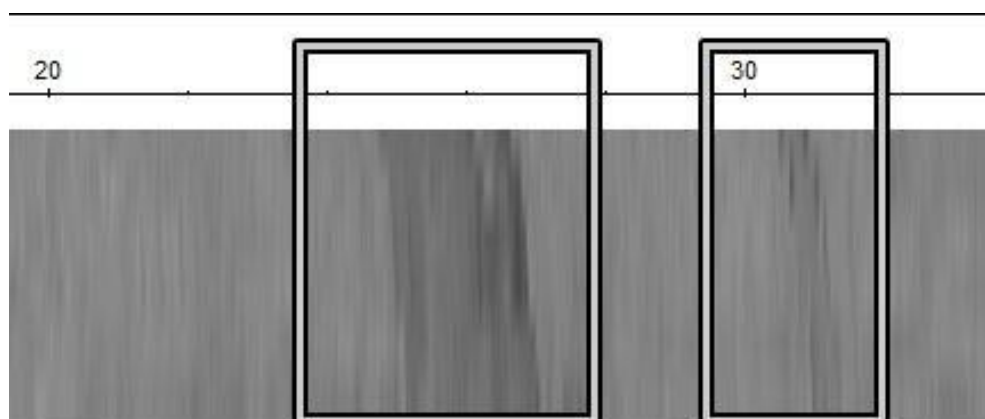


Figure 127. The two areas are the only remarkable features on the survey are both man-made.

Most of the detected roots are in shallowest areas – most often, the first 5cm. This is natural, as roots have little incentive to spread into the deeper parts of the ground, where water is scarcer (unlike soil, water does not permeate through asphalt, so roots have an extra incentive of nearing the surface). However, roots do tend to penetrate in the lines of minimum resistance, and can go to deeper areas in some conditions. Another important mention is that in the case of leaking pipes, the roots can go deeper in the direction of the extra humidity. However, this does not appear to be the case here.

In general, these surveys support the idea that tree root surveys can be more successful when carried on paved surfaces than on soil, as tree roots tend to mimic the dielectric properties of the soil they are in. In addition, urban soils are also more challenging to work with. This type of soil is often a much more compact (as highlighted by different speeds in urban soils compared to reference natural soils) and inhomogeneous material (at least in most of the situations studied here). However, even on paved surfaces, detection remains challenging. In this particular cases, what roots are causing asphalt damage appear to be thin. The interpretation is difficult and is unlikely to identify all the root-affected areas, especially areas of incipient damage. However, even in this case, areas of interest can be highlighted for further monitoring, and some areas likely to be roots have been identified.

Lastly, it is worth mentioning that roots themselves can change soil properties for decades (Pawlik and Kasprzak, 2018), and this mechanism has not been sufficiently investigated in urban areas.

5.10 An integrated GPR/ERT example

Lastly, an example of a mixed survey using both GPR and ERT is presented. Here, the complementarity of these methods was put to the test in an area suspected of tree root damage.

The surveys were carried out in the Harborne area, near a mature linden tree (genus *Tilia*) suspected of causing damage to nearby asphalt.

Two separate GPR surveys were carried out in the vicinity of the tree, one on the paved surface (GPR 1), and another on the soil area between the tree and the asphalt (GPR 2). An ERT survey was also overlaid on the second GPR survey for additional information.

The primary objective of the surveys was the mapping of a root that was visible in the very vicinity of the tree, and then seemed to continue underground in the direction of the asphalt. However, on a more general level, the mapping of all present roots was desired.

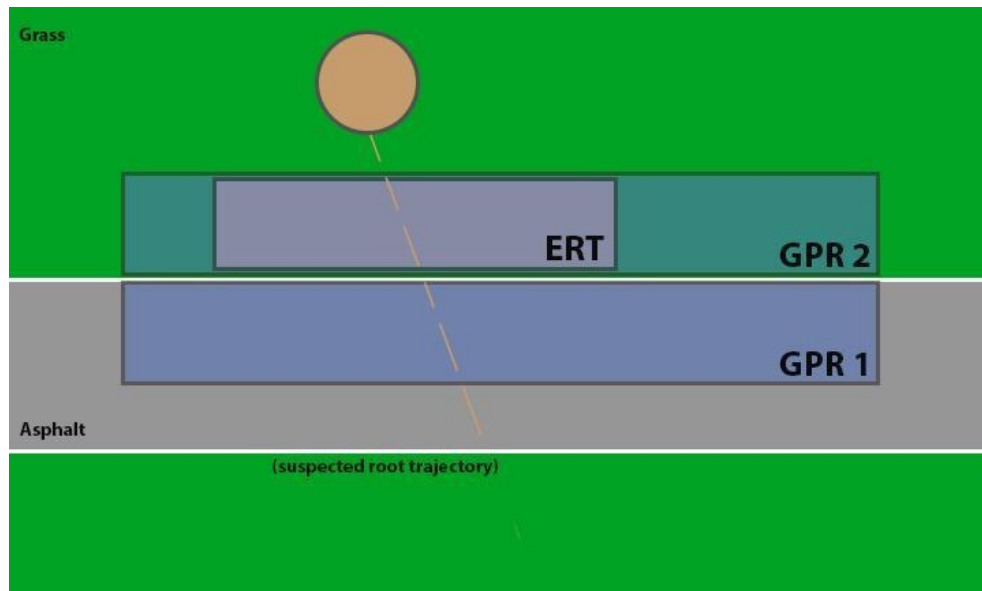


Figure 128. General depiction of the survey area. The survey areas are not to scale.

The GPR surveys were carried out with a 1500 MHz antenna, with a transect spacing of 5 cm. Although the 5 cm separation was found to bring marginal improvements compared to 10 cm, this was preferred as a precaution to ensure data quality. The ERT was carried out using the Dipole-Dipole array, with an electrode distance of 10 cm.

The design of the survey drew from previous experiences. The GPR profiles were approximately 5 meters long, whereas the ERT profiles are 1.5 meters long.

GPR 1

Several areas potentially indicative of root damage were identified on this survey. Root-like features were observed on several radargrams. Nevertheless, the lateral continuity was rather unusual. Instead of exhibiting clear lateral continuity, it appeared

That an entire area was exhibiting deformations.

Two areas appear potentially indicative of a root area. Potential trajectories were identified, but the radargrams were not clear enough to draw definite conclusions.

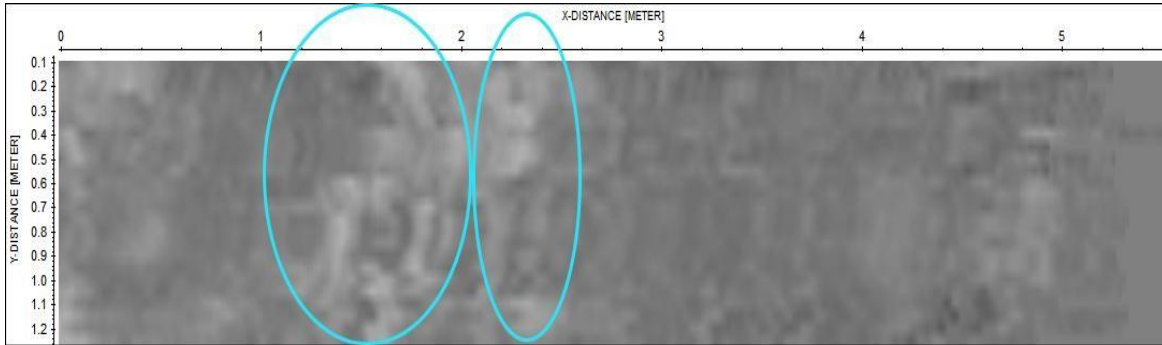


Figure 129. Time slice from an estimated depth of 4 cm from GPR 1.

GPR 2

The data gathered on the soil surveys proved less conclusive. Although the surveyed area was in the vicinity of the tree and the roots were there certainly coarse, both the radargrams and the time slices did not show irrefutable evidence of tree roots.

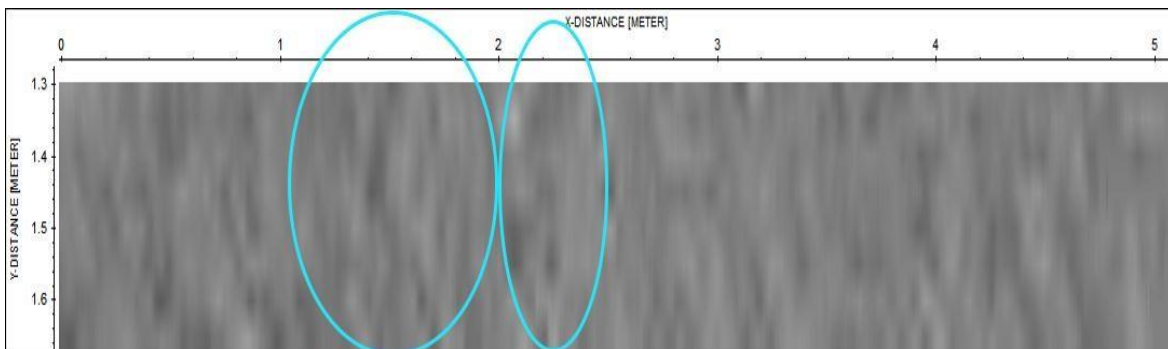


Figure 130. Time slice from an estimated depth of 4 cm. Same areas as above are highlighted.

In one profile, where the root was extremely close to the surface (which was confirmed subsequently by a small-scale soil dredge), there are visible reflections consistent with the observations in GPR 1.

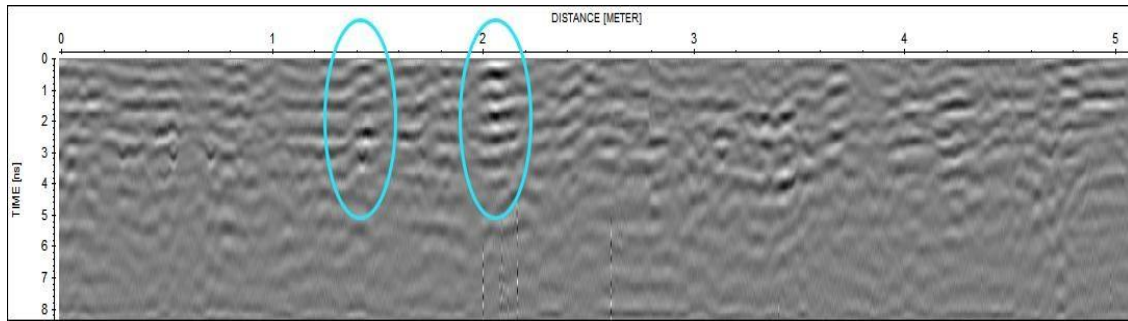


Figure 131. Profile example from GPR 2.

However, given that the lateral continuity is unclear, it is difficult to make strong claims. Indeed, there is little to differentiate the highlighted areas above from other areas, and establishing the lateral continuity of roots is not possible (other areas also appear indicative of roots, but this area alone was focused on in this study).

It should also be said that at the time of the survey, the soil appeared quite wet, and was riddled with pebbles, which made for rather unsuitable GPR surveying conditions.

In order to aid data interpretation, an ERT survey was also deployed.

ERT

A total of 8 parallel ERT profiles (perpendicular on the presumed direction of the roots) were deployed. The dipole-dipole array was used. The electrode positioning was ensured by acrylic plates with holes drilled at regular intervals as per Gereia and Mihai (2019). The RMS errors are all within 2%.

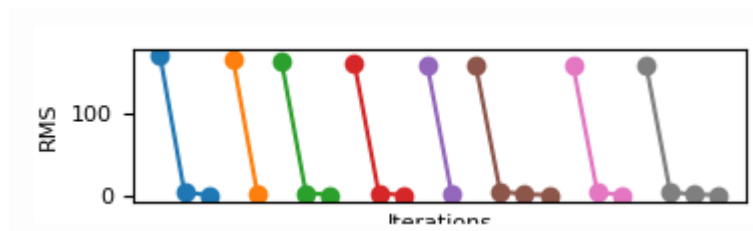


Figure 132. ResiPy representation of the RMS error of the 8 different profiles is very similar. Points represent iterations for every profile.

All profiles show strong positive anomalies. Although the absolute values for inverted resistivity are somewhat varying, this was considered an artifact of inversion rather than an indicator of the true resistivity values of roots and their surrounding areas.

As with the previous example, the positioning and dimension of the anomaly is approximate. The resistivity anomaly tends to exaggerate the dimensions of the root, and if a root is very close to the surface, the anomaly stretches directly to the surface.

Unlike the GPR measurements, however, lateral continuity is readily apparent. Several anomalies are readily visible on all the profiles, although their strength varies.

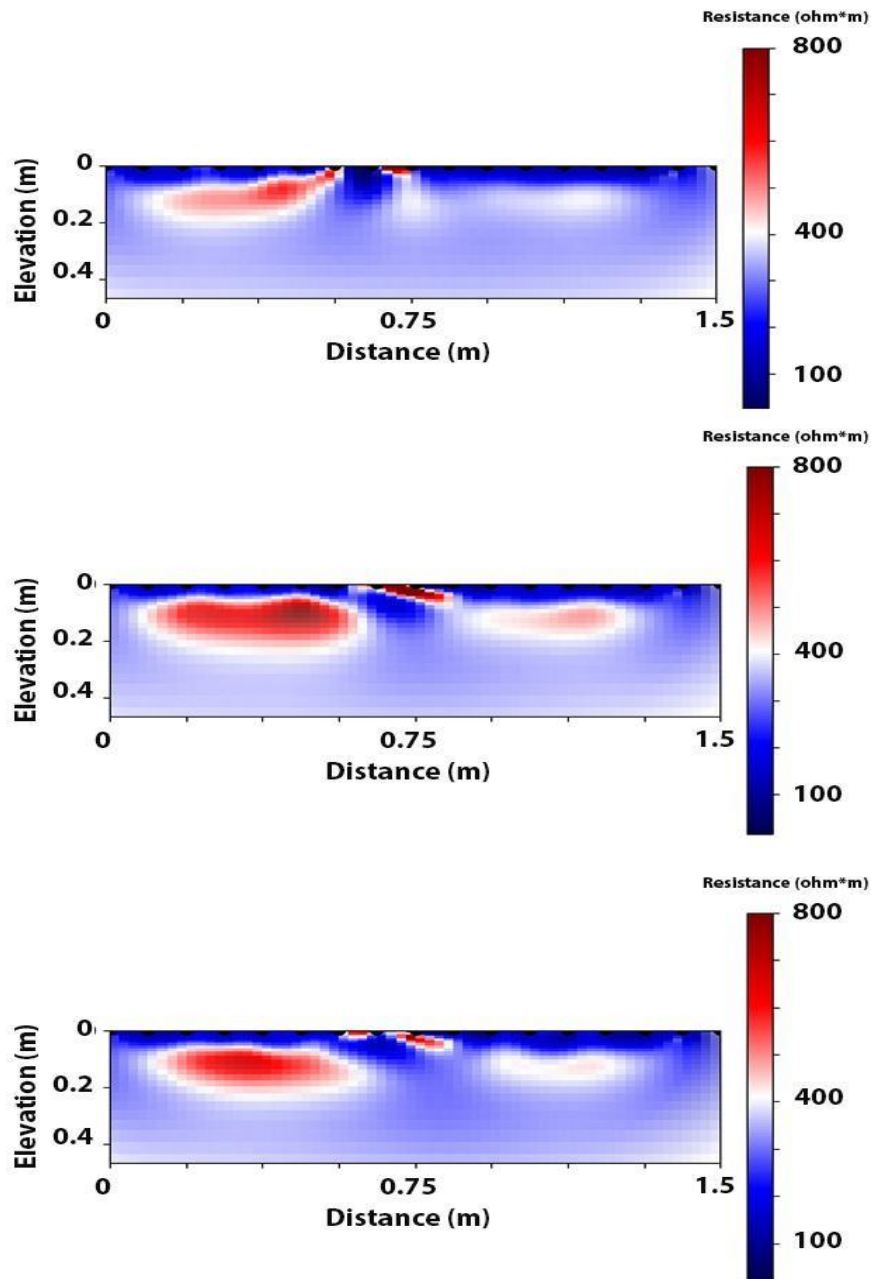


Figure 133. Profiles 1, 2, and 3 of the ERT.

Interpreting whether individual anomalies are indicative of a single root or two roots is not a simple task. A look at profile 2 above, for instance, suggests that the left-hand anomaly is indicative of 2 roots (seemingly having 2 high-resistivity areas). However, profile 3, for instance, is more ambiguous. The central anomaly also appears to have 2 distinct areas on profile 3, but this is misleading – as was subsequently revealed by shallow digging verifications, it was indeed a single root in the centre.

The data was also migrated into 3D using BERT. As previously, the 3D data is approximate in terms of volume and position, but it does highlight nonetheless the existence of at least three different roots. The results were plotted in Paraview and clipped so that the high values are highlighted. The resulting data highlights the estimated position of the roots.

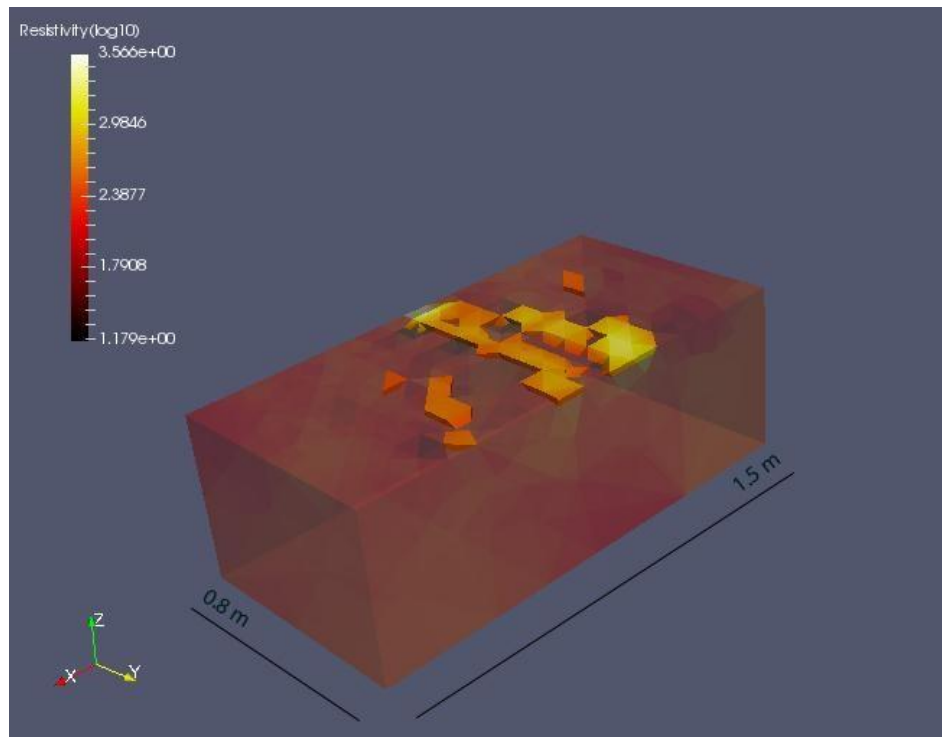


Figure 134. The estimated position of roots from ERT data visualized in Paraview.

There are a few differences when comparing with individual profiles, which highlight some of the potential shortcomings of 3D ERT data (and why individual profiles should still be analysed if 3D data exists). In particular, one of the roots (the one that appears ‘incomplete’ above) is visible individually on all single profiles – but it does not appear continuous on the 3D data. This happens due to a reduced contrast on some of the profiles, but also due to significant background variation on some of the profiles (presumably due to localized differences in moisture).

It is worth mentioning that as they use different inversion and meshing mechanisms,

BERT and Resipy can sometimes have different resistivity results – and this is also the case here (which is why results from two different packages are presented). The Resipy inversion seems to be more clearly contoured here, as is also indicated by the fact that the positive anomalies appear under the surface on Resipy (as was true of the roots), whereas on BERT, they appear on the surface.

Integrating GPR and ERT data

Integrating both GPR and ERT data proved to be particularly fruitful. For instance, when the ERT profiles are overlaid on the GPR profiles, there is a good correlation between the suspected root areas on the GPR and the ERT positive anomalies.

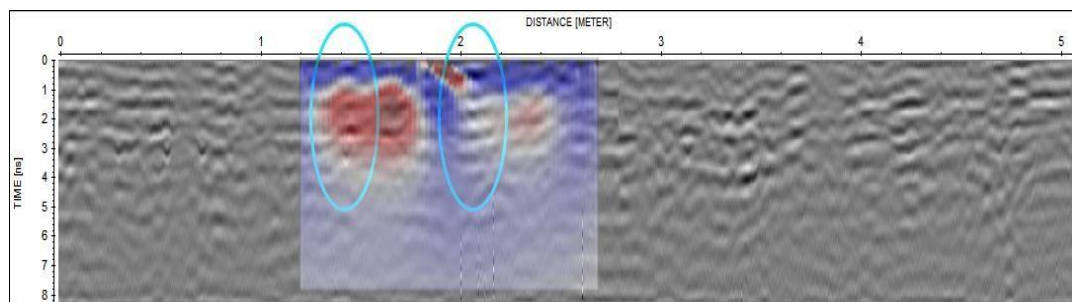


Figure 135. GPR profile 2 and ERT profile 2 overlaid.

The suspected root areas from the GPR correlate with ERT anomalies, which is a reliable root indicator.

The ERT contrasts (highlighted in yellow below) also correlate with visible GPR features. These features, however fade and unclear, appear consistent on multiple profiles. Therefore, they seem to exhibit some lateral continuity, visible on individual profiles (although not in time slices), even though it is not readily apparent from the GPR data alone.

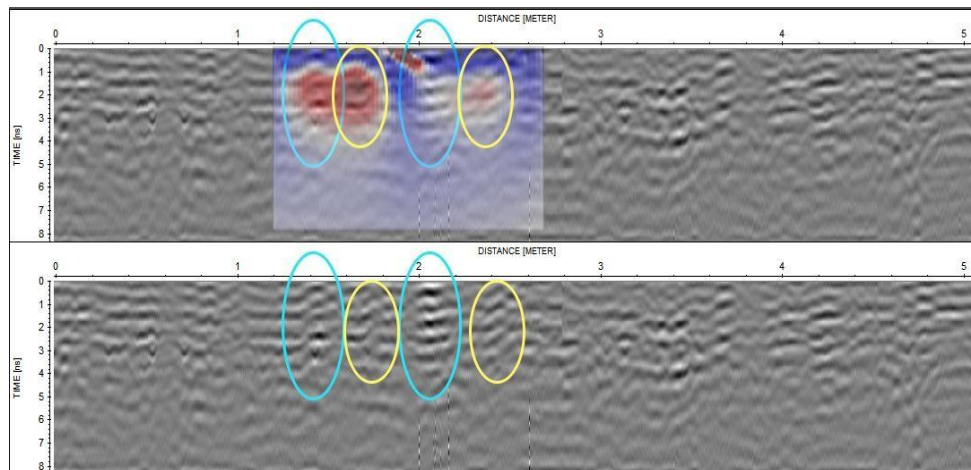


Figure 136. GPR and profile 2 overlaid, with GPR and ERT contrasts highlighted.

This highlights how well GPR and ERT data can work together and complement each other. It is easy to over-interpret or under-interpret GPR data, especially in realistic scenarios, where the urban soils are often inhospitable and unpredictable, frequently containing pebbles and other objects to serve as noise. ERT can serve as an excellent complement to this method, confirming GPR findings.

Given the difference in data acquisition time, it is best if GPR is used as a main method, and if the data is ambiguous, ERT can be employed to add more certainty.

In this case, the geophysical integrated data suggests the existence of not one, but four roots extending into the asphalt. Of course, the surveys on soil cannot exhaustively prove that the roots are extending into the asphalt, but if they extend to the very edge of the asphalt, then it is very likely that some damage has already happened or will happen in the near future.

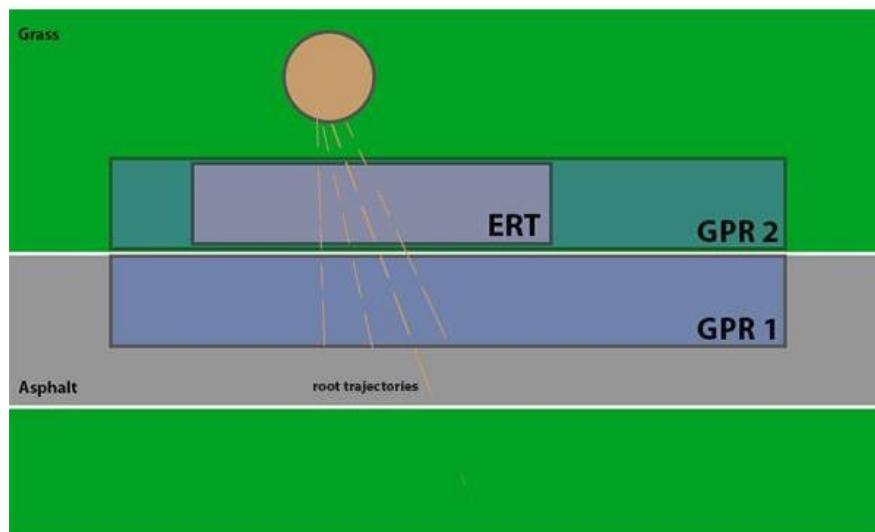


Figure 137. The root trajectories inferred from geophysical surveys.

After the survey, very small, centimetre-sized patches were dug manually, and the existence of 4 roots was confirmed in the area of interest. This confirms the advantages of joint usage of GPR-ERT surveys in the detection of tree roots.

Just as in previous GPR surveys in the literature, the method alone does not appear able to resolve and map all present tree roots. However, this recommends the use of ERT as a complementary geophysical method.

6. CONCLUSIONS AND RECOMMENDATIONS

The thesis analysed the use of geophysical methods to study and detect tree roots in an urban environment, and the potential to assess structural damage to man-made structures. GPR and ERT were the two geophysical methods selected for this purpose.

The study employed a multidisciplinary approach, attempting to bridge together information from multiple fields, using a variety of approaches. This has proven a challenging but rewarding task.

As this study progressed, it became clear that from this multidisciplinary puzzle of geophysical study of tree roots, several pieces are missing, and there are significant knowledge gaps. The biophysical understanding of tree roots is incomplete and the peculiarities and site-specificity of urban soils pose extra difficulties to detection. The mechanisms and behavior of roots penetrating man-made paved surfaces is also understudied. As a result, general conclusions are difficult to draw, and most findings should be interpreted in their own context. Still, the thesis strives to address general issues regarding the geophysical study of tree roots in general. Negative and unclear findings are also discussed, as these can also provide useful directions for future research and can also help shed light on the task at hand.

In the end, this thesis attempts to provide contributions to the field and fill some of these knowledge gaps and with new insights and directions. It is hoped that this effort can inspire additional research in relevant fields and make a practical impact, contributing to making tree root surveys a more reliable and usable tool for urban planners.

6.1 Research questions

In the first part of this study, several research questions were asked. These questions guided the work presented here, and answers (or at least partial answers) can be given.

Main research questions:

a) *Is there a reason to study the interaction between tree roots and infrastructure with geophysics?*

Yes. This part was answered during the literature review, presented in Chapter 2. The destructive interactions between tree roots and paved surfaces can be seen in most if not all urban areas, and this interaction comes at a significant, quantifiable cost, which can be reduced through timely interventions. The need for these interventions can be assessed through geophysical methods.

Tree valuations show that root-infrastructure interactions are significant factors to be considered. Geophysical methods can direct assessment and interventions, with practical and financial implications, and can therefore become a consideration when assessing the economic value of urban trees. In addition, as a “side effect”, studying these interactions can also aid the understanding of other aspects of tree roots (such as disease or carbon storage).

It is hoped that geophysical surveys can become a more integral part of tree management intervention in urban areas, particularly as costs can be reduced for said surveys.

b) *What are the relevant and useful physical parameters of tree roots that can be used for detection, and what methods can detect them?*

Tree roots tend to resemble the soil environment they are in. Physical contrasts are therefore small, which, combined with the small size of most roots, makes geophysical detection very difficult. To make matters even more difficult, urban areas pose unique challenges in terms of geophysical surveys.

Two methods that seem to offer the most potential are GPR and geo-resistivity (especially in the form of ERT). These methods offer the best results in terms of resolution and potential applicability in urban areas of interest. Therefore, permittivity and resistivity are the parameters of interest. A few mentions should be made:

- root size is an important parameter, in addition to the geophysical contrast; resolution is a key challenge in this application, and the smallest of roots can often escape detection in realistic surveys. Even in high-frequency GPR, the resolution might not be sufficient to resolve sub-centimetre roots;

- the two geophysical methods have some similar challenges, and some different ones. GPR offers much better resolution, applicability, and speed, but may not always be able to detect the faint contrasts between the root and its surrounding subsurface. ERT is slower and has worse resolution, but relies on a different geophysical contrast. Adding another geophysical method, even with these limitations, can help to remove substantial uncertainty and resolve tree roots even in difficult conditions. As modern resistivity methods (particularly non-contact methods) become more performant and robust, it is believed that electrical methods can play an even more important role in these surveys. A complementary use of these two methods offers better results;

- in the case of resistivity, coarse roots can be considered resistive, producing strong positive anomalies. However, thin roots can easily escape detection;

- in the case of GPR, high-frequency antennas should be used. Antennas in the 700-

1500 MHz perform adequately, whereas a 4000 MHz antenna does not have sufficient resolution to detect any thinner roots. It is not out of the question that an antenna in the 1500-4000 MHz interval might be useful in some scenarios, where only the first few centimetres are investigated. Having access to two antennas of different central frequencies can be very useful.

c) *What is the span of information we can derive by using these methods?*

This was the most complex question to answer, and to an extent, it still remains an open question. This is a multidisciplinary study and therefore must consider multiple parameters and conditions from multiple different areas (geophysics, biology, soil science, civil engineering). Therefore, the range of derivable information is variable and site-specific.

It is important to be aware that there is no guarantee that all roots, even all coarse roots, can be detected with geophysical methods. This is largely owed to the small geophysical contrast as well as the small size of the root. Direct dielectric measurements show that roots exhibit great permittivity variability, and the root permittivity value can be very close to that of the soil. It is possible that there is a lack of dielectric contrast between roots and the surrounding soil, which hampers GPR surveys on soil. Surveys on paved surface also depend on the type of surface. While some mediums (such as rebar-enforced concrete) are extremely inhospitable and can even render such GPR surveys useless, most paved surfaces are better suited for GPR surveys than soils. However, it can sometimes be difficult to differentiate between the roots themselves and damage caused by the roots (or external factors). In fact, fissure systems created by tree roots inside paved surfaces may be easier to detect than the roots themselves, especially if the fissures are water-filled.

Where GPR produces uncertain results on soil, ERT can serve as a complement. Where these two methods are applied in conjunction, coarse roots (centimetre-sized diameter) are very likely to be detected. While it cannot be said with certainty that all such roots will be detected, the complementarity of these two methods means that positive results can usually be expected.

The determination of root size is still challenging. The challenges of determining the size of objectives using GPR are well known in the literature, and ERT is very unreliable when it comes to estimating sizes, tending to greatly overestimate the size of roots.

d) Is there a way to predict and/or characterize the structural damage that tree roots will do using geophysical techniques?

Assessing tree root damage to paved surfaces using GPR is a realistic expectation in most scenarios, though it is not possible to fully eliminate uncertainty. Cracks around the tree root (particularly if they are water-filled) can facilitate detection. With some notable exceptions (such as paved surfaces that include cobbles or rebar), detection of subsurface roots is more advantageous on paved surfaces compared to soil surfaces. Determining lateral continuity is key to determining whether the damage is root-related or not, as individual profiles are not always conclusive. However, structural deformations that are unrelated to roots can also have continuity, and this can lead to some false positives.

Incipient damage can also be linked to roots, as long as the detected damaged is traced back to a root. The prediction of tree root damage is challenging but can be attempted. It will result in a prediction with likelihood, not certainty, but this can help direct early interventions. Roots can be mapped around the paved surface (or building), and if the roots are in the immediate vicinity, there is a high likelihood of existing or

future damage. It is possible that the roots would simply change the direction of growth (if they have space to grow in other directions). This is where electrical measurements taken in the immediate vicinity can be most helpful to confirm the potential existence of roots extending into the structure.

Overall, while a layer of uncertainty cannot be completely eliminated, it appears that geophysical surveys can direct early or preventive action to reduce tree root damage to infrastructure.

6.2 Other conclusions and secondary research questions

The suitability and applicability of the two discussed geophysical methods in the detection of tree roots in urban areas were assessed. The two methods were analysed separately and several surveys (as well as lab experiments) were carried out. Herein, the secondary questions served as a guide to delimitate the problem and the findings.

In terms of GPR, frequency selection is crucial. The range of frequencies should be selected based on a careful estimation of the expected soil/paved surface conditions, as well as the expected size of the objective. In scenarios that resemble a typical urban area, the range of 750-1500 MHz is excellently suited for this purpose, although the thinnest of tree roots might also escape detection. In this case, bigger is not always better – in some cases, particularly for soils with water-rich clays, a frequency towards the lower end of this spectrum might be desirable. This is not to say that frequencies lower than this cannot be useful in tree root surveys. The lower the frequency goes, the lower the resolution – which brings a cap on what root sizes can be detected. However, low frequency antennas can also be used in detecting coarse roots. Ideally, two antennas of different frequencies will be used in conjunction. For surveys on more favourable paved surfaces, antennas of

higher frequencies typically yield better results.

The direction of GPR surveys may also be significant. Ideally, profiles in two perpendicular directions should be carried out, at distances no larger than 10 cm. If the direction of the objective is known, then profiles perpendicular on that direction can suffice. In some instances, and in particular if accurate positioning can be ensured, profiles at lower spacing can increase data quality

In a scenario where acquisition time is also significant (as traffic may need to be stopped, for instance) and the direction of the objective is completely unknown, it is recommended to carry profiles on X and Y perpendicular, even at the cost of increasing the distance between profiles (ie profiles at a distance of 20 cm in both directions are recommended over 10 cm in just one direction). Total station (and other high-precision positioning systems) can be an excellent aid to GPR positioning, and might even resolve surface bumps that are not readily visible to the naked eye, therefore aiding surface damage even without other geophysical methods.

Forward models can also aid survey planning and data interpretation, by helping the surveyor know what type of response to expect. When an unexpected response is encountered, forward modelling could help the surveyor understand what type of structure created said response. When it comes to GPR data processing, a flow consisting of geometric corrections, de-wow, bandpass, gain, background removal, and potentially stacking, migration, and Hilbert transform can help improve the signal-to-noise ratio. Different sites may require different tweaks in this flow and every site should be treated individually, with different flows compared for assessment.

The measurements of tree root permittivity revealed substantial variation across roots from the same tree, and even different segments from the same root. There is a

realistic chance of the permittivity of the root to approximately coincide with the permittivity of the surrounding soil, in which caseroots cannot be detected.

Urban soils have also raised unexpected challenges. They have noted geophysical differences compared to natural soils and are rich in pebbles and other types of geophysical noise. Generally speaking, surveys carried out in drier soils tend to yield better results. The matter of when a survey should be carried out is not clear, and this is often direct by need, and flexibility is not possible. However, when the season can be chosen, summer (and drier seasons in general) should be favored. A wet soil covered in fallen leaves was found to be extremely unfavourable to this type of survey.

Geo-resistivity can also aid in the detection of tree roots on soil surfaces (future progress in terms of practical equipment is underway and may soon expand the applicability to paved surfaces). The distance between electrodes cannot always be expected to be on the same order of magnitude as the root itself, but should generally lie in the 5-20 centimetre range. Coarse tree roots can be resolved in this way, although the process is time-consuming. Low-cost custom-made equipment was built and used in this purpose, successfully accelerating and improving data quality through the implementation of non-conventional arrays. This is an avenue that warrants further investigation and could be improved upon. Despite significant advancements, the classic Wenner array is still a worthy consideration. Complementary to GPR, ERT might yield the best results in wetter seasons, when soil resistivity is lowest, but this is unlikely to be a major concern. It is recommended to integrate data from these two methods by first carrying out a GPR survey and identifying the areas of interest, and then following up with an ERT in that particular area. The results are consistent with published literature, highlighting that tree roots can be mapped geophysically, but challenges still remain. Joint ERT/GPR surveys for resolving individual roots (as opposed to the entire root area) are very rare in the literature and

represent a good opportunity to address and reduce knowledge gaps. Permittivity data from direct measurements can also help understand why some roots escape detection.

In order to assist surveyors or city planners in the attempt to detect tree roots, a simple guide has been developed. The guide aims to be of practical use for geophysicists and non-geophysicists as well. This is presented in Annex E and aims to serve as a stand-alone practical guide for surveys.

Ultimately, the task of detecting tree roots through geophysical methods remains challenging and site-specific. It something that should be considered by city planners in the case of root-infrastructure interactions, and in many cases, it can save important resources and make significant financial impact by facilitating timely intervention.

6.3 Recommendations for future work

This thesis also strives to help further research and help open up new avenues or further develop the existing findings and incorporate them in a practical scenario. The most immediate consideration is the application of routine surveys for tree root detection and damage assessment/prediction. At the current time, given the costs associated with the survey, it is unrealistic to expect this to be deployed at a large scale. However, it is presumably cost-effective in some particular areas, where the risk of tree root damage is particularly high and/or the cost of repair intervention is high. For instance, a historic or heavily circulated area in the vicinity of several old trees, particularly trees with ‘aggressive’ roots, would warrant surveys and/or regular monitoring. The issue might also warrant investigation in the case of old or leaky pipes, where the damage can be exacerbated by tree roots expanding the leak, with costly results. Lastly, surveys are also recommended where there are concerns of potential damage to buildings (even in private gardens, for instance). The roots might

be causing direct damage or subsidence, and this has taken a toll in the past. Although most structures can withstand roots, older buildings (as is often the case in the UK) can be affected, especially by trees with large and strong roots such as pine or palm trees. Some soils are also more susceptible to this type of damage, as are some types of trees with more vigorous and penetrant roots. In all cases, a prior assessment should be carried out, to evaluate the existing risk and the potential of a geophysical survey. In time, the cost of geophysical equipment (and geophysical surveys) can be also expected to drop, while the cost of infrastructure interventions can be expected to rise. This trend could make surveys more robust and increase positioning accuracy, which is often a contentious matter. Ultimately, smart sensors could potentially be deployed to continuously monitor at-risk areas. High-resolution non-contact resistivity equipment could offer new avenues on paved surfaces.

The geophysical methods could also be used in different scenarios, such as orchards or nurseries. While this was not explored in great detail here, it seems that diseases, pests, and other environmental threats change the physical parameters of the roots, and this change might be detected with proper survey. For instance, a diseased root is expected to have lower permittivity than normal and become inactive in time. Again, the matter of developing this in a cost-effective manner can be challenging, but given an analysis of said parameters, sensors can be deployed in place to monitor changes, saving resources in the long term. Regular GPR surveys can also be used to monitor changes. This is already used in some situations for soil monitoring, and can be adapted for root monitoring with relative ease. This could be used in conjunction with sensors that monitor other relevant parameters (such as soil humidity and porosity). Electrical methods seem like a better fit here, since they are generally cheaper and easily applicable in this scenario.

This approach may also help offer a better understanding of CO₂ absorption by trees,

which is strongly directed by roots. While this is still speculative, it is plausible that increased absorption can affect the parameters and growth of the root. This matter is of utmost importance in a world where man-made global warming is one of the most important and difficult challenges mankind must face.

Confirmation digging is something that is lacking in this work. Setting up a realistic scenario where roots would cause real damage is challenging and time-consuming to set up, and controlled environment simulations would need extreme complexity to replicate the entire system complexity. Therefore, it would be more practical to detect these scenarios already happening and study them extensively. This has proven impossible in this case. However, using a combination of geophysical methods, interdisciplinary approaches, and forward modelling, the author is hopeful that the work can serve as a useful resource for future study. Setting up such study areas can help fill some of the knowledge gaps described here.

Lastly, this type of study could be used to better understand the potential and limitations of geophysical methods (which are seldom used for such minute objectives) and the physical parameters of tree roots. For the important role that they have played since the dawn of humanity, tree roots have received surprisingly little attention, especially in terms of physical studies, and our understanding of roots (and their interactions with other elements) is still incomplete. This is not just a purely scientific pursuit, but given the impact of trees in society, it can also have a substantial role in improving sustainability and can still be greatly expanded.

As climate change can accelerate tree growth and pose new environmental pressures on both trees and urban ecosystems, and as infrastructure is becoming more and more expensive, geophysical studies on tree roots are expected to become more significant and

prevalent.

7. APPENDICES

Appendix A: MATLAB functions and scripts

Array_Slayer: select the type of geometry, plot the measurements real-time, and save geometry in a file

```
clear
```

```
if exist('RS232Port','var')
```

```
fclose(RS232Port);
```

```
clear('RS232Port');
```

```
TheCOMPort = 'Closed'
```

```
end
```

```
%%%%%%%%%% SELECT A COM PORT
```

```
%%%%%%%%%%
```

```
Array_Type = menu('What is the COM
```

```
port?','COM1','COM2','COM3','COM4','COM5','COM6','COM7','COM8','COM9','COM10','COM11','COM12');
```

```
switch Array_Type
```

```
    case 1
```

```
RS232Port =
```

```
serial('COM1','BaudRate',9600,'DataBits',8,'Parity','none','StopBits',2,'FlowControl','none','Terminator','CR/LF');
```

```
    case 2
```

```
RS232Port =
```

```
serial('COM2','BaudRate',9600,'DataBits',8,'Parity','none','StopBits',2,'FlowControl','none','Terminator','CR/LF');
```

case 3

```
RS232Port =  
serial('COM3','BaudRate',9600,'DataBits',8,'Parity','none','StopBits',2,'FlowControl','none','Termin  
ator','CR/LF');
```

case 4

```
RS232Port =  
serial('COM4','BaudRate',9600,'DataBits',8,'Parity','none','StopBits',2,'FlowControl','none','Termin  
ator','CR/LF');
```

case 5

```
RS232Port =  
serial('COM5','BaudRate',9600,'DataBits',8,'Parity','none','StopBits',2,'FlowControl','none','Termin  
ator','CR/LF');
```

case 6

```
RS232Port =  
serial('COM6','BaudRate',9600,'DataBits',8,'Parity','none','StopBits',2,'FlowControl','none','Termin  
ator','CR/LF');
```

case 7

```
RS232Port =  
serial('COM7','BaudRate',9600,'DataBits',8,'Parity','none','StopBits',2,'FlowControl','none','Termin  
ator','CR/LF');
```

case 8

```
RS232Port =  
serial('COM8','BaudRate',9600,'DataBits',8,'Parity','none','StopBits',2,'FlowControl','none','Termin  
ator','CR/LF');
```

case 9

```
RS232Port =  
serial('COM9','BaudRate',9600,'DataBits',8,'Parity','none','StopBits',2,'FlowControl','none','Termin  
ator','CR/LF');
```

```

    case 10

RS232Port =
serial('COM10','BaudRate',9600,'DataBits',8,'Parity','none','StopBits',2,'FlowControl','none','Terminator','CR/LF');

    case 11

RS232Port =
serial('COM11','BaudRate',9600,'DataBits',8,'Parity','none','StopBits',2,'FlowControl','none','Terminator','CR/LF');

    case 12

RS232Port =
serial('COM12','BaudRate',9600,'DataBits',8,'Parity','none','StopBits',2,'FlowControl','none','Terminator','CR/LF');

    otherwise

        disp('You need a COM Port')

end

%%%%%%%%%%
%%%%%%%%%%

iteration=0;

NumberOfElectrodes = 16;

WennerProfiles = 0;

SchlumbergerProfiles = 0;

DipoleProfiles = 0;

OptimizedProfiles = 0;

FileName = sprintf('Report_%s.txt', datestr(now,'mm-dd-yyyy HH-MM'));

RaportWrite=["Number of electrodes: ";num2str(NumberOfElectrodes)];

```

```

while 1

Array_Type = menu('Would you like to carry a measurement?', 'Yes', 'No');

if exist ('RS232Port', 'var')

Intermediate_Port=RS232Port;

fclose(RS232Port);

clear('RS232Port');

TheCOMPort = 'Closed'

end

switch Array_Type

    case 1

iteration=iteration+1

RaportWrite=[RaportWrite;"Profile number "];

RaportWrite=[RaportWrite;num2str(iteration)];

CurrentMeasurement = 0;

Array_Type = menu('What type of array do you want?', 'Wen', 'Sch', 'Dip-dip', 'Opt');

% Handle response

switch Array_Type

    case 1

        disp([Array_Type ' Doing a Wenner array'])

        WennerProfiles = WennerProfiles+1;

        RaportWrite=[RaportWrite;"Wenner"];

%%                               Wenner                               %%

```

```

ElectrodePositions = zeros(10000,4);

ElectrodeIndex = 0;

for ArrayIncrement = 1:(NumberOfElectrodes-1)/3           %Distance between
electrodes

    for C1Electrode = 1:(NumberOfElectrodes-3*ArrayIncrement)

        P1Electrode = C1Electrode + ArrayIncrement;

        P2Electrode = P1Electrode + ArrayIncrement;

        C2Electrode = P2Electrode + ArrayIncrement;

        ElectrodeIndex = ElectrodeIndex + 1;

        ElectrodePositions(ElectrodeIndex,1) = C1Electrode;

        ElectrodePositions(ElectrodeIndex,2) = C2Electrode;

        ElectrodePositions(ElectrodeIndex,3) = P1Electrode;

        ElectrodePositions(ElectrodeIndex,4) = P2Electrode;

    end

end

% Reduce size of the array

ElectrodePositions = ElectrodePositions(1:ElectrodeIndex,:);

changing_rows=1;

position_matrix_wenner_initial = ElectrodePositions;

position_matrix = ElectrodePositions;

%Fix so consecutive P's (M,N) are moved around so the device measures

for fixing = 1:100;

```

```

for invers = 1:(length(position_matrix)-1);

    invers_2=invers + 1;

    invers_0=invers - 1;

    if position_matrix(invers,3) == position_matrix(invers_2,3) | position_matrix(invers,4) ==
position_matrix(invers_2,4)

        position_matrix([changing_rows, invers],:)=position_matrix([invers, changing_rows],:)

        changing_rows=changing_rows+2;

    end

end

end

position_matrix_wenner = position_matrix;

ElectrodePositions = position_matrix;

case 2

    disp([Array_Type ' Doing a Schlumberger'])

    SchlumbergerProfiles = SchlumbergerProfiles + 1;

    TypeOfProfile = 'Schlumberger';

    RaportWrite=[RaportWrite;"Schlumberger"];

%%                Schlumberger                %%

ElectrodePositions = zeros(10000,4);

ElectrodeIndex = 0;

for ArrayIncrement = 1:5;                %Distance between P1P2

    for ArraySpread = ArrayIncrement:(NumberOfElectrodes-ArrayIncrement-1)/2

```



```

%Distance between C and P

for C1Electrode = 1:(NumberOfElectrodes-2*ArraySpread - ArrayIncrement);

    C2Electrode = (C1Electrode + 2*ArraySpread + ArrayIncrement);

    P1Electrode = (C1Electrode + ArraySpread);

    P2Electrode = (P1Electrode + ArrayIncrement);

    ElectrodeIndex = ElectrodeIndex + 1;

        ElectrodePositions(ElectrodeIndex,1) = C1Electrode;

        ElectrodePositions(ElectrodeIndex,2) = C2Electrode;

        ElectrodePositions(ElectrodeIndex,3) = P1Electrode;

        ElectrodePositions(ElectrodeIndex,4) = P2Electrode;

    end

end

end

% Reduce size of the arr
ay

ElectrodePositions = ElectrodePositions(1:ElectrodeIndex,:);

changing_rows=1;

position_matrix_schlumberger_initial = ElectrodePositions;

position_matrix = ElectrodePositions;

%Fix so consecutive P's (M,N) are moved around so the device measures

for fixing = 1:100;

for invers = 1:(length(position_matrix)-1);

    invers_2=invers + 1;

```

```

invers_0=invers - 1;

if position_matrix(invers,3) == position_matrix(invers_2,3) | position_matrix(invers,4) ==
position_matrix(invers_2,4)

    position_matrix([changing_rows, invers],:)=position_matrix([invers, changing_rows],:)

    changing_rows=changing_rows+2;

end

end

end

position_matrix_schlumberger = position_matrix;

ElectrodePositions = position_matrix;

case 3

    disp([Array_Type ' Doing a Dipole-Dipole array'])

    DipoleProfiles = DipoleProfiles + 1;

    TypeOfProfile = 'Dipole';

    RaportWrite=[RaportWrite;"Dipole"];

%%                DipoleDipole                %%

ElectrodePositions = zeros(10000,4);

ElectrodeIndex = 0;

for ArrayIncrement = 1:(NumberOfElectrodes-2)/2;                %Distance between
electrodes

    for C1Electrode = 1:(NumberOfElectrodes-2*ArrayIncrement - 1);

        C2Electrode = C1Electrode + ArrayIncrement;

        for P1Electrode = (C1Electrode + ArrayIncrement + 1):(NumberOfElectrodes -
ArrayIncrement);

```

```

P2Electrode = P1Electrode + ArrayIncrement;

ElectrodeIndex = ElectrodeIndex + 1;

    ElectrodePositions(ElectrodeIndex,1) = C1Electrode;           % Position of C1 current
injection electrode

    ElectrodePositions(ElectrodeIndex,2) = C2Electrode;           % Position of P1 voltage
sensing electrode

    ElectrodePositions(ElectrodeIndex,3) = P1Electrode;           % Position of P2 voltage
sensing electrode

    ElectrodePositions(ElectrodeIndex,4) = P2Electrode;           % Position of C2 current
injection electrode

end

end

end

    % Reduce size of the array

ElectrodePositions = ElectrodePositions(1:ElectrodeIndex,:);

changing_rows=1;

position_matrix_dipole_initial = ElectrodePositions;

position_matrix = ElectrodePositions;

%Fix so consecutive P's (M,N) are moved around so the device measures

for fixing = 1:100;

for invers = 1:(length(position_matrix)-1);

    invers_2=invers + 1;

    invers_0=invers - 1;

    if position_matrix(invers,3) == position_matrix(invers_2,3) | position_matrix(invers,4) ==
position_matrix(invers_2,4)

```

```

position_matrix([changing_rows, invers],:)=position_matrix([invers, changing_rows],:)

changing_rows=changing_rows+2;

end

end

end

position_matrix_dipole = position_matrix;

ElectrodePositions = position_matrix;

case 4

disp([Array_Type 'Doing an Optimized array'])

OptimizedProfiles = OptimizedProfiles+1;

TypeOfProfile = 'Optimized';

RaportWrite=[RaportWrite;"Optimized"];

%%          Ideal Measurements thingie          %%

%% Generate an array of data collection connections

P1 = [1 1 1 1 1 1 2 2 2 2 2 2 3 3 3 3 3 3 4 4 4 4 4 4 5 5 5 5 5 5 6 6 6 6 6 6 7 7 7 7 7 7 8 8 8 8 8 8 9 9
9 9 9 9 10 10 10 10 10 10 11 11 11 11 11 11 12 12 12 12 12 12 13 13 13 13 13 13 14 14 14 14 14
14 15 15 15 15 15 16 16 16 16 16 16 17 17 17 17 17 17 18 18 18 18 18 18 19 19 19 19 19
20 20 20 20 20 20 21 21 21 21 21 21 22 22 22 22 22 22 23 23 23 23 23 24 24 24 24 25 25 25 26
26 27 1 6 1 7 1 11 1 3 12 1 5 1 8 1 1 11 1 3 1 5 1 8 1 1 17 6 2 1 11 4 13 19 1 2 2 1 1 4 10 1 9 2 5 2
12 1 1 14 11 1 1 4 1 16 2 2 1 3 7 1 7 2 1 2 3 1 1 3 5 1 7 1 3 2 7 14 2 2 4 7 1 16 8 2 1 1 2 1 8 4 3 3 1
10 4 3 3 6 4 7 2 1 3 1 12 1 11 2 1 3 4 1 10 1 4 5 5 4 4 1 9 17 3 2 5 1 11 3 2 1 3 7 5 3 9 13 10 1 2 3
4 6 7 4 4 3 20 13 1 1 20 7 3 4 1 1 6 12 1 6 1 1 9 1 4 10 4 5 13 8 3 1 9 5 14 5 2 3 1 9 1 7 11 1 3 2 5
4 10 10 1 15 1 4 6 10 1 1 7 3 1 1 7 2 5 2 3 1 4 2 5 3 3 7 9 6 1 5 6 5 7 2 13 3 1 1 17 7 5 4 8 10 2 3
19 1 5 10 4 4 2 5 6 6 2 5 11 2 3 3 3 2 8 8 5 12 13 2 2 4 6 1 9 12 5 4 5 4 18 5 9 1 3 3 12 3 8 3 7 6 21
8 1 1 4 16 7 8 4 21 1 10 2 1 5 1 8 6 19 1 7 7 5 9 7 5 2 1 11 1 9 5 9 5 12 4 5 6 16 10 2 7 1 2 3 14 1
13 3 5 1 2 3 12 3 10 4 5 13 1 7 3 7 6 3 1 6 6 2 4 17 2 3 8 5 6 9 4 9 6 11 1 3 1 3 7 7 10 3 2 5 20 2 17

```

15 3 4 9 6 8 1 4 11 1 4 11 3 7 6 6 7 5 6 13 12 5 9 15 9 6 6 5 5 8 14 2 11 4 1 5 8 8 3 14 5 3 16 2 1 3
7 12 4 2 6 7 1 3 18 1 4 1 10 1 7 12 3 4 5 10 9 5 4 6 2 1 4 4 11 3 7 6 2 5 10 13 1 3 4 4 14 5 7 9 7 4
18 11 2 7 1 8 12 2 4 2 6 6 1 12 3 16 8 9 7 10 6 14 4 11 4 10 1 5 7 5 4 9 9 15 5 5 17 5 7 8 6 11 4 4 7
3 2 20 10 2 1 2 2 13 3 1 3];

P2 = [2 2 2 2 2 2 3 3 3 3 3 3 4 4 4 4 4 4 5 5 5 5 5 5 6 6 6 6 6 6 7 7 7 7 7 7 8 8 8 8 8 8 9 9 9 9 9 9 10
10 10 10 10 10 11 11 11 11 11 11 12 12 12 12 12 12 13 13 13 13 13 13 14 14 14 14 14 14 15 15
15 15 15 15 16 16 16 16 16 16 17 17 17 17 17 17 18 18 18 18 18 18 19 19 19 19 19 19 20 20 20
20 20 20 21 21 21 21 21 21 22 22 22 22 22 22 23 23 23 23 23 23 24 24 24 24 24 25 25 25 25 26
26 26 27 27 28 2 18 3 15 3 16 3 12 18 3 13 4 14 4 4 15 4 10 13 5 11 5 12 5 3 19 14 4 3 19 17 16
22 4 3 4 2 6 9 15 5 13 5 12 4 16 5 4 17 14 4 3 10 6 20 9 6 7 8 11 6 13 5 11 5 16 3 8 7 9 7 12 7 5 12
10 18 7 5 9 14 4 18 17 6 4 4 4 5 12 14 7 7 10 21 11 6 6 10 11 14 6 3 5 8 15 6 13 5 9 8 7 6 13 6 8 9
10 7 10 9 17 20 4 3 15 5 15 5 7 6 6 13 8 9 13 18 16 5 4 7 7 11 11 6 12 6 21 19 3 4 24 13 8 9 2 7 11
14 6 9 7 6 14 7 7 12 8 10 16 12 5 10 16 8 22 7 6 6 8 12 7 10 14 3 11 5 7 9 14 14 5 17 8 6 10 17 5 7
12 10 15 8 11 9 8 5 15 5 5 4 9 13 8 10 11 19 9 11 8 10 9 7 15 11 6 4 19 20 9 9 10 15 4 7 21 6 12
13 7 8 3 10 9 11 5 14 13 6 7 8 10 8 11 13 7 15 17 6 9 9 10 7 13 15 17 10 9 6 20 8 12 4 5 6 18 7 15
6 13 8 22 12 3 5 8 18 23 12 8 25 3 12 14 2 6 5 11 9 20 4 11 9 9 11 10 15 6 7 14 9 14 10 14 7 14 7
9 11 20 14 7 16 6 4 7 16 8 16 11 10 4 5 6 16 21 16 6 18 18 7 14 9 11 7 5 8 12 10 13 7 18 5 10 10 8
8 13 8 19 14 13 10 8 5 9 13 13 13 8 12 8 22 3 20 18 4 5 12 9 10 7 7 15 6 7 15 7 11 10 11 10 7 11
15 15 10 11 17 15 17 12 10 9 11 15 4 21 26 2 12 9 12 9 17 13 8 17 6 6 13 8 17 12 6 15 9 7 6 19 11
9 5 12 3 24 14 5 29 8 14 14 17 8 8 27 10 19 6 14 8 14 22 10 8 11 14 4 8 11 10 17 6 13 13 9 9 23
13 3 9 29 20 13 30 9 4 13 9 5 16 7 19 12 12 10 16 10 16 5 13 7 12 6 7 18 11 7 11 11 16 11 12 21 7
11 10 16 12 10 10 12 4 9 21 13 9 29 30 4 16 12 9 10];

M = [3 4 5 6 7 8 4 5 6 7 8 9 5 6 7 8 9 10 6 7 8 9 10 11 7 8 9 10 11 12 8 9 10 11 12 13 9 10 11 12
13 14 10 11 12 13 14 15 11 12 13 14 15 16 12 13 14 15 16 17 13 14 15 16 17 18 14 15 16 17 18
19 15 16 17 18 19 20 16 17 18 19 20 21 17 18 19 20 21 22 18 19 20 21 22 23 19 20 21 22 23 24
20 21 22 23 24 25 21 22 23 24 25 26 22 23 24 25 26 27 23 24 25 26 27 28 24 25 26 27 28 29 25
26 27 28 29 26 27 28 29 27 28 29 28 29 29 13 29 16 28 15 28 14 27 28 13 27 19 27 18 17 27 16
26 21 26 20 26 19 12 28 27 17 12 28 28 27 29 15 13 16 9 22 25 27 18 26 19 26 15 27 17 14 27 26
14 11 25 21 28 25 22 23 24 25 20 26 18 26 20 27 11 24 23 24 22 25 21 19 26 24 27 22 17 24 26
13 27 27 19 13 14 14 17 25 26 21 22 25 28 25 21 20 24 25 26 20 10 17 23 26 18 25 16 24 23 22
18 25 19 22 23 24 21 24 24 27 28 14 11 26 16 26 16 21 18 18 25 22 23 25 27 26 15 13 20 20 24
24 19 25 19 28 27 10 12 29 25 22 23 7 20 24 25 17 22 21 17 25 19 19 24 21 23 26 24 15 24 26 21
28 19 18 17 21 24 19 23 25 9 24 15 20 22 25 25 14 26 21 17 23 26 14 19 24 23 26 22 23 23 20 16
26 14 15 12 21 25 20 22 23 27 22 23 20 22 21 20 25 24 16 11 27 27 22 21 22 25 12 19 28 16 24

24 18 20 10 22 21 23 14 25 24 17 18 21 23 20 23 24 18 25 26 16 22 21 22 18 24 25 26 22 21 16
27 19 23 11 14 17 26 18 25 16 24 19 28 23 9 13 19 26 28 23 19 29 8 23 25 6 17 13 22 20 27 11 22
20 20 22 21 25 16 17 24 21 24 22 24 17 24 17 20 22 27 24 17 25 15 11 17 25 20 25 23 21 10 13
15 25 27 25 15 26 26 17 24 20 22 17 13 19 23 21 24 18 26 13 21 21 18 18 23 18 26 24 23 22 18
12 21 23 23 23 18 23 19 28 9 27 26 11 13 22 19 20 16 16 24 14 16 24 16 21 20 21 20 16 21 24 24
20 21 25 24 25 22 20 19 21 24 10 27 29 5 22 19 22 19 25 23 18 25 14 14 23 18 25 22 14 24 19 16
14 26 22 20 12 22 7 28 23 12 21 17 23 23 25 17 17 9 21 26 14 23 17 23 27 20 17 21 23 9 17 21 20
25 14 22 22 18 18 28 22 8 18 23 26 22 7 18 10 22 18 11 24 15 26 21 21 19 24 19 24 12 22 15 21
13 15 25 20 15 20 20 24 20 21 27 15 20 19 24 21 19 19 21 10 18 27 22 18 21 8 10 24 22 19 19];

N = [4 5 6 7 8 9 5 6 7 8 9 10 6 7 8 9 10 11 7 8 9 10 11 12 8 9 10 11 12 13 9 10 11 12 13 14 10 11
12 13 14 15 11 12 13 14 15 16 12 13 14 15 16 17 13 14 15 16 17 18 14 15 16 17 18 19 15 16 17
18 19 20 16 17 18 19 20 21 17 18 19 20 21 22 18 19 20 21 22 23 19 20 21 22 23 24 20 21 22 23
24 25 21 22 23 24 25 26 22 23 24 25 26 27 23 24 25 26 27 28 24 25 26 27 28 29 25 26 27 28 29
30 26 27 28 29 30 27 28 29 30 28 29 30 29 30 30 25 30 24 30 20 30 18 30 30 18 30 28 30 26 23
30 20 30 28 30 26 30 23 19 30 29 25 14 30 29 30 30 19 20 21 11 27 30 29 22 30 26 29 19 29 20
17 30 30 16 20 30 27 30 29 29 28 30 30 24 29 24 29 30 30 13 28 30 30 26 30 24 29 28 30 30 27
24 29 29 18 30 29 23 15 29 23 27 29 30 25 28 28 30 28 30 27 30 29 28 27 20 24 27 29 20 30 19
27 28 30 21 30 26 26 27 28 27 27 28 28 29 22 14 30 26 28 20 26 23 22 30 28 26 28 29 30 21 18
24 25 27 28 27 28 27 30 30 11 18 30 27 27 28 11 25 30 30 19 27 29 22 30 21 23 30 26 27 28 27
18 30 29 27 30 24 26 20 24 30 22 29 29 17 26 23 28 26 27 28 17 30 25 22 30 30 16 24 30 26 29
29 26 30 24 30 27 25 23 24 24 29 22 26 28 29 25 25 26 24 26 28 30 29 18 21 29 30 29 23 27 30
14 26 29 21 28 27 21 25 12 25 26 27 20 29 28 26 20 28 28 23 29 26 23 29 28 19 27 25 27 22 30
27 29 26 27 22 30 22 26 13 23 28 30 24 28 23 28 23 30 25 10 19 21 30 30 27 23 30 24 28 26 10
29 15 25 23 30 12 24 24 22 26 24 29 26 20 28 26 26 30 27 22 29 22 25 26 29 30 19 30 24 15 21
29 28 29 30 25 27 25 20 27 30 28 19 29 28 24 25 24 28 24 18 25 30 27 27 29 29 14 23 28 23 23
27 22 30 29 28 28 20 22 30 25 26 28 21 26 29 29 11 28 27 14 16 25 22 24 19 18 28 24 21 26 20
25 24 24 25 20 23 29 29 22 26 30 27 30 26 23 25 26 30 21 29 30 27 23 26 28 23 29 28 26 30 17
15 24 28 28 24 16 30 27 25 19 30 27 30 13 29 26 30 26 26 22 19 25 27 27 22 21 10 28 28 26 28
20 26 30 21 24 29 28 25 18 27 27 26 17 24 27 24 22 29 24 13 20 24 30 27 8 19 12 25 25 23 28 19
27 24 25 23 27 22 28 15 28 21 25 22 24 30 22 16 26 22 29 24 23 28 17 26 26 26 27 20 24 27 14
20 29 29 21 23 10 11 25 30 28 21];

position_matrix = [P1(:), P2(:), M(:), N(:)];

position_matrix_initial=position_matrix;

```

x = 1;

changing_rows=1;

Number_extra_rows=0;

%Remove rows over number of electrodes

pos = [P1; P2; M; N];

pos_invers = pos';

for i = 1:670

    if (P1(i)<=NumberOfElectrodes)

        if(P2(i)<=NumberOfElectrodes)

            if(M(i)<=NumberOfElectrodes)

                if(N(i)<=NumberOfElectrodes)

                    A_n(x)=position_matrix(i,1);

                    B_n(x)=position_matrix(i,2);

                    M_n(x)=position_matrix(i,3);

                    N_n(x)=position_matrix(i,4);

                    x=x+1;

                end

            end

        end

    end

end

position_matrix = [A_n; B_n; M_n; N_n]';

num_pos = numel(position_matrix)/4;

```

```

position_matrix_optimizat = position_matrix;

%Fix so consecutive P's (M,N) are moved around so the device measures

for fixing = 1:100;

for invers = 1:(length(position_matrix)-1);

    invers_2=invers + 1;

    invers_0=invers - 1;

    if position_matrix(invers,3) == position_matrix(invers_2,3) | position_matrix(invers,4) ==
position_matrix(invers_2,4)

        position_matrix([changing_rows, invers],:)=position_matrix([invers, changing_rows],:)

        changing_rows=changing_rows+2;

    end

end

end

end

ElectrodePositions = zeros(10000,4);

ElectrodeIndex = 0;

for ArrayIncrement = 1:num_pos;                                %Distance between electrodes

    C1Electrode = position_matrix(ArrayIncrement,1);

    C2Electrode = position_matrix(ArrayIncrement,2);

    P1Electrode = position_matrix(ArrayIncrement,3);

    P2Electrode = position_matrix(ArrayIncrement,4);

    ElectrodeIndex = ElectrodeIndex + 1;

        ElectrodePositions(ElectrodeIndex,1) = C1Electrode;        % Position of C1 current
injection electrode

```



```

        ElectrodePositions(ElectrodeIndex,2) = C2Electrode;           % Position of P1 voltage
sensing electrode

        ElectrodePositions(ElectrodeIndex,3) = P1Electrode;         % Position of P2 voltage
sensing electrode

        ElectrodePositions(ElectrodeIndex,4) = P2Electrode;         % Position of C2 current
injection electrode

end

% Reduce size of the array

ElectrodePositions = ElectrodePositions(1:ElectrodeIndex,:);

otherwise

    disp('Aborting')

%ending of switch cases%

end

Comment3 = "";

%% Initialise switching network communication

%Array_Type = menu('What is the COM
port?','COM1','COM2','COM3','COM4','COM5','COM6','COM7','COM8','COM9','COM10','COM
11','COM12');

%switch Array_Type

% case 1

%

%RS232Port =
serial('COM4','BaudRate',9600,'DataBits',8,'Parity','none','StopBits',2,'FlowControl','none','Termin
ator','CR/LF');

%
```

```

% Open Port

RS232Port = Intermediate_Port;

fopen(RS232Port);

fprintf(RS232Port,'reset\n');

%% Display to user the position of the electrodes to be connected

PreviousElectrodePositions = zeros(1,4);

for ElectrodeIndex = 1:length(ElectrodePositions)

    pause(1);

    % Draw a picture

    Figure1Handle = figure(1);

    set(Figure1Handle,'Color','w')

        OutlinePositionsX = 1:NumberOfElectrodes;      % X Positions

    OutlinePositionsY = zeros(size(OutlinePositionsX)); % Y Positions

    plot(OutlinePositionsX,OutlinePositionsY,'k+','MarkerSize',15,'LineWidth',2)

    xlim([0 NumberOfElectrodes+1]);

    ylim([-1.6 +1.6]);

    %%%%%%%%% C1 - 1 // C2 - 2 // P1 - 3 // P2 - 4 %%%%%%%%%

        C1 = ElectrodePositions(ElectrodeIndex,1);

    C2 = ElectrodePositions(ElectrodeIndex,2);

    P1 = ElectrodePositions(ElectrodeIndex,3);

    P2 = ElectrodePositions(ElectrodeIndex,4);

    hold on

```

```

CurrentMeasurement = CurrentMeasurement + 1;

% Use red markers for current injection and blue markers for voltage sense

plot(C1,0,'ro','MarkerSize',15,'LineWidth',2)

plot(C2,0,'ro','MarkerSize',15,'LineWidth',2)

plot(P1,0,'bs','MarkerSize',15,'LineWidth',2)

plot(P2,0,'bs','MarkerSize',15,'LineWidth',2)

    title(['Current Measurement ',num2str(CurrentMeasurement),' ']);

% Use text to label the electrodes

text(C1,-0.2,'C1','HorizontalAlignment','center')

text(C2,-0.2,'C2','HorizontalAlignment','center')

text(P1,0.2,'P1','HorizontalAlignment','center')

text(P2,0.2,'P2','HorizontalAlignment','center')

% Add block for current injection

line([C1 C1],[0 1],'LineWidth',2,'Color','r')

line([C2 C2],[0 1],'LineWidth',2,'Color','r')

BoxX1 = C1 + (C2-C1-2)/2;

BoxX2 = BoxX1 + 2;

line([C1 BoxX1],[1 1],'LineWidth',2,'Color','r')

line([BoxX2 C2],[1 1],'LineWidth',2,'Color','r')

line([BoxX1 BoxX2 BoxX2 BoxX1 BoxX1],[0.7 0.7 1.3 1.3 0.7],'LineWidth',2,'Color','r')

text(BoxX1+1,1.1,'Signal','HorizontalAlignment','center')

text(BoxX1+1,0.9,'Generator','HorizontalAlignment','center')

```

```

% Add block for voltage sense

line([P1 P1],[0 -1],'LineWidth',2,'Color','b')

line([P2 P2],[0 -1],'LineWidth',2,'Color','b')

BoxX1 = P1 + (P2-P1-0.8)/2;

BoxX2 = BoxX1 + 0.8;

line([P1 BoxX1],[-1 -1],'LineWidth',2,'Color','b')

line([BoxX2 P2],[-1 -1],'LineWidth',2,'Color','b')

line([BoxX1 BoxX2 BoxX2 BoxX1 BoxX1],[-0.7 -0.7 -1.3 -1.3 -0.7],'LineWidth',2,'Color','b')

text(BoxX1+0.4,-1,'RX','HorizontalAlignment','center')

hold off

    % Control switching network - switch relays on if there is to be a change
    if ElectrodePositions(ElectrodeIndex,1) ~= PreviousElectrodePositions(1),

        RelayMessage = ['c1,' num2str(ElectrodePositions(ElectrodeIndex,1)) ',on\n'];

        fprintf(RS232Port,'%s',RelayMessage);

        pause(1.1);

    end

    if ElectrodePositions(ElectrodeIndex,2) ~= PreviousElectrodePositions(2),

        RelayMessage = ['p1,' num2str(ElectrodePositions(ElectrodeIndex,2)) ',on\n'];

        fprintf(RS232Port,'%s',RelayMessage);

        pause(1.1);

    end

    if ElectrodePositions(ElectrodeIndex,3) ~= PreviousElectrodePositions(3),

        RelayMessage = ['p2,' num2str(ElectrodePositions(ElectrodeIndex,3)) ',on\n'];

```

```

fprintf(RS232Port,'%s',RelayMessage);

pause(1.1);

end

if ElectrodePositions(ElectrodeIndex,4) ~= PreviousElectrodePositions(4),

    RelayMessage = ['c2,' num2str(ElectrodePositions(ElectrodeIndex,4)) ',on\n'];

    fprintf(RS232Port,'%s',RelayMessage);

    pause(1.1);

end

if mod (CurrentMeasurement, 10) == 0

    pause(4);

end

if ElectrodeIndex < length(ElectrodePositions),

    % Control switching network - switch relays off if there is to be a change

    if ElectrodePositions(ElectrodeIndex,1) ~= ElectrodePositions(ElectrodeIndex+1,1),

        RelayMessage = ['c1,' num2str(ElectrodePositions(ElectrodeIndex,1)) ',off\n'];

        fprintf(RS232Port,'%s',RelayMessage);

        pause(0.001);

    end

    if ElectrodePositions(ElectrodeIndex,2) ~= ElectrodePositions(ElectrodeIndex+1,2),

        RelayMessage = ['p1,' num2str(ElectrodePositions(ElectrodeIndex,2)) ',off\n'];

        fprintf(RS232Port,'%s',RelayMessage);

        pause(0.001);

    end

end

```

```

if ElectrodePositions(ElectrodeIndex,3) ~= ElectrodePositions(ElectrodeIndex+1,3),

    RelayMessage = ['p2,' num2str(ElectrodePositions(ElectrodeIndex,3)) ',off\n'];

    fprintf(RS232Port,'%s',RelayMessage);

    pause(0.001);

end

if ElectrodePositions(ElectrodeIndex,4) ~= ElectrodePositions(ElectrodeIndex+1,4),

    RelayMessage = ['c2,' num2str(ElectrodePositions(ElectrodeIndex,4)) ',off\n'];

    fprintf(RS232Port,'%s',RelayMessage);

    pause(0.001);

end

end

PreviousElectrodePositions = ElectrodePositions(ElectrodeIndex,:);

end

disp('Wenner Profiles:');

disp(WennerProfiles)

disp('Schlumberger Profiles:');

disp(SchlumbergerProfiles)

disp('Dipole-Dipole Profiles:');

disp(DipoleProfiles)

disp('Optimized Profiles:');

disp(OptimizedProfiles)

fclose(RS232Port);

clear('RS232Port');

```

otherwise

```
disp('Thanks, buh-bye!');
```

```
break
```

```
end
```

```
end
```

```
Results = fopen(FileName,'w');
```

```
fprintf(Results, '%s\r\n\r\n',RaportWrite);
```

```
%fclose(FileName);
```

```
%% Clear the tasks
```

```
% Close the switching network comms - close serial port
```

```
fclose(RS232Port);
```

```
clear('RS232Port');
```

Transfer real permittivity data from coaxial probe to a csv

```
data=ans;
```

```
emptyCells = cellfun('isempty', data);
```

```
data(all(emptyCells,2),:) = []
```

```
data(:,2) = [];
```

```
freq = data(1:101,1);
```

```
tabel = cell2table(data);
```

```
writetable(tabel,'bun2.csv');
```

```
perm = data;
```

```
perm(:,1) = [];  
  
perm2 = reshape(perm,[101,40]);  
  
c=[freq,perm2];  
  
d=cell2table(c);  
  
writetable(d,'datele.csv');
```

Transform gpr-Max files to SegY (readable by Reflex)

```
file=hdf5read('all_roots10_all.out', '/rxs/rx1/Ez')  
  
file_t=file.'  
  
WriteSegy('all_roots10.segy', file_t, 'dsf', 5, 'revision',1);
```


Appendix B: GPR-max model examples (both in old and new format)

A few representative models are presented here. GprMax changed its framework at some point over this project. Some files are in legacy format.

Simple 3 cylinder model (example)

#title: B-scan from a metal cylinder buried in a dielectric half-space

#domain: 0.60 0.20 0.002

Domain size in meters

#dx_dy_dz: 0.002 0.002 0.002

Discretisation in meters

#time_window: 4e-9

in seconds

#time_step_limit_type: 2D

#pml_cells: 10 10 0 10 10 0

Insulating box

#material: 6 0 1 0 half_space

material: relative permittivity, conductivity, relative permeability, magnetic loss, name

#material: 9 0 1 0 test_material

#waveform: ricker 1 0.8e9 my_ricker

type of waveform (ricker, gaussian, gaussiandotnorm...), amplitude, frequency Hz, name

#hertzian_dipole: z 0.020 0.170 0 my_ricker

polarization (x,y,z), x, y, z al antenei, name

#rx: 0.060 0.170 0

receiver x y z

#src_steps: 0.002 0 0

#rx_steps: 0.002 0 0

increments pentru moving source

box: 0 0 0 0.6 0.170 0.002 half_space

x y z pentru lower left corner si x y z pentru upper right

box: 0 0 0 0.240 0.100 0.001 test_material

#soil_peplinski: 0.05 0.95 2.0 2.66 0.001 0.25 my_soil
sand fraction, clay fraction, soil density, sand density, clay water, sand water, identifier

#fractal_box: 0 0 0 0.6 0.2 0.002 1.5 1 1 1 50 my_soil my_fractal_box

#cylinder: 0.150 0.100 0 0.150 0.100 0.002 0.010 pec

x,y,z pentru o fata, x y z pentru alta fata, diametru, material (pec e prebuilt)

#cylinder: 0.300 0.100 0 0.300 0.100 0.002 0.020 pec

#cylinder: 0.450 0.100 0 0.450 0.100 0.002 0.030 pec

#geometry_view: 0 0 0 0.60 0.20 0.002 0.002 0.002 0.002 3cylinderclay n

Water with water-filled holes

#title: 4 hole

#domain: 0.80 0.20 0.002

#dx_dy_dz: 0.002 0.002 0.002

#time_window: 8e-9

#time_step_limit_type: 2D

#pml_cells: 10 10 0 10 10 0

#material: 6 0 1 0 half_space

#material: 4 1.0 1.0 0.0 asphalt1

#material: 2 1.0 1.0 0.0 asphalt2

#material: 80 1.0 1.0 0.0 apa

material: 16 0 1 0 pine

material: 48 0 1.0 0.0 rootpine

material: 80 0 1.0 0.0 water

material: 6 0 1.0 0.0 concrete

pine at 40% moisture

#waveform: ricker 1 0.7e9 my_ricker

#hertzian_dipole: z 0.020 0.020 0 my_ricker

```

#rx: 0.034 0.162 0
#src_steps: 0.002 0 0
#rx_steps: 0.002 0 0
#box: 0 0 0 0.6 0.170 0.002 half_space
#box: 0.000 0.000 0 0.800 0.200 0.002 free_space
#box: 0.000 0.000 0 0.800 0.160 0.002 asphalt1
#box: 0.000 0.000 0 0.800 0.094 0.002 asphalt2
#box: 0.100 0.151 0 0.110 0.160 0.002 apa
#box: 0.260 0.151 0 0.280 0.160 0.002 apa
#box: 0.440 0.141 0 0.452 0.161 0.002 apa
#box: 0.628 0.141 0 0.648 0.160 0.002 apa
geometry_view: 0 0 0 0.60 0.20 0.002 0.002 0.002 0.002 9monthtreepipe1 n

```

Simple concrete model

```

.....MEDIUM.....
#medium: 6 0.0 0.0 0.01 1.0 0.0 soil
#medium: 12 0.0 0.0 0.01 1.0 0.0 concrete
#medium: 80 0.0 0.0 0.01 1.0 0.0 water
.....DOMAIN.....
#domain: 0.6 0.2
#dx_dy: 0.003 0.003
#time_window: 0.4e-9
.....PML.....
#abc_type: pml
#pml_layers: 8
.....GEOMETRY.....
#box: 0.025 0.024 0.574 0.141 soil
#cylinder: 0.060 0.059 0.028 pec
#cylinder: 0.555 0.067 0.018 pec

```

```
#cylinder: 0.136 0.057 0.033 concrete
#box: 0.182 0.065 0.515 0.094 concrete
#box: 0.198 0.070 0.207 0.080 water
#box: 0.218 0.074 0.279 0.080 water
#box: 0.321 0.074 0.389 0.078 water
#box: 0.294 0.068 0.304 0.087 water
.....ANALYSIS .....
#analysis: 52 concrete.out a
#line_source: 1.0 1000.0e6 ricker MLSource_1
#tx: 0.038 0.145 MLSource_1 0.0 0.4e-9
#rx: 0.059 0.144
#tx_steps: 0.010 0.000
#rx_steps: 0.010 0.000
#end_analysis:
-----
#messages: y
#title:
#geometry_file: concrete.geo
```

Root sections with different permittivities

```
#title: cylinders and fun
#domain: 0.60 0.20 0.002
#dx_dy_dz: 0.002 0.002 0.002
#time_window: 4e-9
#time_step_limit_type: 2D
#pml_cells: 10 10 0 10 10 0
#material: 6 0 1 0 half_space
#material: 24 0 1 0 pine
#waveform: ricker 1 0.8e9 my_ricker
```

```

#hertzian_dipole: z 0.020 0.020 0 my_ricker
#rx: 0.060 0.02 0
#src_steps: 0.002 0 0
#rx_steps: 0.002 0 0
#soil_peplinski: 0.5 0.5 2.0 2.66 0.001 0.25 my_soil
#fractal_box: 0 0 0 0.6 0.2 0.002 1.5 1 1 1 50 my_soil my_fractal_box
#cylinder: 0.020 0.100 0.002 0.120 0.100 0.002 0.060 pine
#cylinder: 0.120 0.100 0.002 0.220 0.100 0.002 0.040 pine
#cylinder: 0.220 0.100 0.002 0.320 0.100 0.002 0.030 pine
#cylinder: 0.320 0.100 0.002 0.420 0.100 0.002 0.020 pine
#cylinder: 0.420 0.100 0.002 0.440 0.100 0.002 0.010 pine
#cylinder: 0.440 0.100 0.002 0.460 0.100 0.002 0.008 pine
#cylinder: 0.460 0.100 0.002 0.480 0.100 0.002 0.006 pine
#cylinder: 0.480 0.100 0.002 0.520 0.100 0.002 0.004 pine
#cylinder: 0.520 0.100 0.002 0.560 0.100 0.002 0.003 pine
#cylinder: 0.560 0.100 0.002 0.600 0.100 0.002 0.002 pine

```

Asphalt water-filled fissures

```

.....MEDIUM.....
#medium: 24 0.0 0.0 0.01 1.0 0.0 rootpine
#medium: 24 0.0 0.0 0.01 1.0 0.0 water
#medium: 6 0.0 0.0 0 1.0 0.0 concrete
.....DOMAIN.....
#domain: 0.6 0.2
#dx_dy: 0.002 0.002
#time_window: 4.0e-9
.....PML.....
#abc_type: pml
#pml_layers: 8

```

.....GEOMETRY

#box: 0.411 0.089 0.479 0.120 rootpine
#box: 0.347 0.094 0.411 0.116 rootpine
#box: 0.307 0.100 0.348 0.110 rootpine
#box: 0.016 0.016 0.305 0.152 concrete
#box: 0.256 0.101 0.308 0.108 rootpine
--TrUSx--
#triangle: 0.258 0.107 0.258 0.103 0.238 0.103 rootpine
#box: 0.478 0.082 0.582 0.123 rootpine
#box: 0.246 0.091 0.263 0.095 water
#box: 0.258 0.111 0.281 0.113 water
#box: 0.285 0.087 0.299 0.094 water
#box: 0.288 0.117 0.296 0.118 water
#cylinder: 0.296 0.110 0.005 water
#cylinder: 0.277 0.088 0.007 water
#cylinder: 0.248 0.110 0.005 water
#cylinder: 0.233 0.089 0.006 water
#cylinder: 0.226 0.104 0.006 water
#cylinder: 0.241 0.116 0.004 water

.....ANALYSIS

#analysis: 1 filename.out a

#end_analysis:

.....

#messages: y

#title: model of...

#geometry_file: asphalt water.geo

Fractal clay-sand mixture with cylinder roots

#time_window: 4e-9

#time_step_limit_type: 2D
#pml_cells: 10 10 0 10 10 0
#material: 6 0 1 0 half_space
#material: 16 0 1 0 pine
#material: 48 0 1.0 0.0 rootpine
#material: 80 0 1.0 0.0 water
#waveform: ricker 1 1e9 my_ricker
#hertzian_dipole: z 0.020 0.020 0 my_ricker
#rx: 0.015 0.02 0
#src_steps: 0.002 0 0
#rx_steps: 0.002 0 0
#box: 0 0 0 0.6 0.170 0.002 half_space
#soil_peplinski: 0.5 0.5 2.0 2.66 0.001 0.25 my_soil
#fractal_box: 0 0 0 0.6 0.2 0.002 1.5 1 1 1 50 my_soil my_fractal_box
#box: 0.411 0.089 0 0.479 0.120 0.002 rootpine
#box: 0.347 0.094 0 0.411 0.116 0.002 rootpine
#box: 0.307 0.100 0 0.348 0.110 0.002 rootpine
#cylinder: 0.212 0.101 0 0.212 0.101 0.002 0.034 pec
#cylinder: 0.212 0.100 0 0.212 0.100 0.002 0.023 water
#box: 0.256 0.101 0 0.308 0.108 0.002 rootpine
#triangle: 0.258 0.107 0 0.258 0.103 0 0.238 0.103 0 0.002 rootpine
#box: 0.478 0.082 0 0.582 0.123 0.002 rootpine
#geometry_view: 0 0 0 0.60 0.20 0.002 0.002 0.002 0.002 andrei2 n

Complex, noisy subsurface model with roots

[Not fully included as it contains over 1400 lines]

#box: 0.002 0.000 0 1.172 0.270 0.002 soil
#box: 0.002 0.000 0 0.064 0.270 0.002 concrete
#box: 0.000 0.224 0 0.301 0.270 0.002 concrete

#cylinder: 0.693 0.186 0 0.693 0.186 0.002 0.032 pec
#cylinder: 0.447 0.192 0 0.447 0.192 0.002 0.019 pec
#cylinder: 0.693 0.186 0 0.693 0.186 0.002 0.032 pec
#cylinder: 0.951 0.236 0 0.951 0.236 0.002 0.009 pec
#cylinder: 0.446 0.191 0 0.446 0.191 0.002 0.013 water
#box: 0.847 0.199 0 0.892 0.270 0.002 treeroot
#box: 0.855 0.159 0 0.880 0.199 0.002 treeroot
--Start_imageC--
#cylinder: 0.862 0.205 0 0.862 0.205 0.002 0.015 treeroot
--End_imageC--
--Start_imageC--
#cylinder: 0.862 0.205 0 0.862 0.205 0.002 0.015 treeroot
#cylinder: 0.880 0.205 0 0.880 0.205 0.002 0.015 treeroot
--End_imageC--
--Start_imageC--
#cylinder: 0.880 0.205 0 0.880 0.205 0.002 0.015 treeroot
#cylinder: 0.868 0.193 0 0.868 0.193 0.002 0.015 treeroot
--End_imageC--
--Start_imageC--
#cylinder: 0.868 0.193 0 0.868 0.193 0.002 0.015 treeroot
#cylinder: 0.873 0.191 0 0.873 0.191 0.002 0.015 treeroot
--End_imageC--
--Start_imageC--
#cylinder: 0.873 0.191 0 0.873 0.191 0.002 0.015 treeroot
#cylinder: 0.867 0.174 0 0.867 0.174 0.002 0.015 treeroot
[...]

Appendix C: Abstracts from attended conferences

Symposium on the Application of Geophysics to Engineering and Environmental Problems (SAGEEP)

Andrei Mihai and Gereia Alexandra

Detecting Tree Roots in an Urban Environment with a 400 MHz GPR Antenna

Here, we present the results of Ground Penetrating Radar (GPR) surveys carried with a relatively lower frequency antenna (400 Mhz) in an urban environment. The aim of the study was to determine if this frequency can be used to detect tree roots in urban soils and in different types of pavement, and what are the pros and cons of applying this method in a real environment. While GPR studies on tree roots are not novel, applying the method in an urban environment, with realistic challenges is substantially more different and challenging.

EGU General Assembly 2017

Geophysical Research Abstracts
Vol. 19, EGU2017-6867, 2017

The use of Ground Penetrating Radar to detect tree roots in an urban setting

Andrei Mihai and Alexandra Gereia

Here, we discuss the application of Ground Penetrating Radar (GPR) in the detection of tree roots using a broad range of frequencies (from 250 MHz to 4GHz) and several processing flows, assessing the applicability of the method, with its advantages and limitations, using GPR models as well as practical surveys. For many years, geophysical techniques have been successfully applied in a range of environmental, engineering and geotechnical sectors. Especially in urban areas, the rise of near-surface geophysics has been challenging, as not only are the investigation targets often much more subtle and difficult to study remotely, but man-made materials typically make

investigations much more difficult. Tree roots account for between 10 and 65 % of the total biomass, depending on factors such as age, species, soil type, water availability and competition. However, tree roots have rarely been studied with GPR in real, urban environments, despite the fact that they can cause significant damage to buildings, bridges, roads, and sidewalks. We carried out hundreds of profiles over several surfaces and structures commonly found in urban environments and around various species of trees, of different ages and heights and we report on the success and shortcomings we encounter. Several relevant models were developed to aid the study, focusing especially on the minimal detectable geophysical contrast. To our knowledge, GPR (or any other geophysical method) research was not used by any municipality or policy maker to study tree root hazard. We propose it as a means to better understand said hazard as well as to assess the development of trees in urban areas.

Near Surface Geoscience 2018

The Use of Geophysical Methods in Identifying Tree Roots in Urban Areas

Andrei Mihai and Alexandra Gereaa

In recent years, geophysical techniques have been increasingly used for environmental and engineering applications. As a result, there is growing demand for geophysical studies, particularly in urban areas, where surveys have been traditionally difficult to carry. An area of potential interest has been the study of the interaction between tree roots and infrastructure. Trees are generally a welcome sight in urban areas, as they provide a number of environmental services such as pollution mitigation (Escobedo et al. 2011) and even crime reduction, as Kuo and Sullivan (2001) suggest. However, trees can also interact negatively with infrastructure. In particular, tree roots can cause significant damage to buildings (Biddle, 2001), as well as to roads and sidewalks (Randrup et al. 2001). This process often goes unseen before the damage becomes evident on the surface. Assessing infrastructure damage in the early stages of the process, or even predicting it, could be valuable for urban planning and infrastructure management and repair. However, this remains challenging. Here, we use two geophysical methods, Electrical Resistivity Tomography (ERT) and Ground Penetrating Radar (GPR), describing their usage in the detection and study of coarse tree roots in urban areas. We use a mixture of forwards models, lab measurements, and practical surveys in reallife, non-ideal settings, to assess the span of information that can be derived. We also present a custom-made ERT electrode switchbox that can work on any desired tomography configuration; we used this to work with non-standard configurations, such as the

ones proposed by Wilkinson et al. (2006). For the GPR, we used four different antennas, with very different central frequencies (250 MHz, 750 MHz, 1500 MHz, 4000 MHz).

International Geoscience Student Conference (2019)

The use of different GPR frequencies to study tree roots under paved areas

Andrei Mihai and Alexandra Gereaa

Summary

In recent years, near surface and environmental geophysics have greatly developed and expanded their scope. However, urban studies remain challenging due to several reasons (noise owed by human infrastructure, lack of site delimitation in circulated areas, difficulties in applied methods on paved surfaces, etc.). Ground Penetrating Radar has recently emerged as an excellently-suited method for such urban areas, especially thanks to its speed of data acquisition and excellent resolution.

Appendix D: Journal paper

A B S T R A C T

Ground penetrating radar has been used extensively in near-surface studies to detect underground objects and features typically located within a few metres beneath the surface. In urban areas, ground penetrating radar is widely used to study buried utilities such as pipes and cables. A more recent and unconventional application of ground penetrating radar is the detection of tree roots, which can interact negatively with the human infrastructure in a number of ways. However, the geophysical study of tree roots has proven quite challenging and site-specific. Most tree roots (even coarse roots) have a small diameter and are hard to resolve through geophysical methods. In addition, the sheer amount of potential variability regarding the tree species, age, size, health and the subsurface environment (e.g., soil or a man-made material such as concrete or asphalt) makes it very hard to implement a one-size-fits-all approach. This is where robust, easily customizable forward models can be of assistance, indicating the range of detectable geophysical contrast and the limitations of the method, as well as the suitable antenna frequencies. Here, a

vector network analyser with a commercial open-ended coaxial probe was used to take direct measurements of the relative permittivity of freshly cut tree root segments at frequencies from 50 MHz to 3 GHz. The results were used as inputs to ground penetrating radar forward modelling using gprMax open source software, depicting various realistic scenarios which could be encountered in actual field surveys. The developed models help better understand the applicability, potential and limitations of ground penetrating radar surveys for detecting tree roots in different environments, aiding the development of future surveys. The notable variability in the tree roots is a significant consideration for surveys and forward models.

Key words: GPR, gprMax, tree root.

INTRODUCTION

Trees are essentially ubiquitous in both rural and urban areas, where they provide a number of environmental and social services (Gillner et al. 2015; Mcpherson, Doorn and Goede 2016). Roots are a key structural component of trees, offering anchorage as well as water and nutrient absorption and distribution. However, tree roots can also destructively interact with human infrastructure, causing structural damage to roads, sidewalks and buildings, and causing or enlarging pipe fissures (Randrup, McPherson and Costello 2001; Mullaney, Lucke and Trueman 2015). In urban areas, trees can pose significant risks, with the damage to infrastructure ranging from simple cracks or bumps to serious structural damage (Day 1991).

Roots are more difficult to study than the rest of the tree *in situ* since they are inaccessible and generally buried beneath the soil. Roots are also actively exchanging chemical substances with the surrounding soil (through absorption and respiration), which tends to mask their geophysical contrast. Along with their small size, this makes the *in situ* geophysical detection and study especially difficult.

Ground Penetrating Radar (GPR) is a potential method for detecting tree roots (Butnor et al. 2001; Bassuk et al. 2011). GPR is a non-destructive geophysical method which can be operated relatively fast and is generally well suited for urban surveys. Studies have shown that coarse roots can be mapped in some cases (Hruska, Cermak and Sustek 1999; Butnor et al. 2003; Guo et al. 2013), but the extent to which smaller roots can be detected remains unclear and since past studies generally focus on individual case study scenarios, a certain degree of uncertainty exists even in the case of coarse root detection. The suitability of detecting different types of roots in different types of soils with GPR remains a matter of active research. Most studies have been carried out

under controlled conditions or forest/orchard settings, and significant differences between these soils and urban soils can be expected (Lehmann and Stahr 2007), which could have important implications for the GPR detection of roots. However, it is in the urban areas where the interaction between roots and human infrastructure such as roads, pavements, buried utilities and buildings is more likely.

The usage of GPR in tree root detection has fundamental limitations (Hirano & Yamamoto, 2009), and given the inherent variability of parameters in soils, roots and environmental conditions, a significant variation in detection rates can be expected. Root orientation also affects the detection accuracy of GPR (Tanikawa, Hirano and Dannoura, 2013), which adds another layer of uncertainty to surveys.

Several studies describe different scenarios in which tree roots have been detected using GPR, with varying degrees of success (Cermak et al. 2000; Butnor et al. 2003; Morelli et al. 2005; Bassuk et al. 2011; Ow et al. 2012; Zhu et al. 2014; Butnor et al. 2016). However, these usually focus either on experimental scenarios (Barton and Montagu 2004; Bassuk et al. 2011), or natural soil environments like a forest (Morelli et al. 2005; Hirano and Yamamoto 2012). Real-scenario studies in urban settings, which have differences to natural landscapes (more compaction, erosion, higher temperatures, potential elements of human infrastructure or other artefacts), have generally used relatively low frequencies of 400 (Ow and Sim 2012; Zhu et al. 2014) or 500 MHz (Nichols, McCallum and Lucke 2017), which can only resolve the coarsest roots. Notably, Yokota et al. (2011) found that even a frequency of 800 MHz has difficulties resolving roots with a diameter under 3 cm.

However, the literature does not focus on the dielectric properties of the roots (for clarity, and hereafter, the term ‘permittivity’ is used to refer to the real part of the relative permittivity). Furthermore, potentially unsuitable frequencies are still chosen in practice, leaving some roots outside of the detectability range. Hence, establishing a range of expected permittivity values and a generally detectable contrast could allow GPR operators to better design surveys by anticipating the limitations of different antenna frequencies (i.e. resolution and depth of penetration) and the contrast between roots and soil. A robust model in which parameters for local soil are introduced could provide an indication to what antenna is best suited for the survey. Similarly, developing robust forward models in which one needs only to insert the permittivity values of the root and the soil could help with the interpretation of often complex subsurface scenarios.

This paper presents direct permittivity measurements over a substantial range of root samples (and a few branch samples), from trees belonging to four common species: Sycamore

(*Acer pseudoplatanus*), Pine (*Pinus sylvestris*), Ash (*Fraxinus excelsior*) and Oak (*Quercus robur*). These trees are commonly widespread in temperate climates in urban areas and are likely to be encountered by a surveyor in a real-life setting.

These experimental data are integrated into GPR forward models using gprMax, presenting several relevant scenarios, including the permittivity of common soil types and of the measured roots, potentially serving as a foundation for a better understanding of GPR tree root detection in urban areas. The geophysical mapping and characterization of these tree roots could be used to assess or predict interactions with human infrastructure, enabling city councils to make better urban planning decisions regarding trees. Ultimately, with sufficient development and increasing technological affordability, these measurements could be integrated in a smart city system, with sensors monitoring the potential interactions of tree roots and infrastructure.

This is a cross-disciplinary study with multiple considerations from biology, civil engineering and geophysics. Special emphasis is given to the geophysical standpoint, though other implications are also considered.

M E T H O D O L O G Y

Sample collection

A great deal of emphasis was placed on the health and well-being of the trees. All the root samples were collected from mature, healthy trees and only small segments were cut. Roots under 2 cm in diameter were selected and analysed, since the main purpose of the study was to assess roots that would be more difficult to detect. This also ensured that no structural damage was done to the tree by cutting any of its major roots. Root segments were collected close to their termination, so as not to disturb a longer segment of the root. All harvested roots were gathered from the shallowest part of the topsoil (depth <2 cm). The areas from which the roots were harvested were heavily shaded, with very few patches of sun, and no roots were taken from these sunny patches, to avoid a potential source of water content variation. Roots were harvested at a distance of 3-4 m from the trunk.

All root samples were harvested from an urban area around Harborne, Birmingham (UK); freshly cut roots were labelled, placed in air-tight plastic containers and quickly transported to the laboratory where measurements could be taken. The root is a living part of the tree. From the moment it is separated, it starts to undergo a series of changes. Significantly, it starts to slowly

lose some of its water content. Since the measurements could not be carried out *in situ*, it was therefore imperative to perform them as quickly as possible, within 30-60 minutes.

Root samples were cut into segments approximately 10 cm long. Their shape was sometimes irregular which made measurements more difficult, so samples were cut into smaller segments, but never smaller than 5 cm.

Measuring permittivity

The permittivity measurements were carried out with an 85070E dielectric probe, an open-ended coaxial probe (Keysight Technology). The 85070E can measure complex permittivity over a broad range of frequencies. Most measurements were normally taken from 50 MHz to 3 GHz, and sometimes from 100 MHz to 3 GHz, which is a broad frequency range for ground penetrating radar measurements.

While measuring, the transversal part of the root was firmly pressed on the probe surface. The transversal part was cut smoothly to minimize the presence of small pockets of air which would cause lower permittivity values to be measured.

To further reduce uncertainty, 40 individual measurements were taken for every sample, allowing any anomalous measurements (likely resulting from imperfect contact between the probe and the root segment) to be safely eliminated. In most instances, 40 satisfactory measurements were obtained, and in all occasions, at least 30 valid measurements were obtained for each root segment.

Initially, some measurements were taken as a proof-of-concept, as we wanted to assess the feasibility of the method and the potential of using branches as root substitutes for lab measurements (which turned out to not be the case). For subsequent measurements, samples were also weighed on a high-precision scale, placed into an oven at 105°C for 24 hours, after which they were weighed again to calculate the water content.

Forward models

The data obtained were introduced into forward models produced using the gprMax software; gprMax is an open-access software that simulates electromagnetic wave propagation, using the finite difference time-domain method.

Through its nature, gprMax encourages robust models, as key parameters (such as tree root permittivity, in this case) can be changed, often by modifying a single line of code. Its latest version (based on Python) makes it relatively easy to script more complex scenarios, although the models presented here are reasonably simplistic. Overall, given the inherent complexity of ground penetrating radar (GPR) data, developing forward models can be extremely challenging, but gprMax offers a readily available open-source software solution.

Generally, three-dimensional model calculations are significantly more computationally intensive, particularly for high resolution models involving GPR antennas operating at high frequencies. Hence, for the purpose of this study, only two-dimensional models were developed, as the identification of tree roots is primarily done on GPR profiles.

Several variations of the initial models were carried out, highlighting the robustness of the models, which can be easily tweaked based on existing environmental and root conditions. Easily changeable parameters include the permittivity of the roots and surrounding soil, potential soil layers, root size, position and shape, antenna frequency and waveform. Additionally, gprMax offers the possibility of designing a fractal box with a complex mixture of sand and clay with varying water contents.

Several simplifying assumptions were made. The roots were considered to be cylindrical; although they have irregularities, they still follow a cylindrical shape, and the irregularities are unlikely to have a significant effect. All surfaces were considered to be flat and regular.

Two antenna frequencies were used for these models: 750 MHz and 1.5 GHz. These frequencies were selected as relevant to the practical applicability in GPR surveys and the potential of detecting roots. Both the depth of penetration and the resolution are governed by the GPR wavelength in a trade-off relationship: higher frequency means higher resolution and lower depth of penetration. For this type of study, the vertical and lateral resolution must first be considered.

In order for root detection to be possible, the vertical distance between two reflectors must be at least $1/8$ to $1/2$ of the wavelength λ (Mller and Vosgerau 2006). The two important parameters to consider here are wave frequency and velocity, the latter of which can vary significantly in different mediums. Wave theory indicates that the best vertical resolution can be achieved at one quarter of the dominant wavelength (Sheriff 1977). Applying this to clays with relative permittivities ranging between 5 and 40 will yield propagation speeds of 4.7-13 cm/ns (Overmeeren 1994), which for the two antennas yield vertical resolutions of 1.765-4.5 cm and 0.77-1.97 cm, respectively.

Of course, this theoretical range can be worsened in practice by many factors, such as scattering, energy losses or the return centre frequency being typically lower than the nominal centre frequency due to greater attenuation of higher frequencies (Neal 2004). Given a reasonable velocity of 10 cm/ns, the theoretical vertical resolution for the 750 MHz and 1500 MHz antenna can be expected to be 3.5 cm and 1.6 cm, respectively, (Mancuso 2012).

Horizontal resolution, regarded as the minimum distance which should exist between two reflectors to allow detection, is more difficult to calculate, as it also depends on the trace interval, the beam width, the radar cross section of the reflector and the depth of the target (Rial et al. 2009). This horizontal resolution is also determined by the area illuminated by the GPR antenna, the so-called antenna footprint. It is typically worse than the vertical resolution as it includes the $\lambda/4$ factor as well as another factor dependent on depth. The most common approximation for the antenna footprint, which is used to define the horizontal resolution (Vega, Ramon« and Di Capua 2008) is

$$A = \frac{\lambda}{4} + \frac{b}{\sqrt{(\epsilon + 1)}}$$

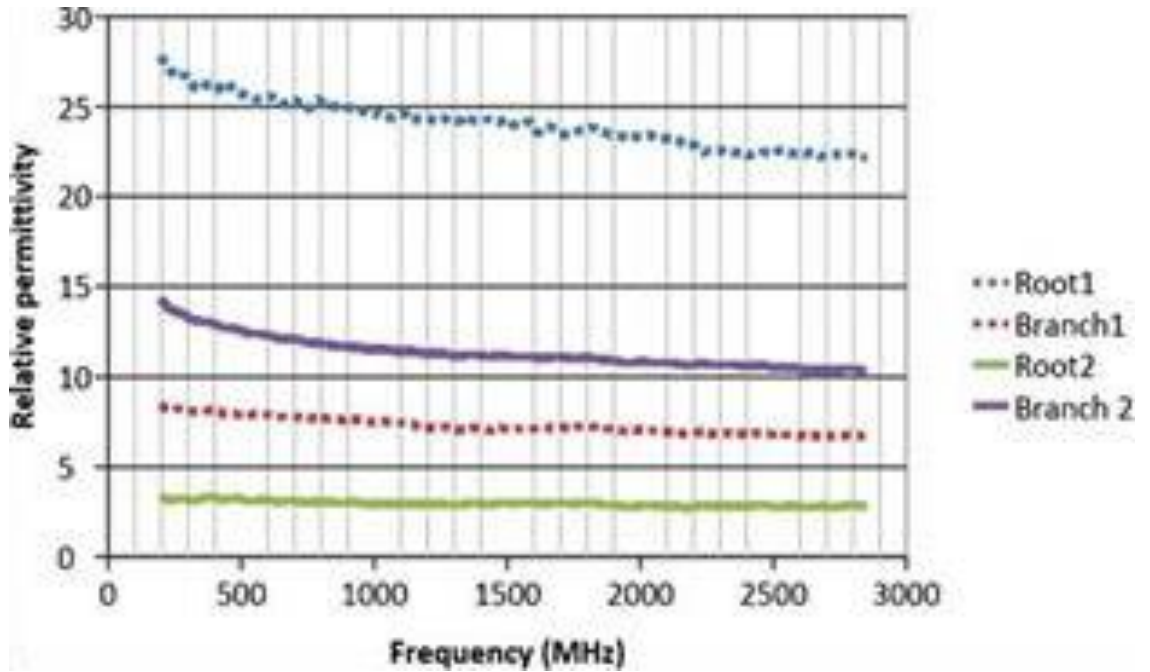
where h is depth and ϵ is the average relative permittivity to depth h.

This effect is diminished since with the exception of tap roots, the vast majority of roots are located within the first 20 cm, but is still significant. For the clay interval, considering a depth of 10 cm, this adds another 1.6-5 cm to the vertical resolution.

The increase in lateral resolution with depth is an important factor in tree root study. Neal (2004) discusses the detailed aspects which can influence practical lateral resolution, including horizontal spacing between GPR profiles (which of course, is not considered on a single profile).

In theory, using higher frequency always seems desirable, but in practice this is not always the case as the depth of penetration is reduced to only a few centimetres due to high

scattering in the topsoil. In the field, topsoil is a heterogeneous and lossy complex medium, with greatly varying dielectric properties (Zhu et al. 2014), which can create an unsuitable medium for very high frequency antennas (2 GHz and above).



The 700-1500 MHz interval range therefore seems like a realistic range for the study of coarse tree roots (thicker roots which have undergone secondary thickening and have a woody structure). While the 700 MHz antenna will be incapable of detecting thinner roots, it is still a frequency commonly used in practice (along with even lower frequencies), and the models highlight the limitations of these lower frequencies.

RESULTS

Experimental results

A set of initial measurements was carried out to assess the suitability of using branches instead of roots, which would have been more easily accessible. However, it was found that

branches and roots have very different permittivity values (as illustrated in Fig. 1), and therefore branches cannot be used as a proxy for roots.

Although there may well be a correlation between the permittivity of roots and branches (influenced by species, overall health and activity of the tree or water content), results indicate that branches are not an accurate proxy for roots.

Table 1 General characteristics of the measured root segments, including the diameter (\emptyset), wet weight (g), dry weight (g) and water content (%)

	1a	1b	2a	2b	3a	3b	4a	4b	6a	6b
Species	yc	yc	yc	yc	yc	yc	ak	ak	ak	ak
\emptyset (mm)					0	0				
Wet weight (g)	.68	.41	.05	.41	.2	.68	.27	.35	.06	.4
Dry weight (g)	.89	.55	.12	.49	.89	.64	.1	.17	.99	.53
Water content (%)	.38	.39	.48	.46	.53	.54	.51	.5	.51	.55
Permittivity 0.5 GHz	5.1	4.5	2	3.5	5.3	7.8	5.1	8.1	8.4	3
Permittivity 1 GHz	3.5	2.9	1	2.2	3.5	6	2.5	6.1	6.3	1.2
Permittivity 1.5 GHz	3	2.4	0.6	2.1	3	5.3	1.6	5.5	5.6	0.5
Species	ak	ak	yc	yc	yc	yc	yc	yc	yc	yc
	6c	6d	7a	7b	8a	8b	9a	9b	10a	10b

Ø											
(mm)											
Weight (g)	Wei	.61	.33	.04	.08	.72	.45	.62	.8	.54	.15
W (g)	Dry	.73	.56	.56	.53	.34	.2	.5	.09	.19	.97
Water %	Wat	.52	.53	.49	.5	.51	.51	.46	.45	.52	.53
Permittivity 0.5 GHz	Per	8.8	1.5	6.8	3.5	8.5	8.6	5	6.5	8.1	2.8
Permittivity 1 GHz	Per	6.9	9.2	5.1	1.6	6.2	6.8	3.3	4.7	6.2	1.3
Permittivity 1.5 GHz	Per	6.2	8.3	4.6	0.9	5.4	6.2	2.9	4.4	5.5	1

Figure 1 shows measurements on roots and branches approximately 1 cm in diameter from a mature Sycamore tree. The curves follow an expected shape, with permittivity values slowly declining with frequency.

The initial measurements also revealed two other aspects: firstly, a minority of the roots have a very low, almost negligible permittivity (<4). Although the water content was not measured for these first samples, they were visibly drier, and possibly diseased or inactive. Secondly, it was immediately visible that the root permittivity values were spread over a wider range and did not cluster around a single value.

There was also a large difference in permittivity between roots and branches of similar diameters, further suggesting that branches are not good substitutes for roots.

Several smaller scale measurement campaigns were carried out, gathering 2-4 roots or 2-4 segments of the same root. Since this was time-consuming and logistically challenging, all surveys but one (describe in the following section) were carried out in this fashion. Additionally, since there is a reasonable reason to believe that environmental conditions such as soil moisture can change the permittivity of the roots, surveys conducted on different days were analysed separately

A larger survey

The largest and most comprehensive survey was carried around the Harborne Walkway, in Birmingham, UK. A total of 20 root segments were successfully harvested and analysed (two segments from eight individual roots, four segments from one individual root). Another four segments from a different root yielded very low permittivity values and were discarded. This ensured that there was time to carry the measurement before the root samples start drying up. All samples were taken from the same soil unit (a wet clay), over a distance of under 1 km, with depths ranging from 0 to approximately 2 cm, from three species: Sycamore, Pine and Oak. Roots were labelled from R1 to R10. Out of the samples, R5 segments were discarded as very dry and potentially diseased/inactive, and four segments were harvested from R6 (R6a, R6b, R6c, R6d). From all other roots, two segments were harvested (a and b). The diameter, weight and dry weight were measured. It was attempted to harvest root segments both from the surface and right beneath the surface. All the 'a' segments were visible on the surface. The 'b' segments were on the same root section as the 'a' segments, in their direct continuation, but right beneath the surface (<2 cm), which did not appear to have a consistent effect on permittivity. For the R6 root, only the 'a' segment was partially visible on the surface.

Table 1 shows the characterization parameters of the tree roots analysed in this study.

Segments from the same root tended to have more similar water content values, typically within 1-2%, although one sample varied by up to 4% (R6 in Table 1). Water content also did not appear to be correlated with diameter.

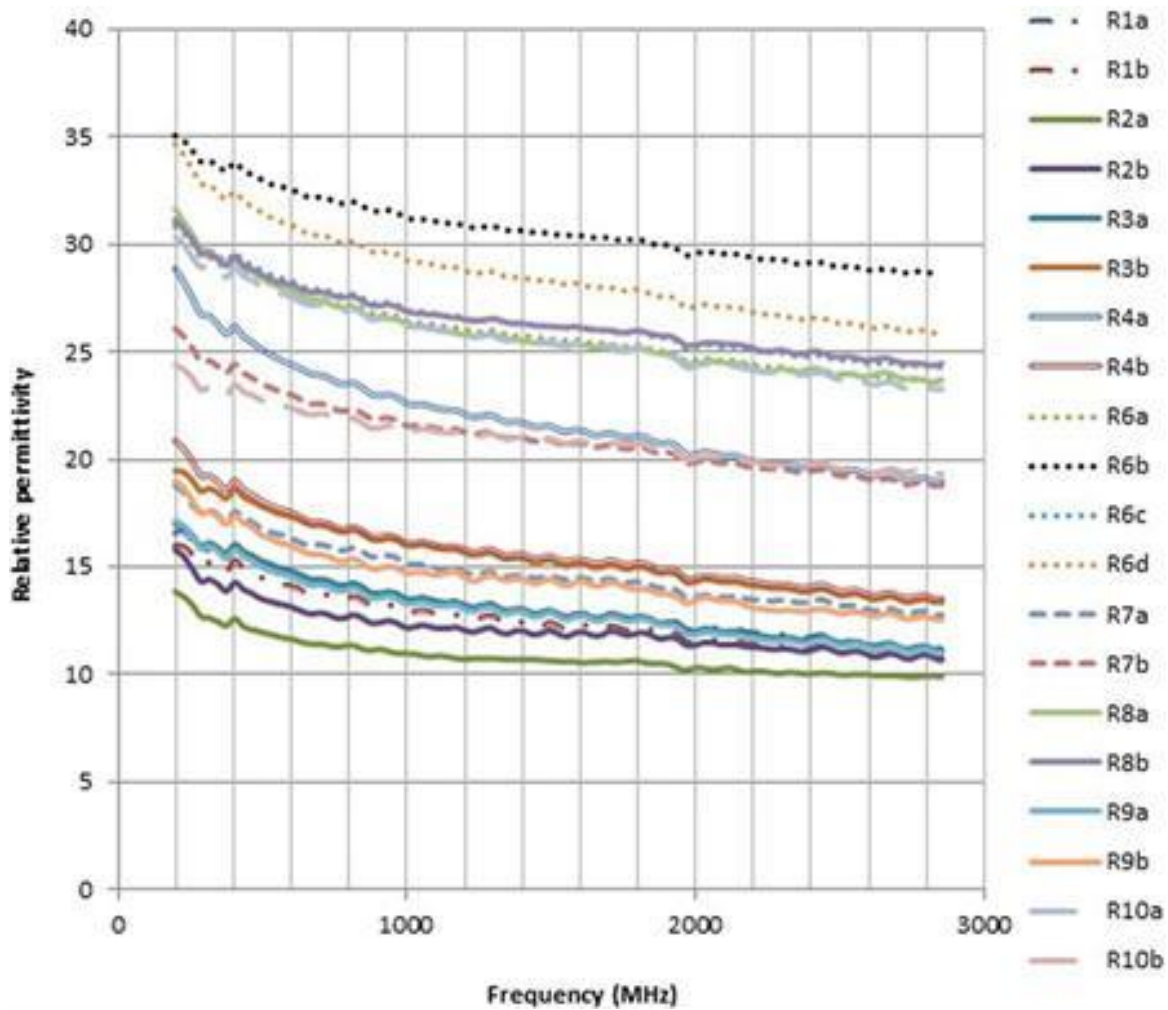


Figure 2 Median permittivity values for root segments R1-R10.

The range of frequencies over which the segments were measured was 50 MHz-3 GHz, with measurements taken at 101 individual frequencies. The first and last five extreme measurements were eliminated, and the median value was calculated.

Figure 2 shows the median permittivity values for root segments R1-R10; the lack of smoothness in the curves is common when taking vector network analyser measurements with open-ended coaxial probes and can be caused by imperfect contact between root sample and probe and possibly by sub-optimal calibration of the probe (note that the measurements shown in Fig. 2 were taken on the same day). However, because all the curves followed a similar shape, we interpret this to be an artefact of the probe measurement, and these irregularities do not affect the conclusion derived from the analysis.

The wide spread of the permittivity values is remarkable. At 1 GHz, permittivity values range from just over 10.9- 31.1. This interval is significant because the permittivity of the soil is

likely to be within this range (Curioni, Chapman and Metje 2017). If the permittivity of the soil is similar to the permittivity of the root, it is unlikely that ground penetrating radar can detect it.

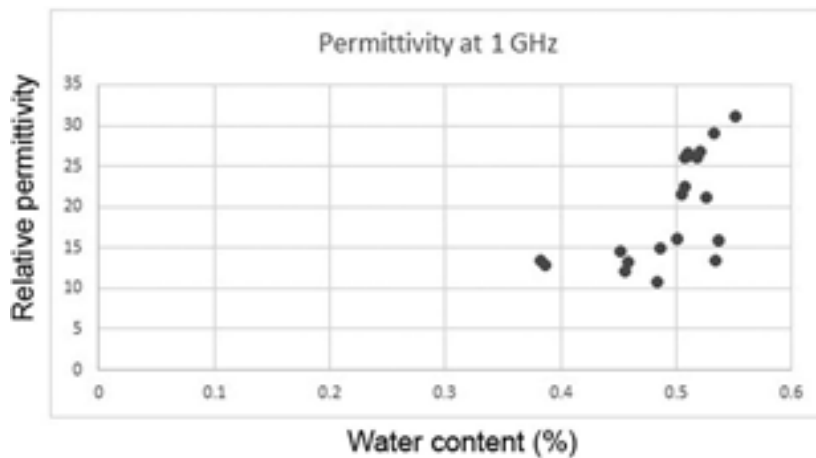


Figure 3 Permittivity values for R1DR10 at 1 GHz. Permittivity values at other frequencies yielded similar trends, which cannot be grouped by any readily available parameter.

Similarly to the water content (see Table 1), the permittivity values show no correlation to the root diameter or tree species.

In most instances, different segments of the same roots had very similar values -- but this was not always the case. Figure 3 shows the relationship between water content and permittivity at 1 GHz.

Although a positive relation exists, the data are spread out and do not appear to follow a predictable behaviour. This suggests that several different factors other than water content are affecting the permittivity value of the roots, producing a notable spread.

The trend did not become clearer when grouping the data points by diameter, tree species or other available characterization parameters. This suggests that unlike other materials (for example soils), tree root permittivity cannot be estimated based on water content alone, and other factors need to be considered.

However, a thorough explanation of this variability was not attempted here as it was not the primary objective of this study and is an area of interest for future work.

The root density and the electrical conductivity caused by sap flow at the time of the sampling are potential parameters which could have played a significant role in affecting the measured permittivity, as suggested by Cermak et al. (2000).

Forward models

The root permittivity values described in the previous section were inserted into the forward models using gprMax.

Two virtual two-dimensional boxes of $0.8 \text{ m} \times 0.3 \text{ m}$ and $0.6 \text{ m} \times 0.2 \text{ m}$, respectively, were constructed in gprMax. The antenna was not modelled, and a simple Tx-Rx system was used, as is readily available in gprMax (Warren, Giannopoulos and Giannakis 2016). Both the permittivity values of the roots and the soil can be changed with ease. Additionally, a complex and real-life mixture of clay and sand can be modelled as an existing feature of the software.

The soils from which the roots were harvested were loamy and clayey. The permittivity values considered in the models cover a broader range, from 2 (a very dry and sandy soil) to 20 (a very wet, clay-rich soil). The values were extracted from existing literature (Daniels 1996) and input into the models (Peplinski, Ulaby and Dobson 1995). Forward models were generated with a time window of 8 ns; discretization step (dx dy dz): 0.001 m; waveform: Ricker; spatial increment for sources and receivers: 0.001 m.

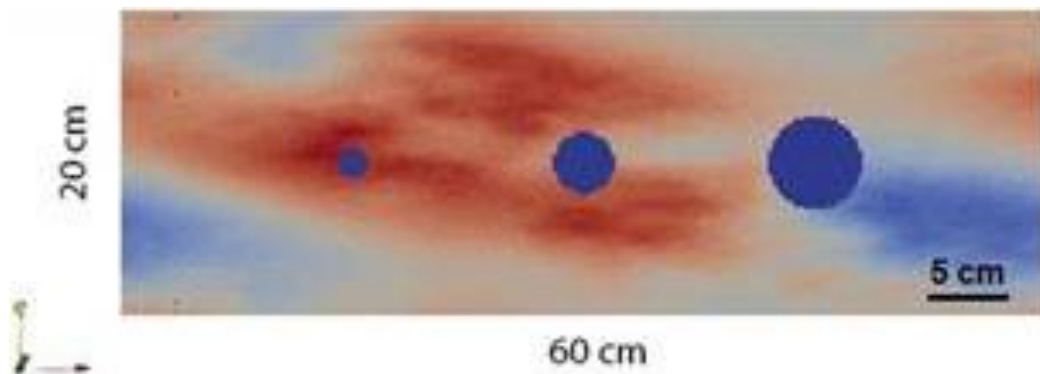


Figure 4 A visualization of a virtual box ($0.6 \text{ m} \times 0.2 \text{ m}$) with three crossing roots of different diameters. The box features a fractal mixture of clay and sand with modifiable water content (Warren et al. 2016), using the Peplinski model (Peplinski et al. 1995). All models generated in this manner feature a 50% clay/sand mixture using a stochastic distribution of dielectric properties and the standard gprMax parameters as currently presented at http://docs.gprmax.com/en/latest/examples_advanced.html (a volumetric water fraction range of 0.001-0.25, bulk density 2 g/cm^3 , sand particle density of 2.66 g/cm^3). Time window: 8 ns;

discretization step (dx dy dz):

0.001 m; Ricker wavelet; spatial increment for sources and receivers: 0.001 m.

For simplicity, the modelled roots were kept horizontal, and most of the generated ground penetrating radar (GPR) profiles were kept perpendicular to the root. However, profiles along the direction of the root were also generated.

After the forward models were outputted, they were imported into ReflexW, where some filtering was applied. Since the data are synthetic, there was no need for processing steps like dewow or bandpass filters, but static corrections (moving start time), background removal (standard ReflexW settings), hyperbola-based migration and Hilbert transforms (standard ReflexW envelope) were applied.

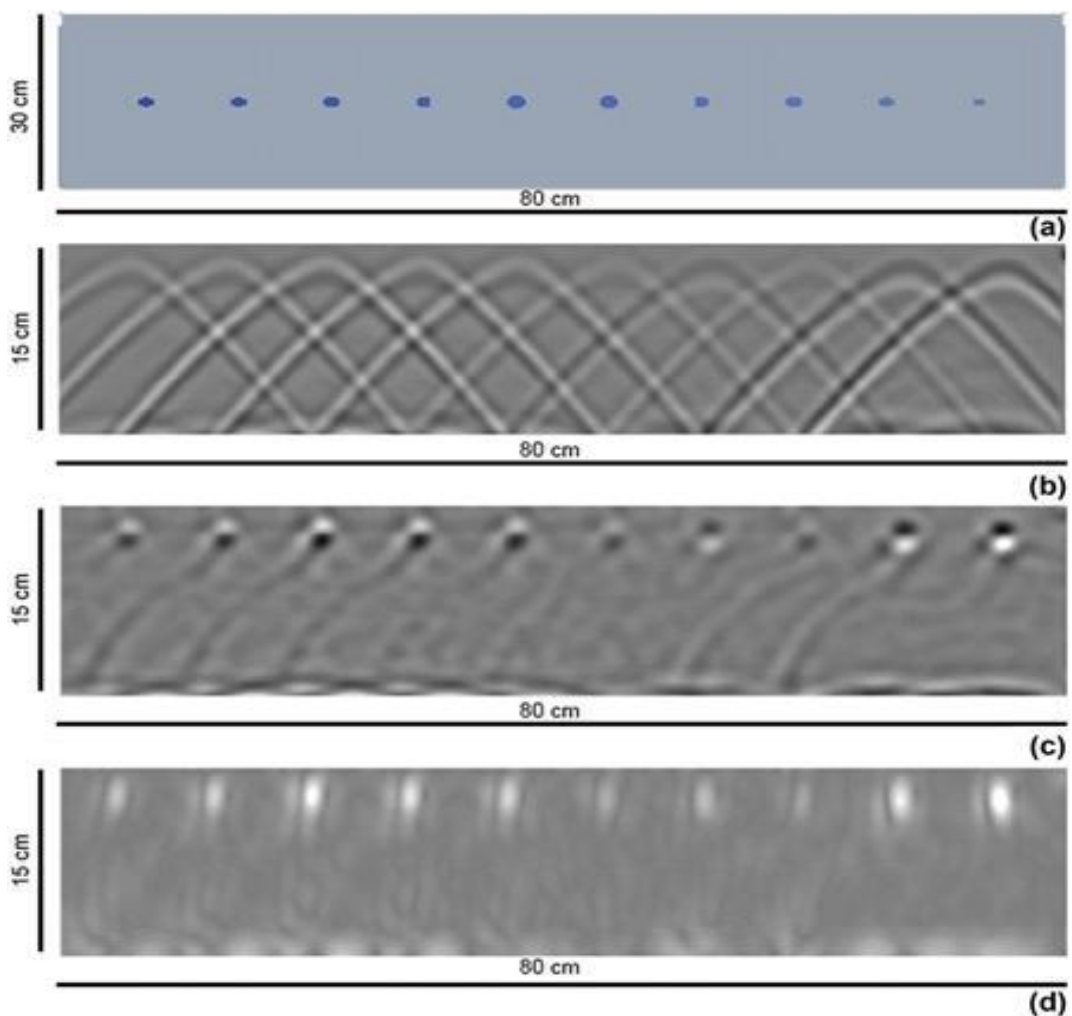


Figure 5 Synthetic radargram generated using data obtained from roots R1aDR6b, including permittivity and diameter values for the roots. Estimated permittivity for the clay from which they were extracted is 20. Radar frequency: 1.5 GHz. The gprMax box geometry (a);

resulting data, with background removal and static corrections (b); migrated data (c); and Hilbert transform (d). Some roots are easier to distinguish than others, depending on the permittivity contrast. Notably, size plays a secondary role – roots with a larger diameter are not easier to detect if the permittivity contrast is not strong. No type of noise was added, thus all results can be considered an ideal case for GPR detectability.

Figure 5 depicts how segments through R1-R6b would generate a GPR response if placed next to each other, in the same soil type, at the same depth. The visual differences caused by a range of real, different permittivity contrasts are presented, using a common processing flow. If the contrast is strong enough, it overshadows the impact of root size, and if the contrast is low enough, detectability becomes much more difficult, and potentially impossible.

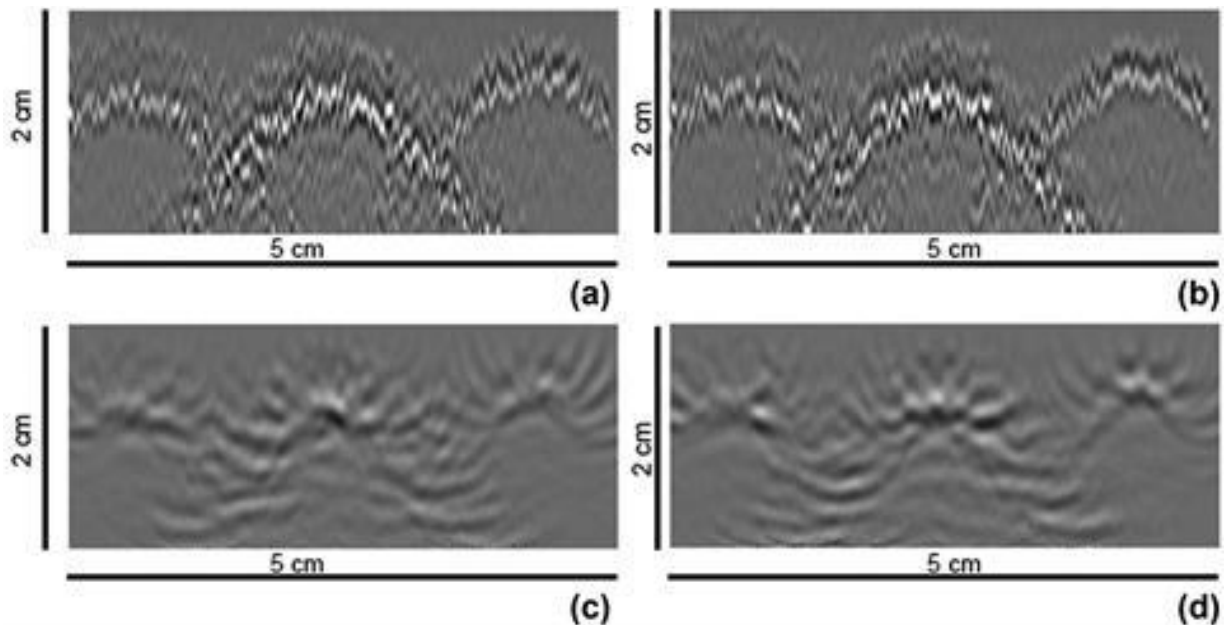


Figure 6 A forward model simulation in a $0.6 \text{ m} \times 0.2 \text{ m}$ virtual box for three roots with varying permittivity values (R3a, R6a, R10b) in a wet clay with a permittivity of 20 (radar frequency: 1.5 GHz). Results show a homogenous root (a) and a root with a 1 mm bark (b), in unmigrated (top) and migrated (bottom) sections.

Some models were also developed with varying bark thickness (Fig. 6 represents a zoom-in section of such a model). However, plausible bark thickness (around 1-2 mm) did not appear to have a major effect, though it did make the contrast slightly more pronounced. In a more realistic soil scenario (which is heterogeneous), data migration can become problematic, potentially causing unwanted effects (migration artefacts). For the practical purpose of a GPR survey, it seems that using non-migrated data may be more useful in the case of resolving tree roots.

As expected, models with a lower permittivity (which mimicked a drier soil) yielded an overall better quality. This was also visible in the Peplinski soil model in Fig. 4: when the fraction of clay (especially wet clay) was higher, the quality of the data was reduced.

It is important to also note that urban soils also have a great variability in terms of permittivity. In addition to the root variation, soil variation is potentially equally significant. In Fig. 7, a dry root is presented in different homogeneous soil conditions, mimicking a very dry clay, a very dry loamy soil, a fertile soil and a wet clay.

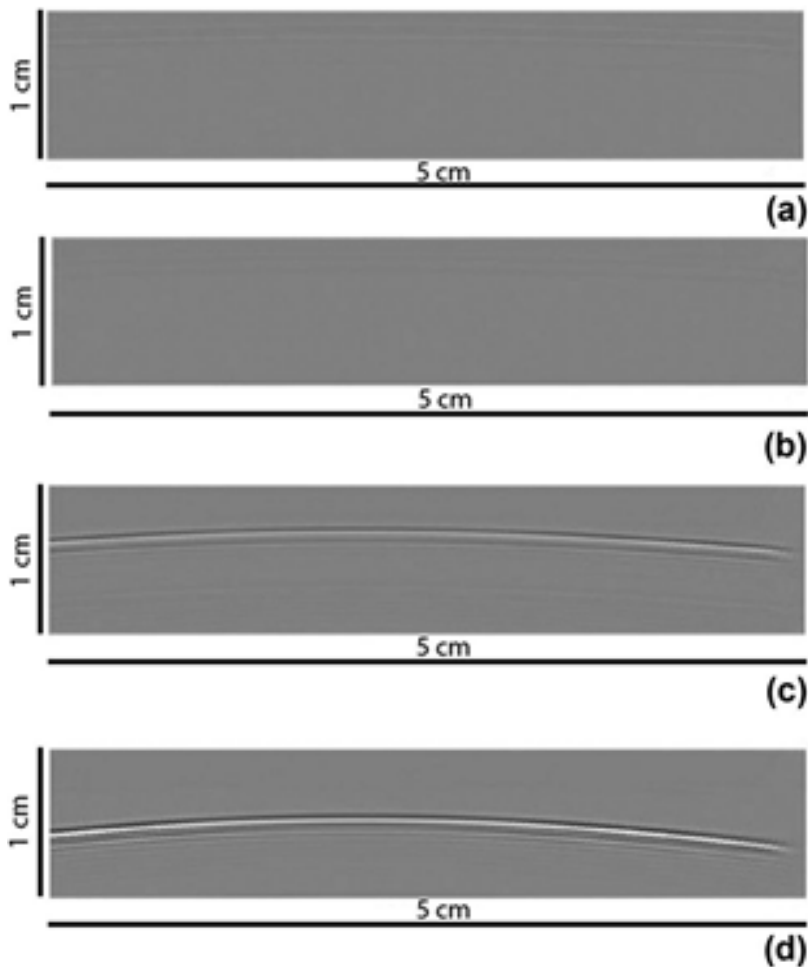


Figure 7 Zoom-in section of a dry root (permittivity value 3) is presented in four different soils, with different permittivity values (2, 3.5, 10, 20 for a, b, c, d, respectively). Radar frequency is 750 MHz.

The unlikely case of carrying out a GPR profile along the line of a tree root is depicted in Fig. 8. Here, the heterogeneous soil is kept unchanged, and instead, the root permittivity value takes different values.

In both cases, when one member of the root-soil system changes permittivity values, the contrast becomes more pronounced as the difference increases. Tree roots can be detected if they have a permittivity contrast to the surrounding soil, regardless of whether it is a positive or negative contrast. In the absence of a permittivity contrast, even a large root can be difficult to detect.

Figure 7 shows that even a dry root, which a surveyor might believe to be easily detectable, is almost completely invisible in the case of very dry soils, though the contrast becomes evident in the case of soils with a higher permittivity. Strong permittivity contrasts (be they positive or negative) make tree root detection possible. In other words, it is the relative permittivity value (between the root and the soil) that enables GPR detection, not the absolute value. This is, of course, a fundamental principle of geophysics, but becomes particularly important here due to the range of permittivity of the target (tree root) and the environment (soil), which can have significant overlap.

Figure 8 shows the type of signal that can be expected in the case of a GPR profile carried in the line of a tree root which thins out towards its termination.

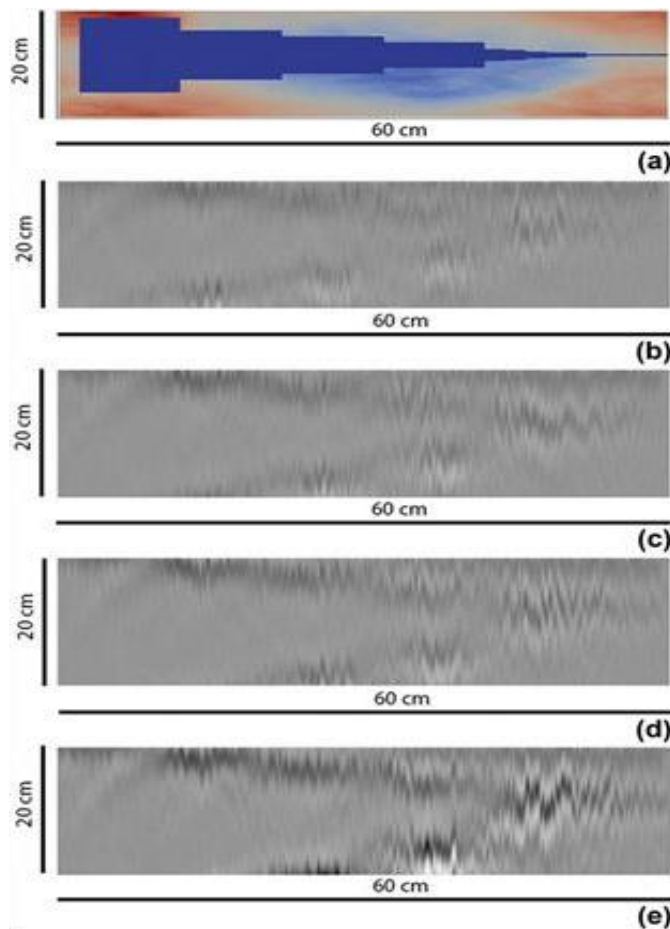


Figure 8 A mixture of sand and clay and a simplified root, which grows thinner from the tree to its termination (a). Different permittivity values are given to the root (12, 16, 20, 24 for b, c, d, and e, respectively). Radar frequency is 700 MHz.

DISCUSSION

Tree roots are complex and highly variable. They exhibit a broad range of permittivity values, depending on factors that do not seem solely limited to water content. The permittivity contrast to the surrounding soil environment critically dictates the ability of ground penetrating radar (GPR) to detect tree roots, which is a practical concern.

Even within a single soil unit, in similar environmental conditions, root permittivity can be spread over a large interval. This permittivity interval has substantial overlap with that of many soil types and therefore there is a high chance that some of the roots will have a permittivity value close to that of the soil, making detection more difficult or, in some cases, impossible. This also explains why GPR seems “blind” to some roots, as the root permittivity is masked by that of the surrounding soil.

Root permittivity does not seem to be correlated with diameter. This suggests that in some scenarios, larger roots can be more difficult to detect than smaller roots, if their permittivity happens to be closer to that of the surrounding soil. Neighbouring segments of the same root can also have varying permittivity values.

Permittivity values for branches show no correlation with permittivity values for roots. Appealing to this proxy is unreliable and not recommended.

The permittivity contrast between the root and the surrounding soil is the defining factor which impacts detectability. This contrast, defined by the permittivity values for the soil and the root, is the parameter which should be most carefully considered in the forward models. It is recommended that a range of permittivities be simulated. The diameter of the root should be considered for the selection of a suitable survey antenna. As expected, results suggest that the 1500 MHz is much better suited for studying finer tree roots, due to its higher resolution. This should also ensure a sufficient depth of penetration in most scenarios.

The root can exhibit a positive or a negative permittivity contrast to the surrounding soil. The positive or negative nature of the contrast does not have a strong impact on detectability,

although, in practice, a negative contrast suggests a higher soil permittivity, where GPR data tends to have lower quality.

The above does not necessarily hold true for paved surfaces, where it is possible to detect roots even when they exhibit similar permittivity values to the surrounding environment as they generate a system of small cracks and fissures which might be detected with GPR.

The presence of bark does not always ensure detectability. Roots with a thin bark (1-2 mm) are only slightly easier to detect, this effect being most significant in a higher permittivity soil, which ensures a higher bark-soil permittivity contrast. If the bark is thin enough, some of the signal is reflected by the root, while some of it passes through the root, which is why sometimes, some roots exhibit a double hyperbola response.

Some roots (including diseased or inactive roots) have an extremely low permittivity (<5). This could be useful, for instance, in an orchard setting, to detect potential health problems of the roots and subsequently, the trees themselves.

Water content, while certainly an important parameter, is not the only influential factor responsible for tree root permittivity. Permittivity might also vary dynamically with water/nutrient uptake and sap flow. Hence, repeating a GPR survey at different times, or under different environmental conditions, could yield different results. A general correlation between the soil and the root permittivity can be assumed and with all things equal, wetter soils (with a higher permittivity) will generally contain wetter roots (also with a higher permittivity), though this does not appear to cancel out the root permittivity variability, just offset it.

The results presented in the study can give surveyors an awareness of the spread of permittivity values of tree roots, and a more realistic expectation of what can be detected, including the fact that some roots may remain undetected even in the case of a well-designed and carefully carried-out survey. This range of permittivity can be then input into forward models along with a predicted or measured value for the soil unit to aid in the understanding of the range of detectable contrasts and the overall expected signal (with the mention that models will provide an 'optimistic' version of detectability; low contrasts barely distinguishable in the simplified forward models are unlikely to be detectable in a real-life scenario). This is an inexpensive, relatively easy way of improving a pre-survey assessment and overall survey design.

Tree root forward models can also aid in the interpretation of GPR data. The identification of tree roots on radar-grams and differentiation from other subsurface reflectors relies on the root's continuity. However, permittivity variation within a single root could mask this continuity. This can be particularly impactful in surveys which map the proximity of tree root growth to elements of infrastructure such as pipes, one of the main objectives of the geophysical study of tree roots. The removal of such tree roots is an expensive and delicate intervention, and a thorough geophysical interpretation could assess whether such an intervention is necessary, saving costs and time. Ideally, pre-emptive surveys would be carried out enabling such interventions before any damage has been done.

Finally, should all the underlying parameters determining root permittivity be determined, a simple, non-invasive radar-gram could reveal important aspects about these parameters and subsequently, about tree health. For instance, it is plausible that diseased tree roots have lower permittivity, and GPR could provide a relatively fast and non-invasive way to help assess the disease spread.

CONCLUSION

The ground penetrating radar (GPR) detection of tree roots remains a difficult and site-specific task. A range of permittivity values for tree roots is introduced, and the impact on detectability is discussed.

This is the first study to combine direct measurements of permittivity and GPR forward modelling techniques. Harvesting and measurement of tree root permittivity is possible, though the process is time-consuming and must be done carefully. The contact between root segment and probe remains a potentially problematic issue, although this can be overcome by collecting a large number of measurements and removing any potential outlier.

Tree root permittivity has a broad range of values, even in the same ground condition. In one of the surveyed areas, the roots' relative permittivity varied between 10.9 and 31.5. Some roots will have a value closer to that of the surrounding soil, which makes detection much more difficult. This information is useful in several ways: it can help develop more realistic survey expectations, it can aid GPR data interpretation, and it can offer a better understanding of the root-soil system from the standpoint of a GPR surveyor.

Whilst the generated synthetic models here have featured a root-soil dynamics, the same type of models can be adapted with relative ease to depict tree root damage to man-made structures (such as concrete or sidewalks) and better understanding this potentially destructive interaction, or used to monitor trees in a controlled setting (such as an orchard).

This study can serve as a starting point for a more thorough understanding of the biophysical parameters of tree roots, which can in turn affect their geophysical detection and characterization. The permittivity variation between the same root segment remains an intriguing finding which warrants further exploration.

The imaginary part of permittivity, not analysed here, deserves further investigation, to see whether it follows the power-law trend described by Jonscher (1977).

Future research should focus on including more complex models that resemble the reality, for example by including more complex root structures and man-made structures, in addition to soil. Additional experimental studies and collection of real data are needed to confirm the findings of this research and shed light on the reasons why tree roots exhibit the large variability measured here, ultimately providing a more effective guidance for tree root detection using GPR.

A C K N O W L E D G E M E N T S

We would like to thank the Antonis Giannopoulos, Craig Warren and everyone else who worked to develop the gprMax software. We also thank the COST initiative TU1208 on Ground Penetrating Radar for their communication sessions and practical workshops which helped us lay the foundation of this study. Also, we would like to thank Michał Dabrowski for his input and suggestions.

Appendix E: Surveying guide

This is meant to serve as a standalone guide for geophysical surveys attempting to detect or study tree roots. The guide is aimed at geophysicists and other surveyors as well and can be distributed freely.

Two geophysical methods can be used in root surveys: Ground Penetrating Radar (GPR) and Electrical Resistivity Tomography (ERT). Out of these two, GPR is by far the more robust and is recommended in most cases. Nevertheless, both methods are described here.

GPR

GPR is an electromagnetic method that can be applied on all smooth surfaces, paved or soil. The method relies on detecting dielectric contrasts between subsurface materials. Surveyors must be aware that in the case of soil surveys, this contrast might be very small or might not exist at all..

a. Equipment selection

Ideally, more than one frequency will be used to survey tree roots: a lower and a higher frequency. The high-frequency antenna will produce high resolution under good survey conditions in the very topsurface (first 10 cm), whereas the lower frequency will have a higher depth of penetration, and will still be reliable under worse survey conditions. In practice, this would mean an antenna of 400-750 MHz, and another of 1000+ MHz. Thankfully, mixed systems have become much more common today and can be deployed efficiently.

Surveyors must pay attention to the lateral and vertical resolution that their antennas can provide, and have realistic expectations (see Mihai et al., 2019). Surveyors should be aware of the potential as well as the limitations of the method, and also be aware that on paved surfaces, cracks might sometimes be more visible than the root itself.

However, the luxury of choice is not always available. In these scenarios, where there is a limited antenna accessibility, surveyors must first consider if the antenna(s) has (have) the capacity to satisfy expectations -- only then, should the survey proceed. Otherwise, there is a good chance of wasting time with inadequate results.

It should be considered that while roots generally have a higher permittivity than their surroundings, this is not necessarily always the case. A strong contrast is required for detection, but this contrast could be both positive and negative.

Resolving individual roots is not always possible for thin roots. However, a root area in the vicinity of the tree should generally be detectable, and this can give indications as to the direction of the roots and the likelihood of existing or impending damage.

b. Survey design

Survey design is crucial. Tree root detection is very site-specific, and any peculiarities of the site should be considered. Several steps can be taken to reduce the risk of unwanted noise and improve the chance of a high-quality survey.

First, the survey area must be considered. If the area includes different types of surfaces (ie, soil and asphalt areas), it is ideal if a different survey is carried out for every individual surface. This will only slightly increase the data acquisition time, and will make data processing much simpler (and more reliable). The reason for this is that different surfaces can obstruct one another with higher-contrast reflections, and joint data interpretation is hampered. Some processing softwares can split the survey into different areas, but this greatly depends on the type of GPR data and processing software. This can also be done in the files, directly, but is laborious and time-consuming. For simplicity, splitting the profiles is best. In addition, it is best if profiles are relatively short, to minimize human positioning errors.

When detecting tree roots, the distance between profiles should not be greater than 10 cm. Sometimes, this is unavoidable, but the quality of the data can decrease sharply at greater distances.

If the direction of the tree roots is known (or if there is one particular direction of interest), profiles should be carried out perpendicular to that direction. In the vast majority of cases, however, this direction cannot be known. Therefore, it is recommended to carry out profiles on perpendicular directions. Given a strict time constraint and no preferential direction, coarser profiles on perpendicular directions are preferred to denser profiles on one direction.

If a total station or another means of precise positioning exists, this can be used with great success, both for the profile geometry and to detect slight elevation (bumps) that might not be visible with the naked eye.

Given the very small dimensions of tree roots in general, the GPR settings should be enabled to improve resolution. It is recommended that the number of scans per trace, and the number of overall traces is increased to the maximum (which may produce files

Some periods of the year are better than others for this type of survey. Autumn, winter, and periods with heavy rain, in general, are not recommended for GPR (especially in clay-rich soils). However, this is of less consequence on paved surface surveys. For instance, fallen leaves can add additional noise to surveys. It is likely that in some yearly conditions, the contrast between roots and surrounding area is increased -- but it is not entirely clear when these periods are. Roots are complex systems that tend to mimic their surroundings. As a rule of thumb, surveys carried out in the summer (over drier parts of the season) tend to have better results.

c. Data acquisition

After the equipment is selected and the survey is designed, the data must be collected carefully. Notes must be taken of any object or structure of interest (bumps, cracks, ducts, etc). The position of any surrounding trees should also be noted.

Special attention must be given to antenna positioning. If the antenna system is asymmetrical (ie there is a wheel ahead or behind the antenna) and meandering profiles are acquired, this should be addressed as a static correction, as there will be an offset

between the real antenna positioning between back and forth profiles.

Operators should be very careful to maintain a steady course. Tapes or strings should be used to help guide the operator and minimize profile deviations (shorter profiles can help). Any positioning anomalies should be dully noted or re-done, if possible.

Surveys on soil should be carried in the same day, in the same meteorological conditions. If a survey is not finished in a day and continued the next one(s), it is best to split this into separate areas, as the soil properties can change significantly from day to day.

d. Data processing

This may vary from case to case as some GPR producers offer proprietary software. However, in most cases, processing should follow a few general steps.

Survey geometry and static corrections are the first steps. This needs to be checked with great attention, to avoid any errors. A frequency filter should be applied as a bandpass. Although every antenna has a frequency, that is only the central frequency, and data is gathered across a much broader spectrum. Therefore, the data should be filtered from $1/2x$ to $2x$ the central frequency. The filter can be narrowed somewhat, but this must be done with extreme attention to ensure that no useful data is removed. As a general rule, noise tends to be more present in the higher frequency, and that is where narrowing the filter is likely to be more effective.

Gain is generally required to compensate for signal attenuation. The type and intensity of gains varies from site to site, but it should be done in a way that reveals as much information as possible from the deeper parts of the survey, while keeping in mind that data quality tends to decrease with depth.

Dynamic corrections and "dewow" filtering can also be considered. A form of background removal (or average subtraction) can also be very useful, highlighting features of interest.

Lastly, migration of data should also be considered. This can be double-edged and data

should always be compared pre-migration and post-migration. The main advantages of migration is hyperbola collapse and depth estimation. However, hyperbolae can be useful in differentiating roots from other features, and accurate depth estimation is not as important since we are dealing with the first centimeters. Especially on paved surfaces, unmigrated data can be more useful than migrated data. This is counterintuitive but is a significant consideration in tree root surveys.

e. Data interpretation

The key to root identification is lateral continuity. Roots exhibit lateral continuity, although not necessarily in a very straight line. Therefore, timeslices are important to detect tree roots.

However, timeslices are not always sufficient for identification. Every profile must also be analysed individually. Areas suspected of being tree roots (or root damage) should be identified both on profiles and on tree roots.

Since there is so much variability in tree root surveys, the interpreter's ability is very important. Features are not always obvious, and identification can be difficult. Experience in GPR interpretation is very useful in this scenario.

Lastly, it is very likely that some areas will be uncertain -- they will be 'suspects' of tree roots, but with some uncertainty. The surveyor should communicate this accordingly, and the expectations should also consider that this sort of survey will likely carry a degree of uncertainty. While this uncertainty can be reduced through careful planning, acquisition, processing, and interpretation, it cannot always be eliminated. Expectations should not deal in the absolute.

f. Other GPR considerations

GPR surveys for tree root damage identification (or prediction) can be a way to save money through timely interventions. As surveying costs have decreased significantly over the years, and the value of infrastructure and environmental services has increased, the

"sweet spot" where surveys are useful has also expanded. These surveys can direct interventions where roots are starting to damage elements of infrastructure. Where suspicions exist, preventive surveys should be carried out and repeated every few months. This might not be feasible in all areas, so the cost of the survey and the cost of potential damage should be balanced.

Root detection can be carried out in conjunction with overall asphalt assessment, which is carried routinely in some areas. This could also direct timely interventions through thorough assessments.

Infrastructure damage is not the only potential application of this type of survey. While there are substantial knowledge gaps in the literature, there are reasons to believe that GPR surveys could also be used in orchard settings or forestry to detect root health and potential diseases. More research is required into these fields.

g. Using ERT as a complement

In areas of interest, where GPR data is inconclusive (or another layer of certainty is required), ERT may be used as a complement to GPR.

Given existing technologies at the time of this writing, ERT is much more time-consuming than GPR and should likely only be carried out as a complement to GPR, or deployed where time is not a constraint.

The applicability of different ERT arrays is site-specific. Optimized arrays (such as those discussed by Wilkinson et al., 2006) can be deployed. However, in most situations, a combination of Wenner and Dipole-dipole arrays is sufficiently robust (and is provided by most commercial equipment).

If the goal is to resolve individual roots, the electrode spacing should not be larger than 10 cm. This means that for instance, in an array of 16 electrodes, only 1.5 meters will be covered at a time. In order to cover a surface of 1.5 x 1.5 meters, this means 16 profiles at a distance of 10 cm between profiles. This can be expected to take several hours. The distance between profiles can be increased, but it should be again considered that lateral

continuity is essential to the identification of tree roots. The classic Wenner array is a worthy consideration here. It has a reduced number of datapoints, which means a low time of acquisition, and often produces high-quality results.

With existing ERT equipment, the method can only be robustly applied on soil surfaces. Since the goal of the survey is to assess or predict root damage on paved surfaces and ERT cannot be used directly on paved surfaces, the best applicability is on soil surfaces right next to paved surfaces (for instance, when trees are surrounded by pavement). In this case, if a root is detected all the way up to the paved surface, then it can be assumed that damage is likely to happen soon or has already happened.

In the case of electrical data, not as much processing is required as with GPR. Eliminating anomalous datapoints is often sufficient. The peculiarities of data inversion should be kept in mind.

ERT and GPR data can be integrated on profiles or in 3D. The results can be compared to confirm the existence of roots on GPR profiles which are often uncertain. However, realistic expectations should be had in the case of ERT surveys of tree roots.

In most situations, it is difficult to justify the use of electrical methods in the detection of tree roots given the constraints. Nevertheless, it can be deployed in some scenarios where digging the topsoil is not possible or not desired and where time is not a strict constraint.

As the available equipment and methodology progresses, it is expected that this method will become more prevalent.

8. REFERENCES

- Alani, A. M., Bianchini Ciampoli, L., Lantini, L., Tosti, F., Benedetto, A. (2018). Mapping the root system of matured trees using ground penetrating radar. *Proceedings of the International Conference on Ground Penetrating Radar, GPR*, 1-6.
- Amato, M., Basso, B., Celano, G., Bitella, G., Morelli, G., & Rossi, R. (2008). In situ detection of tree root distribution and biomass by multi- electrode resistivity imaging. *Tree Physiology*, 28(10), 1441–1448.
- Amato, N. E. D., Sydnor, T. D., Knee, M., & Hunt, R. (2002). Which comes first, the root or the crack? *Journal of Arboriculture*, 28(November), 277–282.
- Annan, A.P. (2009). Electromagnetic Principles of Ground Penetrating Radar. In *Ground Penetrating Radar: Theory and Applications*, edited by Harry M. Jol, pp. 3-40. *Elsevier*, Amsterdam.
- Armson, D., Stringer, P., & Ennos, A. R. (2013). Urban Forestry & Urban Greening The effect of street trees and amenity grass on urban surface water runoff in. *Urban Forestry & Urban Greening*, 12(3), 282–286.
- Barton, C. V. M., & Montagu, K. D. (2004). Detection of tree roots and determination of root diameters by ground penetrating radar under optimal conditions. *Tree Physiology*, 24(12), 1323–1331.
- Bassuk, N., Grabosky, J., Mucciardi, A., & Raffel, G. (2011). *Ground-penetrating Radar Accurately Locates Tree Roots in Two Soil Media Under Pavement*. 37(4), 160–166.
- Berland, A., Shiflett, S. A., Shuster, W. D., Garmestani, A. S., Goddard, H. C., Herrmann, D. L., & Hopton, M. E. (2017). The role of trees in urban stormwater management. *Landscape and Urban Planning*, 162, 167–177.
- Berner, R. A. (1998). The carbon cycle and CO₂ over Phanerozoic time: the role of land plants. *Philosophical Transactions B*, 353(1365), 75-82.
- Binley, A., Kemna, A. (2005). DC Resistivity and Induced Polarization Methods. *Hydrogeophysics*, 50, 129-156.
- Blunt, S. M. (2012). Trees and pavements – are they compatible? *The International Journal of Urban Forestry*, 31 (2), 73-80.
- Boyd, J., Blanchey, G., Saneiyani S., McLahlan, P., Binley, A. (2019). 3D Geoelectrical Problems With ResiPy, an Open Source Graphical User Interface for Geoelectrical Data Processing.

Fast Times, 24, 4, 85-92.

- Brander, L. M., & Koetse, M. J. (2011). The value of urban open space : Meta-analyses of contingent valuation and hedonic pricing results. *Journal of Environmental Management*, 92(10), 2763–2773.
- Butnor, J. R., Doolittle, J. A., Johnsen, K. H., Samuelson, L., Stokes, T., & Kress, L. (2003). *Utility of Ground-Penetrating Radar as a Root Biomass Survey Tool in Forest Systems*. 1607–1615.
- Butnor, J. R., Samuelson, L. J., Stokes, T. A., Johnsen, K. H., Anderson, P. H., & González-benecke, C. A. (2016). Surface-based GPR underestimates below-stump root biomass. *Plant and Soil*, 47–62.
- Cassiani, G., Boaga, J., Vanella, D., Perri, M. T., Consoli, S. (2015). Monitoring and modelling of soil–plant interactions: the joint use of ERT, sap flow and eddy covariance data to characterize the volume of an orange tree root zone. *Hydrology and Earth Systems*, 19, 2213-2225.
- Cassidy, N. J. (2009a). Ground Penetrating Radar Data Processing, Modelling and Analysis. In *Ground Penetrating Radar: Theory and Applications*, edited by Harry M. Jol, pp. 141- 176. Elsevier, Amsterdam
- Cassidy, N. J., Millington, T. M. (2009b). The application of finite-difference time-domain modelling for the assessment of GPR in magnetically lossy materials. *Journal of Applied Geophysics*, 67(4), 296-308.
- Cermak, J., Hrušca, J., & Martinkov, M. (2000). Urban tree root systems and their survival near houses analyzed using ground penetrating radar and sap flow techniques. *Plant and Soil*, 219, 103–116.
- Cermák, J., Ulrich, R., K, Staněk, Z., Koller, J., & Aubrecht, L. (2006). Electrical measurement of tree root absorbing surfaces by the earth impedance method : 2 . Verification based on allometric relationships and root severing experiments. *Tree Physiology*, 26(9), 1113–1121.
- Clark, J. R., Kjelgren, R. (1989) Water as a limiting factor in the development of urban trees. *Environmental Science*, 16(8), 203-208.
- Conyers, L.B. (2004). *Ground Penetrating Radar for Archaeology*, AltaMira Press, Walnut Creek, California, USA.
- Conyers, L. B., 2009. Ground-penetrating radar for landscape archaeology: method and applications. In Campana, S., and Piro, S. (eds.), *Seeing the Unseen: Geophysics and Landscape Archaeology*. Leiden: CRC Press/Balkema, pp. 245–255.

- Cornelis, C., Robert, M., & Barfoed, T. (2019). K benhavn Universitet. Defining urban forestry - a comparative perspective of North America and Europe. *Urban Forestry & Urban Greening*, 4(3-4), 93–103.
- Corwin, D. L., & Lesch, S. M. (2005). Apparent soil electrical conductivity measurements in agriculture. *Computers and Electronics in Agriculture*, 46(1-3), 11–43.
- Costello, L.R., and K.S. Jones. 2003. Reducing infrastructure damage by tree roots: A compendium of strategies. *International Society of Arboriculture*, Symposium, 119 pp,
- Cui, X., Guo, L., Chen, J., Chen, X., & Zhu, X. (2013). Estimating Tree-Root Biomass in Different Depths Using Ground-Penetrating Radar : Evidence from a Controlled Experiment, 51(6), *IEEE Transactions on Geoscience and Remote Sensing*, 51(6), 3410–3423.
- Daniels, D. J. (1996). Surface Penetrating Radar, 2nd edition. *IET Institution of Engineering and Technology*.
- Daniels, D. J. (2004). Ground penetrating radar, 2nd edn. *Institution of Electrical Engineers*, London.
- Davis, J. L., Annan, A. P. (1989). Ground-penetrating radar for high resolution mapping of rock and soil stratigraphy. *Geophysical Prospecting*, 37(5), 531-551.
- Day, R.W. (1991) Damage of structures due to tree roots. *Journal of Performance of Constructed Facilities*, 5, 200-207.
- Demontoux, F., Razafindratsima, S., Bircher, S., Ruffi , G., Bonnaudin, F., Jonard, F., Wigneron, J. P., Sbartai, M., Kerr, Y., (2017). Efficiency of end effect probes for in-situ permittivity measurements in the 0.5–6 GHz frequency range and their application for organic soil horizons study. *Sensors and Actuators A: Physical*, 254 (1), 78-88.
- DiMichelle, W. A., Falcon-Lang, H. J. (2011). Pennsylvanian “ fossil forests ” in growth position (T 0 assemblages): origin, taphonomic bias and palaeoecological insights. *Journal of the Geological Society*, 168, 585–605.
- Donovan, G. H., & Butry, D. T. (2009). The value of shade : Estimating the effect of urban trees on summertime electricity use. *Energy and Buildings*, 41 (6), 662–668.
- Dwyer, J. F., Schroeder, H. W., & Gobster, P. H. (2013). The significance of urban trees and forests: toward a deeper understanding of values. *Journal of Arboriculture*, 17(10), 276-284.
- Edmondson, J. L., Davies, Z. G, McCormack, S. A., Gaston, K. J., Leake J. R. (2011). Are soils in urban ecosystems compacted? A citywide analysis. *Biology Letters*, 7(5), 771-774
- El Said, M.A.H. (1956). Geophysical prospection of underground water in the desert by means of electromagnetic interference fringes: *Pro. I.R.E.*, 44, 24-30.
- Everett, M. E., (2013). *Near-Surface Applied Geophysics*. Cambridge University Press.
- Foster, R. S., & Blaine, J. (1977). Urban Tree Survival: Trees in the sidewalk. *Journal of*

Arboriculture, 4(1), 14–17.

- Francis, J. K., Parresol, B. R., & Patino, J. M. De. (1996). Probability of damage to sidewalks and curbs by street trees in the tropics. *Journal of Arboriculture*, 22(462), 193–197.
- Gaffney, C. (2008). Detecting trends in the prediction of the buried past: A review of geophysical techniques in archaeology. *Archaeometry*, 50(2), 313-336.
- Gastaldo, R. A. (1987). Confirmation of Carboniferous clastic swamp communities. *Nature*, 326, 869-871.
- Gerea, A. G., Mihai, A. E., Atkins, P. (2019). Integrating resistivity and GPR data for plant root study for indoor agricultura environments. *Conference Proceedings, 25th European Meeting of Environmental and Engineering Geophysics*, 2019, 1-5.
- Giannopoulos, A. (2005). Modelling ground penetrating radar by GprMax, Construction and Building Materials. *Construction and Building Materials*, 19(10), 755-762
- Gillner, S., Vogt, J., Tharang, A., Dettmann, S., & Roloff, A. (2015). Landscape and Urban Planning Role of street trees in mitigating effects of heat and drought at highly sealed urban sites. *Landscape and Urban Planning*, 143, 33–42.
- Günther, T., Rücker, C., Spitzer, K. (2006). Three-dimensional modelling and inversion of DC resistivity data incorporating topography—II. Inversion. *Geophysical Journal International*, 166(2), 506-517.
- Guo, L., J. Chen, X. Cui, B. Fan, and H. Lin. 2013. Application of ground penetrating radar for coarse root detection and quantification: a review. *Plant Soil* 362, 1-23.
- Hagrey, S. A., Meissner, R., Werban, U., Rabbel, W., Ismaeli, A. (2004). Hydro-, bio-geophysics. *The Leading Edge*, 23: 670-674.
- Hagrey, S. A. (2007). Geophysical imaging of root-zone, trunk, and moisture heterogeneity. *Journal of Experimental Botany*, 58 (4), 839-854.
- Hirano, Y., & Yamamoto, R. (2012). Detection frequency of *Pinus thunbergii* roots by ground-penetrating radar is related to root biomass. *Plant and Soil*, 360(1-2), 363-373.
- Hoegh, K., Khazanovich, L., Dai, S., Yu, T. (2015). Evaluating asphalt concrete air void variation via GPR antenna array data. *Case Studies in Nondestructive Testing and Evaluation*, 3, 27-33.
- Hubbard, S. S., Peterson, J. E. Jr., Majer, E. L., Zawislanski, P. T. , Williams, , K. H. Roberts, J. , Wobber, F. (1997). Estimation of permeable pathways and water content using tomographic radar data, *The Leading Edge*, 16, 1623-1628.
- Huisman, J. A., Hubbard, S. S., Redman, J. D., & Annan, A. P. (2003). Measuring Soil Water Content with Ground Penetrating Radar : A Review. *Vadose Zone Journal*, 2, 476–491.

- Isaac, M. E., Anglaaere, L. C. N. (2013). An in situ approach to detect tree root ecology: linking ground-penetrating radar imaging to isotope-derived water acquisition zones. *Ecology and Evolution*, 3(5), 1330-1339.
- Jansen, E., Michels, M., van Til, M., Doelman, P. (1994). Effects of heavy metals in soil on microbial diversity and activity as shown by the sensitivity-resistance index, an ecologically relevant parameter. *Biology and Fertility of Soils*, 17, 177–184
- Jim, C. Y., & Chen, W. Y. (2009). Ecosystem services and valuation of urban forests in China. *Cities*, 26(4), 187–194.
- Karaoulis, M. C., Kim, J., & Tsourlos, P. I. (2011). 4D active time constrained resistivity inversion. *Journal of Applied Geophysics*, 73(1), 25–34.
- Kelly, J., Thornton, I., and Simpson, P. R. (1996). “Urban Geochemistry: A Study of the Influence of Anthropogenic Activity on the heavy Metal Content of Soils in Traditionally Industrial and Non-Industrial Areas of Britain,” *Applied Geochemistry*, Vol. 11, No. 1-2, 1996, pp. 363-370. doi:10.1016/0883-2927(95)00084-4
- Kenrick, P., Crane, P. R. (1997). The origin and early evolution of plants on land. *Nature*, 389, 33-39.
- Killicoat, P., & Puzio, E. (2002). The Economic Value of Trees in Urban Areas: Estimating the Benefits of Adelaide’s Street Trees. *Treenet Proceedings of the 3rd National Street Tree Symposium* (September).
- Kirkpatrick, J. B., Davison, A., & Daniels, G. D. (2012). Landscape and Urban Planning Resident attitudes towards trees influence the planting and removal of different types of trees in eastern Australian cities. *Landscape and Urban Planning*, 107(2), 147–158.
- Konstantinovic, M., Wöckel, S., Lammers, P. S., Sachs, J., & Martinov, M. (2007). Detection of Root Biomass using Ultra Wideband Radar – an Approach to Potato Nest Positioning, *IX(1983)*, 1–11.
- Kuras, O., Beamish, D., Meldrum, P. I., Ogilvy, R. D. (2006). Fundamentals of the capacitive resistivity technique. *Society of Exploration Geophysicists*, 71(3).
- La Gioia, A., Porter, E., Merunka, I., Shahzad, A., Salahuddin, S., Jones, M., O’Halloran, M. (2018). Open-Ended Coaxial Probe Technique for Dielectric Measurement of Biological Tissues: Challenges and Common Practices. *Diagnostics*, 8, 40.
- Lal, R. (2005). Forest soils and carbon sequestration. *Forest Ecology and Management*, 220 (1-3), 242–258.
- Loke, M. H. (2000). *Electrical Imaging Surveys for Environmental and Engineering Studies*. RES2DINV publication

- Loke, M. H., Wilkinson, P. B., & Chambers, J. E. (2010). Computers & Geosciences Fast computation of optimized electrode arrays for 2D resistivity surveys. *Computers and Geosciences*, 36(11), 1414–1426.
- Luttik, J. (2000). The value of trees, water and open space as reflected by house prices in the Netherlands. *Landscape and Urban Planning*, 48 (3-4), 161–167.
- Martorana, R., Capizzi, P., Alessandro, A. D., & Luzio, D. (2017). Comparison of different sets of array configurations for multichannel 2D ERT acquisition. *Journal of Applied Geophysics*, 137, 34–48.
- Matos, G. De, Kipnis, R., & Lui, J. (2010). GPR survey at Lapa do Santo archaeological site, Lagoa Santa karstic region, Minas Gerais state, Brazil. *Journal of Archaeological Science*, 37(6), 1141–1148.
- Mavrovic, A., Roy, A., Royer, A., Filali, B., Boone, F., Pappas, C., and Sonnentag, O.: Dielectric characterization of vegetation at L band using an open-ended coaxial probe, *Geosci. Instrum. Method. Data Syst.*, 7, 195–208.
- McDonald, A. G., Bealey, W. J., Fowler, D., Dragosits, U., Skiba, U., Smith, R. I., Nemitz, E. (2007). Quantifying the effect of urban tree planting on concentrations and depositions of PM 10 in two UK conurbations. *Atmospheric Environment*, 41 (38), 8455–8467.
- McPherson, E. G., Peper, P. J. (1996). Cost of street tree damage to infrastructure. *Arboricultural Journal*. 20(2)2, 143-160.
- McPherson, E. G. (2000). Expenditures associated with conflicts between street tree root growth and hardscape in California, United States. *Journal of Arboriculture*, 26, 289–297
- McPherson, E. G., Maco, S. E., Simpson, J. R., Peper, P. J., Xiao, Q., VanDerZanden, A. M., et al.(2002). Western Washington and Oregon community tree guide: Benefits, costs and strategic planting. *Davis, California: International Society of Arboriculture, Pacific Northwest Chapter*.
- McPherson, E. G., & Muchnick, J. (2005). Effects of street tree shade on asphalt concrete pavement performance. *Journal of Arboriculture*, 31(6), 303–310.
- McPherson, E. G., Peper, P. J. (2012). Urban Tree Growth Modeling. *Arboriculture & Urban Forestry*. 38(5): 172-180.
- McPherson, E. G., Doorn, N. Van, & Goede, J. De. (2016). Urban Forestry & Urban Greening Structure, function and value of street trees in California, USA. *Urban Forestry & Urban Greening*, 17, 104–115.
- Meineke, E. K., Dunn, R. R., Sexton, J. O., & Frank, S. D. (2013). Urban Warming Drives Insect Pest Abundance on Street Trees. *PLOS ONE*, 8(3), 2–8.

- Mihai, A. E. (2014). Utilizarea Georadarului in studierea patrimoniului natural si istoric - studiu de caz in regiunea Braga, Portugalia. MSc thesis, University of Bucharest, Faculty of Geology and Geophysics.
- Mihai, A. E., Gereu, A.G., Curioni, G., Atkins, P., Hayati, F. (2019). Direct measurements of tree root relative permittivity for the aid of GPR forward models and site surveys. *Near Surface Geophysics*, 17(3), 299-310.
- Millington, T. M., Cassidy, N. J. (2010). Optimising GPR modelling: A practical, multi-threaded approach to 3D FDTD numerical modeling. *Computers & Geosciences*, 36(9), 1135-1144.
- Moll, G., Ebenreck, S. (1989). Shading our cities: A resource guide for urban and community forests. United States: N. p., 1989. Web.
- Morelli, G. F., Zenone, T., Teobaldelli, M., Fischanger, F., & Matteucci, M. (2005). Use of Ground-Penetrating Radar (GPR) and Electrical Resistivity Tomography (ERT) to study tree roots volume in pine forest and poplar plantation. Proceedings of the 5th International Workshop on Functional-Structural Plant Models p., 21, 1-4.
- Mullaney, J., Lucke, T., Trueman, S. J. (2015). A review of benefits and challenges in growing street trees in paved urban environments. *Landscape and Urban Planning*, 134, 157-166.
- Neubauer, W., Eder-Hinterleitner, A., Seren, S., Melichar, P. (2002). Georadar in the Roman civil town Carnuntum, Austria: an approach for archaeological interpretation of GPR data. *Archaeological Prospection*, 9(3), 135-156.
- Nichols, P., Mccallum, A., & Lucke, T. (2017). Urban Forestry & Urban Greening Using ground penetrating radar to locate and categorise tree roots under urban pavements. *Urban Forestry & Urban Greening*, 27(May), 9–14.
- Nowak, D. J., & Crane, D. E. (2002). Carbon storage and sequestration by urban trees in the USA, *Environmental Pollution*, 116(3), 381–389.
- Nowak, D. J., Hirabayashi, S., Bodine, A., & Hoehn, R. (2013). Modeled PM 2.5 removal by trees in ten U.S. cities and associated health effects. *Environmental Pollution*, 178, 395–402.
- Ow, L. F., Sim, E. K., Ow, L. A. I. F., & Sim, E. N. G. K. (2012). Detection of urban tree roots with the ground penetrating radar. *Plant Biosystems*, 146, 288-297.
- Pandit, R., Polyakov, M., Tapsuwan, S., & Moran, T. (2013). Landscape and Urban Planning. The effect of street trees on property value in Perth, Western Australia. *Landscape and Urban Planning*, 110, 134–142.
- Pawlik, L., Kasprzak, M. (2018). Regolith properties under trees and the biomechanical effects caused by tree root systems as recognized by electrical resistivity tomography (ERT). *Geomorphology*, 300(1), 1-12.
- Ping, X., Yok, P., Edwards, P., & Richards, D. (2018). The economic benefits and costs of trees in

urban forest stewardship : A systematic review. *Urban Forestry & Urban Greening*, 29, 162–170.

- Plati, C., Dérobert, X. (2015). Inspection Procedures for Effective GPR Sensing and Mapping of Underground Utilities and Voids, with a Focus to Urban Areas. *Springer Transactions in Civil and Environmental Engineering*, 125–145. doi:10.1007/978-3-319-04813-0_5
- Pomfret, J. (2006). Ground-penetrating radar profile spacing and orientation for subsurface resolution of linear features. *Archaeological Prospection*, 13(2), 151-153.
- Pretzsch, H., Biber, P., Uhl, E., Dahlhausen, J., Schütze, G., Perkins, D., Lefer, B. (2017). Climate change accelerates growth of urban trees in metropolises worldwide. *Scientific Reports*, 7, 1–10.
- Quigley, M. F. (2004). Street trees and rural conspecifics: Will long-lived trees reach full size in urban conditions? *Urban Ecosystems*, 7(1), 29–39.
- Raich, J. W., Schlesinger, W. H. (1992). The global carbon dioxide flux in soil respiration and its relationship to vegetation and climate. *Tellus*, 44(2), 81-99.
- Randrup, T. B., McPherson, E. G., Costello, L. R. (2001). A review of tree root conflicts with sidewalks, curbs, and roads. *Urban Ecosystems* 5, 209–225.
- Retallack, G. J. (1997). Early Forest Soils and Their Role in Devonian Global Change. *Science*, 276(5312), 583–586.
- Rodríguez-Robles, U., Arredondo, T., Huber-Sannwald, E., Ramos-Leal, J. A., Yépez, E. A. (2017). Technical note: Application of geophysical tools for tree root studies in forest ecosystems in complex soils. *BioGeosciences*, 14, 5343-5357.
- Roman, L. A., & Scatena, F. N. (2011). Urban Forestry & Urban Greening Street tree survival rates : Meta-analysis of previous studies and application to a field survey in Philadelphia, PA, USA. *Urban Forestry & Urban Greening*, 10(4), 269–274.
- Rossi, R., Amato, M., Bitella, G., Bochicchio, R., Ferreira Gomes, R. R., Lovelli, S., Martorella, E., Favale, P. (2011). Electrical resistivity tomography as a non-destructive method for mapping root biomass in an orchard. *European Journal of Soil Science*, 2011, 62, 206-215.
- Roy, S., Byrne, J., & Pickering, C. (2012). Urban Forestry & Urban Greening A systematic quantitative review of urban tree benefits, costs, and assessment methods across cities in different climatic zones. *Urban Forestry & Urban Greening*, 11(4), 351–363.
- Rücker, C., Günther, T., Spitzer, K. (2006). Three-dimensional modelling and inversion of dc resistivity data incorporating topography—I. Modelling. *Geophysical Journal International* 166(2), 495-505.
- Rücker, C., Günther, T. (2011). The simulation of finite ERT electrodes using the complete electrode model, *Geophysics*, 76(4).
- Sarajevs, V. (2011). Street tree valuation systems. *Forestry Commission*, 1–6.

- Sasaki, Y. (1992). Resolution of Resistivity Tomography Inferred from Numerical Simulation, *Geophysical Prospecting*, 40(4), 453-563.
- Satriani, A., Loperte, A., Proto, M., & Bavusi, M. (2010). Advances in Geosciences Building damage caused by tree roots : laboratory experiments of GPR and ERT surveys. *Advances in Geoscience*, 24, 133–137.
- Schultz, J. J., Martin, M. M. (2011). Controlled GPR grave research: Comparison of reflection profiles between 500 and 250 MHz antennae. *Forensic Science International*, 209(1-3), 64-69.
- Selmi, W., Weber, C., Rivière, E., Blond, N., Mehdi, L., & Nowak, D. (2016). Urban Forestry & Urban Greening Air pollution removal by trees in public green spaces in Strasbourg. *Urban Forestry & Urban Greening*, 17(2), 192–201.
- Skiera, B., Moll, G. (1992). The sad state of city trees. *American Forests*, 98, 61-64.
- Smiley, E. T. (2008). Comparison of Methods to Reduce Sidewalk Damage from Tree Roots. *Arboriculture & Urban Forestry*, 34(3), 179–183.
- Soares, A. L., Rego, F. C., Mcpherson, E. G., Simpson, J. R., Peper, P. J., & Xiao, Q. (2011). Urban Forestry & Urban Greening Benefits and costs of street trees in Lisbon, Portugal. *Urban Forestry & Urban Greening*, 10(2), 69–78.
- Soria, A., & Decombeix, A. (2010). The land plant cover in the Devonian: a reassessment of the evolution of the tree habit. *Geological Society of London, Special Publications*, 399 (59–70).
- Stokes, A., Fourcaud, T., Hruška, J., Čermák, J., Nadezhdina, N., Nadyezhdin, V., Praus, L. (2002) An evaluation of different methods to investigate root system architecture of urban trees in situ: Ground-Penetrating Radar. *Journal of Arboriculture*, 28, 2-10.
- Stolt, E. (1982). Vegetationens förmåga att minska expositionen för bilavgaser (The ability of vegetation in decreasing exposure to car fumes). Göteborgs Universitet pauppdrag av Göteborgs Hälsovårdsavdelning (quoted from Svensson and Eliasson 1997, in Swedish).
- Stovin, V. R., Jorgensen, A., & Clayden, A. (2012). Street Trees and Storm water Management. *The International Journal of Urban Forestry*, 30(4), 1375.
- Stummer, P., Maurer, H., & Green, A. G. (2004). Experimental design: Electrical resistivity data sets that provide optimum subsurface information. *Geophysics*, 69(1), 120–139.
- Svensson, M. and Eliasson I. (1997). Grönstrukturens betydelse för stadens ventilation (The importance of green areas for the ventilation of the city). Naturvårdsverkets rapport 4779, Stockholm (in Swedish).
- Szalai, S., Szarka, L. (2008). On the classification of surface geoelectric arrays. *Geophysical Prospecting*, 56, 159-175.

- Tanikawa, T., Hirano, Y., & Dannoura, M. (2013). Root orientation can affect detection accuracy of ground-penetrating radar. *Plant and Soil*, 373 (1-2).
- Tiwary, A., Sinnett, D., Peachey, C., Chalabi, Z., Vardoulakis, S., Fletcher, T., Hutchings, T. R. (2009). An integrated tool to assess the role of new planting in PM 10 capture and the human health benefits : A case study in London. *Environmental Pollution*, 157(10), 2645–2653.
- Trinks, I., Johansson, B., Gustafsson, J., Emilsson, J., Friberg, J., Gustafsson, C., Hinterleitner, A. (2010). Efficient, Large-scale Archaeological Prospection using a True Three-dimensional Ground-penetrating Radar Array System. *Archaeological Prospection*, 186(July), 175–186.
- Troy, A., Grove, J. M., & Neil-dunne, J. O. (2012). Landscape and Urban Planning The relationship between tree canopy and crime rates across an urban – rural gradient in the greater Baltimore region. *Landscape and Urban Planning*, 106(3), 262–270.
- Urban, J., Bequet, R., Mainiero, R. (2011). Assessing the applicability of the earth impedance method for in situ studies of tree root systems. *Journal of Experimental Botany*, 62(6), 1857-1869.
- Villain, G., Ihamouten, A., Dérobert, X., (2017). Determination of concrete water content by coupling electromagnetic methods: Coaxial/cylindrical transition line with capacitive probes. *NDT & E International*, 88, 59-70.
- Volder, A., Watson, T., & Viswanathan, B. (2009). Potential use of pervious concrete for maintaining existing mature trees during and after urban development. *Urban Forestry & Urban Greening*, 8(4), 249–256.
- Warren, C., Giannopoulos, A., Iraklis, G. (2016). gprMax: Open source software to simulate electromagnetic wave propagation for Ground Penetrating Radar. *Computer Physics Communications*, 209, 163-170.
- Warren, C., Giannopoulos, A., Gray, A., Giannakis, I., Patterson, A., Wetter, L., & Hamrah, A. (2018). A CUDA-based GPU engine for gprMax: Open source FDTD electromagnetic simulation software. *Computer Physics Communications*, 237, 208-218.
- Werban, U., al Hagrey, S. A., Rabbel, W. (2008). Monitoring of root-zone water content in the laboratory by 2D geoelectrical tomography, *Journal of Plant Nutrition and Soil Science*, 171 (6), 927-935.
- Wilkinson, P. B., Loke, M. H., Meldrum, P. I., Chambers, J. E., Kuras, O., Gunn, D. A., & Ogilvy, R. D. (2012). Practical aspects of applied optimized survey design for electrical resistivity tomography. *Geophysical Journal International*, 189(1), 428–440.

- Wilkinson, P. B., Meldrum, P. I., Chambers, J. E., Kuras, O., & Ogilvy, R. D. (2006). Improved strategies for the automatic selection of optimized sets of electrical resistivity tomography measurement configurations. *Geophysical Journal International*, 167(3) 1119–1126.
- Xihong, C. U. I., Jin, C., Jinsong, S., Xin, C. A. O., Xuehong, C., & Xiaolin, Z. H. U. (2011). Modeling tree root diameter and biomass by ground-penetrating radar. *Science China Earth Sciences*, 54(5), 711–719.
- Yang, J., Chang, Y., & Yan, P. (2015). Ranking the suitability of common urban tree species for controlling PM2.5 Atmospheric Pollution. *Atmospheric Pollution Research*, 6(2), 267–277.
- Yee, K. S. (1966). Numerical solution of initial boundary value problems involving Maxwell's equations in isotropic media. *IEEE T Antenn Propag*, 14 (1966), 49-58.
- Zanetti, C., Weller, A., Vennetier, M., Meriaux, P. (2011). Detection of buried tree root samples by using geoelectrical measurements: A laboratory experiment. *Plant and Soil*, 339(1), 273-283.
- Zenone, T., Morelli, G., Teobaldelli, M., Fischanger, F., Mateucci, M., Sordini, M., Armani, A., Ferrè, C., Chiti, T., Seufert, G. (2008). Preliminary use of ground-penetrating radar and electrical resistivity tomography to study tree roots in pine forests and poplar plantations. *Functional Plant Biology*, 35, 1047-1058.
- Zhu, S., Huang, C., Su, Y., & Sato, M. (2014). 3D Ground Penetrating Radar to Detect Tree Roots and Estimate Root Biomass in the Field. *Remote Sensing*, 6(6), 5754–5773.